

ABSTRACT

Title of Dissertation: SMALL MOLECULE INHIBITORS OF
CYCLIC DI-AMP SIGNALING

Clement Opoku-Temeng
Doctor of Philosophy
2018

Dissertation directed by: Professor Herman O. Sintim,
Department of Chemistry and Biochemistry
University of Maryland, College Park, Maryland

Drug Discovery Institute, Department of
Chemistry,
Purdue University, West Lafayette, Indiana.

Globally, it is estimated that more than 700,000 people die annually from infections caused by drug-resistant bacterial pathogens. Resistant strains of bacteria continue to be isolated in healthcare and community settings. At the same time, the antibiotic pipeline remains dry – exemplified by the paucity of new antibiotics introduced into clinical use. Consequently, antibiotic-resistant strains are rapidly spreading, and antibiotic-resistant infections persist. Additionally, the existing antibiotics target one of the common targets – DNA, RNA, protein and cell wall synthesis. There is an apparent need to identify antibacterial agents against novel targets to slow down the generation of resistance. Cyclic dinucleotides have emerged as central regulators of bacterial physiology. Particularly, cyclic di-AMP (c-di-AMP) regulates cell wall homeostasis, cell size, potassium ion transport, virulence and biofilm formation in

various Gram-positive pathogens including *Staphylococcus aureus*, *Enterococcus faecalis*, *Listeria monocytogenes* and *Streptococcus pneumoniae*. It has been demonstrated that under standard laboratory conditions, deletion of the diadenylate cyclase genes that encode c-di-AMP synthesizing enzymes (diadenylate cyclase, DAC) was lethal in human pathogens like *S. aureus* and *L. monocytogenes*. Hence, DACs have been suggested as potential antibiotic targets. Thus far, the effect of c-di-AMP on bacterial physiology has been studied using genetic approaches whereby the key players of the second messenger signaling are deleted, inactivated or overexpressed to create conditions of varying intracellular c-di-AMP levels. However, these approaches are not amenable to drug development. Cell permeable small molecule modulator or c-di-AMP levels are required to validate the druggability of c-di-AMP signaling.

This dissertation reports the identification of different small molecules that potently inhibit c-di-AMP synthesis. The cell permeable inhibitors possess the ability to decrease the intracellular concentration of c-di-AMP. Furthermore, the antibacterial activities of the cell permeable c-di-AMP synthesis inhibitors have been characterized. Efforts towards the development of antibiotics have also been discussed.

SMALL MOLECULE INHIBITORS OF CYCLIC DI-AMP SIGNALING

by

Clement Opoku-Temeng

Dissertation submitted to the Faculty of the Graduate School of the
University of Maryland, College Park, in partial fulfillment
of the requirements for the degree of
Doctor of Philosophy
2018

Advisory Committee:
Professor Herman O. Sintim, Chair
Dr. Douglas Julin, Co-chair
Professor Lai-Xi Wang
Dr. Theodore Kwaku Dayie
Dr. Sergi Sukharev

© Copyright by
Clement Opoku-Temeng
2018

Dedication

This is dedicated to my mother, Ms. Nora Aninakwah. Your constant support and encouragement have made this possible.

Acknowledgements

“A charge to keep I have, a God to glorify, a never dying soul to save and fit it for the sky” (Charles Wesley; The United Methodist Hymnal, No. 413). I am first and foremost grateful to the Almighty God, who has kept me through the highs and lows of graduate school.

My sincerest of appreciations goes to my research advisor and mentor Prof. Herman O. Sintim. He instilled in me the qualities of a good scientist. Your enthusiasm for ‘research that makes an impact’ forged in me a unique perspective to research. I had the opportunity of acquiring a great deal of skills as well as general knowledge under your mentorship. You pushed me beyond my limits and out of my comfort zone to get the best out of me. Thank you for investing time and other valuable resources in training me.

I am also grateful to my dissertation committee members – Prof. Douglas Julin, Prof. Kwaku Dayie and Prof. Lai-Xi Wang. Your constructive criticisms, continuous encouragement and support over the years have shaped my research focus. I could not have asked for a better dissertation committee.

I am also grateful to past graduate students from the Sintim Research group including Dr. Yue Zheng, Dr. Jie Zhou, Dr. Min Guo and Dr. Benjamin Roembke who shaped my research etiquettes. Both Dr. Jie Zhou and Dr. Yue Zheng directly mentored me whilst our times in the Sintim group overlapped.

To my current colleagues, Dr. Neetu Dayal, Dr. Clinton Mikek and other members of the Sintim group, I say thank you for the help and collaborative atmosphere. I had a lot of memorable experiences being around rich minds like yours.

I will also like to thank the Graduate Office of the Chemistry and Biochemistry Department at University of Maryland, especially Diane Canter. Diane was always at hand to respond to my numerous e-mails and phone calls while I was at Purdue University in West Lafayette.

My sincerest appreciation to my dad, Mr. George Amoako-Temeng. I couldn't have gotten to this level without your support over the years. A big thank you to my sister Nana Ama Temeng and all members of the Aninakwah family for the constant prayers and moral support.

Finally, to Ms. Linda Ayidzoe, my fiancée, the lady that kept me grounded through this topsy-turvy journey, I appreciate your calming influence and all manner of contributions you made towards me achieving this goal. I love you.

Table of Contents

Dedication.....	ii
Acknowledgements.....	iii
Table of Contents.....	v
List of Tables.....	vii
List of Figures.....	viii
List of Abbreviations.....	xv
Chapter 1: Introduction.....	1
1.1 Background.....	1
1.1 Cyclic di-GMP signaling.....	3
1.1.1 Synthesis of c-di-GMP: GGDEF domain proteins.....	5
1.2.2 Degradation of c-di-GMP: EAL or HD-GYP domain proteins.....	5
1.2.3 c-di-GMP receptors.....	6
1.3 Cyclic di-AMP signaling.....	7
1.3.1 Cellular metabolism of c-di-AMP.....	8
1.3.1.1 Cyclic di-AMP synthases and phosphodiesterases.....	8
1.3.1.2 Cellular c-di-AMP concentration and bacterial physiology.....	14
1.3.1.3 Bacterial receptor and effector molecules of c-di-AMP.....	16
1.3.1.4 Mammalian receptors of c-di-AMP: Host-pathogen interactions.....	18
1.3.2 Inhibiting c-di-AMP signaling.....	19
1.4 Cyclic GMP-AMP signaling.....	21
1.4.1 Bacterial cyclic GMP-AMP (3',3'-cGAMP).....	21
1.4.2 Mammalian cyclic GMP-AMP (3',3'-cGAMP).....	22
1.5 The antibiotics resistance crisis.....	22
1.5.1 Resistance mechanisms.....	23
1.5.2 Approaches to reduce the rate of antibiotic resistance.....	24
Chapter 2: Identification suramin and theaflavin-3,3'-digallate as inhibitors of c-di-AMP synthase, DisA.....	27
1.2 Potent inhibition of cyclic diadenylate monophosphate cyclase by the antiparasitic drug, suramin.....	27
1.2.1 Introduction.....	27
1.2.2 Results and Discussion.....	30
1.2.3 Conclusions.....	40
1.2.4 Experimental section.....	40
1.3 Inhibition of cyclic deadenylate cyclase, DisA, by polyphenols.....	44
1.2.1 Introduction.....	44
1.2.2 Results.....	49
1.2.3 Discussion.....	57
1.2.3 Methods.....	60
Chapter 3: Identification and characterization of cell-permeable c-di-AMP synthesis inhibitors.....	63

3.1 Hydroxybenzylidene-indolinones, c-di-AMP synthase inhibitors, have antibacterial and anti-biofilm activities and also re-sensitize resistant bacteria to methicillin and vancomycin	63
3.1.1 Introduction.....	63
3.1.2 Results and Discussion	66
3.1.3 Conclusions.....	79
3.1.4 Methods.....	80
Chapter 4: Proteomic analysis of bacterial response to a 4-hydroxybenzylidene indolinone compound, which re-sensitizes bacteria to traditional antibiotics	85
4.1 Introduction.....	85
4.2 Results.....	86
4.3 Discussion	99
4.4 Conclusions.....	108
4.5 Methods.....	108
Chapter 5: Discovery of a bacteriostatic antibiotic with potency against drug-resistant bacteria	117
5.1 N-(1,3,4-oxadiazol-2-yl)benzamide analogs, bacteriostatic agents against methicillin- and vancomycin-resistant bacteria	117
5.1.1 Introduction.....	117
5.1.2 Results and Discussion	119
5.1.3 Conclusions.....	135
5.1.4 Materials and methods	136
Chapter 6: Conclusions and future perspectives.....	142
5.1 Conclusions and future perspectives.....	142
Appendices.....	149
Bibliography	150

List of Tables

Table 3.1. MIC values of active hydroxybenzylidene-indolinones against select bacteria	75
Table 3.2. Potentiation of methicillin and vancomycin by hydroxybenzylidene-indolinone	78
Table 4.1. Functional classification of proteins downregulated in <i>S. aureus</i> after treatment with compound 3.1	95
Table 4.2. Sequence of primers used in RT-PCR.....	116
Table 5.1. MIC ($\mu\text{g/mL}$) of compounds screened against a panel of Gram-positive bacterial pathogens.....	122
Table 5.2. The minimum inhibitory concentration (MIC, in $\mu\text{g/mL}$) and minimum bactericidal concentration (MBC, in $\mu\text{g/mL}$) of compound 5.4 and select antibiotics.....	123
Table 5.3. MIC of compound 5.4 against selected Gram-negative bacterial pathogens.....	125
Table 5.4. MIC ($\mu\text{g/mL}$) of 5.12 (F6-5) and vancomycin against a panel of Gram-positive bacterial pathogens.....	134
Table 5.5. Activity (MIC in $\mu\text{g/mL}$) of 5.4-cis against select Gram-positive bacteria.....	135

List of Figures

- Figure 1.1. Structures of cyclic dinucleotides discovered in bacteria and mammals...4
- Figure 1.2. Regulation of intracellular pool of c-di-AMP. The membrane-integrated DACs CdaA (found in *B. subtilis*, *S. aureus* etc) and CdaM (found in *M. pneumoniae*) as well as cytosolic DACs DisA (found in *B. subtilis*, *M. tuberculosis*, *T. maritima* etc) and CdaS (found in *B. subtilis*, *Clostridium* spp) synthesis c-di-AMP while the membrane-bound PDEs, PgpH (found in *L. monocytogenes*) and GdpP (found in *L. monocytogenes*, *S. aureus*, *B. subtilis* etc) degrade the signal. In some bacteria, like *L. monocytogenes*, transporters are involved in decreasing the intracellular c-di-AMP concentration by secreting the second messenger into the extracellular milieu.....12
- Figure 2.1. Schematic of the synthesis of c-di-AMP by DisA from ATP. A DAC inhibitor will hinder the synthesis of c-di-AMP.....28
- Figure 2.2. Structures of suramin and other sulfonated molecules tested against DisA. Abbreviations: ANTS is 8-aminonaphthalene-1,3,6-trisulfonic acid; APTS is 8-aminopyrene-1,3,6-trisulfonic acid.....29
- Figure 2.3. Coralyne assay of suramin and suramin-related compounds. For the coralyne assay, emission fluorescence intensity of coralyne (at 475 nm) increases as the concentration of c-di-AMP increases. BDS stands for benzothiazole-2,5-disulfonic acid. 8-aminonaphthalene-1,3,6-trisulfonic acid (ANTS) is highly fluorescent so could not be tested using the coralyne assay. Each experiment was done in triplicate.....30
- Figure 2.4. HPLC analysis of DisA reactions. The results from further analysis of hits from coralyne assay showing reactions of 1 μM DisA with **A.** No inhibitor, **B.** 20 μM Trypan Blue and **C.** 20 μM suramin. **D.** The HPLC chromatogram of APTS reaction which was not tested by coralyne assay. Only suramin significantly inhibited DisA activity. ATP and c-di-AMP peaks with respective retention times of 10 min and 14.6 min are indicated with arrows on the No inhibitor chromatogram..... 31
- Figure 2.5. Molecular docking with AutoDock Vina 1.1.1 used to obtain a suramin/TmaDisA complex. **A.** Suramin (magenta) binds in the nucleotide-binding pocket of TmaDisA. **B.** Overlay of TmaDisA with modeled structure of *B. subtilis* DisA. Images were generated with PyMOL visualization software.....33
- Figure 2.6. Dose-reponse curves for the inhibition of DisA (1 μM) activity. **A.**The IC₅₀ of suramin was determined at 100 μM , 500 μM or 1 mM α -³²P-ATP/ATP in reaction buffer. The IC₅₀ values at 100 μM , 500 μM and 1 μM ATP were 1.1 μM , 3.1 μM and 5.4 μM . **B.** The IC₅₀ values of bromophenol

thiohydantoin, 3'-deoxyATP and suramin were determined to be 67.2 μM , 3.8 μM and 2.3 μM respectively at 300 μM ATP and 1 μM DisA. Experiments were done in triplicate. Error bars represent mean \pm SEM generated using GraphPad Prism 4.0 Software (La Jolla, CA, USA).....35

Figure 2.7. Analysis of the binding interaction between DisA and suramin. **A.** The fluorescence emission of DisA (5 μM) was observed to be quenched in the presence of increasing suramin concentration. **B.** Plot of relative fluorescence of DisA (5 μM) at 340 nm as a function of suramin concentration. The data was fitted to the non-linear regression, eqn (2.3). **C.** Stern-Volmer plot of the relative fluorescence (at 340 nm) as a function of suramin concentration. Eqn 2.1 was used for the linear regression. **D.** Stern-Volmer plot generated by fitting the fluorescence emission at 340 nm to eqn (2.2). GraphPad Prism 4.0 Software was used to obtain plots from triplicate measurements.....37

Figure 2.8. HPLC analysis of YybT reactions. The effect of suramin on 1 μM YybT **A.** without suramin and **B.** with 20 μM suramin at 37 °C was analyzed by HPLC. There was no difference between the reaction with and without suramin. The arrows point to the product, pApA and substrate, c-di-AMP which had retention times of 13.7 min and 14.4 min respectively.....39

Figure 2.9. Cellular processes affected by c-di-AMP signaling. Fluctuations in the levels of cellular c-di-AMP cause a myriad of phenotypic changes in different bacteria.....45

Figure 2.10. Structures of polyphenols tested against DisA.....48

Figure 2.11. Screening of polyphenols against DisA. Coralyne assay results of 14 polyphenols screened against DisA (1 μM); λ_{ex} = 420 nm and λ_{em} = 475 nm. Polyphenols that yielded at least 50% inhibition were selected for further analysis.....49

Figure 2.12. Effect of polyphenols on DisA activity. HPLC analysis of DisA reactions (1 μM) reactions **A.** without inhibitor, with **B.** 20 μM TA **C.** 20 μM TF3 and **D.** 20 μM TF2B. The ATP and c-di-AMP peaks are labeled with arrows.....50

Figure 2.13. Inhibition of DisA by polyphenol. Half maximum inhibitory concentration, IC₅₀ curves of **A.** polyphenol inhibitors TF2B, TF3 and TA at 1 μM DisA at 300 μM ATP and **B.** TA at 0.5 μM DisA, 1 μM DisA, 5 μM and 10 μM DisA using 300 μM ATP. Error bars represent the mean and SEM of triplicate experiments. Curves were generated with GraphPad Prism 4 software.....52

Figure 2.14. Dose-response curves for the inhibition of DisA (0.5 μ M) by TF3 at 100 μ M ATP, 300 μ M ATP and 500 μ M ATP. Error bars represent the mean and SEM of triplicate experiments. Curves were generated with GraphPad Prism 4.0 Software53

Figure 2.15. HPLC chromatogram of YybT reactions **A.** without inhibitor **B.** with 20 μ M TA **C.** 20 μ M TF3 and **D.** 20 μ M TF2B. The pApA and c-di-AMP peaks are labeled with arrows.....55

Figure 2.16. Intrinsic fluorescence analysis of DisA. **A.** Fluorescence emission trace of DisA (5 μ M) in phosphate buffer (50 mM, pH 7.5) titrated with indicated concentrations of TF3 at room temperature; λ_{ex} = 290 nm and λ_{em} = 300–450 nm. **B.** Plot of normalized fluorescence intensity (at 340 nm) as a function of TF3 concentration. **C.** The modified Stern-Volmer plot of DisA fluorescence quenching by TF3. F_0 is the maximum fluorescence intensity in absence of TF3 and F is the fluorescence intensity in presence of TF3. Data points represent the mean and SEM of triplicate measurements plotted using GraphPad Prism 4.0 Software56

Figure 3.1. Schematic of c-di-AMP metabolism and the processes regulated by the second messenger. Hydroxybenzylidene-indolinones inhibit c-di-AMP synthesis and also possess antibacterial and anti-biofilm activities.....65

Figure 3.2. **A.** Principle of the coralyne assay detection of c-di-AMP. In the presence of c-di-AMP, coralyne fluorescence, which is otherwise quenched by iodide ions, is increased due to the formation of c-di-AMP/coralyne complex. **B.** Plot of percent fluorescence (emission 475 nm) of coralyne against time for the screening of compound **3.1** (20 μ M) against DisA (0.5 μ M). **C.** Radioactive TLC confirmation of the inhibition of DisA (0.25 μ M) by compound **3.1** (20 μ M).....67

Figure 3.3. **A.** Synthetic strategy for making hydroxybenzylidene-indolinones; **B.** Structures of hydroxybenzylidene-indolinones that were synthesized.....69

Figure 3.4. **A.** (Top) Schematic of inhibition of c-di-AMP synthesis. (Bottom) Percent activity of DisA (0.5 μ M) in the presence of hydroxybenzylidene-indolinones (20 μ M) as determined by coralyne assay after 30 min of reaction. Each bar is the mean of 3 replicates and error bars represent standard error of the mean. Plots were generated using GraphPad Prism version 5 statistical software. **B.** HPLC analysis of synthesis of c-di-AMP by DisA (0.25 μ M) in the presence of selected benzylidene-indolinones (20 μ M). ATP and c-di-AMP peaks are at 9 min and 14 min respectively.....70

Figure 3.5. HPLC analysis of benzylideneindolinones that did not inhibit DAC activity of DisA. Compounds were tested at 20 μ M in a 40 mM Tris-HCl pH 7.5, 100 mM NaCl and 10 mM MgCl₂ reaction buffer with 100 μ M ATP and 0.25 μ M DisA for 2 h. ATP and c-di-AMP peaks are as indicated on DMSO control.....72

Figure 3.6. Antibacterial activities of DAC inhibitors tested at 16 µg/mL in MHB. **A.** Evaluation of compounds 3.1 – 3.16 against *S. aureus* and *E. coli*. **B.** Activity of compound 1 against *E. coli* in the presence of colistin (0.03125 µg/mL). **C.** Selected active compounds against *S. aureus* (Sa), *L. monocytogenes* (Lm), *E. coli* (Ec) and *P. aeruginosa* (Pa). Every bar is the mean of 2 replicates and error bars represent the standard error of the mean. Plots were generated using GraphPad Prism version 5 statistical software.....74

Figure 3.7. Inhibition of MRSA ATCC 33592 biofilms. **A.** Representative wells of crystal violet stained biofilms of MRSA ATCC 33592. Compounds tested are as labelled to the left and the concentrations used are indicated on top. **B.** IC₅₀ curves and **C.** table of IC₅₀ and IC₁₀₀ values of biofilm inhibition by hydroxybenzylidene-indolinones. Every data point is the mean of 4 replicates and error bars represent the standard error of the mean. Plots were generated using GraphPad Prism version 5 statistical software (La Jolla, CA, USA).....77

Figure 4.1. Effect of 4-hydroxybenzylidene-indolinones on the intracellular concentration of c-di-AMP. DacA protein expression was induced in exponentially growing *E. coli* and the cells were treated with 16 µg/mL of test compounds for 3 hours. C-di-AMP was extracted using acetonitrile:methanol:water (2:2:1, v/v/v) extraction solvent and quantified by LC-MS/MS. **A.** Structures of compounds analyzed. **B.** Percent c-di-AMP extracted from *E. coli* harboring *S. aureus* DacA (SaDacA) plasmid in the presence of 16 µg/mL of compounds. Experiments were performed in triplicate, and the mean ± SD values are shown in each bar. **P* < 0.05; ***P* < 0.001; ****P* < 0.0001 relative to DMSO treatment.....87

Figure 4.2. Interactions between compound 3.1 and 10 antibiotics in MRSA and VRE. Plot of ΣFIC indices of various antibiotics tested in combination with compound 3.1 against MRSA (red) and VRE (blue). The checkerboard assay was used to determine the types of interactions existing between compound 3.1 and antibiotics with different modes of action. From the FICI values, synergy was defined as ΣFICI: ≤0.5, additive was ΣFICI:>0.5 and ≤1, indifferent was ΣFICI: >1 and ≤2 and antagonistic was ΣFICI: >2. Dotted gridline at ΣFICI of 0.5 depicts the cutoff for synergy.....89

Figure 4.3. Effect of compound 3.1 on macromolecular biosynthesis. *S. aureus* was treated with increasing concentrations of compound 3.1 and 8× MIC of established antibiotics and assayed for incorporation of **A.** [3H]-thymidine for DNA synthesis, **B.** [3H]-uridine for RNA synthesis, **C.** [3H]-L-Leucine for protein synthesis and **D.** [3H]-N-acetyl-D-glucosamine for cell wall synthesis. Data represent the mean±SD of triplicates.....90

Figure 4.4. Global proteomics analysis of *S. aureus* cells treated with compound 3.1. *S. aureus* was treated in triplicates with GW5074 (compound 3.1) and the levels of proteins assessed. **A.** Venn diagram for comparison of proteins identified in DMSO-treated cells alone, compound 3.1-treated cells alone and in both treatments. **B.**

Representative correlation plots for the replicates of (i) DMSO and (ii) compound **3.1**.....92

Figure 4.5. Analysis of differentially expressed protein from *S. aureus* cells treated with compound **3.1**. **A**. Heatmap analysis of global proteomics data showing differentially expressed proteins between replicates of DMSO-treated and compound **3.1**-treated (GW) *S. aureus*. **B**. Volcano plot of global proteomics data showing the statistical *p*-value (y-axis) vs the relative abundance ratio, Log₂ fold change (Log₂FC, x-axis). Insert represents key to the differently color dots. Select proteins have been labeled. Dotted horizontal line represents the adjusted p-value threshold of 0.05 whilst the dotted vertical lines represent the Log₂FC cut-offs. Significant differential expression was defined as either $p \leq 0.05$ and $\text{Log}_2\text{FC} \geq 2$ for upregulated proteins or $p \leq 0.05$ and $\text{Log}_2\text{FC} \leq -2$ for downregulated proteins. **C**. Bar chart representation of the top 20 proteins which were downregulated, **D**. Table of select proteins that were identified to be present in DMSO-treated samples only. **E**. Bar chart representation of top 20 upregulated proteins. The Log₂FC values were plotted for the corresponding proteins using OriginPro 2017 Software (OriginLab, Massachusetts, USA). Data analysis was performed using the Perseus software. Volcano plot was generated with OriginPro 2017 Software (OriginLab, Massachusetts, USA).....93

Figure 4.6. Relative mRNA expression of select targets from global proteomics analysis. The of compound 3.1 treatment on the transcription of A. *purL*, B. *agrA*, C. *sarX* and D. *sceD*. Total RNA isolated from *S. aureus* treated with either DMSO or 2 µg/mL compound 3.1 was reversed transcribed and cDNAs were quantified by qRT-PCR using target-specific primers. The data represents the mean±SD of triplicate experiments normalized with 16S RNA. Statistically significant differences between DMSO-treatment and compound 3.1-treatment as determined by Student's t-test analysis (unpaired, two-tailed) is represented as * $p \leq 0.05$, ** $p \leq 0.01$ and *** $p \leq 0.001$98

Figure 4.7. Purine biosynthesis pathway. The enzymes encoded by the *pur*-operon sequentially catalyze the conversion of PRPP to IMP. PurQ and PurL are known to participate in the same step, and PurS is thought to play a role in this step. The enzymes shown in green were differentially downregulated or were only found in DMSO-treated samples.....101

Figure 4.8. Predicted functional protein-protein association networks for select downregulated proteins. Predicted association of **A**. AgrA, the response regulator interacts with other components of *agr* system encoded by the *agrBDCA* operon and **B**. SarR transcriptional regulator with other SarA homologs. Figures were generated by STRING v 10.5 online database.....103

Figure 4.9. The *S. aureus agr* system. RNAIII modulates the expression of several virulence factors (upregulated factors are indicated with red lines and downregulated factors are indicated with the green lines). Regulation of *agr* by select SarA homologs is depicted as well. AgrA, AgrC, SarR and SarV were downregulated whilst SarX

was upregulated in *S. aureus* when treated with GW5074.....105

Figure 5.1. Structures of antibacterial compounds. Note: F6 (*cis* : *trans* = 10:1). Compounds were obtained from Life Chemicals Inc. (Ontario, Canada).....120

Figure 5.2. Inhibition of growth of *S. aureus* ATCC 25923 by antibacterial compounds. *S. aureus*, at early exponential growth, was treated with either DMSO or 16 µg/mL of compounds and OD600 measured after 24 h. Error bars represent standard error of the mean of duplicates.....120

Figure 5.3. Time-kill analysis of compound **5.4** against MRSA USA300 using linezolid as a control antibiotic. MRSA USA300 was incubated with compound **5.4** (12 µg/mL) or linezolid (6 µg/mL) vancomycin (6 µg/mL) or DMSO and the number of cells estimated at the indicated time points. Experiment was performed in triplicates.....124

Figure 5.4. Multi-step resistance selection of compound **5.4 (F6)** and ciprofloxacin against MRSA. MRSA USA400 was serially passaged daily over a 14-day period and the broth microdilution assay was used to determine the minimum inhibitory concentration of both **F6** (compound **5.4**) and ciprofloxacin (control antibiotic) against MRSA after each successive passage. A four-fold shift in MIC would be indicative of bacterial resistance forming to the test agent.....126

Figure 5.5. Toxicity analysis of compound **5.4 (F6)** against mammalian cell lines. Percent viable mammalian cells (measured as average absorbance ratio (test agent relative to DMSO)) after exposure to compound **F6** (tested in triplicate) at concentrations ranging from 2 to 256 µg/mL against **A.** murine macrophage (J774) cells, or **B.** human colorectal (Caco-2) cells using the MTS 3-(4,5-dimethylthiazol-2-yl)-5-(3-carboxymethoxyphenyl)-2-(4-sulfophenyl)-2H-tetrazolium) assay. Dimethyl sulfoxide (DMSO) was used as a negative control to determine a baseline measurement for the cytotoxic impact of each compound. Error bars represent standard deviation values for triplicates. A two-way ANOVA, with post hoc Sidak's multiple comparisons test, determined statistical difference (denoted by the asterisk) ($P < 0.05$) between the values obtained for compound **5.4** and DMSO (negative control, used as solvent for the compound).....127

Figure 5.6. Efficacy of compound **5.4 (F6)** in an *in vivo* mouse skin wound infection model. Average log₁₀ reduction in MRSA USA300 CFU/mL in wounds of mice after five days (two doses per day) of treatment. A one-way ANOVA with post-hoc Dunnet's multiple comparisons found statistical significance (*, $P < 0.05$) between mice treated with fusidic acid and compound **5.4**, compared to mice receiving the vehicle (petroleum jelly) alone.129

Figure 5.7. Structural analogs of compound **5.4**, synthesized in our laboratory. **A.** Schematic representation of the synthesis of the analogs studied. Conditions used: (i)

MeLi, THF, -78 °C to rt, 14 h; (ii) EDC·HCl, DMAP, CH₂Cl₂, rt, 16 h; (iii) a) T3P, CH₂Cl₂, rt, 1h b) TEA, DMAP, rt, overnight; (iv) BOP reagent, DIPEA, DMF, rt, 16 h; **B**. Structures of analogs synthesized. Note: The starting material **S-I** existed as 4 :1 *cis* to *trans* form. The product obtained as **5.9** (*cis* : *trans* = 10 :1), **5.10** (*cis* : *trans* = 4 :1), **5.11** (*cis* : *trans* = 20 :1), **5.12** (*cis* : *trans* = 6 :1), **5.13** (*cis* : *trans* = 13 :1), **5.14** (*cis* : *trans* = 6:1); **5.15** (*cis* : *trans* = 5 :1), **5.16** (*cis* : *trans* = 6 :1), **5.17** (*cis* : *trans* = 4 :1), **5.18** (*cis* : *trans* = 6 :1), **5.19** (*cis* : *trans* = 6 :1), **5.20** (*cis* : *trans* = 4 :1).....131

Figure 5.8. Antibacterial activity of analogs of compound **5.4**. Compounds were tested at 16 µg/mL for their ability to inhibit *S. aureus* growth. The OD600 of compounds were normalized to that of the DMSO control.....133

Figure 5.9. Structure of compound **5.4 - cis** (*cis* : *trans* = 30 :1).....134

List of Abbreviations

2',3'-cGAMP	cyclic [G(2',5')pA(3',5')p]
3',3'-cGAMP	cyclic [G(3',5')pA(3',5')p]
agr	accessory gene regulator
AMP	adenosine monophosphate
ATP	adenosine triphosphate
CDC	Centers for Disease Control and Prevention
c-di-GMP	cyclic diguanylate monophosphate
cGAS	cyclic GMP-AMP synthase
DAC	diadenylate cyclase
DGC	diguanylate cyclase
DisA	DNA integrity scanning protein A
DUF147	Domain of unknown function 147
ELISA	enzyme-linked immunosorbent assay
ENPP1	ectonucleotide pyrophosphatase/phosphodiesterase 1
GdpP	GGDEF domain protein containing phosphodiesterase
GEMM-I	Genes for the Environment, Membranes, and Motility
GMP	guanosine monophosphate
GTP	guanosine triphosphate
HPLC	high pressure liquid chromatography
IFN	interferon
IRF3	interferon regulatory factor 3

LC-MS/MS	liquid chromatography with tandem mass spectrometry
MRSA	Methicillin-resistant <i>Staphylococcus aureus</i>
pApA	5'-phosphoadenylyl-(3'-5')-adenosine
PAS	Per-Arnt-Sim
PBP	penicillin binding protein
PDB	protein data bank
PDE	phosphodiesterase
pGpG	5'-phosphoguanylyl-(3'-5')-guanosine
ppGpp	guanosine tetraphosphate
PRR	pattern recognition receptor
RCK	regulator of conductance of K ⁺
RECON	Reductase controlling NF-κB
sar	staphylococcal accessory regulator
SCCmec	staphylococcal chromosomal cassette <i>mec</i>
STING	Stimulator of interferon genes
TBK1	TANK-binding kinase 1
TEAA	triethylammonium acetate
TLC	thin layer chromatography
VISA	vancomycin intermediate resistant <i>S. aureus</i>
VRE	vancomycin-resistant Enterococcus
VRSA	Vancomycin-resistant <i>S. aureus</i>

Chapter 1: Introduction

1.1 Background

The history of medicine, particularly the treatment of bacterial infections was transformed following the landmark discovery of penicillin and its subsequent introduction into the clinic in the 1940s. Infections which previously claimed lives became treatable. Notably, penicillin was tagged ‘the miracle drug’, as it helped save many lives during World War II.¹ This discovery paved way for the identification of many classes of antibiotics during what has been termed the ‘antibiotic era’.² However, bacteria rapidly developed resistance to penicillin and the many other antibiotics later developed, rendering them ineffective. In fact, resistance to almost all antibiotics has been observed in some bacterial isolates, leading to the term multidrug-resistant bacteria. Consequently, the US Centers for Disease Control and Prevention (CDC) has classified several bacterial pathogens including carbapenem-resistant *Klebsiella* spp, multidrug-resistant *Acinetobacter*, vancomycin-resistant *Enterococcus* and methicillin-resistant *Staphylococcus aureus* (MRSA) as significant threats to public health.³ Such infections are associated with enormous medical costs as well as increasing mortality rates.³

The evolution of resistance has been attributed to factors such as misuse of antibiotics in humans and in agriculture. It has also been proposed that bacteria possess resistance mechanisms, which are activated with antibiotic exposure.⁴ In a study by Wright and colleagues, bacteria strains sampled from a cave left untouched for over 4 million years were resistant to 14 structurally different antibiotics.⁴ Paradoxically,

there is a wide gap between the rate of antibiotic resistance and the development of new and effective antibiotics.⁵ The CDC cites the development of new antibiotics as one of the core actions to solving the antibiotics resistance crisis.³ Considering that most antibiotics target one of a few cellular processes, new antibiotics with novel targets may be required to mitigate resistance.

Bacteria pathogens utilize finely tuned molecular programs in response to specific host environments to successfully establish infections and persist. The interception of such regulatory programs has become the focus of novel approaches to prevent or treat infections. The role of nucleotide-based signaling molecules in bacterial physiology is well established.^{6, 7} For example, the intracellular concentration of the second messenger cyclic AMP signals the energy level of the cell.⁸ The discovery of cyclic di-GMP (c-di-GMP) changed the scenery of nucleotide-based signaling.⁹ Although discovered in 1980s, it did take close to two decades before the scientific community realized that cyclic dinucleotides are key signaling molecules.⁹ In Gram-negative bacteria, the role of c-di-GMP as a master regulator has been established.^{6, 7} In 2008, Hopfner and colleagues discovered the similar but distinct cyclic di-AMP in *Thermatoga matima*.¹⁰ Subsequently, the hybrid 3',3'-cGAMP was discovered to be essential during intestinal colonization of *V. cholerae*.¹¹ These bacterial second messenger are not produced by mammalian cells but could however be detected by mammalian immune systems.¹² In 2012, the eukaryotic cyclic dinucleotide 2',3'-cGAMP was discovered to be synthesized by mammalian cells with a role in inducing immune response.^{13, 14} In both bacteria and mammalian cells, cyclic dinucleotides have emerged as central regulatory molecules.

Considering the pivotal roles of cyclic dinucleotides, efforts have been directed towards understanding the molecular details of the signaling controlled by these second messengers and how to harness them in the development of various therapeutics.⁷ The succeeding sections briefly describe the signaling roles of c-di-GMP and cGAMP (2'3' and 3'3'). Cyclic di-AMP signaling is extensively (but not exhaustively) discussed.

1.1 Cyclic di-GMP signaling

Cyclic dimeric guanosine 3'5'-monophosphate is a ubiquitous second messenger predominant in Gram-negative bacteria but also present in some Gram-positive bacteria (see Figure 1.1 for structure).⁶ Cyclic di-GMP signaling has now been shown in several clinically relevant bacteria, including *Pseudomonas aeruginosa*, *Yersinia pestis*, *Vibrio cholerae*, *Salmonella typhimurium*, *Clostridium difficile* and *Escherichia coli*.⁶ Following the discovery of c-di-GMP in 1987,¹⁵ the relevance of the second messenger was not immediately apparent. It will take over two decades before researchers realized the central role of c-di-GMP.^{16, 17} The second messenger has now been established as a master regulator of various processes including virulence factor production, biofilm formation, cell cycle and motility.^{6, 18, 19}

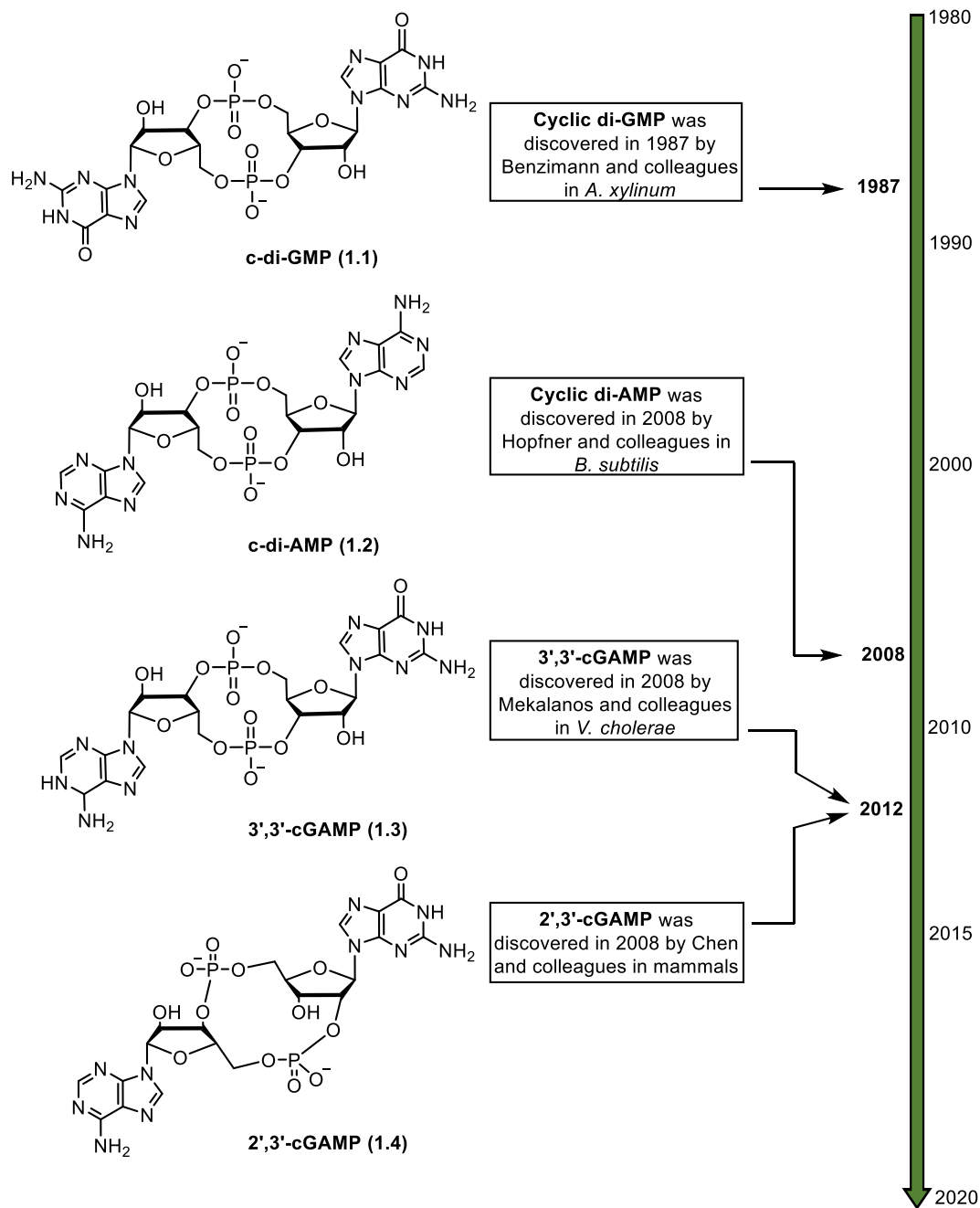


Figure 1.1. Structures of cyclic dinucleotides discovered in bacteria and mammals.

1.1.1 Synthesis of c-di-GMP: GGDEF domain proteins

The bacteria that utilize c-di-GMP signaling possess enzymes known as diguanylate cyclases (DGC) that catalyze the synthesis of the c-di-GMP from two molecules of GTP to first form the linear 5'pppGpG and then cyclizing it to c-di-GMP. DGCs contain the conserved GGDEF (Gly-Gly-Asp-Glu-Phe) or GGEEF (Gly-Gly-Glu-Glu-Phe) motifs essential for DGC activity. In 1995, Hecht and Newton characterized the first GGDEF domain-containing protein PleD, a response regulator in *Caulobacter crescentus*.²⁰ An inhibitory site (I-site) with the RxxD motif (where x is any amino acid) is often present on DGC enzymes.²¹ Binding of c-di-GMP to the I-site allosterically inhibits c-di-GMP synthesis.²¹ Other DGC examples are Wspr²² from *P. aeruginosa* as well as YdaM from *Escherichia coli*²³ and DgcK and DgcL from *Vibrio cholerae*.²⁴ More than one DGC may be present in a given cell, each contributing to increasing either the local or global c-di-GMP concentration.²⁵ *P. aeruginosa* has 33 GGDEF containing-proteins localized either in the cytoplasm or on the cytoplasmic membrane.^{6, 19, 26} It has been suggested that DGCs may directly interact with their targets to effect signaling. The I-site of the *P. fluorescens* DGC GcbC was found to be involved in interacting with the target protein LapD.²⁷

1.2.2 Degradation of c-di-GMP: EAL or HD-GYP domain proteins

Cyclic di-GMP specific phosphodiesterases (PDEs) degrade the signaling molecule.^{18, 19, 28} Two types of PDEs have been documented based on residues in their catalytic pocket. The EAL (Glu-Ala-Leu) domain-containing PDEs are able to hydrolyze c-di-GMP into the linear 5'-phosphoguanylyl-guanosine (5'-pGpG) although they have

been shown to degrade 5'-pGpG into GMP. Some examples of EAL domain-containing PDEs include YahA, YhjH and DosP from *E. coli*,²⁸⁻³⁰ RocR from *P. aeruginosa*.³¹ HD-GYP (His-Asp and Gly-Tyr-Pro) domain-containing PDEs are the second group c-di-GMP specific PDEs.³² These enzymes are capable of hydrolyzing c-di-GMP directly into two GMP molecules.³³ Examples of HD-GYP domain-containing PDEs include RpfG from *Xanthomonas campestris* pv. *Campestris*,³⁴ Bd1817 from *Bdellovibrio bacteriovorus*,³⁵ PmGH from *Persephonella marina*³⁶ and PA4781 from *Pseudomonas aeruginosa*.³⁷ Like with the DGCs, multiple c-di-GMP PDEs exist in a given strain.^{25, 26}

1.2.3 c-di-GMP receptors

The signal transduction function of c-di-GMP is exerted via binding to receptors and effector molecules including various enzymes, transcription factors and riboswitches. The first and perhaps most characterized c-di-GMP binding receptor, the PilZ domain was identified in 2006 and eventually found to regulate various phenotypes.³⁸ Binding of c-di-GMP to the PilZ domain of Alg44 regulates cellulose synthesis in *P. aeruginosa* whereas in *C. crescentus* the PilZ domain containing protein DgrA regulates motility.^{29, 39, 40} C-di-GMP binding regulates enzyme activity. The cell cycle kinase, CckA in *C. crescentus* switches enzymatic activity from kinase to phosphatase upon binding to c-di-GMP.^{41, 42} As earlier stated, the RxxD motifs of DGCs bind to c-di-GMP leading to inhibition of c-di-GMP synthesis. The RxxD motif of PopA regulates cell cycle progression in *C. crescentus* whilst PelD of *P. aeruginosa* is involved in exopolysaccharide production.^{43, 44} C-di-GMP can also bind

to degenerate GGDEF or EAL domain-containing proteins that lack DGC or PDE activity respectively. The *P. aeruginosa* EAL domain protein FimX, binds c-di-GMP and regulates twitching motility of the bacteria.^{45, 46} Thus far, two classes of c-di-GMP riboswitches have been documented, types I and II which are ubiquitous in bacteria. Binding of c-di-GMP to a riboswitch could either enhance or suppress gene expression.^{19, 47-50} Also, during intracellular infection of bacteria in mammalian immune cells, c-di-GMP has been shown to directly bind and activate STING (Stimulator of Interferon Genes, also known as MITA, MPYS and ERIS) leading to the induction of type I interferon response.⁵¹ STING is a transmembrane protein associated with the endoplasmic reticulum. STING regulates the transcription of several host defense genes that encode type I interferons and pro-inflammatory cytokines.^{52, 53} STING is also activated by binding to c-di-AMP and 2',3'-cGAMP (discussed below).

1.3 Cyclic di-AMP signaling

In a seminal paper published in 2008, Hopfner and colleagues showed that DNA Integrity Scanning protein A (DisA), a *Bacillus subtilis* protein that had been implicated in regulating sporulation by scanning for DNA damage, had a nucleotide-binding domain that binds to ATP to make a novel cyclic dinucleotide, cyclic dimeric adenosine 3'5'-monophosphate (c-di-AMP) (see Figure 1.1 for structure).¹⁰ The nucleotide-binding domain DUF147, was renamed diadenylate cyclase (DAC) domain.¹⁰ It turned out that the presence of DNA structures that would interfere with proper chromosome segregation such as Holliday junctions caused DisA to halt the

production of c-di-AMP.¹⁰ Hopfner also predicted that many bacteria harbored proteins that contained the DAC domain and hence c-di-AMP could have a wider role in bacteria, beyond reporting DNA strand breaks.¹⁰ The importance of Hopfner's discovery became apparent when soon thereafter many reports by other laboratories confirmed that c-di-AMP was indeed widely distributed across Firmicutes such as *Listeria monocytogenes* and *Staphylococcus aureus*, and in Actinobacteria like *Mycobacterium tuberculosis* and *M. smegmatis*.^{33, 54-58} Cyclic di-AMP signaling has been identified in some Gram-negative bacteria such as *Chlamydia trachomatis*.^{58, 59} C-di-AMP has now been shown to control a dazzling array of processes in different bacteria, including cell wall formation,⁶⁰ cell size regulation,⁶¹ biofilm formation,^{61, 62} heat stress,⁶³ virulence,⁶⁴ ion transport,⁶⁵ resistance to acid⁶⁶ and others.^{56, 67}

1.3.1 Cellular metabolism of c-di-AMP

1.3.1.1 Cyclic di-AMP synthases and phosphodiesterases

The intracellular concentration of c-di-AMP is under the control of diadenylate cyclases (DACs) and phosphodiesterases (PDEs).⁶⁸ The first DAC domain containing protein to be described was DisA. The crystal structure of DisA from *T. maritima* was published by Hopfner and colleagues, an effort that serendipitously led to the discovery of c-di-AMP.¹⁰ The monomeric unit of DisA contains three distinct domains; a globular nucleotide-binding domain (DAC domain, DisA_N Pfam PF02457), an alpha helical linker domain and a terminal DNA binding domain. A dimer of tetramers forms an octameric dumbbell-shaped complex with the DAC domains at the center.¹⁰ With this architecture each opposing monomer binds an ATP

unit at the DAC domain and the two bound ATP molecules are condensed into c-di-AMP.¹⁰ Hopfner and colleagues showed that the DAC activity of DisA was inhibited by DNA structures with three- and four-way junctions but not single-stranded or double stranded DNA.¹⁰ The DisA class of DAC enzymes is found mostly in spore-forming bacteria like *B. subtilis* where it checks the DNA integrity during sporulation.^{69, 70}

Before entry into sporulation, DisA forms a focus which non-specifically binds to DNA and moves rapidly across the cell with an average focus speed of 0.22 $\mu\text{m}/\text{sec}$ scanning for chromosomal damage.^{69, 70} Treatment of cells with DNA-damaging agents like mitomycin C or nalidixic acid, resulted in significantly decreased number of spores in DisA mutant compared to wildtype *B. subtilis*.^{69, 70} The DisA foci was observed to have stalled in cells treated with DNA-damaging agents with a corresponding decrease in intracellular c-di-AMP levels.^{69, 70} Interestingly, exogenous addition of c-di-AMP to sporulating cells could recover sporulation.⁶⁹ A D77N mutant DisA, which lacks DAC activity, prevents the formation of the DisA foci. Hence DAC activity is essential for DisA foci assembly and in effect DNA integrity scanning.⁶⁹ The lack of DAC activity in the presence of DNA damage, hinders the activation of Spo0A, a master regulator of sporulation in *B. subtilis*, leading to delayed entry into sporulation.⁷⁰ Campos *et al.* also noted a role for DisA during germination and outgrowth of *B. subtilis* spores.⁷¹ Spores lacking the AP endonucleases Nfo and Exo had slow germination and outgrowth rates.⁷¹ However, inactivating DisA in such cells restored germination and outgrowth to rates similar to wildtype, implying that DisA serves as a checkpoint for spore germination to

vegetative growth transition.⁷¹ In exponentially growing *B. subtilis* cells however, DisA foci is not stalled in the presence of DNA-damaging agents.⁷² Homologs of DisA have been found in *M. tuberculosis* (MtDisA)⁷³ and *M. smegmatis* (MsDisA)⁷⁴ as well as *T. maritima*,¹⁰ which are all non-sporulating cells, implying that it has other functions beyond enforcing DNA integrity during sporulation and spore germination. The DAC activity of DisA is modulated by RadA (Radiation-sensitive gene A) protein which is encoded by *radA* gene that forms an operon with *disA*. RadA is a DNA repair protein required for DNA recombination.⁷⁵ Burghout *et al.* revealed that mutating the *radA* gene rendered *S. pneumoniae* sensitive to DNA-damaging agents.⁷⁵ A similar observation was made in *B. subtilis*.⁷⁶ RadA was found to directly interact with DisA with a resultant inhibition DAC activity in many bacteria.^{72, 74} A recent publication by Gándara *et al.* revealed that the DisA foci predominantly moved on the nucleoids whilst RadA moved in spaces without DNA.⁷² The observation that RadA and DisA co-localized only transiently on sites on the nucleoid enforced the assertion that DisA recruits RadA.⁷² Additionally, the presence of the Holliday junction (HJ) resolvase RecU and the branch migration translocase RecG is critical to the formation and dynamic movement of the DisA foci.⁷² An increased amount of HJ intermediates is present in $\Delta recU$ and $\Delta recG$ cells. In such cells, a decrease in dynamic movement of DisA foci was observed.⁷² Consequently, RecU and RecG may interact with DisA in repairing recombination intermediates. However, the role of the concentration of c-di-AMP in these processes remains to be clearly elucidated.⁷⁷

Another class of DAC enzymes is the CdaA (also called DacA) which is found in *B. subtilis*^{78, 79} and the human pathogens *S. aureus*,⁸⁰ *L. monocytogenes*,⁸¹ *Streptococcus*

pyogenes,⁸² *S. pneumoniae*⁵⁵ and *Chlamydia trachomatis*.⁵⁹ CdaA is a membrane-bound protein (Figure 1.2) with three transmembrane (TM) domains and a cytosolic DAC domain.^{12, 83} It interacts with the membrane-integrated regulator protein CdaR.⁸³ The *B. subtilis* CdaR was shown to enhance the DAC activity of CdaA.⁷⁸ However, in *L. monocytogenes*, the DAC activity of CdaA is inhibited by interaction with CdaR.⁸⁴ CdaR did not affect the synthesis and membrane-localization of CdaA⁸⁴ and given that it is also not present in some CdaA-containing bacteria⁷⁷ its function may not be universal. The cytosolic portion of CdaA also interacts with the glucosamine-6-phosphate mutase GlmM.^{77, 83} GlmM is an essential enzyme which synthesizes glucosamine-1-phosphate, an intermediate in the synthesis of the peptidoglycan precursor UDP-N-acetylglucosamine (UDP-NAG).⁷⁷ In *Lactococcus lactis*, GlmM was found to negatively regulate the activity of CdaA when lower c-di-AMP levels were observed in mutant GlmM cells compared to wildtype.⁸⁵ Additionally, high levels of UDP-NAG were observed in *gdpP* mutant *L. lactis* strains (signifying high c-di-AMP levels) compared to wildtype, suggesting a role for c-di-AMP in peptidoglycan homeostasis.⁸⁵ In pathogenic bacteria *S. aureus*, *L. monocytogenes* and *S. pneumoniae*, the DAC gene has been said to be essential for bacterial survival.^{57, 86, 87} This is because it was not possible to generate mutant strains without the DAC gene. The central role of c-di-AMP signaling in these pathogens and the essentiality of the DAC coupled with the knowledge that c-di-AMP signaling is not present in human cells, it has been suggested that this second messenger signaling is a potential antibiotic target.¹²

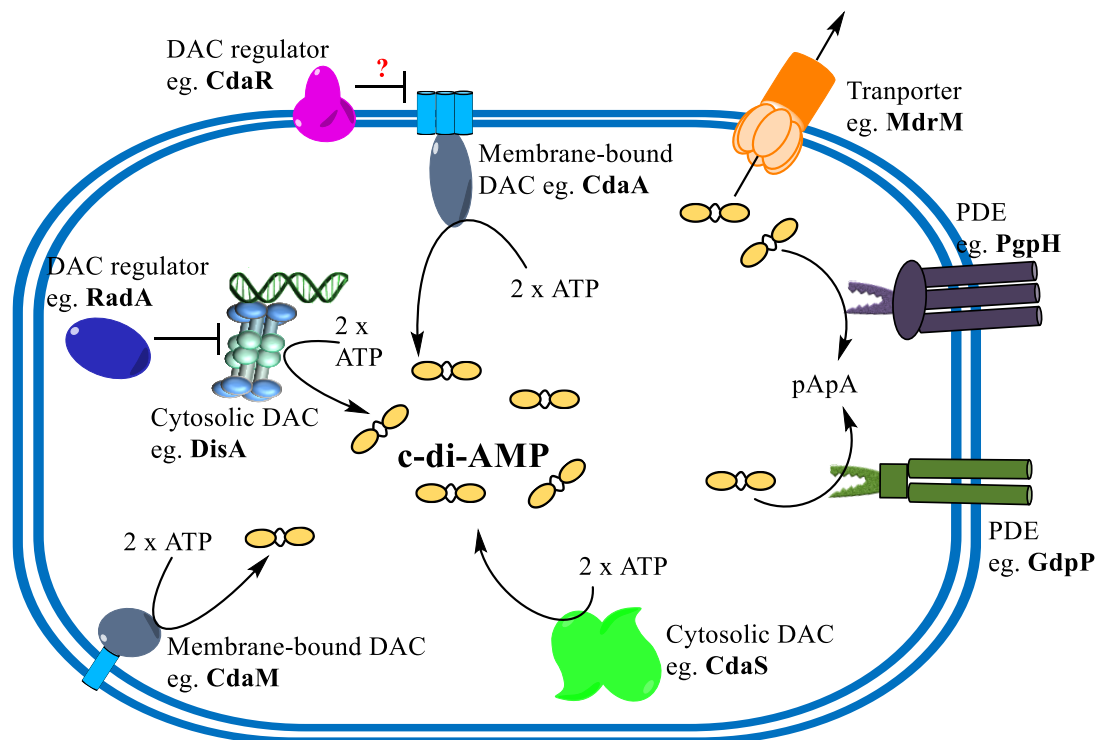


Figure 1.2. Regulation of intracellular pool of c-di-AMP. The membrane-integrated DACs CdaA (found in *B. subtilis*, *S. aureus* etc) and CdaM (found in *Mycoplasma pneumoniae*) as well as cytosolic DACs DisA (found in *B. subtilis*, *M. tuberculosis*, *T. maritima* etc) and CdaS (found in *B. subtilis*, *Clostridium* spp) synthesis c-di-AMP while the membrane-bound PDEs, PgpH (found in *L. monocytogenes*) and GdpP (found in *L. monocytogenes*, *S. aureus*, *B. subtilis* etc) degrade the signal. In some bacteria, like *L. monocytogenes*, transporters are involved in decreasing the intracellular c-di-AMP concentration by secreting the second messenger into the extracellular milieu. Reproduced with permission from ⁷ Published by The Royal Society of Chemistry.

The last two classes are the CdaS and CdaM DAC proteins. The CdaS DAC enzyme is required for spore germination and has been found in *B. subtilis* and *Clostridium spp.*^{56, 88} The CdaS protein consists of an N-terminal domain which possesses autoinhibitory activity over the C-terminal DAC domain.⁸⁸ Deletion of the N-terminal domain resulted in enhanced DAC activity.⁸⁸ Recently, Blötz *et al.* also demonstrated that the DAC enzyme, CdaM was present in *Mycoplasma pneumoniae*.⁸⁹ The DAC domain of CdaM shares similarity with that of CdaS but CdaM has a transmembrane (TM) domain with an architecture different from the three TM domains found in CdaA.⁸⁹

By synthesizing c-di-AMP, DACs increase the intracellular concentration of the second messenger. Unlike in c-di-GMP signaling where bacteria could have multiple DGCs most bacteria that utilize c-di-AMP signaling have single DAC encoding genes. Multiple DAC enzymes are found in *B. subtilis* (DisA, CdaA and CdaS)⁷⁹ and *Clostridium spp* (DisA, CdaS).⁵⁶ However, at least one DAC has to be present for cell survival.⁷⁹

Cyclic dinucleotide PDEs carry out the degradation of c-di-AMP (Figure 1.2).⁹⁰ It has been shown that a catalytic DHH/DHHA1 domain is required for c-di-AMP specific PDE activity.⁶⁶ One of the earliest identified examples was YybT (renamed GdpP) from *B. subtilis*.⁶⁶ YybT is anchored to the membrane by a transmembrane domain. The cytosolic portion contains a Per-Arnt-Sim (PAS) sensory domain, a modified GGDEF domain with ATPase activity and a DHH/DHHA1 domain with c-di-AMP PDE activity.⁶⁶ Degradation may yield either the linear pApA or AMP.^{66, 91} Some reported examples of DHH/DHHA1 domain-containing PDEs are PdeA from *L.*

monocytogenes,⁹² GdpP from *Staphylococcus aureus*,⁶¹ and Pde1 and Pde2 from *S. pneumoniae*.⁹³ Aside from the DHH/DHHA1 domain-containing PDEs, a second family was discovered by Woodward and coworkers in *L. monocytogenes*. This family of c-di-AMP PDEs contained a catalytic Asp-His (HD) domain.⁹¹ The PDE, PgpH, was found to be dominant during broth growth of *L. monocytogenes* whilst the DHH/DHHA1 domain-containing PdeA effected its PDE activity mostly during intracellular infections.⁹¹ Suppressor mutations that lead to the inactivation of c-di-AMP PDEs have been noted to result in resistance to β -lactam resistance. In *B. subtilis*, resistance to cefuroxime and other β -lactams is conferred by the sigma factor σ^M . Resistance to cefuroxime in σ^M mutants was found to be restored by mutations in the PDE *gdpP*.⁷⁹ In methicillin-resistant *S. aureus* strains, disruption of *gdpP* permits growth of strains lacking lipoteichoic acid, a component of the Gram-positive bacterial cell wall.⁶¹

An additional mechanism of regulating the intracellular concentration of c-di-AMP is seen in bacterial pathogens like in *L. monocytogenes* and *M. tuberculosis*.⁶⁰ These bacteria possess multidrug-resistant (Mdr) transporters that secrete endogenous c-di-AMP into the extracellular milieu. In *L. monocytogenes*, MdrM and MdrT were shown to be involved in secreting c-di-AMP into the host cytoplasm during intracellular infection with a resultant increase in type I interferon response.^{57, 94}

1.3.1.2 Cellular c-di-AMP concentration and bacterial physiology

As stated above, DACs and PDEs work in concert to regulate the global cellular concentration of c-di-AMP.⁶ The basal concentration of c-di-AMP in *S. aureus* was

found to be 2.1 μM , which increased to 8 μM during stationary phase.^{61, 87} In ΔgdpP strains, c-di-AMP concentrations could get as high as 31.5 μM to 54.93 μM .^{61, 87} In *B. subtilis*, the concentration is 1.7 μM during vegetative growth and could get to 5.1 μM during sporulation.⁶⁹ The increased c-di-AMP concentration in *B. subtilis* during sporulation was attributed to the DAC activity of DisA because in ΔdisA sporulating cells, the elevation in c-di-AMP was lower.⁶⁹ To better understand the role c-di-AMP signaling plays in bacterial physiology and pathogenesis, researchers have looked at the effects of cellular concentration of c-di-AMP in various bacteria. In *B. subtilis*, deletion of YybT, which signifies a condition of high cellular c-di-AMP level led to mutant cells which were resistant to acid stress.⁶⁶ Also, the spores of the mutant cells were resistant to DNA-damaging agents.⁶⁶ High c-di-AMP concentration as a result of the overexpression of MsDisA in *M. smegmatis* resulted in minute colonies.⁹⁵ In *L. monocytogenes*, the gene *lmo2120* (which they renamed *dacA*) was found to encode a DAC domain protein that produced c-di-AMP, which could be secreted into the environment.⁵⁷ When bone marrow-derived macrophages were infected with the intracellular pathogen, the secreted c-di-AMP induced a host cytosolic surveillance pathway, which was dependent on the Stimulator of Interferon Genes (STING).⁶⁰ The group also demonstrated that overexpression of the PDE PdeA (signifying a condition of low cellular c-di-AMP level) resulted in reduced growth rate and virulence and an increased susceptibility of *L. monocytogenes* to peptidoglycan-targeting antibiotics.⁹² A similar observation was made in *S. aureus* where the deletion of the PDE GdpP (depicting a condition of high cellular c-di-AMP level) resulted in increased peptidoglycan cross-linking and resistance to cell wall targeting antibiotics, implying

a role for c-di-AMP in cell size and envelope stress.⁶¹ Although much work has been done through genetic manipulations to unravel the intricacies of c-di-AMP concentration in bacteria, our understanding of how bacteria regulate the accumulation of c-di-AMP is still minimal.

1.3.1.3 Bacterial receptor and effector molecules of c-di-AMP

To transduce a signal, a second messenger must interact with cellular targets. Following the identification of c-di-AMP, there was a surge in reports that sought to demonstrate c-di-AMP signaling in different bacteria and to identify the key players. The identification of effector proteins and riboswitches that interact with the second messenger was central to this process.⁶⁸ In 2013, He and colleagues reported the first c-di-AMP receptor regulator DarR, a TetR family regulator in *M. smegmatis*.⁹⁶ Binding of DarR to c-di-AMP, a process characterized by a K_d of $2.3 \pm 0.5 \mu\text{M}$, was observed to enhance the DNA binding ability of the receptor.⁹⁶ When bound to its target DNA, DarR was found to repress the expression of its target genes in *M. smegmatis*.⁹⁶ Cyclic di-AMP has been shown to interact with several RCK_C (Regulator of Conductance of K⁺) domain-containing protein that function to regulation potassium ion homeostasis in bacteria. In *S. aureus*, KtrA the membrane-associated component of the K⁺ transporter KtrA-KtrB, is required for *S. aureus* survival under low-potassium conditions.⁸⁰ Cyclic di-AMP binds to KtrA at its C terminus resulting in the inhibition of K⁺ uptake in *S. aureus*.⁸⁰ A similar c-di-AMP binding protein CabP, is required for K⁺ uptake and growth under low-potassium conditions in *S. pneumoniae*.⁹⁷ CabP interacts with the membrane-integrated

component SPD_0076. Like in the case of KtrA-KtrB in *S. aureus*, binding of c-di-AMP to CabP inhibits potassium uptake in *S. pneumoniae*.⁸⁰

CpaA, a cation/proton anti-porter in *S. aureus* also binds c-di-AMP at its RCK_C domain. This protein functions to exchange intracellular proton with potassium or sodium ions.⁸⁰ Contrary to the effect of c-di-AMP binding to the earlier described potassium transporters, binding of c-di-AMP to CpaA was found to enhance the antiporter activity of CpaA.⁹⁸ Cyclic di-AMP also binds to the histidine kinase KdpD of the two-component system KdpD-KdpE in *S. aureus*.^{80, 99} It has been shown that KdpD-KdpE regulates K⁺ homeostasis in bacteria by controlling the expression of the Kdp-ATPase high-affinity potassium pump required under low salt conditions.¹⁰⁰ Binding of c-di-AMP to the histidine kinase KdpD leads to the downregulation of the expression of Kdp and decreased survival of *S. aureus* under low potassium conditions.⁹⁹

In *L. monocytogenes*, high c-di-AMP levels have been shown to diminish the uptake of osmolytes such as carnitine.¹⁰¹ The binding of the carnitine importer OpuC in *L. monocytogenes* to c-di-AMP decreases its carnitine import activity.¹⁰¹ This observation was also made with the carnitine uptake system in *S. aureus* where the OpuC transporter directly binds c-di-AMP.¹⁰² In $\Delta gdpP$ strains (signifying high cellular c-di-AMP concentration), carnitine accumulation was observed to be decreased compared to wildtype.¹⁰² Hence in both *L. monocytogenes* and *S. aureus*, c-di-AMP signaling inhibits osmolyte transport.

A fine balance of ions and osmolytes are required by cells to maintain membrane integrity. Cyclic di-AMP inhibits ion and osmolyte transport which will lead to

detrimental effects on cell integrity. The changes in cell size, cell wall formation, β -lactam resistance among others associated with c-di-AMP signaling could stem from its effect on ion and osmolyte transport. This is an emerging theme for the central role of c-di-AMP signaling in bacteria.¹⁰³

1.3.1.4 Mammalian receptors of c-di-AMP: Host-pathogen interactions

The innate immune system has evolved mechanisms to recognize nonself molecules. These mechanisms, known as pattern recognition receptors (PRRs) are localized either on the cell surface or in the intracellular milieu. Extracellular receptors such as Toll-like receptors identify conserved patterns on pathogens during extracellular infection whilst DNA-sensing mechanisms are in place to recognize intracellular infections, particularly nucleic acids.^{104, 105} Bacteria that utilize cyclic di-AMP signaling release the second messenger into extracellular milieu either *via* the use of non-specific transporters or *via* cell lysis.^{57, 60, 94} Given that c-di-AMP is not made by mammalian cells, it is recognized as a foreign agent and hence elicits immune response *via* cytosolic DNA-sensing mechanisms.⁵⁸ Woodward *et al.* first showed that c-di-AMP secreted by *L. monocytogenes* induces type I interferon response.⁵⁷ It was subsequently determined that bacterial cyclic dinucleotides directly bind to and activate STING.⁵¹ Further research revealed that cytosolic PRR DDX41, an RNA helicase binds to c-di-AMP.^{106, 107} It turns out that STING has lower affinity for c-di-AMP compared to the mammalian 2'5' cGAMP and that binding of DDX41 to c-di-AMP leads to a STING-DDX41 complex that enhances the affinity of STING for c-di-AMP. Recently, Woodward and colleagues identified another c-di-AMP sensor,

the mouse oxidoreductase RECON.¹⁰⁸ Compared to STING, RECON has higher c-di-AMP affinity and does not bind c-di-GMP.¹⁰⁸ Binding of RECON to c-di-AMP relieves its inhibition on NF- κ B thereby increasing proinflammatory response leading to decreased bacterial survival.¹⁰⁸

To survive attack by mammalian cells, bacteria first need to regulate the concentration of c-di-AMP. Some bacteria encode cell surface PDEs, known as ectonucleotidases, which degrade c-di-AMP secreted into the cytosol during infection to decrease the STING-dependent type I interferon response.^{109, 110} In *Streptococcus agalactiae* (Group B Streptococcus), CdnP on the cell surface hydrolyzes extracellular c-di-AMP resulting in decreased IFN- β .¹⁰⁹ Recently, Sintim, Bishai and colleagues demonstrated that aside decreasing c-di-AMP concentrations, the *M. tuberculosis* PDE CdnP can degrade the host response by hydrolyzing 2'5' cGAMP.¹¹⁰ This might be an additional virulence strategy employed by *M. tuberculosis* and other bacteria to survive in immune cells.

1.3.2 Inhibiting c-di-AMP signaling

Undoubtedly, c-di-AMP is essential in many Gram-positive bacteria including the human pathogens *L. monocytogenes*, *S. pneumoniae* and *S. aureus*.^{57, 85, 86} As described above, most studies into the molecular mechanisms behind c-di-AMP signaling has involved genetic manipulation of the bacteria by deletion mutations or overexpression of c-di-AMP DACs and PDEs. Indeed, these molecular biology approaches have improved our understanding of c-di-AMP signaling. Unlike these approaches, the use of small molecule probes to investigate c-di-AMP is yet to gain

the same level of attention. Consequently, there is a dearth of inhibitors against c-di-AMP synthesis and degradation.⁷ Aside the fact that the understanding of c-di-AMP is still increasing, the limited number of inhibitors could be due to the paucity of assays for screening large libraries. High performance liquid chromatography (HPLC) and liquid chromatography-mass spectrometry (LC-MS) approaches have been used to quantify c-di-AMP levels and to determine enzyme activity, but these are not amenable to high-throughput screening.^{61, 68, 72, 77} Using HPLC analysis, Rao *et al.* identified the alarmone guanosine tetraphosphate (ppGpp) as an inhibitor of the PDE activity of YybT.⁶⁶ Detection and quantification of c-di-AMP using an ELISA approach was documented by Bai and colleagues in 2014.¹¹⁰ This assay was useful in determining c-di-AMP concentrations in bacterial extracts.¹¹⁰ Although this assay could be used to determine the effect of compounds on the intracellular concentration of c-di-AMP, a direct measure of enzyme activity may not be possible. Hopfner and colleagues used the colorimetric phosphate quantification assay (BIOMOL Green reagent, Enzo, Farmingdale, NY, USA) to determine cordycepin triphosphate (3'-deoxyATP) as an inhibitor of *Thermotoga maritima* DisA (TmaDisA) with an IC₅₀ of 3 mM at 26 nM TmaDisA.¹¹¹ In 2014, Sintim and colleagues developed the coralyne assay for the detection of c-di-AMP levels.¹¹² In line with the observation that coralyne could bind to polyadenosine,^{113, 114} coralyne was found to complex with c-di-AMP with a resultant change in fluorescence which depended on the c-di-AMP concentration.¹¹² The coralyne assay led to the identification of the first DAC inhibitor bromophenol thiohydantoin, from screening a 1,000 compound library.¹¹⁵

Following this initial success, I have identified several DAC inhibitors.^{7, 117-119} Of note, some of these inhibitors possess activity against Gram-positive bacteria. These findings are discussed in the succeeding chapters of this document.

1.4 Cyclic GMP-AMP signaling

1.4.1 Bacterial cyclic GMP-AMP (3',3'-cGAMP)

Davies *et al.* discovered the novel hybrid cyclic dinucleotide, cyclic GMP-AMP (3',3'-cGAMP) (see Figure 1.1 for structure) while exploring the contribution of the *Vibrio* seventh pandemic island-1 (VSP-1) to pathogenesis in *V. cholerae*.¹¹ Cyclic GMP-AMP (3',3') was observed to be synthesized by the novel cyclase DncV, a member of the nucleotidyltransferase superfamily which is encoded by the *dncV* gene located on the VSP-1.¹¹ A conserved G[G/S]X₉-13DX[D/E] active site motif in DncV was observed to be required for catalytic activity. DncV was found to repress chemotaxis.¹¹ Hence, in an infant mouse model, deletion of *dncv* resulted in decreased intestinal colonization.¹¹ Hydrolysis of 3',3'-cGAMP has been found to be carried out by HD-GYP domain proteins V-cGAP1, V-cGAP2 and V-cGAP.¹²⁰ Apart from V-cGAP1 which can degrade 3',3'-cGAMP to 5'-ApG, the other two PDEs hydrolyze the cyclic dinucleotide to 5'-pApG.¹²⁰ Although their genome does not encode DncV, 3',3'-cGAMP was found in the extracts of *Geobacter sulfurreducens*¹²¹ implying that the signaling molecule was present in that bacteria. GEMM-Ib, a GEMM-I class riboswitch (GEMM-Ib, Genes for the Environment, Membranes, and Motility), was found to be a receptor for 3',3'-cGAMP in *Geobacter sulfurreducens*.¹²¹

1.4.2 Mammalian cyclic GMP-AMP (3',3'-cGAMP)

Thus far, the only cyclic dinucleotide of mammalian origin is 2',3'-cGAMP (see Figure 1.1 for structure) which was discovered in 2012.¹³ This second messenger contains a unique phosphodiester linkage between the 2'-OH of GMP and 5'-phosphate of AMP which makes it distinct from 3',3'-cGAMP and other bacterial cyclic dinucleotides.¹²² Synthesis of 2',3'-cGAMP from ATP and GTP is mediated by cyclic GMP-AMP synthase (cGAS). It has become apparent that cGAS is involved in sensing cytosolic DNA and its 2',3'-cGAMP activity is dependent on the presence of DNA.^{123, 124} The second messenger then binds to STING leading to the induction of type I interferon response.^{123, 124} Degradation of 2',3'-cGAMP is attributed to PDE function of ectonucleotide pyrophosphatase/phosphodiesterase 1 (ENPP1) which hydrolyzes the second messenger into AMP and GMP.¹²⁵ Sintim, Bishai and colleagues demonstrated that the *M. tuberculosis* c-di-AMP PDE, CdnP could hydrolyze 2',3'-cGAMP, suggesting a function for the bacterial PDE in interfering with host immune response.¹⁰⁹

1.5 The antibiotics resistance crisis

Humans have been at the end of several disease outbreaks throughout history. A standout example is the so-called “Black death” plague which laid waste to Europe in the mid-thirteenth century.¹²⁶ It was discovered that the bacterium *Yersinia pestis* was the cause of the plague.¹²⁶ The discovery of antibiotics increased the chances of successfully treating deadly bacterial infections. However, antibiotic exposure is concomitant with the emergence of resistance in bacteria. Multidrug-resistant bacteria

are continuously isolated and present an enormous public health treat.¹²⁷ Infections caused by the likes of methicillin-resistant *S. aureus* (MRSA) and vancomycin-resistant Enterococcus (VRE) result in high mortality rates as well as significant financial burden on healthcare.³

1.5.1 Resistance mechanisms

Various mechanisms have been described to be employed by bacteria that are antibiotic resistant. Mechanisms to modify the antibiotic are utilized by bacteria to inactivate antibiotics.^{128, 129} Bacteria achieve this by encoding enzymes that functionalize groups on the antibiotic. For example, the acetylation of chloramphenicol or the phosphorylation of aminoglycosides introduces bulk groups which reduce the ability of the targets to interact with the antibiotics.¹²⁹ Another example is the production of hydrolytic enzymes like in the case of β -lactam antibiotics such as penicillins, cephalosporins and carbapenem. Bacteria encode β -lactamases which hydrolyze β -lactam antibiotics.¹²⁸

Increased efflux of antibiotics by efflux pumps limit the tendency for antibiotics to accumulate in bacteria.¹²⁹ Hence, antibiotics with intracellular targets such as those involved in DNA or protein synthesis inhibition are more susceptible to this mechanism. This is particularly prominent in Gram-negative bacteria. Efflux pumps specific for antibiotic classes as well as multidrug pumps have been described.¹³⁰ In *E. coli*, the AcrAB-TolC efflux system, which is one of the well characterized efflux pumps, is responsible for the expulsion of a wide variety of chemical scaffolds from the cytoplasm to the extracellular milieu.^{130, 131}

Also, bacteria have been observed to modify the antibiotic targets. Vancomycin binds tightly to the D-alanyl-D-alanine (D-Ala-D-Ala) dipeptide of the pentapeptide component of the Lipid II molecule of the nascent peptidoglycan.¹³² In vancomycin resistance, the terminal alanine residue is mutated to a lactate (D-Lac) to give D-Ala-D-Lac which has a significantly decreased binding affinity for vancomycin.¹³³ A similar situation is observed with methicillin resistance in *S. aureus*. Methicillin, which is resistant to β -lactamases, acts by binding to the transpeptidase, penicillin binding protein 2 (PBP 2) involved in peptidoglycan synthesis.¹²⁹ *S. aureus* encodes a modified PBP 2 known as PBP 2a which has lower affinity for methicillin. The *mecA* gene, which encode PBP 2a is located on the staphylococcal chromosomal cassette *mec* (SCC*mec*), a mobile genetic element.¹²⁹

Beyond these mechanistic modes of antibiotic resistance, it has been suggested that antibiotic mechanisms already exist given that antibiotic exposure predates the “antibiotic era”.¹³⁴ A wide variety of antibiotics are produced by bacteria for defense against other bacteria in the environment. Hence, to survive attack, bacteria must evolve resistance mechanisms. Consequently, ‘intrinsic’ resistance to antibiotics may be present in bacteria even before the discovery of the antibacterial agent.¹²⁹ There is also the human contribution to antibiotic crisis which mostly borders on misuse of antibiotics.

1.5.2 Approaches to reduce the rate of antibiotic resistance

It is almost certain that at some point bacteria will develop resistance to any new antibiotic deployed. Several strategies have been used to limit or eradicate antibiotic resistance.¹²⁷

First, efforts to develop antibacterial agents with novel chemical scaffolds should be facilitated.¹²⁷ Several antibiotic classes, like the β -lactams, have different generations which are only derivatives of the first class. It only takes a few years for bacteria to develop resistance to derivatized antibiotics, since such resistance mechanisms will already exist in bacteria. For example, modified versions of penicillin like methicillin, amoxicillin and ampicillin have all become ineffective over a relatively short period of time. Consequently, a push towards identification of small molecule antibacterial agents with limited resemblance to the natural product antibiotics should be encouraged.

Alongside finding novel antibiotics, the identification of novel targets will be paramount to a successful reducing antibiotic resistance.¹²⁹ Majority of existing antibiotics target one of a few cellular processes including cell wall synthesis, DNA and protein synthesis and membrane integrity.¹³⁵ Some prospective antibiotics targets include quorum sensing, virulence factors, cyclic dinucleotide signaling, two component systems^{7, 134} among others.

Another proven strategy is by ‘resurrecting’ current ineffective antibiotics by combining them with small molecules.¹³⁶ β -lactamase inhibitors such as sulbactam, clavulanic acid and tazobactam have been used to enhance the efficacy of β -lactams sensitive to such as amoxicillin and ampicillin. Antibiotic-adjuvant combinations introduce secondary targets with a potential to decrease the tendency for bacteria to develop resistance.¹³⁶ Several research groups including the Sintim group have interests in this approach.^{119, 136, 137} In Chapter 3, I will discuss hydroxybenzylidene-indolines which were identified as DAC inhibitors and were found to possess

antibiotic potentiation activity. Efforts towards understanding the mechanism of action of GW5074 and related compounds will be discussed in Chapter 4. Additionally, the identification of a novel antibacterial agent is discussed in Chapter 5.

Chapter 2: Identification suramin and theaflavin-3,3'-digallate as inhibitors of c-di-AMP synthase, DisA.

1.2 Potent inhibition of cyclic diadenylate monophosphate cyclase by the antiparasitic drug, suramin.

This section (2.1) was originally published as: Opoku-Temeng, C. and Sintim, H.O. "Potent inhibition of cyclic diadenylate monophosphate cyclase by the antiparasitic drug, suramin." *Chem. Commun.*, 2016, 52, 3754

1.2.1 Introduction

Cyclic diadenylate monophosphate (c-di-AMP) is an important second messenger found in Gram-positive Firmicutes and Actinobacteria.¹⁻³ It is synthesized from two molecules of adenosine triphosphate (ATP) by diadenylate cyclases, DAC (Figure 2.1), and degraded by c-di-AMP-specific phosphodiesterases (PDE).⁴⁻⁷ C-di-AMP has been shown to regulate important processes in bacteria, such as virulence,⁸ cell wall formation,^{8, 9} cell size,¹⁰ ion transport¹¹ among others. For some Gram-positive bacteria, such as *Bacillus subtilis* and *Listeria monocytogenes*, it has been demonstrated that low intracellular levels of c-di-AMP increased the sensitivity of the cells to β -lactam antibiotic treatment; an effect attributed to defective peptidoglycan synthesis.^{12, 13} Attempts to delete DAC from human pathogens *L. monocytogenes*¹³ and *Streptococcus pneumoniae*,¹⁴ failed and this was probably due to the essentiality of DAC for maintaining the integrity of the peptidoglycan.

Considering that most antibiotics target peptidoglycan synthesis, there is an obvious interest in discovering inhibitors of DAC enzymes.¹⁵⁻¹⁷

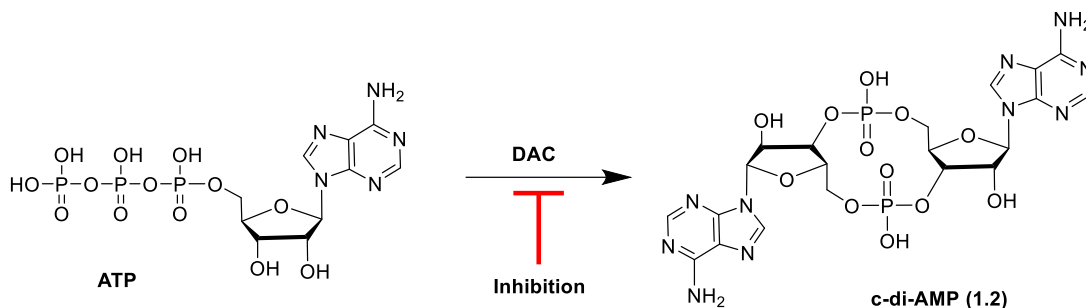


Figure 2.1. Schematic of the synthesis of c-di-AMP by DisA from ATP. A DAC inhibitor will hinder the synthesis of c-di-AMP.¹⁵

Motivated by the potential of DAC inhibitors as antibacterial targets we developed an interesting fluorescent assay for monitoring c-di-AMP synthesis, using readily available coralyne fluorophore.¹⁸ Using this assay, we discovered the first small molecule inhibitor of a DAC (DisA), bromophenol thiohydantoin (or bromophenol- TH).¹⁵ Bromophenol-TH is however a weak inhibitor of DisA (IC₅₀ of 56 mM at 5 mM DisA)¹⁵ and attempts to improve its potency *via* modifications were unfruitful.¹⁷ Recently, Müller *et al.* showed that cordycepin triphosphate (3'-deoxyATP) was an inhibitor of *Thermotoga maritima* DisA (TmaDisA) with an IC₅₀ of 3 mM at 26 nM TmaDisA.¹⁶

In an effort to identify more potent and non-nucleotide-based inhibitors of c-di-AMP synthesis, we employed the coralyne assay to screen a library of 2000 known drugs against DisA. This effort led to the identification of suramin (Figure 2.2), a drug used to treat parasitic infections, as a potent inhibitor of DisA.

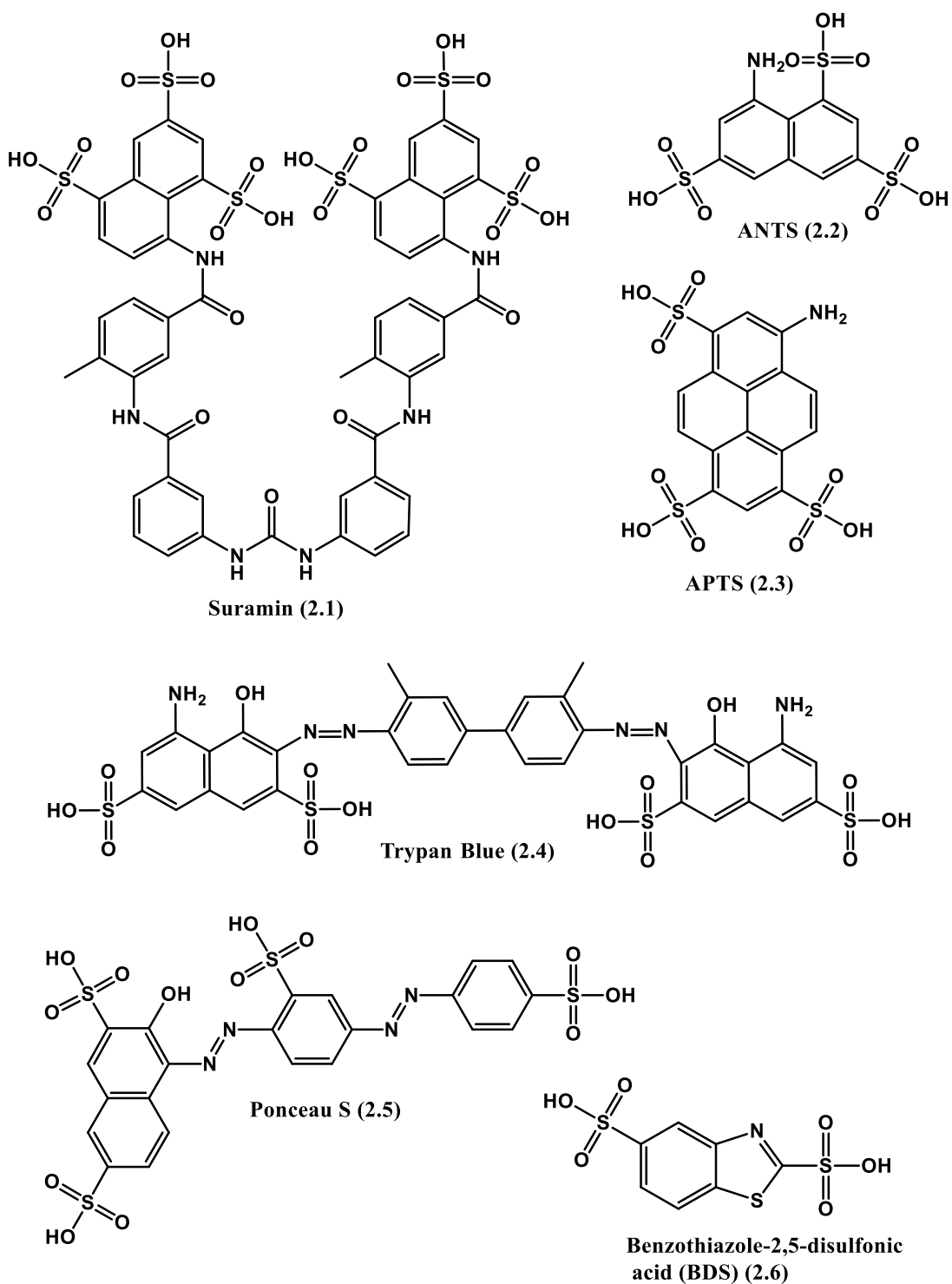


Figure 2.2. Structures of suramin and other sulfonated molecules tested against DisA. Abbreviations: ANTS is 8-aminonaphthalene-1,3,6-trisulfonic acid; APTS is 8-aminopyrene-1,3,6-trisulfonic acid.

2.1.2 Results and Discussion

Suramin is a symmetrical polysulfonated urea derivative that has long been used as an anti-parasitic drug for the treatment of African trypanosomiasis as well as onchocerciasis.^{19, 20} To delineate which moieties on suramin are responsible for DisA inhibition, we tested the enzyme against five structurally related compounds (Figure 2.2) using the coralyne assay. Suramin and trypan blue inhibited DisA activity (Figure 2.3). 8-aminonaphthalene-1,3,6-trisulfonic acid (ANTS), Ponceau S and benzothiazole-2,5-disulfonic (compounds that contain two or more sulfonic acid groups) did not inhibit DisA significantly compared to suramin and trypan blue (Figure 2.3), indicating that the presence of sulfonic acid alone was not sufficient to cause DisA inhibition.

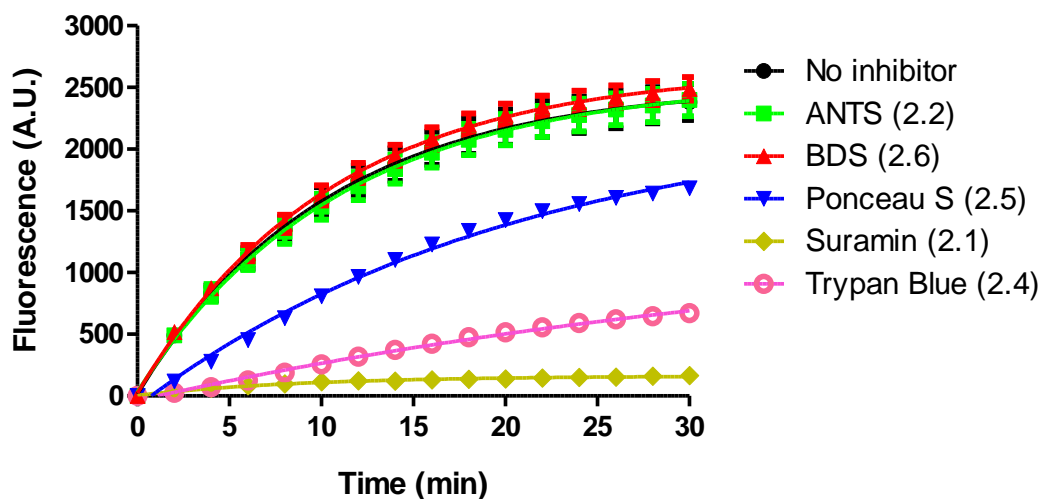


Figure 2.3. Coralyne assay of suramin and suramin-related compounds. For the coralyne assay, emission fluorescence intensity of coralyne (at 475 nm) increases as the concentration of c-di-AMP increases.^{15, 17} BDS stands for benzothiazole-2,5-disulfonic acid. 8-aminonaphthalene-1,3,6-trisulfonic acid

(ANTS) is highly fluorescent so could not be tested using the coralyne assay. Each experiment was done in triplicate.

To eliminate the possibility that a positive hit from the coralyne assay was not due to the quenching of coralyne's fluorescence by the tested compounds, we also used HPLC to monitor the DisA reaction in presence the active compounds and APTS (was not be tested in the coralyne assay). Both trypan blue and suramin inhibited DisA (Figure 2.3) but suramin was a better inhibitor. APTS did not inhibit DisA activity.

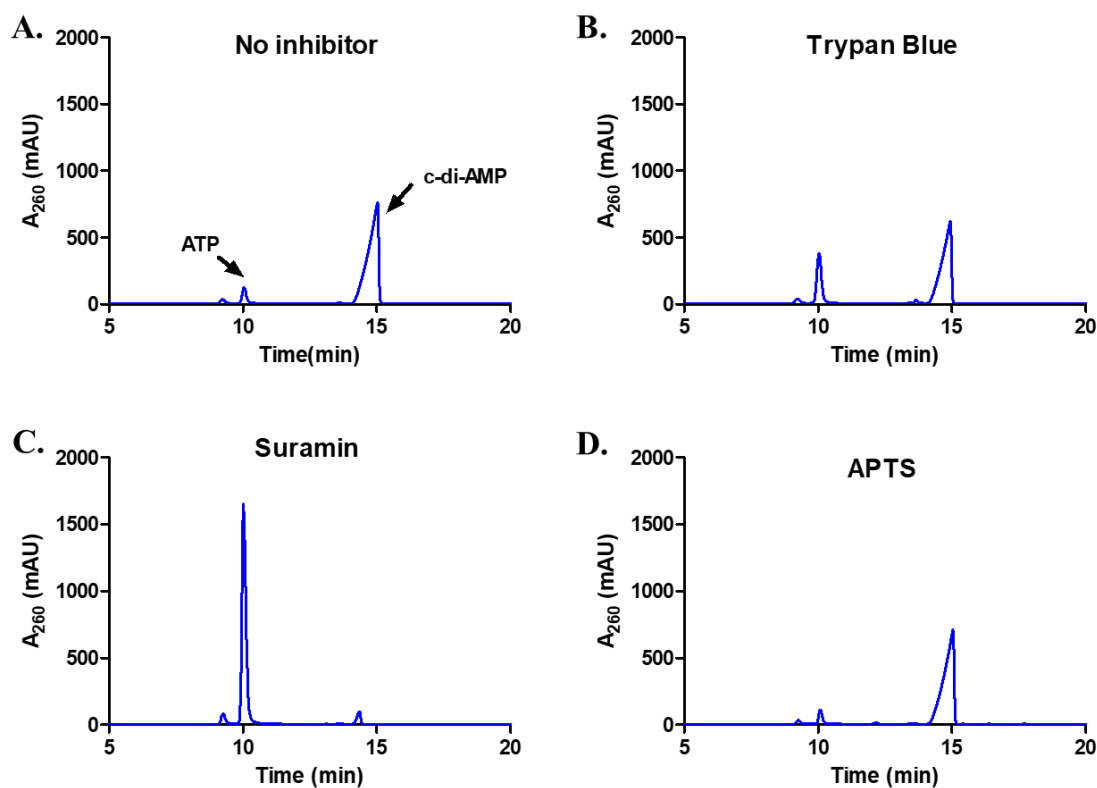


Figure 2.4. HPLC analysis of DisA reactions. The results from further analysis of hits from coralyne assay showing reactions of 1 μ M DisA with **A.** No inhibitor, **B.** 20 μ M Trypan Blue and **C.** 20 μ M suramin. **D.** The HPLC chromatogram of APTS reaction

which was not tested by coralyne assay. Only suramin significantly inhibited DisA activity. ATP and c-di-AMP peaks with respective retention times of 10 min and 14.6 min are indicated with arrows on the No inhibitor chromatogram.

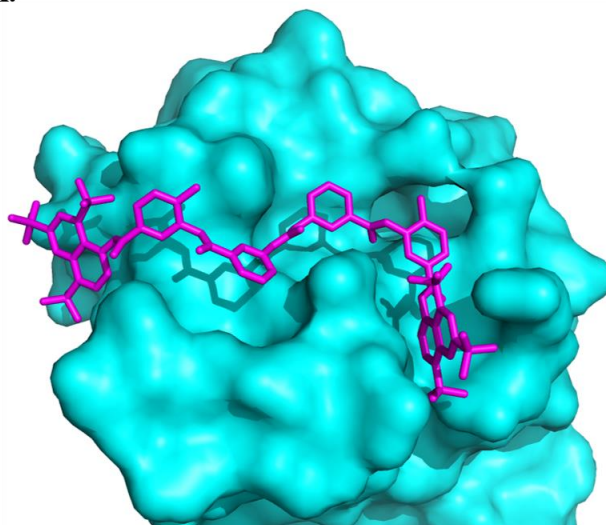
Using HPLC to monitor the DisA reaction (Figure 2.4), we noted that that at 20 μM , suramin inhibited DisA activity by 90% after 30 min while trypan blue only showed 20% inhibition. The coralyne assay indicated about 80% inhibition with trypan blue; the discrepancy between the coralyne and HPLC results for trypan blue inhibition is probably due to partial fluorescence quenching by trypan blue, which contains an azo moiety. Therefore, although the coralyne assay is more convenient than HPLC analysis for high throughput screening to discover c-di-AMP synthase inhibitors, it is crucial to use counter screens, such as HPLC analysis, to confirm “hits”.

We wondered if suramin was inhibiting DisA *via* ATP- competitive mechanism. Previous report by Avliyakov *et al.* indicated that binding of suramin to L3, a ribosomal protein from *Trypanoplasma borreli*, completely abolished ATP binding.²¹ Also, Morgan *et al.* crystallized suramin bound to the ATP binding site of *Leishmania mexicana* pyruvate kinase.²² These precedents provide evidence of suramin binding to the nucleotide binding pockets of proteins.

Docking of suramin with a monomer of TmaDisA(PDB:3C1Z)³ revealed that suramin bound to the ATP binding site of TmaDisA (Figure 2.5) with binding affinity of $-9.4 \text{ kcal mol}^{-1}$. Future crystallography studies, beyond the scope of

this work, should reveal if the docked structure is accurate and could provide more insight into how to design potent DisA inhibitors. *B. subtilis* DisA is similar to TmaDisA; computationally modelled 3D structure²³ of *B. subtilis* DisA aligned well with TmaDisA (Figure 2.5).

A.



B.

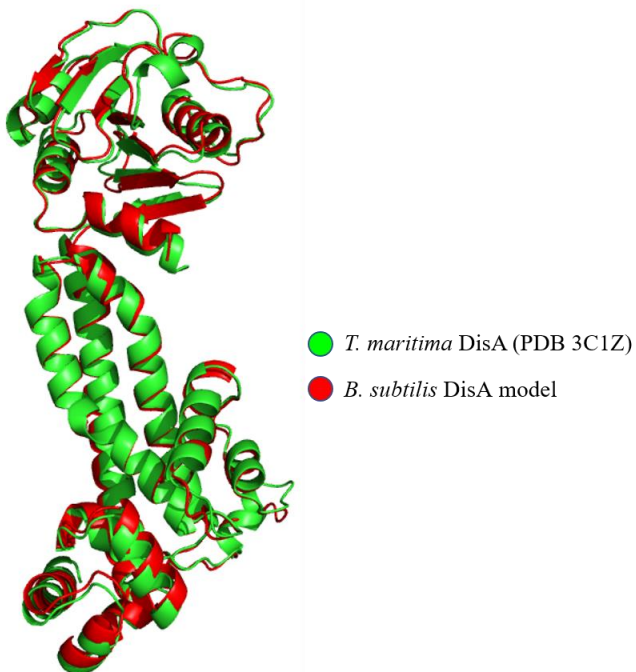


Figure 2.5. Molecular docking with AutoDock Vina 1.1.1 used to obtain a suramin/TmaDisA complex. A. Suramin (magenta) binds in the nucleotide-

binding pocket of TmaDisA. **B.** Overlay of TmaDisA with modeled structure of *B. subtilis* DisA. Images were generated with PyMOL visualization software.

To provide some experimental confirmation that suramin and ATP compete for the same binding site in DisA, we determined the IC₅₀ values at various ATP concentrations (100 μM, 500 μM and 1 mM, see Figure 2.6A). The formation of α-³²P-c-di-AMP/c-di-AMP from α-³²P-ATP/ATP by 1 μM DisA in the presence of increasing concentrations of suramin at the various ATP concentrations was monitored *via* TLC. IC₅₀ values of 1.1 μM, 3.1 μM and 5.4 μM were obtained at the ATP concentrations of 100 μM, 500 μM and 1 mM respectively.

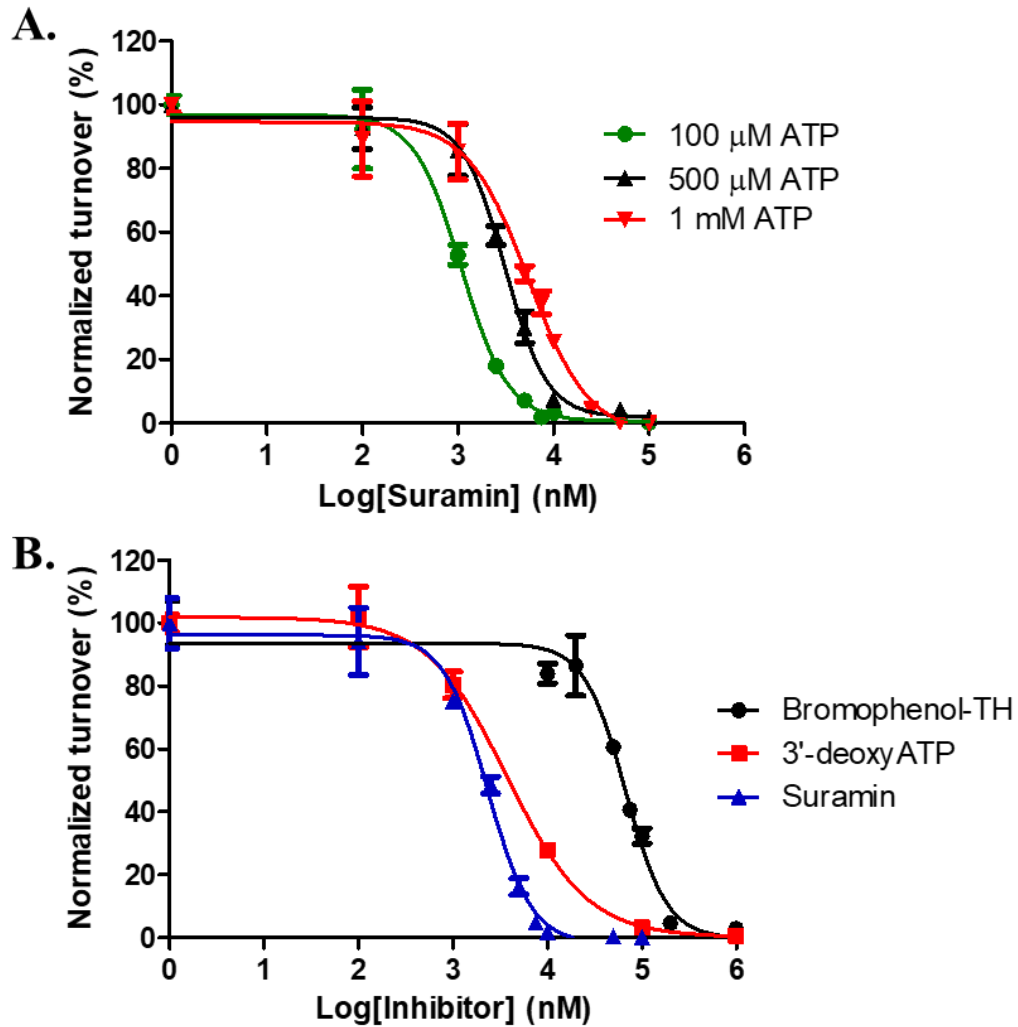
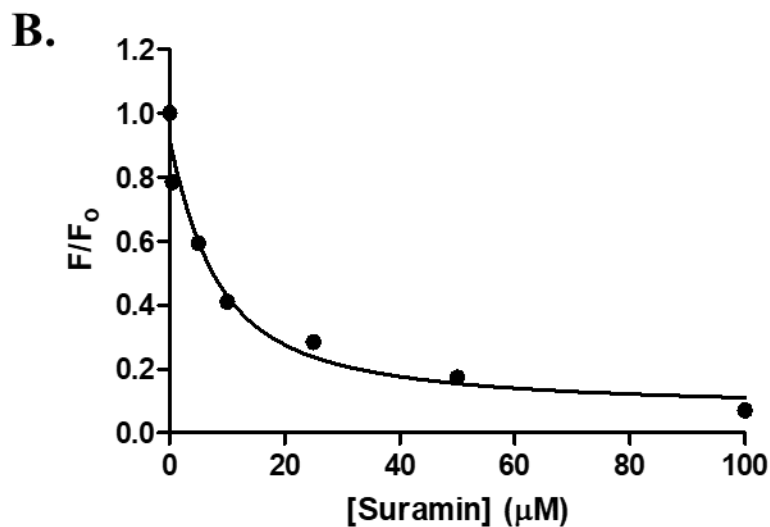
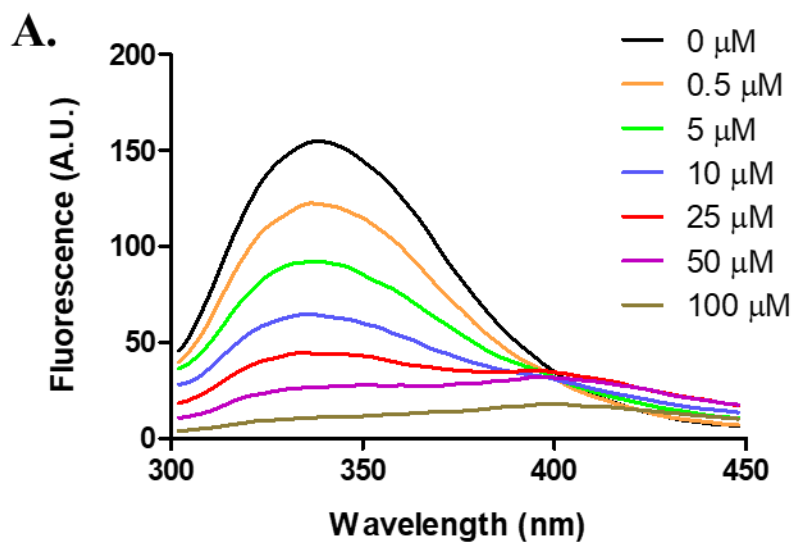


Figure 2.6. Dose-reponse curves for the inhibition of DisA (1 μ M) activity. **A.** The IC₅₀ of suramin was determined at 100 μ M, 500 μ M or 1 mM α -³²P-ATP/ATP in reaction buffer. The IC₅₀ values at 100 μ M, 500 μ M and 1 μ M ATP were 1.1 μ M, 3.1 μ M and 5.4 μ M. **B.** The IC₅₀ values of bromophenol thiohydantoin, 3'-deoxyATP and suramin were determined to be 67.2 μ M, 3.8 μ M and 2.3 μ M respectively at 300 μ M ATP and 1 μ M DisA. Experiments were done in triplicate. Error bars represent mean \pm SEM generated using GraphPad Prism 4.0 Software (La Jolla, CA, USA).

The observed increase in IC_{50} values upon increasing ATP concentration is consistent with both molecules competing for similar binding site. We also compared the potency of suramin's inhibition with that of 3'-deoxyATP and bromophenol-TH. Here, IC_{50} values of 2.3 μM , 3.8 μM and 67.2 μM (DisA concentration was 1 μM) were obtained for suramin, 3'-deoxyATP and bromophenol-TH respectively (Figure 2.6B). This indicates that suramin is more potent than either of the two previously identified inhibitors of DisA (Figure 2.6B).



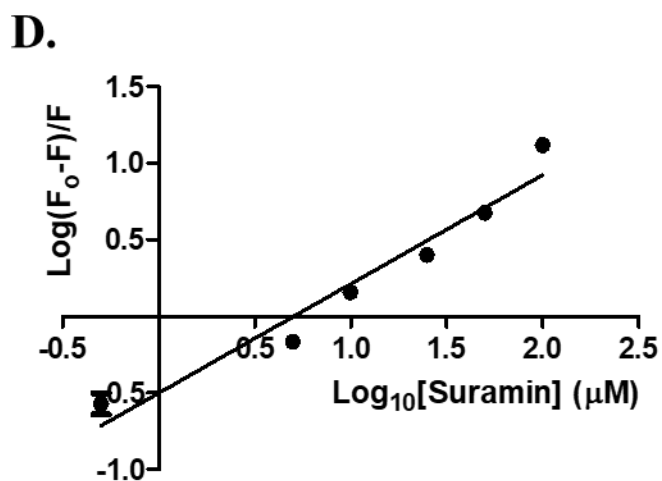
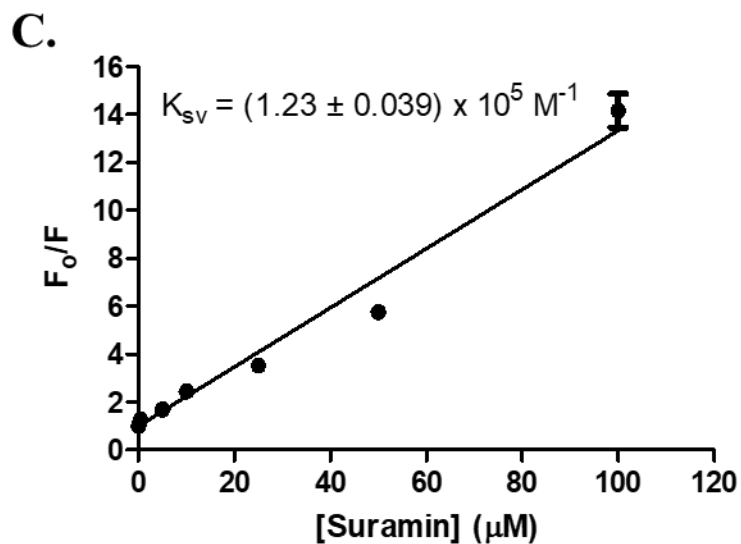


Figure 2.7. Analysis of the binding interaction between DisA and suramin. **A.** The fluorescence emission of DisA (5 μM) was observed to be quenched in the presence of increasing suramin concentration. **B.** Plot of relative fluorescence of DisA (5 μM) at 340 nm as a function of suramin concentration. The data was fitted to the non-linear regression, eqn (2.3). **C.** Stern-Volmer plot of the relative fluorescence (at 340 nm) as a function of suramin concentration. Eqn 2.1 was used for the linear regression. **D.** Stern–Volmer plot generated by fitting the fluorescence emission at 340 nm to eqn

(2.2). GraphPad Prism 4.0 Software was used to obtain plots from triplicate measurements.

The addition of suramin to DisA resulted in a decrease in the protein intrinsic fluorescence, probably due to changes in the microenvironment(s) of the tyrosine residues in the protein. Therefore, we were able to determine the apparent K_d of suramin binding to DisA *via* fluorescence titration of the inhibitor with 5 μM DisA (Figure 2.7A). The apparent K_d was determined to be 5.4 μM (Figure 2.7B), assuming a 1:1 binding. Bromophenol-TH bound to DisA with an apparent K_d of 21 μM ,¹⁵ so it appears that suramin binds tighter to DisA, compared to bromophenol-TH.

We also analyzed the fluorescence quenching data using the Stern–Volmer equation.^{24, 25} The data was fitted to the linear equation²⁴:

$$F_o/F = 1 + k_q\tau_o[Q] = 1 + K_{sv}[Q] \quad (2.1)$$

where F_o and F are respectively the fluorescence intensities of a biomolecule (DisA) without and with a quencher (suramin) at concentration Q , k_q is the quenching rate constant of the biomolecule, τ_o is the fluorescence lifetime of biomolecule (about 10^{-8} s)²⁶ and K_{sv} is the Stern-Volmer constant. From the above equation, K_{sv} was estimated to be $1.23 \pm 0.039 \times 10^5 M^{-1}$ (Figure 2.7C) and so we determined k_q was $1.23 \times 10^{13} M^{-1}s^{-1}$. Since the estimated value of k_q is greater than the diffusion-controlled quenching rate, $2 \times 10^{10} M^{-1}s^{-1}$ a static quenching mechanism prevails in the DisA-suramin complex.²⁶

The data was also fitted to the modified form of the Stern–Volmer equation

(eqn (2.2) and Figure 2.7),²⁷

$$\text{Log} \frac{(F_0 - F)}{F} = \text{Log}K + n\text{Log}[Q] \quad (2.2)$$

where F and F_0 are respectively the fluorescence intensities (at 340 nm) in the presence and absence of the quencher (suramin) at concentration Q , the binding constant K (reciprocal of which gives the dissociation constant, K_d) is the y-intercept of the line and the slope gives the number of binding sites, n on the protein (DisA). From eqn (2.2), an apparent K_d of 3.2 μM was determined and the number of binding sites (n) was found to be 1, implying a 1: 1 binding between DisA and suramin.

Suramin did not inhibit the activity of *B. subtilis* YybT, a c-di-AMP specific phosphodiesterase (Figure 2.8), indicating that the observed DisA inhibition is somehow specific.

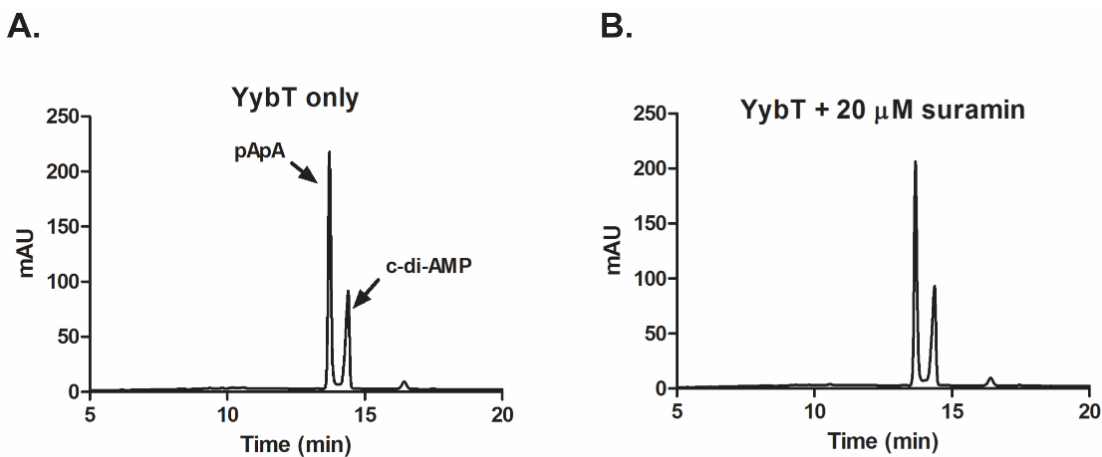


Figure 2.8. HPLC analysis of YybT reactions. The effect of suramin on 1 μM YybT **A.** without suramin and **B.** with 20 μM suramin at 37 $^{\circ}\text{C}$ was analyzed by HPLC. There was no difference between the reaction with and without suramin. The arrows

point to the product, pApA and substrate, c-di-AMP which had retention times of 13.7 min and 14.4 min respectively.

2.1.3 Conclusions

In conclusion, we have identified suramin as a potent inhibitor of DisA. Suramin is already used in the clinic to treat parasitic infection and has also been shown to have anti-cancer²⁸ and anti-viral²⁹ properties. Recently Nautiyal *et al.* showed that suramin inhibited *Mycobacterium tuberculosis* RecA protein with submicromolar IC₅₀.³⁰ They also showed that suramin potentiated the activity of ciprofloxacin against *M. smegmatis*.³⁰ Here, we show that suramin also inhibits cyclic diadenylate cyclase enzyme and represents an interesting scaffold, which could be used to develop cyclic dinucleotide signaling inhibitors. The advances made in the identification of c-di-AMP related enzymes, receptor proteins and RNA far outpace the number of small molecule inhibitors of these proteins. This paper sets the tone for the discovery of such small molecules, which could find use in unravelling the intricacies of cyclic dinucleotide signaling as well as being used as antibacterial agents.

2.1.4 Experimental section

2.1.4.1 Protein expression and purification

E. coli BL21(DE3) cells transformed with plasmids of enzymes were grown at 37 °C in LB medium amended with 50 µg/mL Kanamycin. Cultures were grown to an OD₆₀₀ of 0.6, and expression was induced by adding 1 mM isopropyl-β-D-thiogalactopyranoside (IPTG). YybT expression was induced for 6 h at 30 °C whilst DisA was induced for 18 h at 16 °C. Cell pellets were harvested by centrifugation at

4,000 rpm for 15 min and resuspended in lysis buffer (10 mM Tris-HCl, pH 8.0, 100 mM NaCl for YybT and 50 mM sodium phosphate buffer, pH 8.0, 300 mM NaCl for DisA). The cells were lysed by sonication and the lysates were centrifuged at 25,000 rpm for 25 min at 4 °C to collect the supernatant. The hexahistidine-tagged proteins were purified from the supernatants by affinity chromatography using a GE HisTrap™ HP 1 mL column mounted onto a Bio-Rad NGC™ Chromatography System. Protein concentration was determined by measuring the UV absorbance at 280 nm and the purified proteins were stored with 10 % glycerol in their respective lysis buffers at - 80 °C.

2.1.4.2 The coralyne assay

The initial screening of the library was done at the Johns Hopkins University ChemCORE facility. Suramin and suramin-related compounds were stored as 10 mM stock solutions in DMSO. Triplicate 100 µL reactions were set up containing 300 µM ATP, 10 µM coralyne, 3 mM KI and 20 µM compound or DMSO in a 40 mM Tris-HCl pH 7.5, 100 mM NaCl and 10 mM MgCl₂ reaction buffer. The reactions were started by adding 1 µM DisA. The fluorescence of coralyne over the course of 30 min was measured on a Molecular Devices SpectraMax M5e microplate reader with $\lambda_{\text{ex}}=420$ nm and $\lambda_{\text{em}}=475$ nm at 30 °C.

2.1.4.3 HPLC analysis

Reactions containing 20 µM suramin or related compounds, 300 µM ATP and 1 µM DisA were set up and allowed to go for 30 min at 30 °C. The reactions were then terminated by heating at 95 °C for 5 min and the precipitated proteins were filtered off. Components of the filtrate were then analyzed on a COSMOSIL C18-MS-II Packed column (5 µm) using 0.1 M TEAA in water (Buffer A) and acetonitrile

(Buffer B). The samples were eluted with 99 %→87 % Buffer A at 0 to 16 min, 87 %→10 % Buffer A at 16 to 22 min and kept at 10% Buffer A till 25 min, detecting signals at room temperature with a 260 nm UV detector. For the effect of suramin on YybT, HPLC reactions were set up containing 50 μM c-di-AMP and 1 μM YybT in the presence or absence of 20 μM suramin for 30 min at 37 °C in reaction buffer (100 mM Tris-HCl, pH 8.3, 20 mM KCl, 0.5 mM MnCl₂ and 1 mM DTT). The reaction was analyzed as described above.

2.1.4.4 IC₅₀ determination

Half maximal inhibitory concentrations (IC₅₀) were determined in 10 μL reactions containing ATP (at either 100 μM, 300 μM, 500 μM or 1 mM), 11 nM ³²P-ATP and increasing concentrations of suramin mixed in reaction buffer (40 mM Tris-HCl pH 7.5, 100 mM NaCl and 10 mM MgCl₂). Reactions were initiated by adding 1 μM DisA at 30 °C for 1 hour. Afterwards, 0.4 μL aliquots of the reaction mixtures were spotted on TLC plates (EMD Millipore TLC Cellulose) and spot separation was achieved in a 1:1.5 (vol/vol) saturated (NH₄)₂SO₄ and 1.5 M KH₂PO₄ buffer.

2.1.4.5 Measurement of intrinsic fluorescence of DisA

DisA (5 μM) was incubated with various concentrations of suramin at 25 °C for 1 hour. Protein intrinsic fluorescence was measured on a Cary Eclipse Fluorescence Spectrophotometer (Agilent) with λ_{ex} = 290 nm and λ_{em} = 300 - 450 nm. Initially, apparent *K_d* (assuming 1:1 binding ratio) was calculated using fluorescence intensity at 340 nm according to the equation³¹:

$$F = F_0 + \Delta F \frac{(K_d^{app} + P_t + Q_t) - \sqrt{(K_d^{app} + P_t + Q_t)^2 - 4P_tQ_t}}{2P_t} \quad (2.3)$$

Where F is the fluorescence intensity at 340 nm, F_0 is the fluorescence intensity at 340 nm in the absence of ligand, ΔF is the change in fluorescence upon ligand binding, K_d^{app} is the apparent dissociation constant, P_t is the total protein (DisA) concentration and Q_t is the total ligand (suramin) concentration.

For Stern-Volmer analysis of the fluorescence emission spectra, the emission at 340 nm at each suramin concentration was used to generate the Stern-Volmer plots^{24, 27} according to the equations (1) and (2) from which the Stern-Volmer constant, K_{sv} dissociation constant, K_d and number of binding site, n were estimated.

2.1.4.5 Molecular docking and computational modelling

We used Autodock Vina 1.1.1³² to perform docking calculations. TmaDisA PDB file (3C1Z) was downloaded from RCBS Protein Data Bank and used as AutoDock protein. Suramin was converted into a PDB file using ChemDraw and used as AutoDock ligand. AutoDockTools was used to convert the PDB files to the required PDBQT file format. A grid box large enough to cover the globular nucleotide binding domain of TmaDisA (Center X = -20, Center Y = 10, Center Z = 75, Size X = 92, Size Y = 96, Size Z = 68) was selected. We set the exhaustiveness value to 32 and conducted the molecular docking experiment. The best pose was determined as the one with the highest binding affinity. PyMOL viewer version 1.3.49 was used to visualize the docking results. For computational modelling, the FASTA sequence of DisA was obtained from UniProt ([A0A0C2Q1A6](#)) and submitted to the Phyre2 web portal for protein modelling²³. PyMOL was then used to align the 3D model with the structure of TmaDisA.

1.3 Inhibition of cyclic deadenylate cyclase, DisA, by polyphenols

This section (2.2) was originally published as: Opoku-Temeng, C. and Sintim, H.O. “Inhibition of cyclic deadenylate cyclase, DisA, by polyphenols.” *Sci. Rep.*, 2016, 6:25445

2.2.1 Introduction

Nucleotides play critical roles in cells, some of which include serving as a source of energy, as components of biomolecules like DNA and RNA and as cofactors of enzymes. It has long been known that mononucleotides such as cAMP and ppGpp regulate several processes in bacteria.^{2, 33} In the late 1980s Benziman and colleagues identified cyclic dinucleotide bis-(3'-5')-cyclic dimeric guanosine monophosphate (c-di-GMP) as an allosteric regulator in the bacterium *Acetobacter xylinum* (now called *Gluconacetobacter xylinus*).³⁴ It would take close to two decades before the microbiology community fully appreciated that c-di-GMP is a master regulator of bacterial physiology.³³ In Gram-negative bacteria c-di-GMP controls the transition from planktonic to the biofilm state and there has been an explosion of research activities dedicated to unravelling the intricacies of c-di-GMP signaling. Just as c-di-GMP research was taking shape, another related cyclic dinucleotide, bis-(3'-5')-cyclic dimeric adenosine monophosphate (c-di-AMP) was identified by Hopfner and colleagues during their study of the *Bacillus subtilis* checkpoint protein, DNA integrity scanning protein A (DisA).³

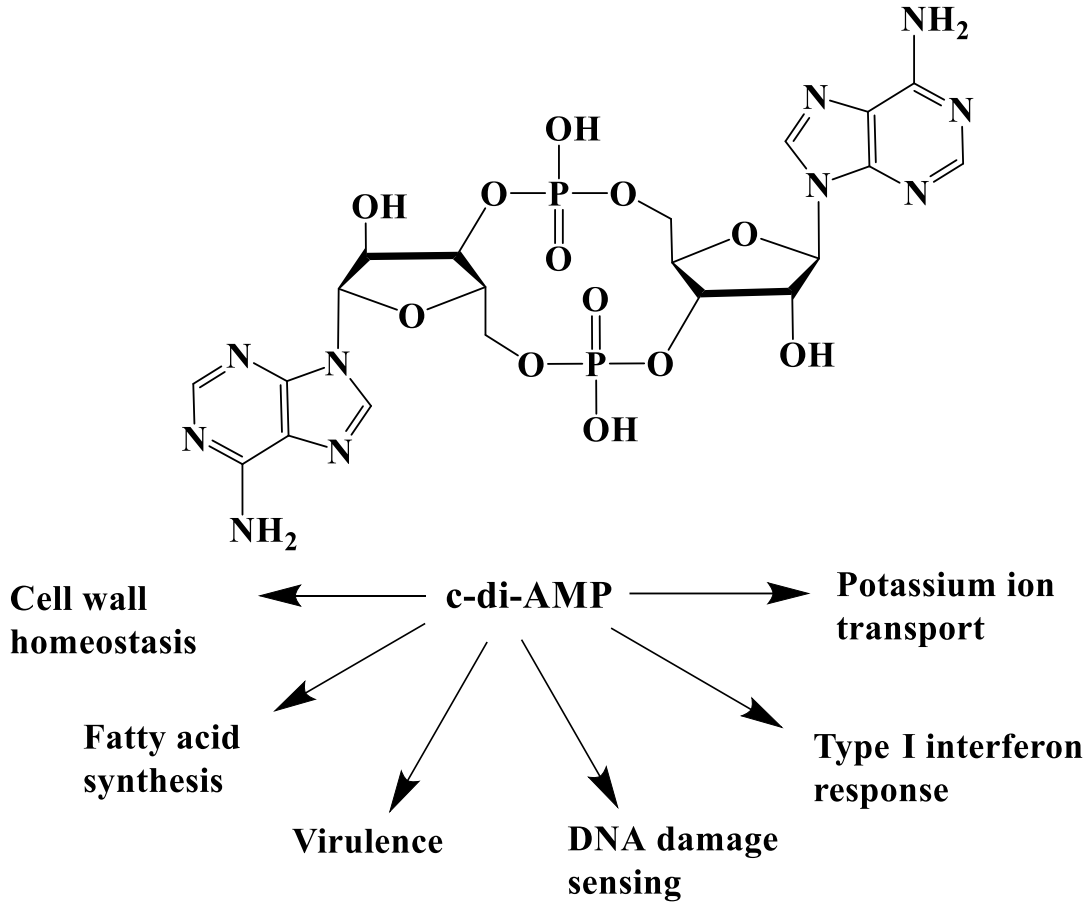


Figure 2.9. Cellular processes affected by c-di-AMP signaling. Fluctuations in the levels of cellular c-di-AMP cause a myriad of phenotypic changes in different bacteria.

Just like the analogous c-di-GMP, c-di-AMP is also emerging as an important signaling second messenger in several bacteria and has been found to regulating several physiological processes including but not limited to cell wall homeostasis,^{8, 9} fatty acid metabolism,³⁵ cell size regulation¹⁰ and virulence⁸ (Figure 2.9). C-di-AMP has been found to be mainly produced predominantly in Gram-positive Firmicutes, Actinomycetes and mycobacteria.^{1, 2} The intracellular levels of c-di-AMP are tightly regulated by two opposing enzymes: diadenylate cyclases (DAC), which synthesize c-

di-AMP from two molecules of ATP/ADP and phosphodiesterases (PDE), which degrade c-di-AMP into pApA or AMP.⁴⁻⁷ This tight regulation is important in keeping an optimal intracellular c-di-AMP concentration as overproduction or underproduction of the signaling molecule has been observed to cause interesting changes in bacteria physiology.^{8, 10, 12} In *Listeria monocytogenes*, overexpression of PdeA led to low levels of intracellular c-di-AMP and resulted in reduced growth rate and avirulent phenotype.⁸ Decreased intracellular concentration of c-di-AMP in *L. monocytogenes* also resulted in a higher susceptibility to peptidoglycan-targeting antibiotics.⁸ An opposite observation was made when the PDE GdpP of *Staphylococcus aureus* was deleted, leading to an increase in peptidoglycan cross-linking and resistance to cell wall-targeting antibiotics.¹⁰

Studies that aimed to knock out the DAC gene however proved futile since the DAC domain in several bacteria, including the pathogens *L. monocytogenes*¹³ and *S. pneumoniae*^{7, 14} is essential. Thus, to study the role of DAC in such bacteria, researchers have resorted to conditional depletion of the gene.⁸ Arguably, there is a need to identify small molecules that can modulate the functions of c-di-AMP metabolism enzymes for use as chemical probes to interrogate c-di-AMP-mediated processes. Also, since c-di-AMP has been shown to affect peptidoglycan synthesis or remodeling, it is likely that inhibitors of c-di-AMP synthesis or degradation could also be utilized as antibacterial agents or used in synergy with traditional antibiotics.

We have been interested in the development of technologies that could aid the identification of inhibitors of cyclic dinucleotide metabolism enzymes.^{18, 36, 37} These probes have facilitated the identification of the first DisA inhibitor, bromophenol

thiohydantoin,^{15, 17} which are weak inhibitors of DisA. In an effort to discover more potent inhibitors of DisA and motivated by the dazzling arrays of enzymes that polyphenols regulate,^{38, 39} we turned our attention to evaluating polyphenols as DisA inhibitors. The biological properties of plant polyphenols have long been established.^{40, 41} Tea polyphenols for example are known for their antioxidant properties and have been studied for their anticancer, antiviral and antibacterial properties.^{42, 43} Strikingly, some tea polyphenols like catechin have been shown to potentiate the action of antibiotics, particularly cell wall targeting antibiotics like oxacillin and ampicillin, against methicillin resistant *S. aureus*.⁴⁴ We were therefore interested in investigating if polyphenols could inhibit c-di-AMP metabolism proteins. Since c-di-AMP has emerged as important second messenger that regulates diverse processes in bacteria, we wondered if perhaps some of the activity of polyphenols against bacteria was due to inhibition of c-di-AMP metabolism enzymes. Thus, we tested 14 polyphenols (Figure 2.10) against *B. subtilis* DisA.

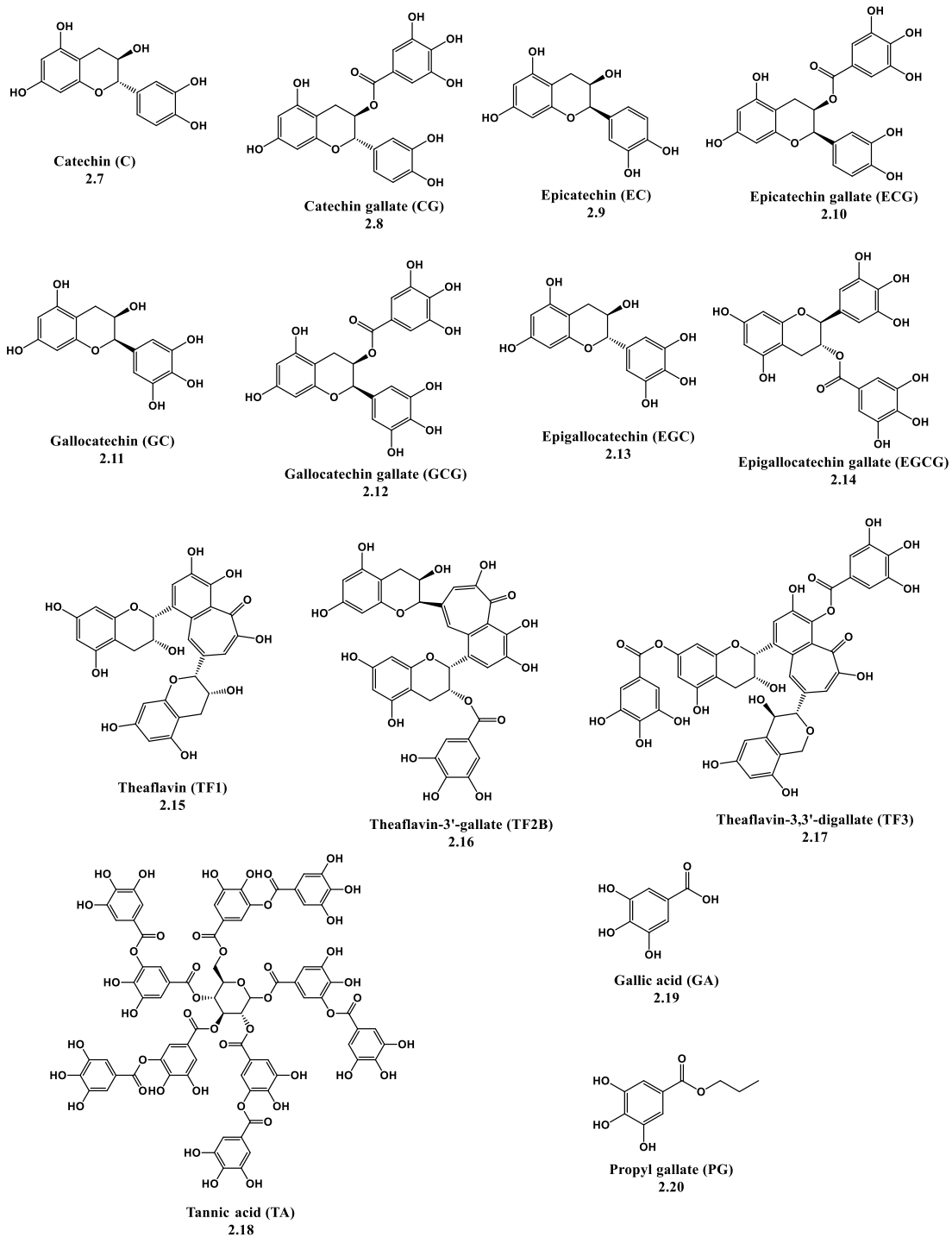


Figure 2.10. Structures of polyphenols tested against DisA

2.2.2 Results

2.2.2.1 Coralyne assay identifies TA, TF2B and TF as DisA inhibitors.

We utilized the coralyne assay¹⁸ developed by our group to evaluate the inhibitory effect of 14 polyphenols (compounds **2.7** to **2.20**) on DisA. For structures of these compounds, see Figure 2.10. From the coralyne assay results, we selected compounds that yielded 50% or more inhibition, after 30 min. At 20 μ M inhibitor concentration and 1 μ M DisA concentration, TA completely inhibited c-di-AMP formation (Figure 2.11).

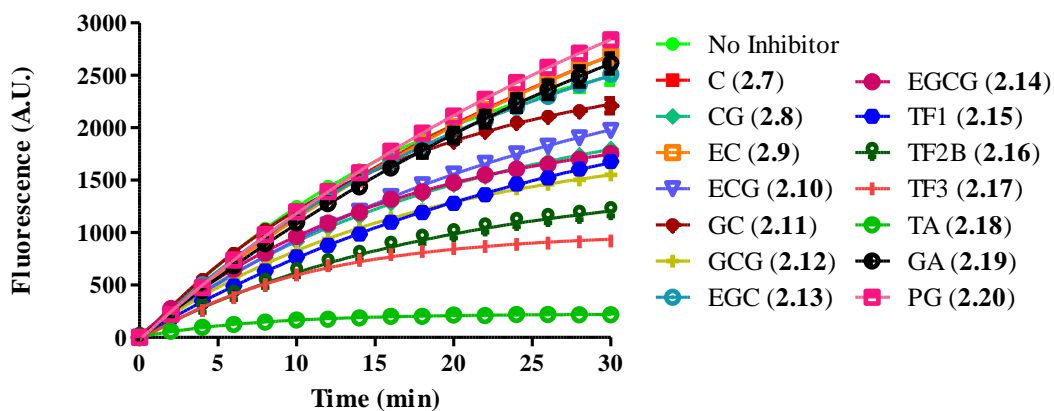


Figure 2.11. Screening of polyphenols against DisA. Coralyne assay results of 14 polyphenols screened against DisA (1 μ M); λ_{ex} = 420 nm and λ_{em} = 475 nm. Polyphenols that yielded at least 50% inhibition were selected for further analysis.

TF2B and TF3 also inhibited DisA activity, albeit not as potent as tannic acid (Figure 2.11). It appears that as the number of gallates on a polyphenol increased, so did the potency of inhibition. For example, TF1 (compound **2.15**), TF2B (compound **2.16**) and TF3 (compound **2.17**) contain the same theaflavin moiety and only differ by the number of attached gallate units (TF1 contains no gallates; TF2B contains one gallate and TF3 contains two gallates); inhibition was observed to increase from TF1 to TF3.

Control experiments with gallic acid (GA, compound **2.19**) and propyl gallate (PG, compound **2.20**) did not lead to any inhibition (Figure 2.11). From these experiments, we conclude that it is the combination of both the theaflavin and gallic acid units that results in DisA inhibition.

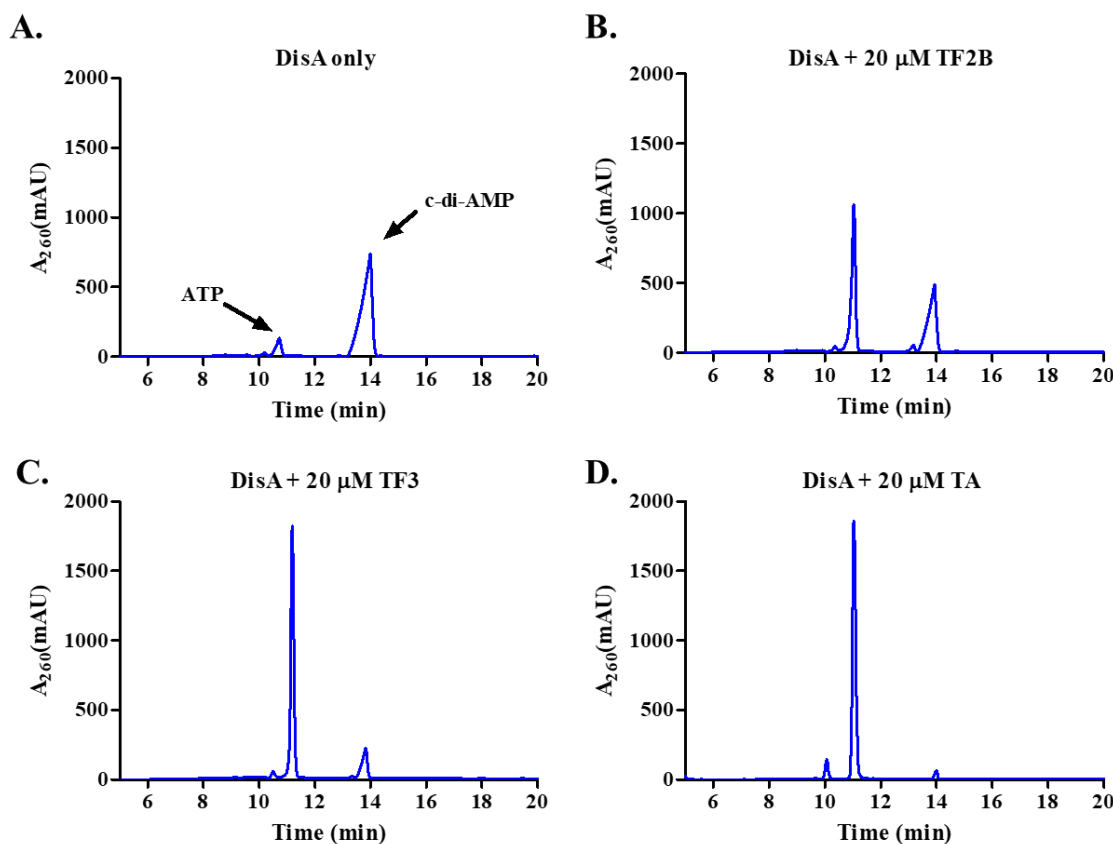


Figure 2.12. Effect of polyphenols on DisA activity. HPLC analysis of DisA reactions (1 μ M) reactions **A.** without inhibitor, with **B.** 20 μ M TA **C.** 20 μ M TF3 and **D.** 20 μ M TF2B. The ATP and c-di-AMP peaks are labeled with arrows.

To further explore the inhibition of TA, TF2B and TF3, we first performed HPLC analysis of their respective reactions. Consistent with the results from the coralyne assay, TA was observed to be the most potent of the three; with ~97% inhibition at 20

μM TA when $1\ \mu\text{M}$ DisA was used (Figure 2.12). TF3 and TF2B followed in that order with $\sim 83\%$ and $\sim 78\%$ inhibition respectively (Figure 2.12). We then proceeded to determine the half maximal inhibitory concentration, IC_{50} of TA, TF2B and TF3. Different concentrations of TA, TF2B and TF3 were incubated with $1\ \mu\text{M}$ DisA, $300\ \mu\text{M}$ ATP and $11\ \text{nM}$ ^{32}P -ATP at $30\ ^\circ\text{C}$. The amount of c-di-AMP synthesized in the presence or absence of inhibitor was normalized with respect to the amount in the absence of inhibitor and used to estimate the IC_{50} values. A steep dose-response curve was observed when TA (but not TF2B and TF3) was titrated against $1\ \mu\text{M}$ DisA (Figure 2.13). Steep dose-response curves have been shown to be caused by promiscuous enzyme inhibitors and for such inhibitors, the IC_{50} values have been observed to increase linearly with enzyme concentration.⁴⁵ Hence, we determined the IC_{50} of TA at four enzyme concentrations. The IC_{50} values increased from $1.8\ \mu\text{M}$ at $0.5\ \mu\text{M}$ DisA to $3.4\ \mu\text{M}$ at $1\ \mu\text{M}$ DisA, $16.2\ \mu\text{M}$ at $5\ \mu\text{M}$ DisA and $18.3\ \mu\text{M}$ and $10\ \mu\text{M}$ DisA (Figure 2.13); consistent with the observations made for non-specific enzyme inhibitors.⁴⁵

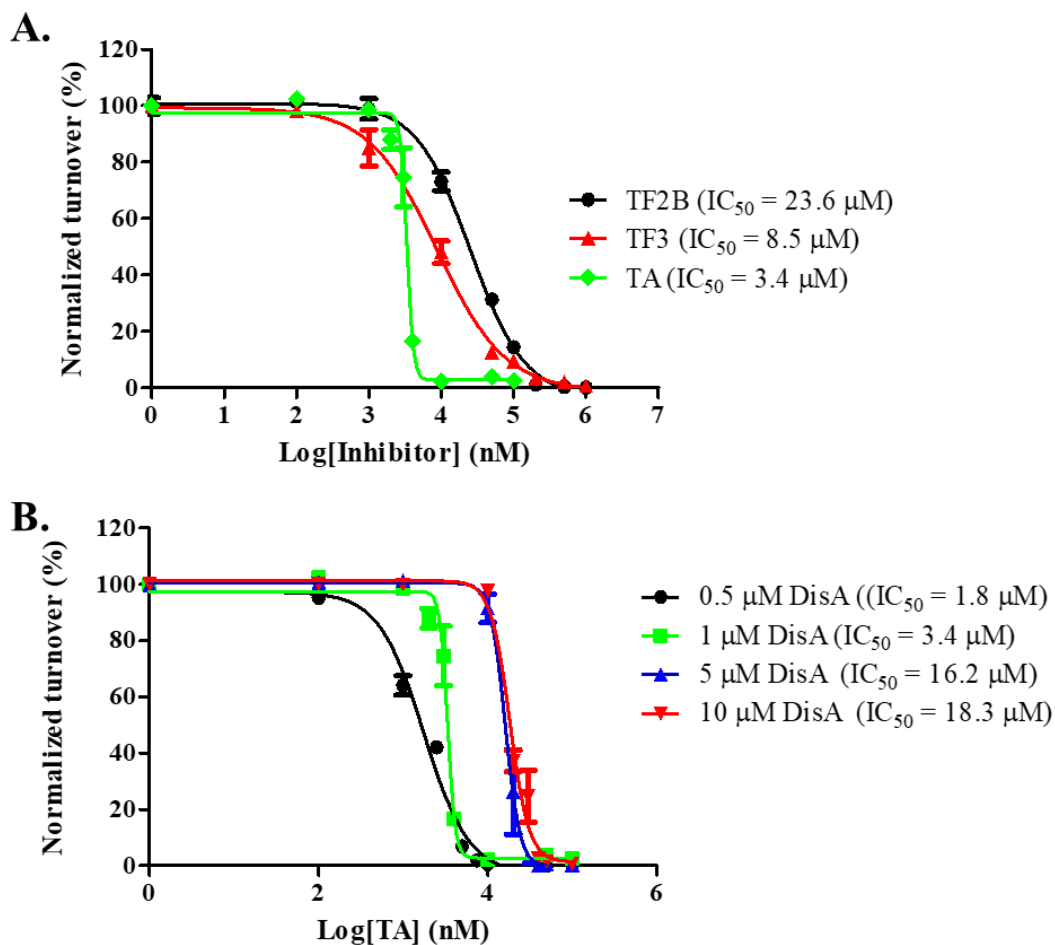


Figure 2.13. Inhibition of DisA by polyphenol. Half maximum inhibitory concentration, IC₅₀ curves of **A.** polyphenol inhibitors TF2B, TF3 and TA at 1 μM DisA at 300 μM ATP and **B.** TA at 0.5 μM DisA, 1 μM DisA, 5 μM and 10 μM DisA using 300 μM ATP. Error bars represent the mean and SEM of triplicate experiments. Curves were generated with GraphPad Prism 4 software.

The dose response curves for TF2B and TF3 were not as steep as for tannic acid and presumably these two compounds are not promiscuous protein inhibitors. At 1 μM DisA, the IC₅₀ values of TF2B and TF3 were 23.6 μM and 8.5 μM respectively (Figure 2.13), which is lower than what was obtained for the first reported DisA inhibitor,

bromophenol thiohydantoin.¹⁵

2.2.2.2 TF3 inhibition does not depend on ATP concentration.

Because TA was deemed a promiscuous inhibitor, it was not investigated further. TF3 was selected for further investigation and to gain insight into the type of inhibition exhibited by TF3 (ATP competitive or non-competitive), we determined the IC_{50} of TF3 at various ATP concentrations. Here, we incubated DisA (0.5 μ M) with either 100 μ M ATP, 300 μ M ATP or 500 μ M ATP and increasing concentrations of TF3. IC_{50} values of 3.8 μ M, 3.4 μ M and 4.4 μ M were obtained at 100 μ M ATP, 300 μ M ATP and 500 μ M ATP respectively (Figure 2.14). Since the IC_{50} barely increased upon 3-fold and 5-fold increases of ATP concentration, we conclude that TF3 inhibits DisA in an ATP non-competitive manner.

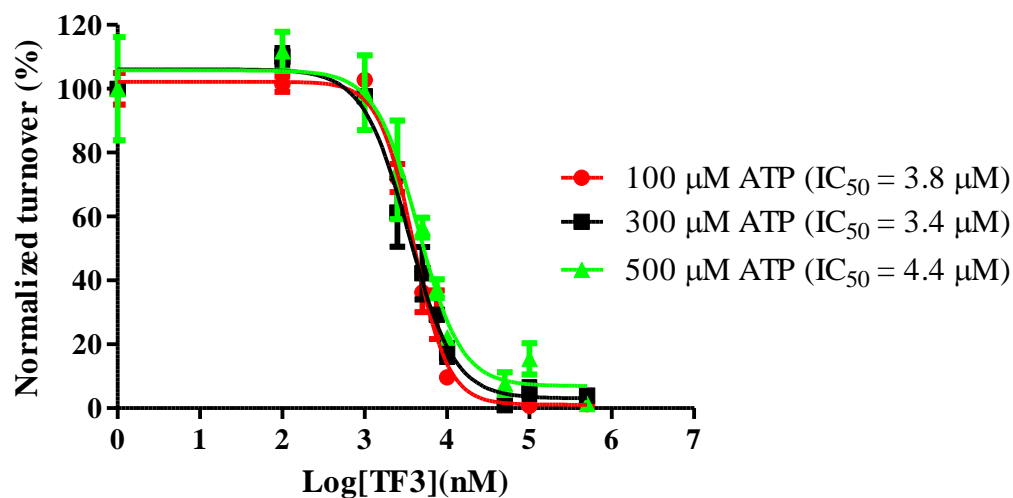


Figure 2.14. Dose-response curves for the inhibition of DisA (0.5 μ M) by TF3 at 100 μ M ATP, 300 μ M ATP and 500 μ M ATP. Error bars represent the mean and SEM of triplicate experiments. Curves were generated with GraphPad Prism 4.0 Software.

2.2.2.3 TF3B and TF3 are specific inhibitors of DisA

Cyclic di-AMP signaling in *B. subtilis* is regulated by DisA, CdaS and CdaA,^{3, 46} which act as DACs and YybT⁴⁷ (recently renamed as *B. subtilis* GdpP¹²) which is the cognate PDE.⁴⁷ To determine whether the inhibitors of DisA identified were specific for the c-di-AMP synthase but not phosphodiesterase, HPLC analyses of YybT hydrolysis of c-di-AMP in the absence or presence of the inhibitors were analyzed. About 50% inhibition of YybT activity was observed when incubated with TA (Figure 2.15). Furthermore, it has been shown that tannic acid inhibition is abolished in the presence of non-ionic surfactants.⁴⁸ When incubated with 0.1% Triton X-100, the inhibition of DisA by TA was completely abolished. TF2B and TF3 did not inhibit YybT (Figure 2.15), confirming our initial assessment (from the DisA dose-response curves) that TA is a promiscuous inhibitor whereas TF2B and TF3 are not promiscuous.

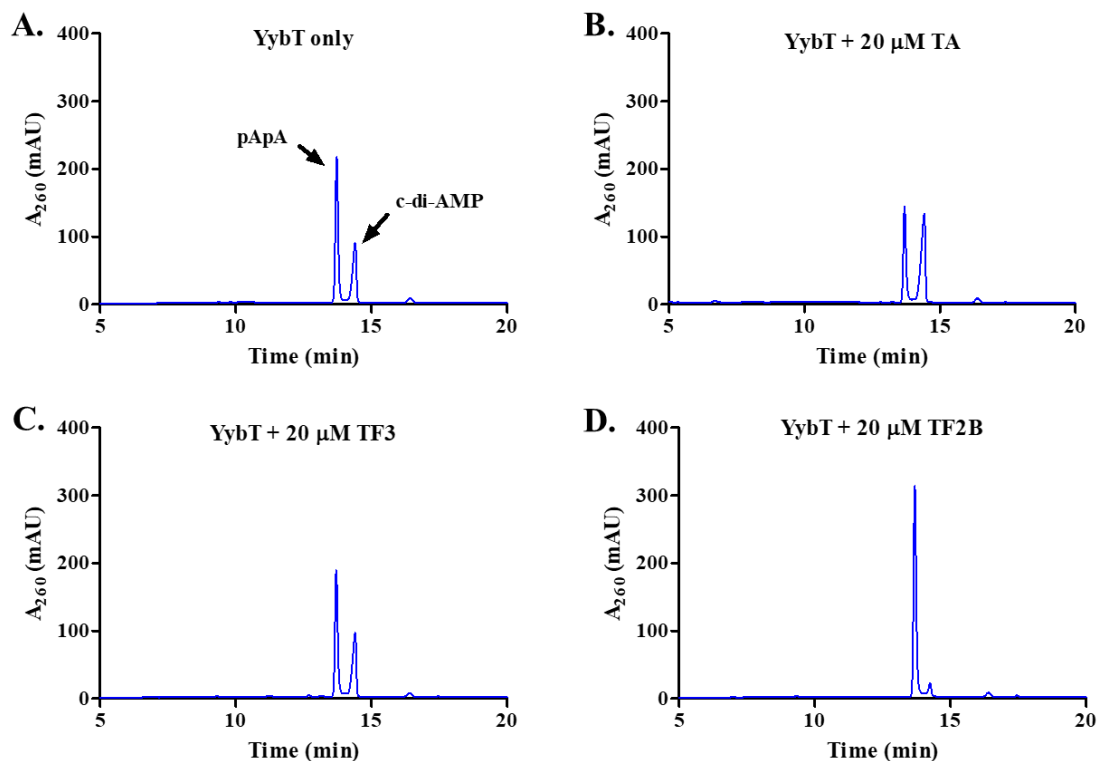


Figure 2.15. HPLC chromatogram of YybT reactions **A.** without inhibitor **B.** with 20 μM TA **C.** 20 μM TF3 and **D.** 20 μM TF2B. The pApA and c-di-AMP peaks are labeled with arrows.

2.2.2.4 Analysis of binding of TF3 to DisA

We determine the binding affinity of TF3 to DisA by measuring the intensity of DisA intrinsic fluorescence when incubated with different concentrations of TF3. When excited with light of wavelength 290 nm, DisA has intrinsic fluorescence with maximum emission at 340 nm. We found that when incubated with TF3, the fluorescence of DisA decreased (Figure 2.16). Assuming a 1:1 binding, we determined the apparent K_d of DisA (5 μM) binding to TF3 using equation (2.3).³¹ The apparent dissociation constant, K_d^{app} was estimated to be 23 μM (Figure 2.16).

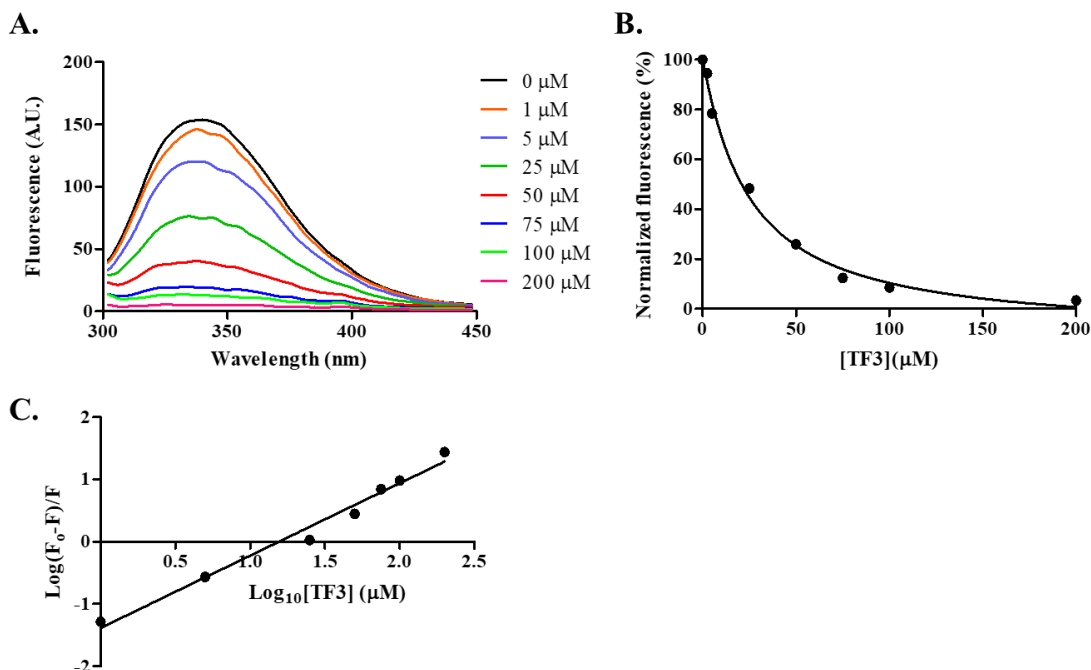


Figure 2.16. Intrinsic fluorescence analysis of DisA. **A.** Fluorescence emission trace of DisA (5 μM) in phosphate buffer (50 mM, pH 7.5) titrated with indicated concentrations of TF3 at room temperature; $\lambda_{\text{ex}} = 290 \text{ nm}$ and $\lambda_{\text{em}} = 300\text{--}450 \text{ nm}$ **B.** Plot of normalized fluorescence intensity (at 340 nm) as a function of TF3 concentration. **C.** The modified Stern-Volmer plot of DisA fluorescence quenching by TF3. F_0 is the maximum fluorescence intensity in absence of TF3 and F is the fluorescence intensity in presence of TF3. Data points represent the mean and SEM of triplicate measurements plotted using GraphPad Prism 4.0 Software.

The decrease in DisA fluorescence upon TF3 binding denote fluorescence quenching. Hence, we also used equation (2.2), the modified form of the Stern-Volmer equation²⁷ to determine the binding constant, K_a and number of binding sites, n at different inhibitor concentrations, Q (Figure 2.16). A binding constant, K_a of $4.25 \times 10^4 \text{ M}^{-1}$ was obtained and a reciprocal of this gave a dissociation constant, K_d of 23.5 μM .

This agrees with the apparent K_d initially determined from equation (2.3). The number of binding sites, n on DisA was also estimated to be approximately equal to 1, implying that DisA has a single binding site for TF3. This observation is also in agreement with the earlier 1:1 binding assumption made from equation (2.2).

2.2.3 Discussion

C-di-AMP is emerging as a central second messenger that controls various functions in bacteria. Small molecule modulators of c-di-AMP could potentially have applications in medicine, agriculture and synthetic biology. Thus far there is a paucity of small molecules that can be used to “switch” off c-di-AMP synthesis in bacteria and our goal is to identify various small molecules that could be used to inhibit DisA, a c-di-AMP synthase. Polyphenols represent a class of natural products that are primarily known for their antioxidant and antibacterial properties and we were curious to know if these interesting biologically active molecules also inhibit c-di-AMP metabolism enzymes. Indeed, there are a few literature reports that suggest that polyphenols inhibit processes in bacteria. Takahashi *et al.*⁴⁴ and Zhao *et al.*⁴⁹ have shown that polyphenols can affect bacterial cell wall. Interestingly some of these tested polyphenols also affect the c-di-AMP synthase, *vide infra*.

Tannic acid (TA), theaflavin-3'-gallate (TF2B) and theaflavin-3,3'-digallate (TF3) were found to inhibit the activity of DisA. Of the three, TA was shown to inhibit DisA better than TF3 and TF2B as depicted in Figures 2.11 – 2.13. Of note, the inhibition of DisA appeared to depend on the number of gallate moieties on a given aglycone unit. For example, TF3 was more effective than TF2B, which was also more effective than

TF1. Also, EGCG was more effective than EGC whilst GC was less effective than GCG and so on. Yet gallic acid on its own or propyl gallate did not inhibit DisA (Figure 2.11), meaning that it is not just the presence of gallate moiety *per se* that caused DisA inhibition but rather the proper spatial presentation of the gallate group that was critical for enzymatic inhibition. It has been reported that gallic acid has antimicrobial activity and it is effective against *S. mutans*, which is one of the causative agents of dental caries.⁵⁰ Our data suggests that the effect of gallic acid on bacteria is not via DisA inhibition and is probably via the inhibition of another target; it appears that the gallate moiety is indeed a polypharmacophore unit.

The dose-response curve of TA had a steep slope (Figure 2.13), a signature of a non-specific inhibitor. When tested against YybT, a PDE from *B. subtilis*, TA was found to inhibit the PDE activity of YybT (Figure 2.15). Others have also reported the inhibition of several enzymes by tannic acid. For example, TA has been shown to inhibit the activity of α -glucosidase, an enzyme targeted in the development of antidiabetic drugs⁵¹ This inhibition was observed to be stronger than that seen with the antidiabetic drug acarbose⁵¹. The study also noted the inhibitory effect on trypsin by TA.⁵¹ Yang *et al.* showed TA as a strong inhibitor of epidermal growth factor tyrosine kinase.¹¹ They also observed that the plant polyphenol inhibited other protein kinases including protein kinase C, mitogen-activated protein kinase and cAMP-dependent protein kinase.⁵² The activity of gastric H⁺,K⁺-ATPase⁵³ has also been shown to be inhibited by TA. Based on the perceived promiscuity of tannic acid and the fact that it is not drug-like, we decided to focus more on TF2B and TF3, which were observed to specifically inhibit DisA but not YybT (Figure 2.11 – 2.15). The IC₅₀

of TF3 against DisA (8.5 μM) was lower than that of TF2B (23.6 μM), highlighting the importance of the gallate moiety. Regarding the mode of inhibition, there was no direct correlation between ATP concentration and IC_{50} values TF3 (Figure 2.14), implying that TF3 might be binding to a site on DisA distinct from the nucleotide-binding domain. The binding interaction between DisA and TF3 was found to have an apparent K_d of 23 μM (Figure 2.16), which shows moderate affinity.

A number of studies have shown that polyphenols synergize with traditional cell wall-targeting antibiotics and in some cases antibiotic-resistant bacteria could become susceptible to antibiotics via polyphenol potentiation.⁵⁴⁻⁵⁶ C-di-AMP has been shown to modulate bacterial cell wall synthesis^{8, 10} so the expectation is that inhibitors of c-di-AMP synthesis could potentiate the effects of cell wall-targeting antibiotics. This work has uncovered a few polyphenols that could be used to modulate c-di-AMP in bacteria but for these molecules or analogs thereof to find practical applications, some limitations need to be addressed. Friedman *et al.* showed that black tea theaflavins possessed antibacterial activity against *B. cereus* at nanomolar levels⁵⁷. However, several other studies have reported rather high minimum inhibitory concentrations for such molecules against other bacteria.^{54, 56} The latter observation might be due to the difficulty of the molecules to enter bacteria. Use on whole animals might also be limited by rapid metabolism. Perhaps the limitation on membrane permeation could be addressed in the future via acylation of the phenolic moieties. It is likely that the acyl groups would be deprotected by esterases inside cells to uncover the active molecules. Furthermore, the essential gallate moieties are attached to the theaflavin unit *via* an ester linkage but this type of linkage is unstable towards enzymatic hydrolysis so a

more stable analog of theaflavin gallates will have to be developed. Beyond the practical application of these molecules to reduce c-di-AMP synthesis in bacteria, the molecules identified in this manuscript could be used to identify the binding site (probably an allosteric site) that would be targeted for the development of potent and specific inhibitors of DisA. Future work, beyond the scope of this paper, will be aimed at gaining structural insights into the binding mode of polyphenols to DisA and could lead to new tactics or design principles to inhibit DisA and ultimately inhibit bacterial cell wall synthesis or other processes that are regulated by DisA.

2.2.3 Methods

2.2.4.1 Protein expression and purification.

For protein expression, overnight cultures of *E. coli* containing plasmids of either DisA or YybT were inoculated into 1 L LB medium and cultured at 37 °C. At OD₆₀₀ of 0.6, the cultures were supplemented with 1 mM IPTG to induce expression and incubated at 16 °C with 250 rpm for 18 h. The induced cells were centrifuged at 4 °C and pellets resuspended in lysis buffer [50 mM sodium phosphate buffer, pH 8.0, 300 mM NaCl for DisA and 10 mM Tris-HCl, pH 8.0, 100 mM NaCl for YybT]. The resuspended cells were lysed by sonication and centrifuged at 25,000 rpm for 25 min at 4 °C. The supernatants were passed through HisTrap HP 1 mL columns (GE) and the proteins purified using the Bio-Rad NGC™ Chromatography System at a 1 mL/min flowrate. Elution of proteins was achieved by adding 200 mM imidazole to the lysis buffer. The concentrations of the purified proteins were determined by measuring their A₂₈₀.

2.2.4.2 Screening of polyphenols

The polyphenols were screened for DisA inhibition as earlier described¹⁵. Briefly, reactions containing 300 μM ATP, 10 μM coralyne, 3 mM KI, 20 μM inhibitor and 1 μM DisA in reaction buffer (40 mM Tris-HCl, pH 7.5, 100 mM NaCl and 10 mM MgCl_2) were set up in triplicates at 30 °C in 96 well plates. A Molecular Devices SpectraMax M5e plate reader was used to measure the fluorescence of coralyne with excitation and emission wavelengths of 420 nm and 475 nm respectively for 30 min with 2 min intervals.

2.2.4.3 Enzyme inhibition assays

To analyze the effect of the identified polyphenol inhibitors on DisA, HPLC reactions containing 300 μM ATP and 1 μM DisA with or without 20 μM polyphenol inhibitors were set up at 30 °C. After 30 min the reaction mixture was heated at 95 °C for 5 min and the precipitated proteins were filtered off using a 3 K centrifugal filter (VWR International). Components of the filtrate were then analyzed on a COSMOSIL C18-MS-II Packed column (5 μm) using 0.1 M TEAA in water and acetonitrile, detecting signals at room temperature with a 260 nm UV detector.

To determine the half maximum inhibitory concentration IC_{50} , triplicate reactions containing ATP (at either 100 μM , 300 μM or 500 μM), 11 nM ^{32}P -ATP and increasing concentrations of polyphenol inhibitors were mixed in reaction buffer. The reactions were then initiated by adding 1 μM DisA (or as indicated) at 30 °C for 1 hour. The radioactive components were separated by spotting 0.4 μL aliquots on TLC plates (EMD Millipore TLC Cellulose). The spots were separated using 1:1.5 (vol/vol) saturated $(\text{NH}_4)_2\text{SO}_4$ and 1.5 M KH_2PO_4 buffer.

The effect of polyphenol inhibitors on YybT was tested by setting up HPLC reactions containing 50 μM c-di-AMP and 1 μM YybT with or without 20 μM polyphenol inhibitors for 30 min at 37 °C in reaction buffer (100 mM Tris-HCl, pH 8.3, 20 mM KCl, 0.5 mM MnCl_2 and 1 mM DTT). The reactions were analyzed as described for the DisA reactions.

2.2.4.4 Fluorescence spectroscopy and binding characteristics

The binding affinity studies was performed by monitoring the protein fluorescence at 340 nm. Triplicate solutions containing various concentrations of TF3 and DisA (5 μM) were incubated at room temperature in 50 mM sodium phosphate buffer pH 7.5 for 1 hour. Fluorescence spectra were recorded on a Cary Eclipse Fluorescence Spectrophotometer (Agilent) using a 1.0 cm quartz cell. The excitation wavelength of DisA was 290 nm and emission spectra were collected from 300 nm to 450 nm. Data was analyzed using equations 2.2 and 2.3.

Chapter 3: Identification and characterization of cell-permeable c-di-AMP synthesis inhibitors

3.1 Hydroxybenzylidene-indolinones, c-di-AMP synthase inhibitors, have antibacterial and anti-biofilm activities and also re-sensitize resistant bacteria to methicillin and vancomycin

This section (3.1) was originally published as: Opoku-Temeng, C., Dayal, N., Miller, J. and Sintim, H.O. “Hydroxybenzylidene-indolinones, c-di-AMP synthase inhibitors, have antibacterial and anti-biofilm activities and also re-sensitize resistant bacteria to methicillin and vancomycin.” *RSC Adv.*, 2017, 7, 8288

3.1.1 Introduction

Each year millions of people become infected with drug-resistant bacteria and a significant number succumb to the pathogens. It has been estimated that if new antibacterial agents or adjuvants that re-sensitize resistant bacteria to traditional antibiotics are not developed/found, in the near future (by 2050) deaths due to bacterial infections will surpass 10 million.¹ In light of this gloomy forecast, several groups have embarked on the search of essential pathways or proteins that could be targeted to develop a new generation of antibacterial agents.² Recently, it was revealed that cyclic dimeric adenosine 3',5'-monophosphate (c-di-AMP), initially discovered as a ligand bound to the DNA integrity scanning protein A (DisA) of *Thermatoga maritima*,³ is an important second messenger that is present in a myriad of clinically-relevant bacteria, including *Staphylococcus aureus*,⁴ *Listeria*

monocytogenes,⁵ *Streptococcus pyogenes*,⁶ *Mycobacterium tuberculosis*,⁷ and *Chlamydia trachomatis*⁸ among others. The physiological roles of c-di-AMP include peptidoglycan homeostasis,^{9, 10} cell size regulation,⁴ fatty acid metabolism and transport,¹¹ ion transport,¹² biofilm formation¹³ and a host of other physiological processes (Figure 3.1).

C-di-AMP is synthesized by diadenylate cyclases (DACs) from two molecules of ATP (Figure 3.1). The DAC gene has been shown to be essential in some Gram-positive bacteria such as *L. monocytogenes*, *S. aureus* and *S. pneumoniae*,^{5, 10, 14, 15} and this raises the potential that new drugs against these problematic bacteria could be found by screening for inhibitors of c-di-AMP synthesis. Of note c-di-AMP regulates cell wall homeostasis^{9, 10} and because many antibiotics in clinical use also target the cell wall,¹⁶ it is anticipated that inhibitors of c-di-AMP could potentiate the action of several cell wall-acting antibiotics. In a seminal study by Gründling, it was disclosed that depletion of intracellular c-di-AMP via the over-expression of a c-di-AMP PDE (GdpP) sensitized *S. aureus* to the β -lactams oxacillin and penicillin G.⁴ The *gdpP* mutant strain was observed to have increased biofilm formation relative to the wildtype.⁴ Recently, another important work from Peng *et al.* revealed that c-di-AMP regulates biofilm formation in *S. pneumoniae*.¹³ These insights regarding the role of c-di-AMP in biofilm formation is interesting (it is known that biofilm bacteria are several orders of magnitude more resistant to antibiotics than planktonic bacteria) and could lead to new treatment paradigms against Gram-positive bacteria.¹⁷

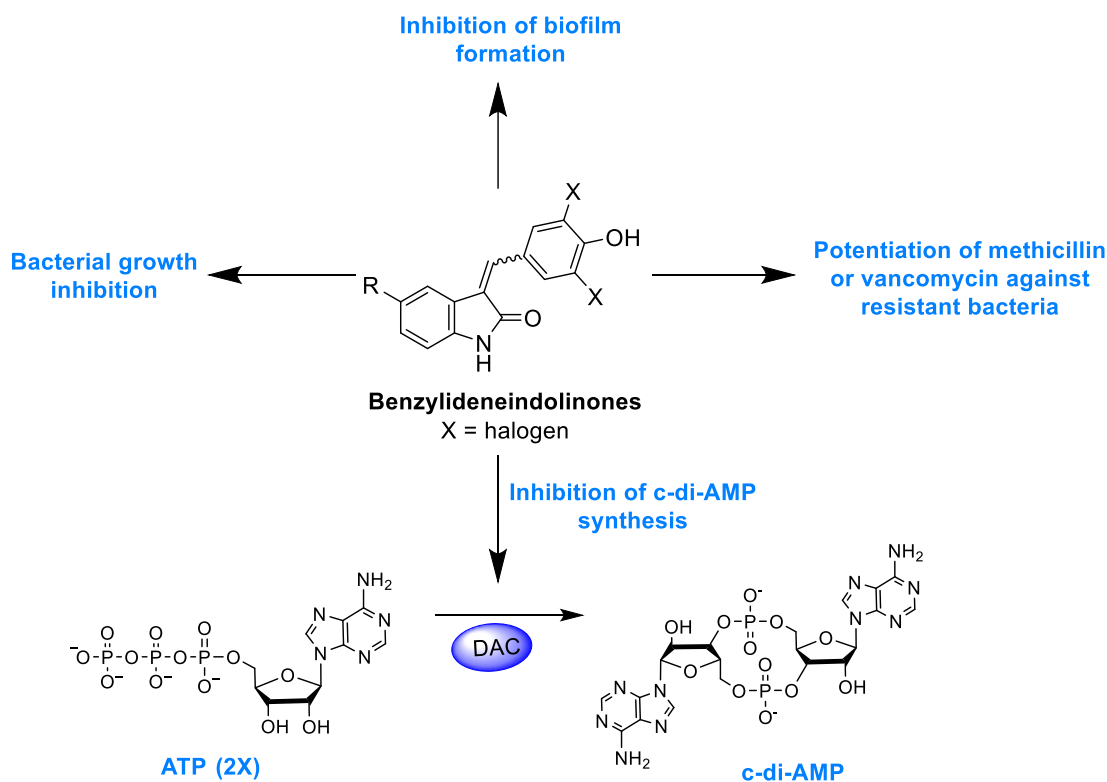


Figure 3.1. Schematic of c-di-AMP metabolism and the processes regulated by the second messenger. Hydroxybenzylidene-indolinones inhibit c-di-AMP synthesis and also possess antibacterial and anti-biofilm activities.

Motivated by the central role played by c-di-AMP in some bacteria, especially in *S. aureus*, our group has been pursuing inhibitors of c-di-AMP synthesis with the hope that some of these compounds could be developed into antibacterial agents. Previously we revealed that bromophenol-TH,¹⁸ suramin¹⁹ and theaflavin digallate²⁰ inhibit the prototypical c-di-AMP synthase, DisA. The first-generation c-di-AMP synthase inhibitors are however not drug-like. For example suramin,¹⁹ is polyanionic and suffers from poor cell penetration and the theaflavins are easily metabolized *in*

vivo.²¹ 3'-deoxyATP, a nucleotide analog was also identified as DAC inhibitor by Müller and others²² but this molecule also suffers from cell permeation (it is polyanionic as well). In our continuing efforts to identify cell-permeable compounds that also inhibit c-di-AMP synthesis, we identified a benzylidene-indolinone derivative as a cell permeable inhibitor of c-di-AMP synthesis. This molecule and analogs thereof demonstrate potent antibacterial properties and could synergize the action of other antibiotics.

3.1.2 Results and Discussion

We previously used the coralyne assay²³ (Figure 3.2) to identify bromophenol-TH,¹⁸ suramin¹⁹ and theaflavin digallate²⁰ as inhibitors of c-di-AMP synthase DisA from *B. subtilis*. Based on the success of the coralyne assay, we screened a 20,000-compound library containing pharmacologically active compounds in order to identify cell permeable inhibitors of DAC.

From the screen we identified a hydroxybenzylidene-indolinone derivative, compound **3.1** as an inhibitor of c-di-AMP synthesis (Figure 3.2). The DAC inhibition was confirmed using α -³²P-ATP assays (Figure 3.2). Compound **3.1** (GW5074), was originally developed as a selective c-Ras inhibitor. It is non-toxic to mammalian cells and has been used in a few mouse studies without showing any adverse effects.^{24, 25} Compound **3.1** possesses neuroprotective properties and in an *in vivo* model of Huntington's disease, it was shown to protect neurons via resisting 3-NP-induced striatal neurodegeneration.²⁴ Compound **3.1** was also shown to suppress sidestream smoke-induced airway hyper responsiveness in mice.²⁵ Based on its safety

profile and hence high potential for clinical translation we proceeded to make a small library of this class of molecules following the synthetic strategy shown in Figure 3.3. A total of 15 analogs with subtle changes to the indolinone and benzylidene moieties were easily synthesized (Figure 3.3) and screened for DAC inhibition.

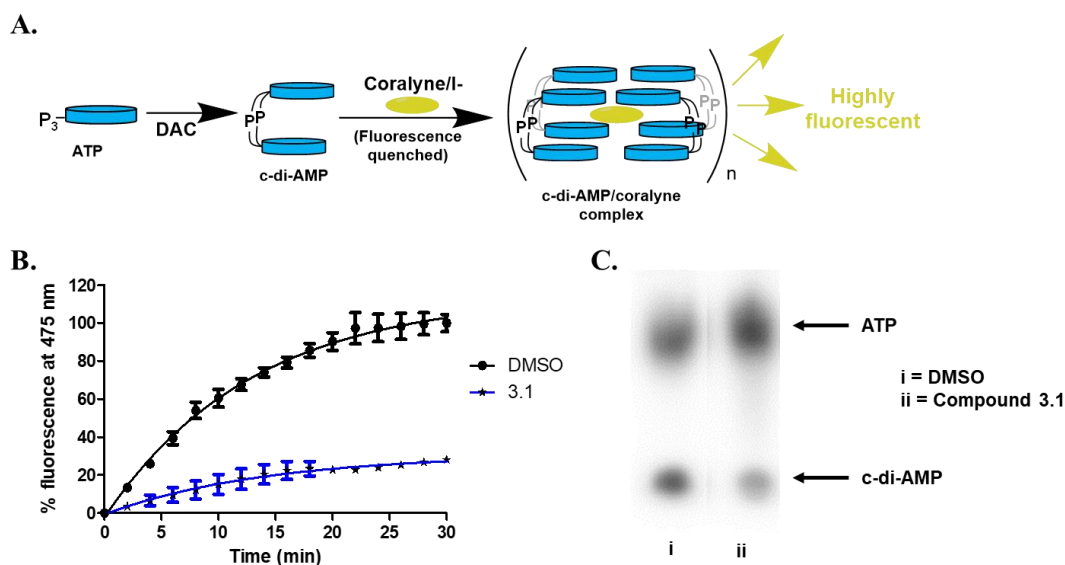


Figure 3.2. **A.** Principle of the coralyne assay detection of c-di-AMP. In the presence of c-di-AMP, coralyne fluorescence, which is otherwise quenched by iodide ions, is increased due to the formation of c-di-AMP/coralyne complex. **B.** Plot of percent fluorescence (emission 475 nm) of coralyne against time for the screening of compound **3.1** (20 μ M) against DisA (0.5 μ M). **C.** Radioactive TLC confirmation of the inhibition of DisA (0.25 μ M) by compound **3.1** (20 μ M).

The “hit” compound **3.1** is decorated with an iodo group at the 5-position of the indolinone. Compounds **3.2 – 3.9** were designed to identify which substituent at the 5-position of the indolinone core was optimal for DAC inhibition. Compound **3.2** did not have any substitution at position 5, whereas compounds **3.3** and **3.4** contained bromo and trifluoromethyl groups (both groups are similarly as hydrophobic as the iodo group). Compounds **3.3, 3.4, 3.5, 3.6** and **3.7** were 5-bromo, 5-trifluoromethyl, 5-hydroxy, 5-cyano and 5-amino substitutions respectively. Compounds **3.5 – 3.9** contained the polar groups OH (**3.5**), CN (**3.6**), NH₂ (**3.7**), CO₂Me (**3.8**) and CO₂H (**3.9**). We expected the ester group to be converted into the acid moiety inside the cell, although the ester compound (a pro-drug) could have different permeation properties than the acid. Compound **3.14** contained an iodo moiety at the 6-position of the indolinone and is ideal for comparing 5- vs. 6-substitutions of the indolinone. To investigate the importance of the bromo groups on the benzyldene portion of the molecule, we synthesized compounds **3.10 – 3.12** whereby the bromo groups were replaced with H, F and Cl. Finally, the importance of the hydroxyl group at the 4-position of the benzyldene was investigated by making compounds **3.13** and **3.15**, which did not contain a phenol or compound **3.16**, which had the OH group moved from the 4-position to the 2-position on the benzyldene. With these compounds in hand, we proceeded to investigate which compounds inhibited DisA, using the coralyne assay²³.

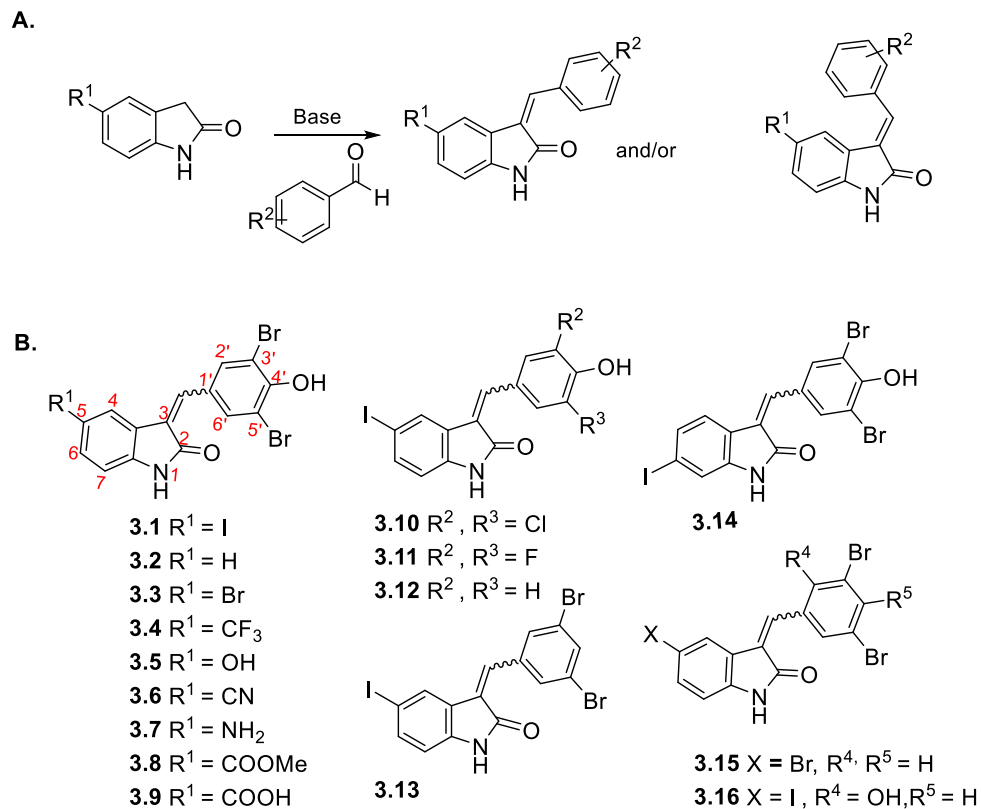


Figure 3.3. **A.** Synthetic strategy for making hydroxybenzylidene-indolinones; **B.** Structures of hydroxybenzylidene-indolinones that were synthesized.

DAC activity assay, in the presence of the synthesized compounds revealed that substitution of the indolinone moiety with hydrophilic groups (OH (**3.5**), CN (**3.6**), NH_2 (**3.7**), CO_2Me (**3.8**) and CO_2H (**3.9**)) lead to compounds that were weak DAC inhibitors. On the contrary, substitution of indolinone moiety with iodo or CF_3 group at the 5-position (compounds **3.1**, **3.4** or **3.10**) afforded potent inhibitors of DAC. At 20 μM , compounds **3.1** and **3.4** completely inhibited the synthesis of c-di-AMP by DisA (0.25 μM), see Figure 3.4.

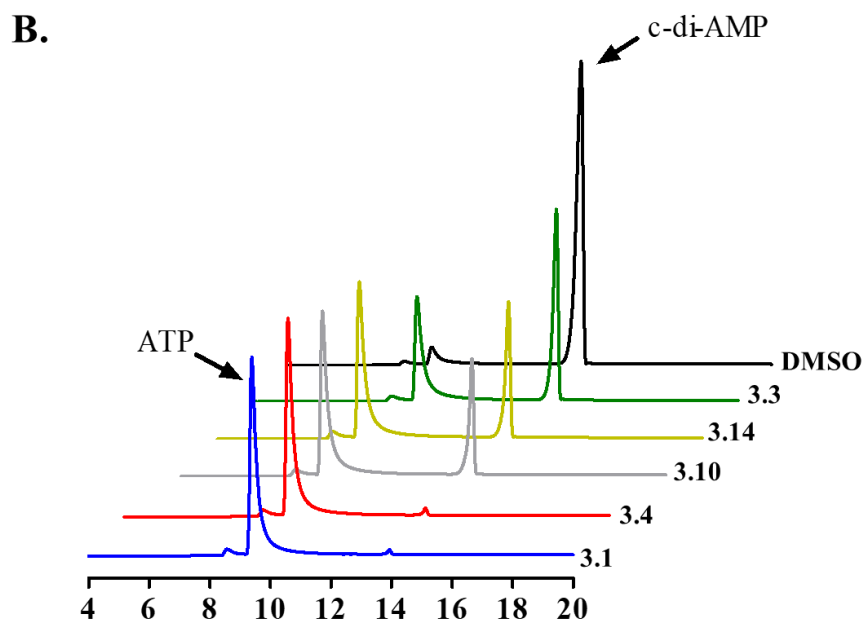
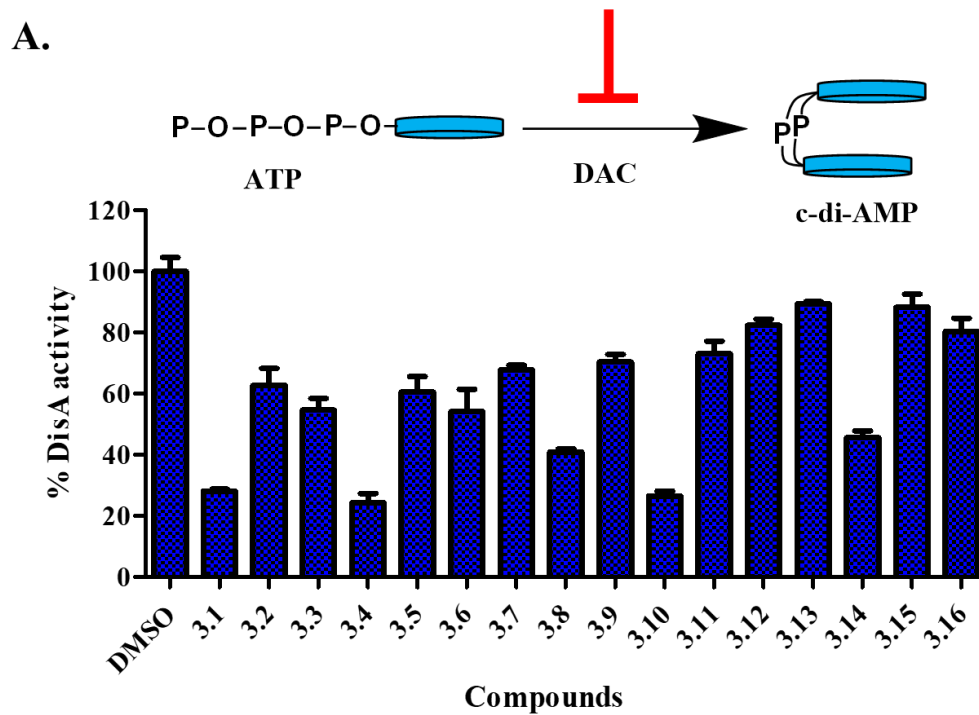


Figure 3.4. A. (Top) Schematic of inhibition of c-di-AMP synthesis. (Bottom) Percent activity of DisA (0.5 μ M) in the presence of hydroxybenzylidene-indolinones (20 μ M) as determined by coralyne assay after 30 min of reaction. Each bar is the mean

of 3 replicates and error bars represent standard error of the mean. Plots were generated using GraphPad Prism version 5 statistical software. **B.** HPLC analysis of synthesis of c-di-AMP by DisA (0.25 μ M) in the presence of selected benzylidene-indolinones (20 μ M). ATP and c-di-AMP peaks are at 9 min and 14 min respectively.

The substitution pattern of the benzylidene group was also critical for DAC inhibition. The 4-OH group on the benzylidene group was essential as compound **3.15**, which lacked OH group or compound **3.16**, bearing 2-OH (but not 4-OH) did not inhibit c-di-AMP synthesis. The nature of the halogen on the benzylidene moiety was also critical for DAC inhibition. Substitution of positions 3 and 5 of the benzylidene with Br or Cl afforded DAC inhibitors (compounds **3.1** and **3.10**) whereas compounds bearing H or F substituents at the 3 and 5 positions of the benzylidene were not active (compounds **3.11** and **3.12**) (Figures 3.4 and 3.5).

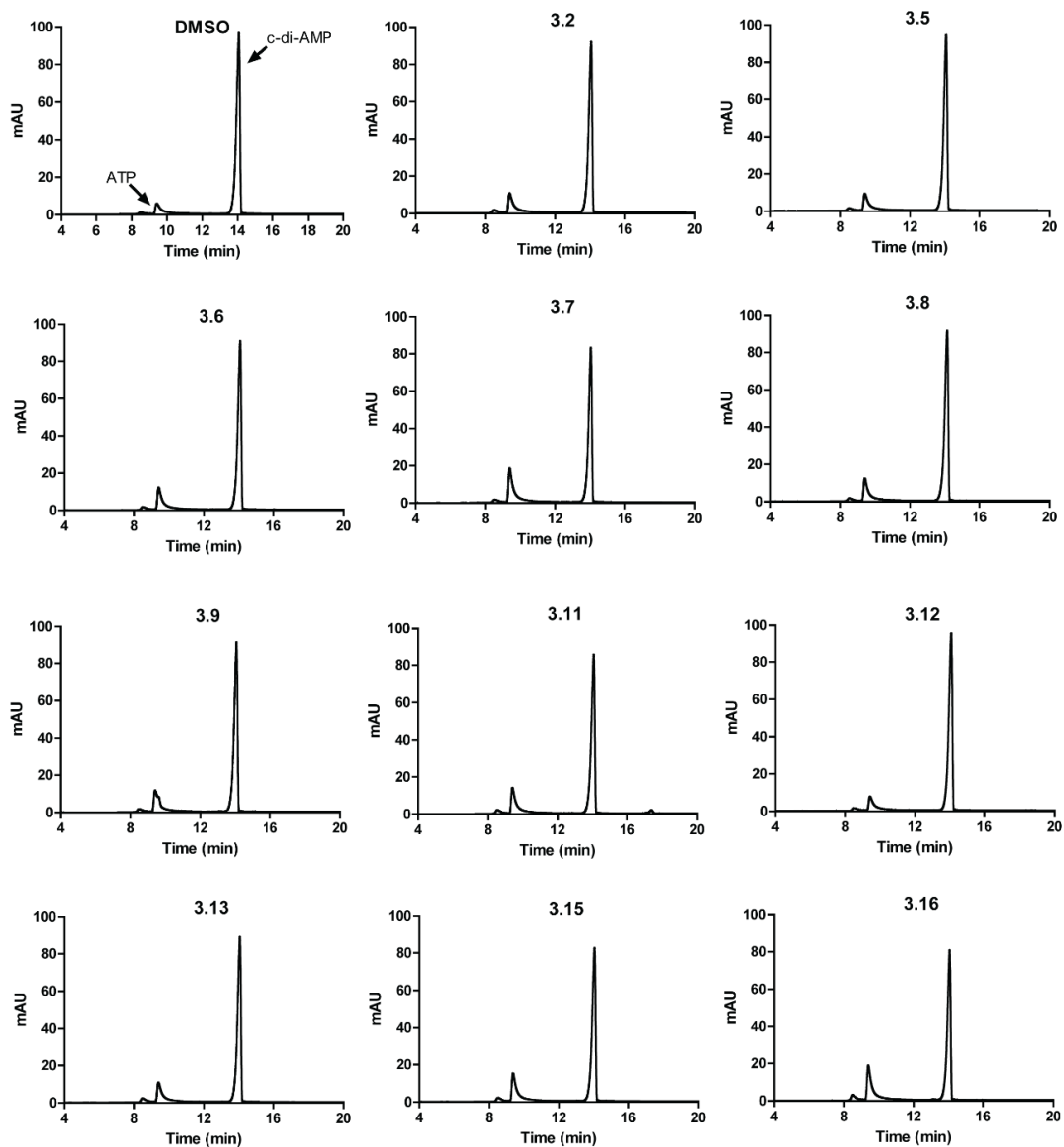


Figure 3.5. HPLC analysis of benzylideneindolinones that did not inhibit DAC activity of DisA. Compounds were tested at 20 μ M in a 40 mM Tris-HCl pH 7.5, 100 mM NaCl and 10 mM MgCl₂ reaction buffer with 100 μ M ATP and 0.25 μ M DisA for 2 h. ATP and c-di-AMP peaks are as indicated on DMSO control.

As previously stated, a myriad of physiological processes are regulated by c-di-AMP signaling, such as cell wall homeostasis^{9, 10} and coupled with the essentiality of DACs of human pathogens,^{5, 10, 14, 15} we hypothesized that cell permeable inhibitors of c-di-AMP synthesis, such as the ones identified above could also possess antibacterial properties. We therefore decided to investigate the effects of the hydroxybenzylidene-indolinones compounds on bacterial viability. Initially, we screened the compounds against *S. aureus* (ATCC 25923) and *E. coli* (ATCC 25923) (as representative Gram-positive and Gram-negative bacteria). The bacteria were cultured in the presence of 16 µg/mL of the hydroxybenzylidene-indolinones in Mueller Hinton broth (MHB) for 24 h at 37 °C with 250 rpm shaking. Post incubation, we measured the optical density at 600 nm (OD₆₀₀) of the cultures. For each bacterial species, an equivalent amount of DMSO, not exceeding 0.1% was used as negative control. Compounds **3.1**, **3.2**, **3.3**, **3.4**, **3.10** and **3.14** (but not compounds **3.5 – 3.9** or **3.11 – 3.13** or **3.15 – 3.16**) significantly inhibited the growth of *S. aureus*. None of the compounds affected *E. coli* growth (Figure 3.6).

To rule out the possibility that the lack of activity against *E. coli* was not due to permeation issue, we also investigated the activity of compound **3.1** (16 µg/mL) in the presence of ¼ the MIC value of colistin (0.03125 µg/mL). Treating *E. coli* with ¼ the MIC of colistin (a non-toxic concentration) would make the bacteria permeable to compounds. Even in the presence of colistin, compound **3.1** did not inhibit the growth of *E. coli* (Figure 3.6). This experiment suggests that the hydroxybenzylidene-indolinones work via a Gram-positive specific mechanism. For the active compounds, we expanded the panel of bacteria to include *L. monocytogenes* (ATCC 19115) and

Pseudomonas aeruginosa (ATCC 27853) and also observed that they were active against the Gram-positive *L. monocytogenes* but not against the Gram-negative *P. aeruginosa* (Figure 3.6).

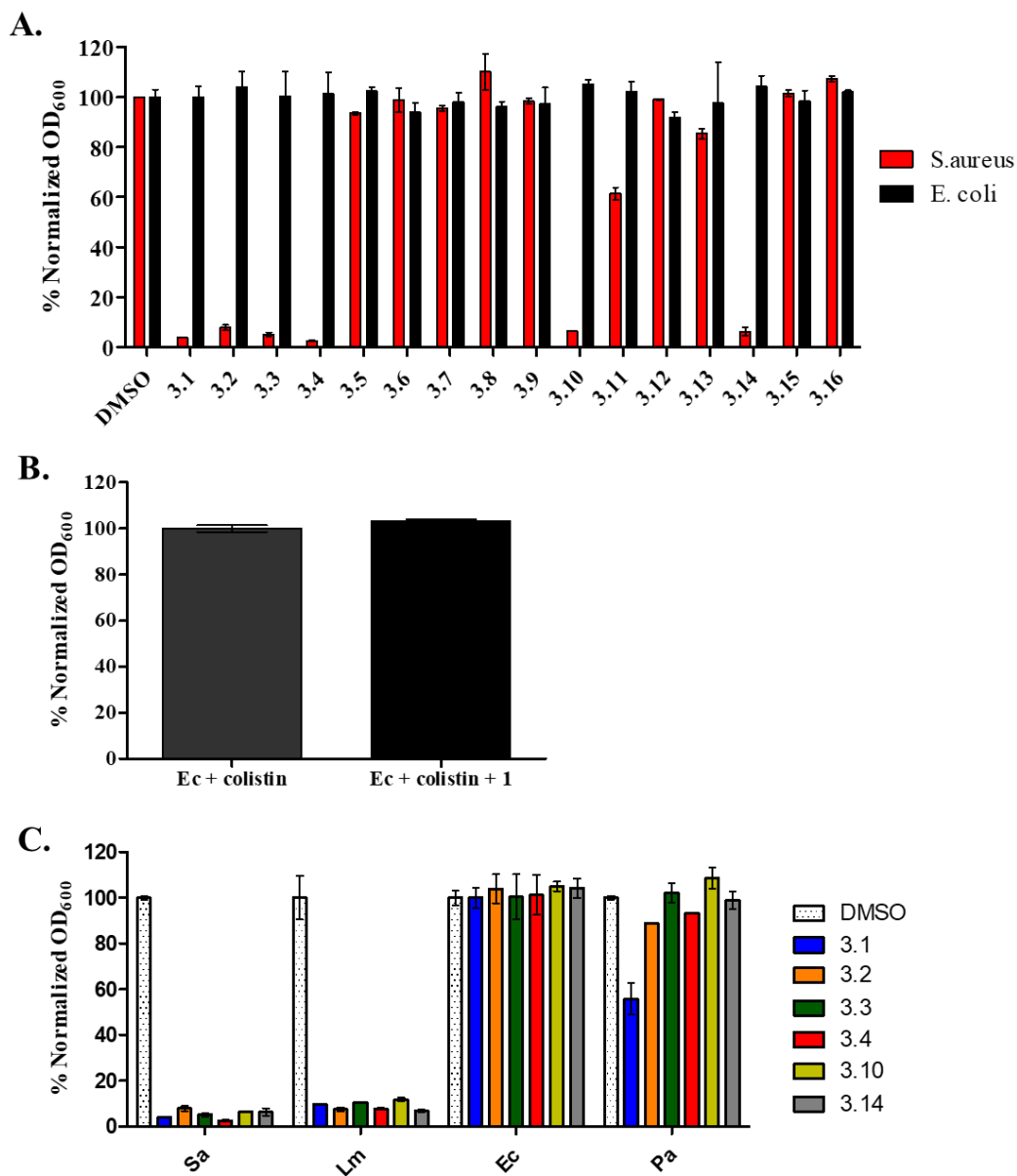


Figure 3.6. Antibacterial activities of DAC inhibitors tested at 16 $\mu\text{g}/\text{mL}$ in MHB. **A.** Evaluation of compounds 3.1 – 3.16 against *S. aureus* and *E. coli*. **B.** Activity of compound 1 against *E. coli* in the presence of colistin (0.03125 $\mu\text{g}/\text{mL}$). **C.** Selected

active compounds against *S. aureus* (Sa), *L. monocytogenes* (Lm), *E. coli* (Ec) and *P. aeruginosa* (Pa). Every bar is the mean of 2 replicates and error bars represent the standard error of the mean. Plots were generated using GraphPad Prism version 5 statistical software.

Having established the susceptibility of bacteria to the compounds, we sought to determine their minimum inhibitory concentration (MIC). For this we also included antibiotic resistant strains MRSA ATCC 33592 and vancomycin-resistant *E. faecalis* (ATCC 51575). The MIC values obtained are as shown in Table 3.1.

All compounds had good MIC values against *S. aureus* and MRSA, ranging from 4 µg/mL to 16 µg/mL but not against VRE faecalis. Compounds **3.4**, **3.10** and **3.14** appeared to be particularly potent against *L. monocytogenes*, with MIC values ranging from 2 µg/mL to 4 µg/mL (Table 3.1).

Table 3.1. MIC values of active hydroxybenzylidene-indolinones against select bacteria

Test compounds	MIC (µg/mL)			
	<i>S. aureus</i>	MRSA	<i>L. monocytogenes</i>	VRE faecalis
3.1	8	8	8	16
3.2	8	16	16	128
3.3	8	8	16	>128
3.4	8	4	2	32
3.10	8	4	2	64
3.14	4	4	4	>128
Vancomycin	1	1	1	>128
Methicillin	2	>128	ND	ND

ND represents Not determined

As earlier stated, biofilm-associated infections continue to be a major public health threat. Biofilms in general are difficult to treat, due in part to the reduced penetration of antibiotics into the biofilm.²⁶ Very recently Peng *et al.* demonstrated that the deletion of *pdeA*, gene that encodes the *S. pneumoniae* PDE resulted in an increased *S. pneumoniae* biofilm formation.¹³ Also, Gründling and colleagues showed that in *S. aureus*, deletion of GdpP (PDE) resulted in increased biofilm formation relative to wildtype.⁴ These observations implicated c-di-AMP signaling in regulating biofilm formation.^{4, 13} A report by the United States Centers for Disease Control and Prevention in 2013, characterized MRSA as being at the threat level of serious; implying that these require immediate attention.²⁷ Staphylococcal infections are problematic in the healthcare setting primarily as a result of biofilm formation on host tissues, implants and medical devices.²⁸ Others have pursued small molecules that inhibit MRSA biofilm formation.^{29, 30} Motivated by these studies, we tested all 16 compounds for their effect on MRSA biofilm formation. The microtiter plate biofilm formation³¹ was employed using compounds at concentrations ranging from 16 µg/mL to 0.03125 µg/mL. We observed that 6 compounds (**3.1**, **3.2**, **3.3**, **3.4**, **3.10** and **3.14**) potently inhibited biofilm formation (Figure 3.7). The IC₅₀ values for biofilm inhibition for the compounds were 0.19 µg/mL for compound **3.1**; 0.11 µg/mL for compound **3.2**; 0.81 µg/mL for compound **3.3**; 0.69 µg/mL for compound **3.4**; 0.70 µg/mL for compound **3.10** and 0.40 µg/mL for compound **3.14** (Figure 3.7). The concentration of maximum biofilm inhibition, IC₁₀₀, (Figure 3.7) were observed to be similar to the MIC values (Table 3.1), implying that the anti-biofilm activities were derived from growth inhibition.

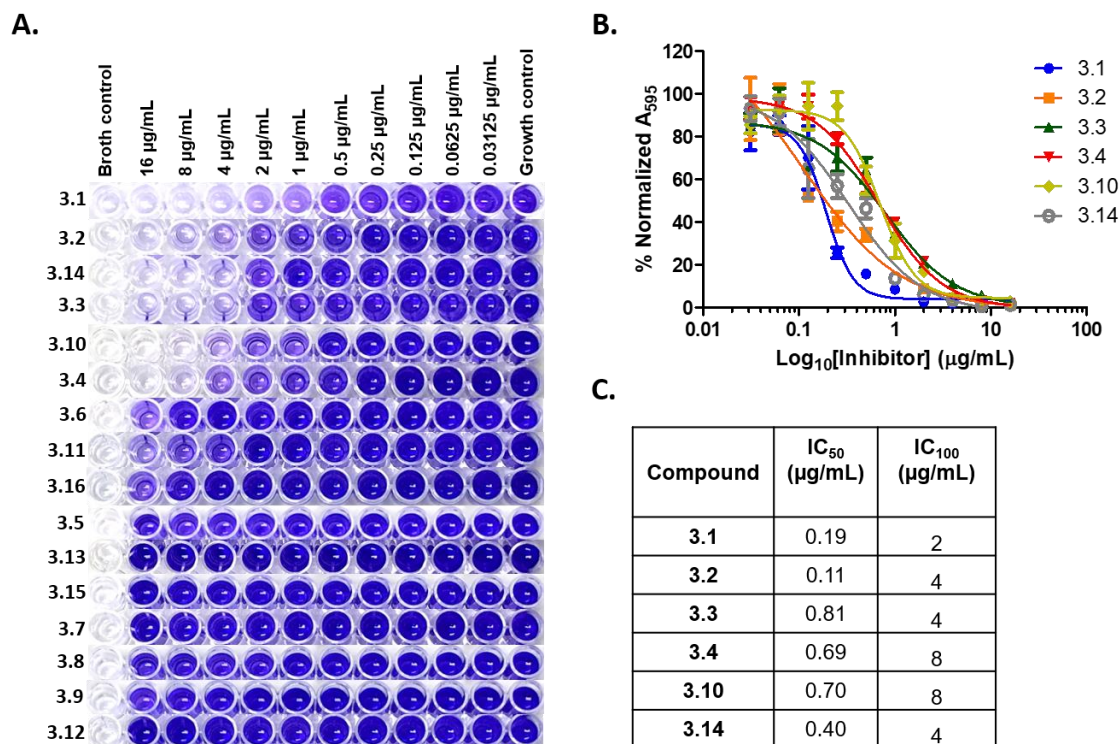


Figure 3.7. Inhibition of MRSA ATCC 33592 biofilms. **A.** Representative wells of crystal violet stained biofilms of MRSA ATCC 33592. Compounds tested are as labelled to the left and the concentrations used are indicated on top. **B.** IC₅₀ curves and **C.** table of IC₅₀ and IC₁₀₀ values of biofilm inhibition by hydroxybenzylidene-indolinones. Every data point is the mean of 4 replicates and error bars represent the standard error of the mean. Plots were generated using GraphPad Prism version 5 statistical software (La Jolla, CA, USA).

‘Resurrecting’ antibiotics that have been rendered ineffective due to resistance by combining them with small molecules “adjuvants” is now being pursued as a strategy to combat antibiotic resistance.³²⁻³⁴ Recently several groups have reported several small molecules that could re-sensitize MRSA or VRE to β -lactams or vancomycin

respectively.³⁵⁻³⁸ Having observed that the compounds were active against MRSA and VRE faecalis, we investigated the ability of hydroxybenzylidene-indolinones to re-sensitize MRSA and VRE faecalis to methicillin and vancomycin respectively. MRSA is resistant to methicillin with an MIC of greater than 128 $\mu\text{g/mL}$. In the presence of 2 $\mu\text{g/mL}$ of compound **3.1** and **3.4**, an MIC of 2 $\mu\text{g/mL}$ was obtained for methicillin against MRSA; signifying a fold change in MIC of greater than 64-fold (Table 3.2). Compounds **3.3** and **3.10** also reduced the MIC of methicillin by greater than 32-fold from >128 $\mu\text{g/mL}$ to 4 $\mu\text{g/mL}$.

Table 3.2. Potentiation of methicillin and vancomycin by hydroxybenzylidene-indolinones

Resistant Bacteria	Antibiotic-compound combinations	MIC ($\mu\text{g/mL}$)	Fold change
MRSA	Methicillin (Meth)	>128	NA
	Meth + 3.1 ^a	2	>64
	Meth + 3.3 ^a	4	>32
	Meth + 3.4 ^a	2	>64
	Meth + 3.10 ^a	4	>32
VRE faecalis	Vancomycin (Van)	>128	NA
	Van + 3.1 ^b	2	>64
	Van + 3.3 ^c	2	>64
	Van + 3.4 ^c	2	>64
	Van + 3.10 ^c	2	>64
	Van + 3.14 ^c	1	>128

a = 2 $\mu\text{g/mL}$, *b* = 4 $\mu\text{g/mL}$ and *c* = 8 $\mu\text{g/mL}$ of compound NA stands for Not Applicable

Similarly, the MIC of vancomycin for VRE faecalis was determined to be greater than 128 $\mu\text{g/mL}$. When combined with compound **3.1** at 4 $\mu\text{g/mL}$ (1/4 MIC) we observed a greater than 64-fold improvement in MIC of vancomycin (Table 3.2). On their own, compounds **3.3**, **3.4**, **3.10** and **3.14** have weak activity against VRE faecalis (Table 3.1). Interestingly, at 8 $\mu\text{g/mL}$ of **3.3**, **3.4** and **3.10**, the MIC of vancomycin improved by greater than 64-fold. At that same concentration we observed that compound **3.14** could reduce the MIC of vancomycin for VRE faecalis from >128 $\mu\text{g/mL}$ to 1 $\mu\text{g/mL}$ (Table 3.2). In both instances, we observed that compound **3.2** could not potentiate the activity of either methicillin or vancomycin. Due to the interesting biological activities displayed by these compounds, we attempted to generate bacteria that were resistant to these compounds in order to confirm the mechanism of action. Unfortunately, we have been unable to generate mutants that are resistant to these compounds, despite numerous efforts, in order to identify mechanism of action.

3.1.3 Conclusions

In our continual efforts to identify compounds that inhibit cyclic dinucleotide signalings^{17, 39} we uncover hydroxybenzylidene-indolinones as new inhibitors of c-di-AMP synthesis *in vitro*. Interestingly these compounds could potentiate resistant bacteria to methicillin and vancomycin. Further work in our laboratory is focused on lead optimization to arrive at more potent analogs of the compounds reported in this manuscript.

3.1.4 Methods

3.1.4.1 General synthesis of hydroxybenzylidene-indolinones

GW5074 was purchased from Cayman Chemicals (Ann Arbor, MI, USA). Analogs of GW5074 were synthesized by Dr. Neetu Dayal (postdoctoral fellow) and Jacob Miller (undergraduate researcher).

3.1.4.2 Bacterial strains and growth conditions

Standard strains of *S. aureus* (ATCC 25923 and MRSA ATCC 33592), *L. monocytogenes* ATCC 19115, vancomycin-resistant *E. faecalis* ATCC 51575, *E. coli* ATCC 25922 and *P. aeruginosa* ATCC 27853 were routinely cultured in Mueller–Hinton broth 37°C unless otherwise stated.

3.1.4.3 Protein expression and purification

The enzyme used in this study were expressed from *E. coli* BL21 (DE3) cells harboring specific plasmids³. Briefly, protein expression was induced at OD₆₀₀ of 0.6 by the addition of 1 mM isopropyl β-D-1-thiogalactopyranoside (IPTG) and the culture temperature reduced to 16 °C. Expression was performed for 18 hours after which cultures were centrifuged at 5000 rpm for 15 min at 4 °C. The cell pellets were then resuspended in lysis buffer (50 mM sodium phosphate buffer, pH 8.0, 300 mM NaCl) and lysed by sonication. The supernatant of the lysate was collected by centrifugation and proteins were purified by nickel affinity chromatography. Aliquots of purified proteins were stored in 10% glycerol at – 80 °C.

3.1.4.4 Screening

The screening was performed using the coralyne assay as previously described.¹⁸ Briefly, the compounds were stored as 10 mM DMSO stock solutions. Aliquots of the compounds (20 μ M) or DMSO were added to a reaction mixture containing 10 μ M coralyne, 300 μ M ATP and 3 mM KI in a 40 mM Tris-HCl pH 7.5, 100 mM NaCl and 10 mM MgCl₂ reaction buffer. We then initiated the reactions by adding DisA at 0.5 μ M and incubated at 30 °C. The change in coralyne fluorescence at 475 nm when excited at 420 nm was monitored on a BioTek Cytation 5 Cell Imaging Multi-Mode Reader for 30 min. Compounds that reduced the fluorescence of coralyne were selected and further analysed by HPLC. The reaction components (as above but without coralyne and KI) were mixed up 30 °C. After 2 hours, the reaction was heated at 95 °C for 5 min and the precipitated proteins were filtered off. Components of the filtrate were then analyzed on a COSMOSIL C18-MS-II Packed column (5 μ m) using 0.1 M TEAA in water (Buffer A) and acetonitrile (Buffer B). The samples will be eluted with 99 % \rightarrow 87 % Buffer A at 0 to 16 min, 87 % \rightarrow 10 % Buffer A at 16 to 22 min and kept at 10% Buffer A till 25 min, detecting signals at room temperature with a 260 nm UV detector.

For radioactive TLC assay, compound 1 (20 μ M) was incubated with 100 μ M ATP, 11.1 nM ³²P-ATP and DisA (0.25 μ M) in the same reaction buffer as above for 2h. An equal volume of DMSO was used as control. Aliquots of the reaction were spotted on TLC plates and separated using a saturated (NH₄)₂SO₄ and 1.5 M KH₂PO₄ buffer. The spots were imaged on a Typhoon FLA 9500 scanner.

3.1.4.5 Effect of hydroxybenzylidene-indolinones on bacterial viability

The effect on the growth of *S. aureus*, *L. monocytogenes*, *P. aeruginosa* and *E. coli* strains was determined by assessing culture turbidity after 24 h. Briefly, overnight cultures of the bacteria were diluted 1:10000 in MHB and cultured for 2-3 h (early exponential) at 37 °C. Aliquots were then dispensed into sterile glass tubes containing stock solutions of compounds in DMSO to yield a final concentration of 16 µg/mL. For the *E. coli* with colistin experiment, 0.03125 µg/mL colistin was added to the cultures before adding either compound 1 or an equal volume of DMSO. The cultures were incubated at 37 °C for 24 h and the OD₆₀₀ of each culture was measured using a BioTek Cytation 5 Cell Imaging Multi-Mode Reader.

3.1.4.6 Minimum inhibitory concentration and synergy assays

The MIC of active compounds were determined according to the guideline of the Clinical and Laboratory Standards Institute (CLSI). Cation-adjusted Mueller-Hinton broth was routinely used. Aliquots of 0.5 McFarland standardized inoculum were dispensed into wells of 96 well plate to 5×10^5 CFU/mL with test compounds at final concentrations from 128 µg/mL to 0.5 µg/mL. Vancomycin and methicillin were routinely used as the antibiotic control and was tested within the same range of concentrations. The cultures were incubated at 35 °C for 20 h after which wells were visually inspected for turbidity. The MIC was defined as the lowest concentration of compound or antibiotic to result in no visible growth.

For synergy assay, compounds were serially diluted along the ordinate of a 96 well plate whilst methicillin or vancomycin was diluted along the abscissa of same microtiter plate. MRSA and VRE were standardized by the 0.5 McFarland standard

and aliquoted into respective wells. The plates were incubated in a static incubator at 37 °C for 18 – 20 hours before the MIC was determined.

3.1.4.7 Biofilm studies

MRSA biofilm inhibition was performed in tissue culture treated 96 well plates (CellTreat Sci. Pdt, MA, USA). Overnight cultures of MRSA ATCC 33592 were diluted 1:100 in fresh tryptic soy broth (TSB) supplemented with 1% glucose. The diluted culture was inoculated into wells with compound (at 8 µg/mL to 1 µg/mL). The plates were incubated at 37 °C for 24 h after which the medium was carefully removed, and the unattached cells washed away. The biofilms were stained with 0.1 % crystal violet for 30 min. The crystal violet was removed, and wells washed until no crystal violet was present in the wash. The dye was solubilized with 100% ethanol for 1 h and the biofilm mass was quantified by measuring absorbance at 595 nm on a BioTek Cytation 5 Cell Imaging Multi-Mode Reader. The A₅₉₅ value for any absorbance reading, A was normalized to the no compound (A_T) and broth (A_o) controls using the equation

$$\% \text{ Normalized } A_{595} = \left(\frac{A - A_o}{A_T - A_o} \right) \times 100$$

3.1.4.8 Antibiotic- hydroxybenzylidene-indolinones combination analysis

We used the standard checkerboard assay to determine the ability of the hydroxybenzylidene-indolinones to potentiate the activity of antibiotics (methicillin and vancomycin)⁴⁰. Briefly, the antibiotics were serially diluted along the abscissa of a 96 well microtiter plate to achieve a starting concentration of 128 µg/mL whilst the hydroxybenzylidene-indolinones were diluted along the ordinate. An inoculum equal

to a 0.5 McFarland turbidity standard was prepared for both MRSA ATCC 33592 and VRE faecalis ATCC 51575 in sterile saline. Aliquots of the standardized inoculum were dispensed into the microtiter plates to give 5×10^5 CFU/mL. The plates were then incubated at 35 °C for 20h. Guided by the MIC values of the compounds and antibiotics, we calculated the fold change for wells with no visible turbidity.

Chapter 4: Proteomic analysis of bacterial response to a 4-hydroxybenzylidene indolinone compound, which re-sensitizes bacteria to traditional antibiotics

This chapter constitutes a manuscript under preparation. The initial proteomics data acquisition was done by Dr. Uma Aryal, manager of the Proteomics Core Facility of Bindley Bioscience Center at Purdue University. I performed all other experiments and bioinformatics analysis of proteomics data.

4.1 Introduction

Shortly after the introduction of antibiotics into clinical use, bacteria that were resistant to them¹ were identified. Antibiotic resistance is now widespread and consequently infections caused by antibiotic-resistant bacteria and deaths related to such infections continue to surge, particularly in healthcare settings. Currently, deaths due to infections caused by drug-resistant bacteria claim the lives of ~700,000 people yearly and this is estimated to reach 10 million by 2050.^{2,3} Clearly, there is a need for measures to be put in place to delay if not stop the onset of the ‘post-antibiotic era’.⁴ The discovery of novel antibiotics has significantly decreased, probably due to the closure of antibiotic discovery programs at major pharmaceutical companies and/or the fact that most “low hanging” antibacterial targets have now been targeted.^{5,6} In the absence of bacterial resistance, many traditional antibiotics are capable of clearing infections. Therefore antibiotic adjuvants, compounds that have little to no bactericidal or static properties themselves but enhance the activity of established antibiotics could improve bacterial infection management.^{7,8} Significant efforts have been directed towards the identification of small molecules with antibiotic adjuvant properties.^{7,9} An example of successful application of an antibiotic adjuvant is the combination of β -lactams with β -lactamase inhibitors, such as Augmentin

(amoxicillin + clavulanic acid).⁷ Drug resistance in bacteria could also be thwarted by using antibiotic combination therapy.^{10, 11} The synergistic effect obtained from combining two or more antibiotics stems from the fact that simultaneous mutation of two or more targets in bacteria is slower than mutation of a single target.¹¹ The combination of a novel antibiotic with an established drug leverages the pre-existing pharmacological profiles of the approved antibiotic and reduces the risk of translating two novel compounds with unknown pharmacological properties.¹²

We recently reported that GW5074 (compound **3.1**), an inhibitor of cyclic diadenylate monophosphate (c-di-AMP) synthase, re-sensitized methicillin-resistant *Staphylococcus aureus* (MRSA) and vancomycin-resistant *Enterococcus faecalis* (VRE) to methicillin and vancomycin respectively.¹³ Initial attempts to generate resistance strains to compound **3.1** failed and so we rationalized that compound **3.1** kills bacteria or synergizes with other antibiotics via the targeting of an essential target (such as c-di-AMP synthase) or multiple pathways (it is difficult for resistant clones to emerge if multiple essential targets are inhibited). Efforts that delineate the mechanism(s) of compounds, which re-sensitize bacteria to traditional antibiotics, could reveal new tactics to deal with the challenge of antibiotic resistance.

4.2 Results

4.2.1 Compound **3.1** and related analogs reduce cellular c-di-AMP levels

We previously showed that 4-hydroxybenzylidene indolinones (Figure 4.1) which inhibited c-di-AMP synthesis *in vitro* and also possessed antibacterial activity against staphylococcal strains.¹³ This prompted us to investigate whether the antibacterial

activity of such compounds could be at least in part due to their effect on cellular c-di-AMP levels. *E. coli* harboring a plasmid encoding the DAC from *S. aureus*, DacA was has been used to evaluate the c-di-AMP synthesis activity of *S. aureus* DacA. This allows to leverage the fact that *E. coli* does not produce c-di-AMP¹⁴ and that the compounds were not active against *E. coli*. Interestingly, all compounds could reduce the cellular levels of c-di-AMP produced by SaDacA relative to the DMSO control (Figure 4.1). Although we did not have access to purified SaDacA, this observation points to an inhibition of the enzyme activity by the compounds. Compounds that decrease the intracellular concentration of the similar but distinct c-di-GMP in Gram-negative bacteria have been previously documented.^{15, 16} To the best of our knowledge, DAC inhibitors that also reduce cellular c-di-AMP levels have not been previously demonstrated.

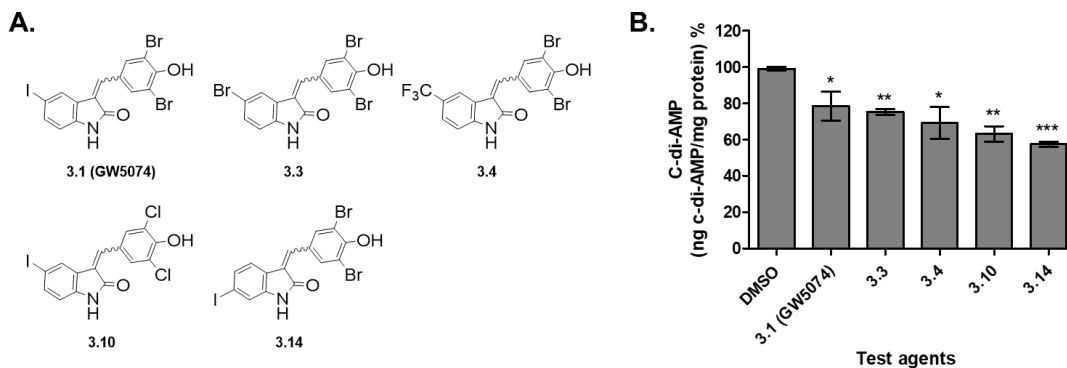


Figure 4.1. Effect of 4-hydroxybenzylidene-indolinones on the intracellular concentration of c-di-AMP. DacA protein expression was induced in exponentially growing *E. coli* and the cells were treated with 16 $\mu\text{g/mL}$ of test compounds for 3 hours. C-di-AMP was extracted using acetonitrile:methanol:water (2:2:1, v/v) extraction solvent and quantified by LC-MS/MS. **A.** Structures of compounds analyzed. **B.** Percent c-di-AMP extracted from *E. coli* harboring *S. aureus* DacA

(SaDacA) plasmid in the presence of 16 µg/mL of compounds. Experiments were performed in triplicate, and the mean ± SD values are shown in each bar. * $P < 0.05$; ** $P < 0.001$; *** $P < 0.0001$ relative to DMSO treatment.

4.2.2 Compound **3.1** synergizes with antibiotics of different classes

One of the interesting observations about the antibacterial activities of compound **3.1** and related compounds was that they could potentiate methicillin and vancomycin against MRSA and VRE.¹³ Considering that methicillin and vancomycin are both cell wall targeting antibiotics, we wondered whether the synergistic activity was limited to cell wall targeting antibiotics. The checkerboard assay¹⁷ was used to probe interactions between compound **3.1** and 10 other antibiotics in MRSA ATCC 33592 and vancomycin-resistant *E. faecalis* ATCC 51575 (VRE). In both bacteria pathogens, synergy was observed with the cell wall-targeting antibiotics ampicillin, ceftriaxone, cloxacillin and methicillin as well as the cell membrane-targeting antibiotic colistin (Figure 4.2). Of note, based on their fractional inhibitory concentration indexes, the synergy with ampicillin, cloxacillin and methicillin appeared to be better against MRSA than VRE. On the other hand, ceftriaxone and colistin had lower FIC indexes against VRE than MRSA when combined with compound **3.1**. Vancomycin was found to synergize with compound **3.1** only in the VRE strain (Figure 4.2). The aminoglycosides, gentamicin and kanamycin, which inhibit protein synthesis, synergized with compound **3.1** in both MRSA and VRE strains (Figure 4.2). The DNA synthesis inhibitor ciprofloxacin and folic acid

synthesis inhibitor trimethoprim only synergized with compound **3.1** in the tested MRSA strain (Figure 4.2).

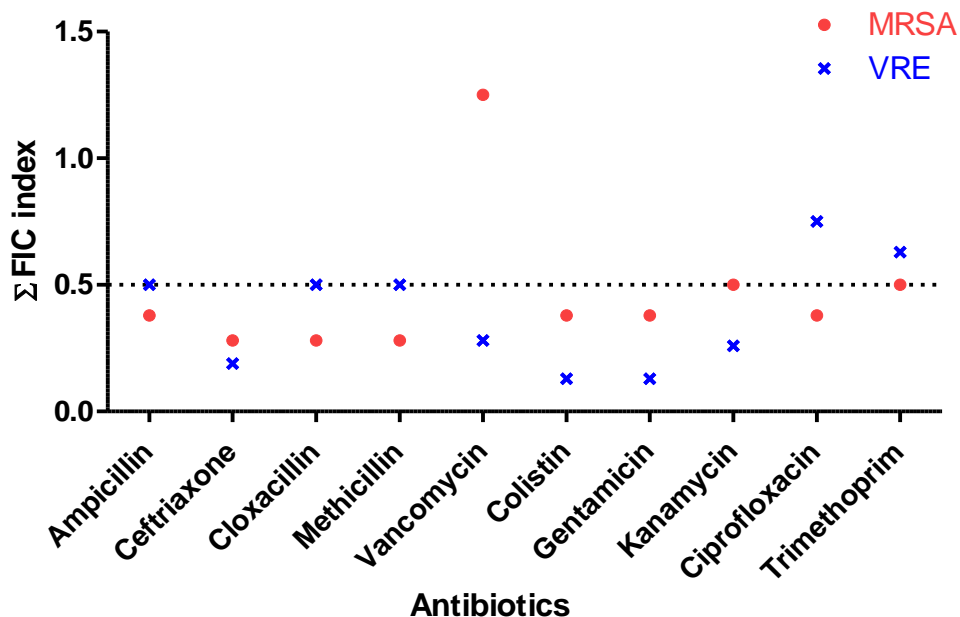


Figure 4.2. Interactions between compound **3.1** and 10 antibiotics in MRSA and VRE. Plot of Σ FIC indices of various antibiotics tested in combination with compound **3.1** against MRSA (red) and VRE (blue). The checkerboard assay was used to determine the types of interactions existing between compound **3.1** and antibiotics with different modes of action. From the FICI values, synergy was defined as Σ FICI: ≤ 0.5 , additive was Σ FICI: > 0.5 and ≤ 1 , indifferent was Σ FICI: > 1 and ≤ 2 and antagonistic was Σ FICI: > 2 . Dotted gridline at Σ FICI of 0.5 depicts the cutoff for synergy.¹⁷

4.2.3 Compound **3.1** inhibits the biosynthesis of major macromolecules

Incorporation of radiolabeled precursors into the biosynthesis of macromolecules is used to investigate the mechanism of action of antibacterial agents.¹⁸ Using

radiolabeled precursors for DNA, RNA, cell wall and protein biosynthesis, we determined that compound **3.1** inhibited the biosynthesis of these macromolecules. At $0.5\times$ MIC through $2\times$ MIC, significantly high inhibition of DNA, RNA, protein and cell wall biosynthesis was observed (Figure 4.3). Even at a low concentration of $0.25\times$ MIC, the incorporation of $[3H]$ -thymidine and $[3H]$ -uridine precursors into DNA and RNA respectively were still significantly inhibited (Figure 4.3).

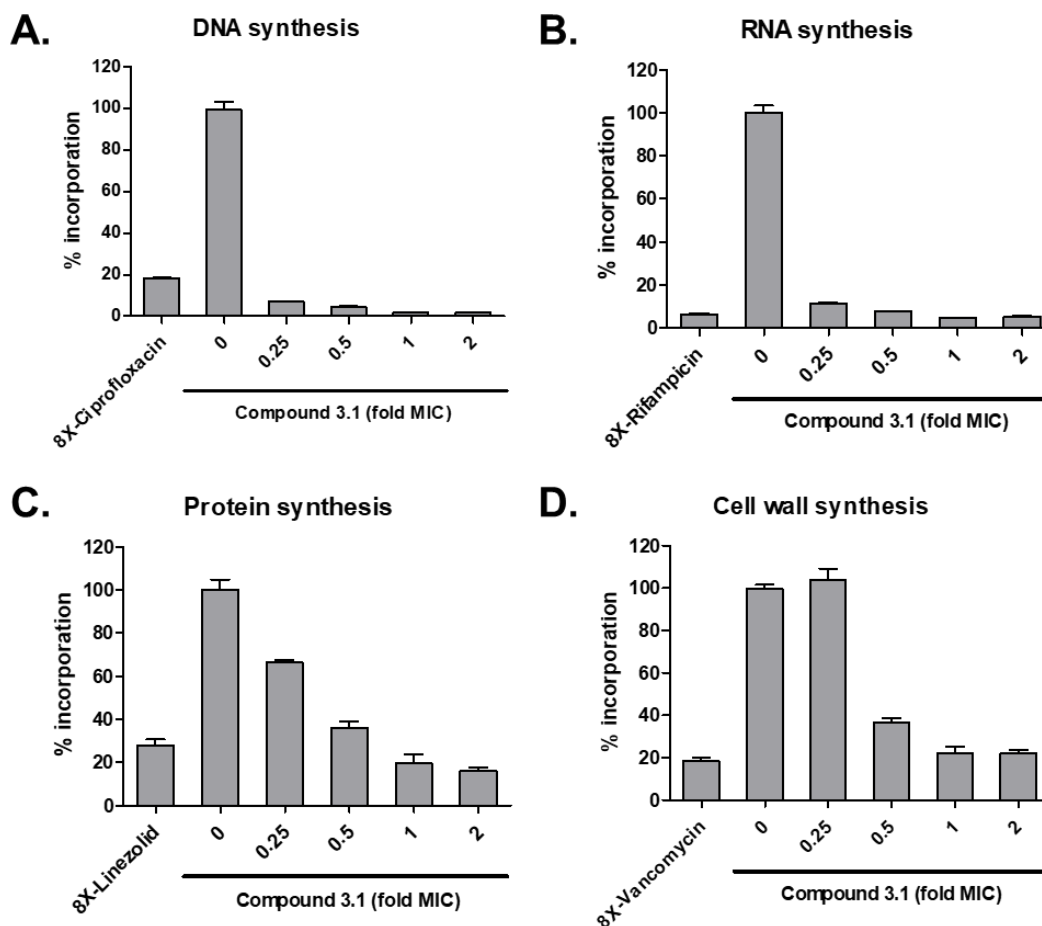


Figure 4.3. Effect of compound **3.1** on macromolecular biosynthesis. *S. aureus* was treated with increasing concentrations of compound **3.1** and $8\times$ MIC of established antibiotics and assayed for incorporation of **A.** $[3H]$ -thymidine for DNA synthesis, **B.** $[3H]$ -uridine for RNA synthesis, **C.** $[3H]$ -L-Leucine for protein synthesis and **D.**

[3H]-N-acetyl-D-glucosamine for cell wall synthesis. Data represent the mean±SD of triplicates.

4.2.3 Effect of compound **3.1** on global proteomics in *S. aureus*

To identify pathways and proteins that are impacted by compound **3.1** treatment, we embarked on a global proteomics study. Exponentially growing *S. aureus* cells were exposed to compound **3.1** or DMSO (control) and the resulting proteomics changes were profiled. From the analysis of the proteomics data, we identified a total of 1451 proteins with molecular weight ranging from 3.5 kDa to 163 kDa. Out of this number, 1233 proteins (85%) were observed to be shared by both DMSO control and compound **3.1** whilst 96 proteins (6.6%) were unique to DMSO control and 122 proteins (8.4%) were unique to compound **3.1** (Figure 4.4). From correlation analysis using scatter plots, we observed good correlation of the biological replicates, with $r = 0.98 - 0.99$ (Figure 4.4).

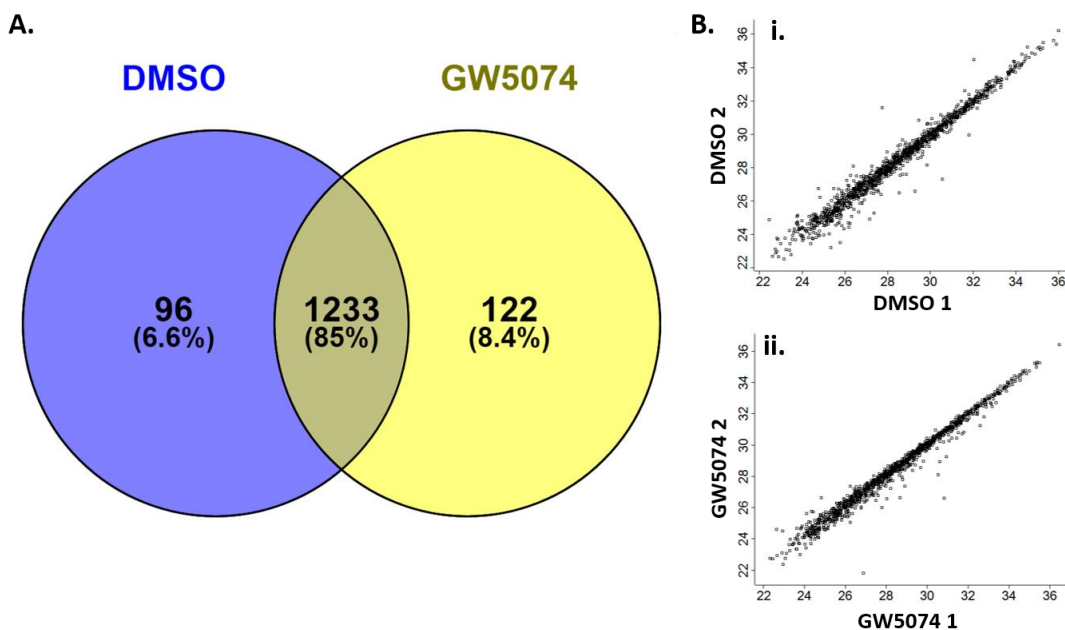


Figure 4.4. Global proteomics analysis of *S. aureus* cells treated with compound **3.1**. *S. aureus* was treated in triplicates with GW5074 (compound **3.1**) and the levels of proteins assessed. **A.** Venn diagram for comparison of proteins identified in DMSO-treated cells alone, compound **3.1**-treated cells alone and in both treatments. **B.** Representative correlation plots for the replicates of (i) DMSO and (ii) compound **3.1**.

In the presence of compound **3.1**, 62 proteins were observed to be downregulated ($p \leq 0.05$ and $\text{Log}_2\text{FC} \leq -2$) whilst 29 proteins were upregulated ($p \leq 0.05$ and $\text{Log}_2\text{FC} \geq 2$) from the 1233 differentially expressed proteins (Figure 4.5). From hierarchical clustering we observed that the control and treatment samples clustered into two groups (Figure 4.5). The purine biosynthesis enzyme PurL was strongly downregulated with about 9-fold reduction (p -value = 0.000186) in abundance. Pathway analysis revealed that several other enzymes involved in the *de novo* purine biosynthesis were observed to be downregulated. This included PurC, PurD, PurE and PurH, all of which were present in the top 20 downregulated proteins (Figure 4.5 and 4.6). Additionally, PurF, PurM, PurN, PurK, PurQ and PurS were only present in the DMSO samples implying that these were strongly downregulated in the presence of compound **3.1** (Figure 4.5).

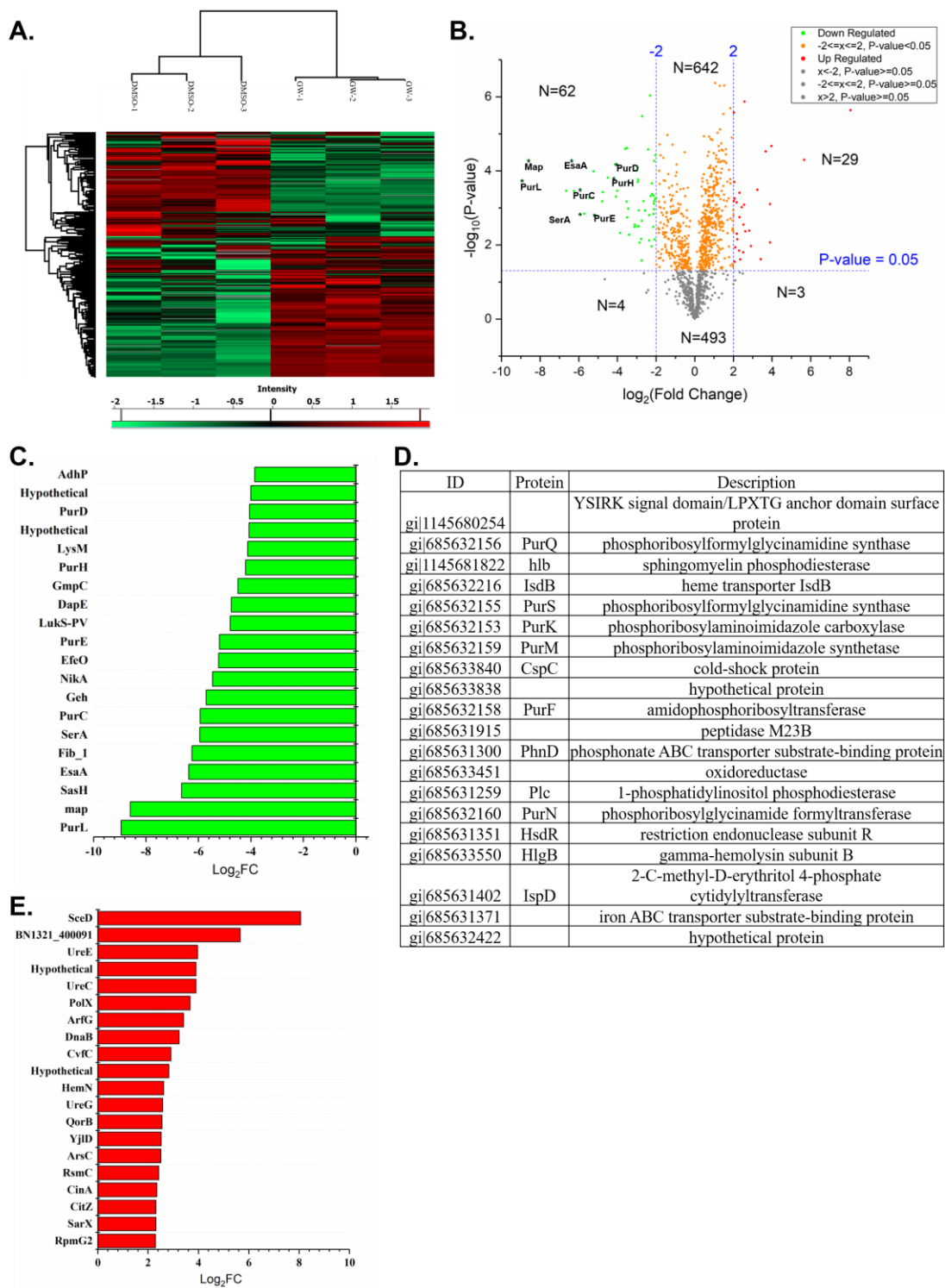


Figure 4.5. Analysis of differentially expressed protein from *S. aureus* cells treated with compound **3.1**. **A.** Heatmap analysis of global proteomics data showing differentially expressed proteins between replicates of DMSO-treated and compound

3.1-treated (GW) *S. aureus*. **B.** Volcano plot of global proteomics data showing the statistical p -value (y-axis) vs the relative abundance ratio, Log₂ fold change (Log₂FC, x-axis). Insert represents key to the differently color dots. Select proteins have been labeled. Dotted horizontal line represents the adjusted p -value threshold of 0.05 whilst the dotted vertical lines represent the Log₂FC cut-offs. Significant differential expression was defined as either $p \leq 0.05$ and Log₂FC ≥ 2 for upregulated proteins or $p \leq 0.05$ and Log₂FC ≤ -2 for downregulated proteins. **C.** Bar chart representation of the top 20 proteins which were downregulated, **D.** Table of select proteins that were identified to be present in DMSO-treated samples only. **E.** Bar chart representation of top 20 upregulated proteins. The Log₂FC values were plotted for the corresponding proteins using OriginPro 2017 Software (OriginLab, Massachusetts, USA). Data analysis was performed using the Perseus software.¹⁹ Volcano plot was generated with OriginPro 2017 Software (OriginLab, Massachusetts, USA).

Aside purine biosynthesis, the downregulated proteins belonged to a range of functional classifications (Table 4.1). The relative abundance of several components of membrane transporters responsible for solutes (eg. OpuCC), metal ions (eg. NikA) and peptide transport (eg. OppA, MetN, MetQ) were also downregulated (Table 4.1). We also found that proteins involved in amino acid biosynthesis and metabolism, like SerA, a critical enzyme in L-serine biosynthesis and DapE, an enzyme in L-lysine biosynthesis pathway were downregulated significantly. Others included MetE and PatA as well as the ribosomal protein S1, RpsA were observed to be significantly downregulated. *S. aureus* virulence factors such as the type VII secretion protein

EsaA (-6.4 fold), gamma-hemolysin subunits A and B, the response regulator AgrA (-2.2 fold), and cysteine protease staphopain A (SspC) were also downregulated by compound **3.1** treatment (Figure 4.5 and Table 4.1). Beta hemolysin (also called sphingomyelin phosphodiesterase, hlb) was only present in the DMSO-treated sample (Figure 4.5). The histidine kinase AgrC and the glutamyl endopeptidase SspA were observed only in the DMSO-treated sample (Table 4.1). The ATP-dependent Clp protease ATP-binding subunit ClpX was also downregulated (Table 4.1). The ClpX ATPase, a chaperone protein interacts with ClpP protease to perform protein refolding and degradation functions (Table 4.1).^{20, 21} One cell wall-associated protein, a LysM domain containing protein, which is involved in cell wall degradation²² was found to be downregulated (-4.1 fold). Others included proteins involved in carbohydrate metabolism (AdhP, LdhD, ButA etc), transcription (CspC) and translation (RpsA). A significant number of hypothetical/uncharacterized proteins, making up ~27% of identified downregulated proteins were also observed (Table 4.1). The HTH-type transcriptional regulators SarR and SarV were also downregulated (-2.4 and -2.2 fold respectively) by compound **3.1** treatment (Table 4.1).

Table 4.1. Functional classification of proteins downregulated in *S. aureus* after treatment with compound **3.1**

ID	Protein	Classification	Log ₂ FC	p-value
		Nucleotide metabolism		
gi 685632157	PurL	phosphoribosylformylglycinamide synthase	-8.94	0.000186
gi 685631236		5-nucleotidase	-6.64	0.000345
gi 685632154	PurC	phosphoribosylaminoimidazole-succinocarboxamide synthase	-5.93	0.000324
gi 1145680706	PurE	5-(carboxyamino)imidazole ribonucleotide mutase	-5.20	0.001566
gi 685632161	PurH	phosphoribosylaminoimidazolecarboxamide formyltransferase	-4.20	0.000161
gi 685632162	PurD	phosphoribosylamine--glycine ligase	-4.05	6.75E-05
		Membrane transporters		
gi 685633599	NikA	nickel ABC transporter substrate-binding protein	-5.46	0.000533

gi 685631614	MetQ	methionine ABC transporter substrate-binding protein	-4.50	0.000153
gi 685631881	OpuCC_2	glycine/betaine ABC transporter permease	-3.41	0.000203
gi 685631972	MetN	methionine ABC transporter ATP-binding protein	-2.93	0.000172
gi 685632054	OppA_2	peptide ABC transporter substrate-binding protein	-2.89	0.003127
gi 685633640		ABC transporter permease	-2.72	3.34E-06
gi 685633492	LctP	L-lactate permease	-2.13	0.000466
gi 685633639	EcsA	lantibiotic ABC transporter ATP-binding protein	-2.10	5.41E-05
		Virulence		
gi 685633121		Protein map	-8.60	5.18E-05
gi 685631438	EsaA	type VII secretion protein EsaA	-6.37	5.32E-05
gi 685632243	Fib_1	fibrinogen-binding protein	-6.25	0.00035
gi 685631476	Geh	Glycerol ester hydrolase;Lipase (EC 3.1.1.3)	-5.71	0.00144
gi 685631499		Efem/EfeO family lipoprotein	-5.23	0.000103
gi 685633122		gamma-hemolysin subunit B	-4.79	0.000669
gi 685631950		extracellular matrix protein-binding protein emp	-3.10	0.002843
gi 685631717	SdrD	hydrolase	-2.99	9.8E-05
gi 685633549	HlgC	gamma-hemolysin subunit A	-2.96	0.003199
gi 685633090	SspC	cysteine protease staphopain A	-2.65	0.00066
		Amino acid biosynthesis		
gi 685632900	SerA	D-3-phosphoglycerate dehydrogenase	-5.95	0.001489
gi 685633123	DapE	succinyl-diaminopimelate desuccinylase	-4.75	0.000378
gi 685632899		aminotransferase class V	-3.50	0.001806
gi 685631513	MetE	5-methyltetrahydropteroyltriglutamate--homocysteine methyltransferase	-2.89	0.001172
gi 685633124	DapE	succinyl-diaminopimelate desuccinylase	-2.32	9.37E-07
gi 685632136	DapC	N-acetyl-L,L-diaminopimelate aminotransferase	-2.11	0.000769
		Carbohydrate metabolism		
gi 685631760	AdhP	ethanol-active dehydrogenase/acetaldehyde-active reductase	-3.85	0.004803
gi 685631372	PlfB	formate acetyltransferase	-3.39	0.005306
gi 685633649	LdhD	lactate dehydrogenase	-2.28	0.000476
gi 685632476		4-oxalocrotonate tautomerase	-2.05	0.000569
gi 685631284	ButA	acetoin reductase	-2.00	0.000548
		Cell envelope		
gi 685631268		peptidoglycan-binding protein LysM	-4.12	6.75E-05
		Folding, sorting and degradation		
gi 685633675	ClpX	Clp protease ClpX	-2.95	8.34E-05
gi 685631411	ScdA	iron-sulfur cluster repair protein ScdA	-2.74	0.026313
		Signal transduction		
gi 1145679415	AgrA	DNA-binding response regulator	-2.22	0.000219
gi 685632905	HtrA	serine protease	-2.10	0.000654
		Transcription		
gi 685631953	CspC	cold shock protein	-2.85	0.00863
gi 685633415	SarR	MarR family transcriptional regulator	-2.41	2.64E-05
gi 685633386	SarV	MarR family transcriptional regulator	-2.20	0.000422
		Translation		
gi 685632586	RpsA	30S ribosomal protein S1	-2.04	3.77E-05
		Hypothetical/uncharacterized proteins		
gi 685633613		hypothetical protein	-4.07	0.000497
gi 685632805		hypothetical protein	-4.01	0.000348
gi 685633308		hypothetical protein	-3.53	0.000672
gi 685631865		hypothetical protein	-3.50	2.41E-05
gi 685631435		hypothetical protein	-3.11	0.003302
gi 685633494		hypothetical protein	-2.94	0.0002
gi 685631327	SrpF	alpha-helical coiled-coil protein	-2.78	0.006918
gi 685633773		hypothetical protein	-2.74	0.002238
gi 685631768		hypothetical protein	-2.57	0.001186
gi 685632106		hypothetical protein	-2.36	0.007578
gi 685633111		membrane protein	-2.35	0.001568

gi 685632424		LSM domain protein	-2.23	0.010939
gi 685632806		hypothetical protein	-2.15	0.003249
gi 685632405		hypothetical protein	-2.13	0.001454
gi 685633778		phage infection protein	-2.10	0.001089
gi 1145683535		DUF2648 domain-containing protein	-2.08	0.007076

The highest upregulated protein was the peptidoglycan hydrolyase, SceD which had 8-fold increase in expression (p -value = 2.29×10^{-6}) (Figure 4.5). Three out of the 29 upregulated proteins are involved in urea degradation. Urease subunit alpha, UreC, one of three structural urease proteins was observed to be upregulated (Figure 4.5). The other two structural proteins, UreA and UreB were overexpressed and found only in the compound **3.1**-treated samples. Two urease accessory proteins UreE and UreG were observed to be upregulated upon treatment with compound **3.1** (Figure 4.5). Also, upregulated were the DNA-templated-DNA polymerase, PolX as well as the DNA helicase, DnaB. Expression of SarX, a transcriptional regulator for the *agr* locus was upregulated (Figure 4.5).

4.2.4 GW5074 affects the mRNA levels of target proteins

From the proteomics analysis, we observed the differential regulation of several proteins following GW5074 treatment. We performed real-time RT-PCR analysis of select targets to validate the observed differential protein levels. The mRNA levels of *purL* and *sceD* that respectively correspond to the most downregulated protein PurL and the most upregulated protein, SceD were analyzed. Additionally, given the effect of GW5074 on the *agr* locus and virulence production, we also quantified the mRNA levels of *agrA* and *sarX* which encode the downregulated response regulator AgrA and the upregulated transcriptional regulator SarX respectively. In line with the observations from the global proteomics analysis, we observed decreased *purL* and

agrA mRNA levels and increased *sceD* and *sarX* mRNA levels (Figure 4.6). These observations suggest that GW5074 regulates the target mRNA expression which leads to differential protein abundance.

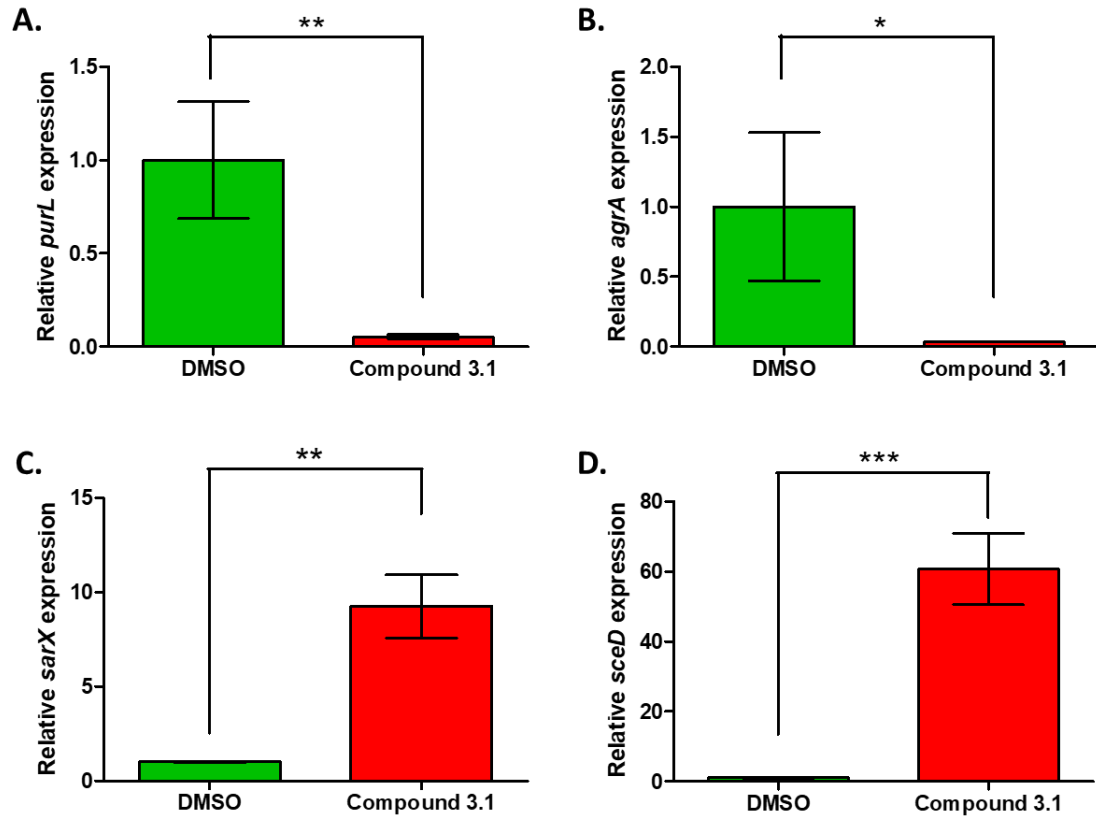


Figure 4.6. Relative mRNA expression of select differentially regulated targets from global proteomics analysis. The of compound **3.1** treatment on the transcription of **A.** *purL*, **B.** *agrA*, **C.** *sarX* and **D.** *sceD*. Total RNA isolated from *S. aureus* treated with either DMSO or 2 $\mu\text{g}/\text{mL}$ compound **3.1** was reversed transcribed and cDNAs were quantified by qRT-PCR using target-specific primers. The data represents the mean \pm SD of triplicate experiments normalized with 16S RNA. Statistically significant differences between DMSO-treatment and compound **3.1**-treatment as

determined by Student's t-test analysis (unpaired, two-tailed) is represented as * $p \leq 0.05$, ** $p \leq 0.01$ and *** $p \leq 0.001$.

4.3 Discussion

S. aureus has demonstrated the capacity to develop resistance to antibiotic therapy and hence continues to be a major health threat in both hospital and community settings.^{23, 24} We previously reported that the 4-hydroxybenzylidene indolinone, GW5074 (compound **3.1**) and related compounds could inhibit c-di-AMP synthesis.¹³ The observation that the compounds could reduce intracellular c-di-AMP levels is exciting. In the similar but distinct c-di-GMP signaling, inhibitors of cellular c-di-GMP synthesis have been link with modulating processes controlled by c-di-GMP such as biofilm formation.¹⁵ Like any second messenger signaling, the central role of c-di-AMP stems from the intracellular concentration of the molecule. Compounds that can reduce the cellular concentration, like those discussed here could have use in study bacterial physiology with respect to c-di-AMP signaling.

With the modest antibacterial activities, the compounds were observed to synergize with methicillin against MRSA and vancomycin against VRE.¹³ Combined with the observed effect on intracellular c-di-AMP, which is essential in rich media, we evaluated the mechanism of antibacterial action of compound **3.1** and related compounds against *S. aureus*.

The scope of antibiotic interaction of compound **3.1** is not limited to methicillin and vancomycin. We found that against MRSA, compound **3.1** could synergize with the ampicillin, ceftriaxone and cloxacillin in addition to methicillin. β -lactam antibiotics inhibit cell wall synthesis by binding to and inhibiting the transpeptidase activity of

penicillin-binding proteins.²⁵ Resistance to methicillin and all β -lactam antibiotics is conferred by the *mecA* gene present on the staphylococcal cassette chromosome *mec* (SCC*mec*).²⁵ The *mecA* gene encodes the low affinity penicillin-binding protein, PBP2a which has transpeptidase activity even in the presence of methicillin.

To better understand the mechanism of antibacterial action, we observed that compound **3.1** potently inhibited DNA and RNA synthesis whilst moderately affecting protein and cell wall synthesis from macromolecular biosynthesis assays. Their effect on nucleotide metabolism was also confirmed in the global proteomic analysis. Enzymes encoded by the *pur*-operon (*purEKCSQLFMNHD*) were observed to be significantly downregulated either among the differentially expressed proteins or were completely degraded and hence found only in the DMSO control. These enzymes sequentially catalyze the *de novo* synthesis of inosine monophosphate (IMP) from phosphoribosyl pyrophosphate (Figure 4.7). Downregulation of some of the enzymes following treatment with antibacterial agents is often observed in *S. aureus*.²⁶⁻²⁸ Purine biosynthesis enzymes have been implicated in virulence, persistence and tolerance to stresses such as antibiotics in *S. aureus*.^{29, 30} For example, *purC* mutants were growth-defective.³¹ In another study, PurL, PurN, PurM and PurE were found to be critical for *S. aureus* fitness in abscess formation.³² Furthermore, *purH* mutant *S. aureus* was found to have significantly decreased virulence and *in vivo* survival compared to wildtype.³³ The global proteomics data revealed that compound **3.1** affected all enzymes encoded by the *pur*-operon (PurL, PurC, PurD, PurE and PurH were downregulated whilst PurF, PurM, PurN, PurK, PurQ and PurS were only present in the DMSO-treated sample). Such an extensive effect could be

caused the compound potentially modulating the transcription of the operon. The PurR transcriptional repressor of the *pur*-operon was however not significantly affected. Therefore, it is possible that PurR is allosterically activated upon compound **3.1**-treatment, given that *purL* mRNA expression was also decreased. Varying effectors act on the expression and activation of *purR* in different bacteria. In *E. coli*, hypoxanthine and guanine co-repress PurR whilst adenine activates PurR to repress the *pur*-operon in *B. subtilis*.^{34, 35} Taken together, the purine biosynthesis pathway is important for normal growth of *S. aureus* as well as effective pathogenesis. Hence a complete shut-down of the *de novo* purine biosynthesis pathway, such as caused by compound **3.1**-treatment will have fitness costs.

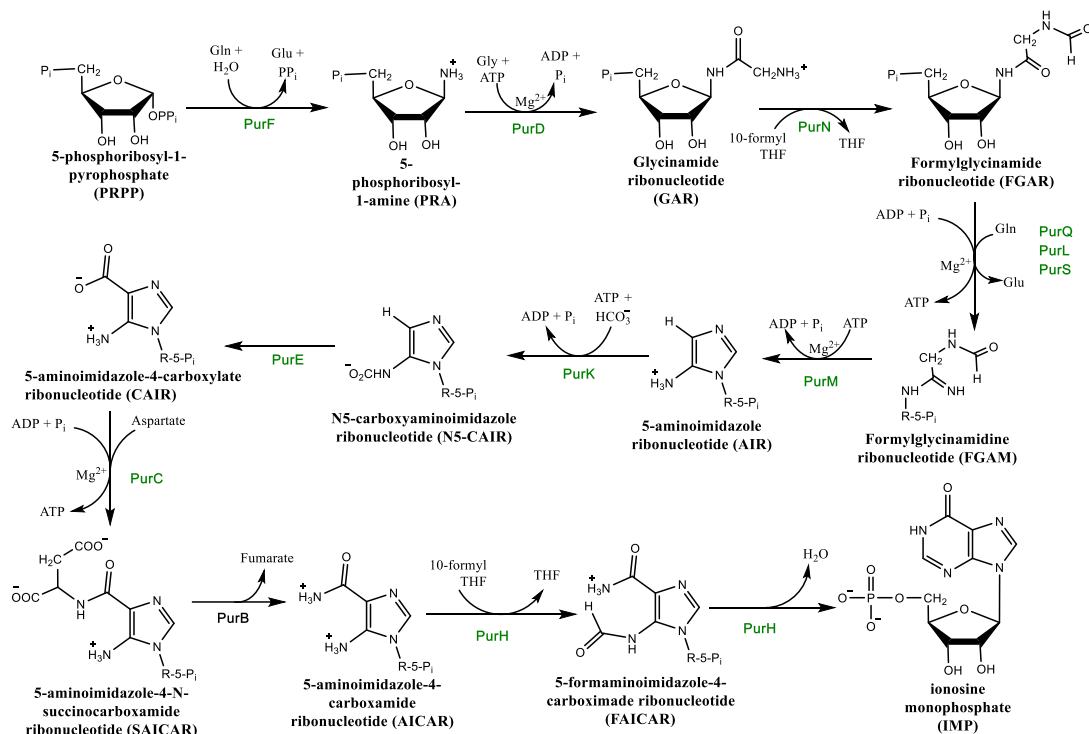


Figure 4.7. Purine biosynthesis pathway. The enzymes encoded by the *pur*-operon sequentially catalyze the conversion of PRPP to IMP. PurQ and PurL are known to participate in the same step, and PurS is thought to play a role in this step. The

enzymes shown in green were differentially downregulated or were only found in DMSO-treated samples.

From the proteomics analysis, several virulence-related proteins were downregulated upon treatment with compound **3.1**. The second highest downregulated protein, Map (MHC class II analog protein, $\text{Log}_2\text{FC} = - 8.6$), is a cell surface protein that has been shown to bind to fibrinogen, fibronectin, vitronectin and other extracellular matrix (ECM) components of host cells.³⁶ Although *map*⁻ mutant *S. aureus* was not deficient in adhering to ECM components,³⁷ the mutant strains were observed to have decreased pathogenicity as abscess formation, osteomyelitis and arthritis levels were reduced compared to wildtype strains.³⁸ In nude mice however, no significant difference in the virulence of *S. aureus* was observed between mutant and wildtype strains, an indication that Map may function to modulate the immune system to facilitate *S. aureus* survival and virulence.³⁸

EsaA, an essential component of the ESAT-6 like Secretion system (ESS), was also downregulated ($\text{Log}_2\text{FC} = - 6.4$). The ESS is a Type VII secretion system that plays a critical role in *S. aureus* pathogenesis.^{39, 40} EsaA, EssA, EssB and EssC form the membrane components of the ESS that cooperate to transport the secreted virulence factors EsxA, EsxC, EsxB, EsxD, and EsaD. Consequently, EsaA is proposed to interact with the components of the ESS. Indeed, deletion of EsaA revealed its essential role in the transport of EsxA and EsxC.⁴¹ Hence, downregulation of EsaA will affect *S. aureus* virulence.

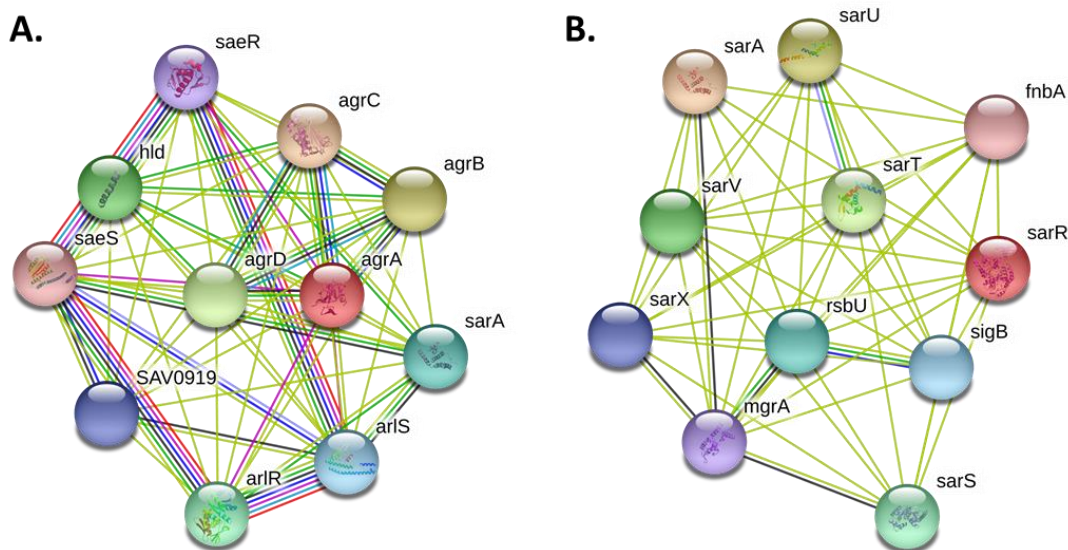


Figure 4.8. Predicted functional protein-protein association networks for select down-regulated proteins. Predicted association of **A.** AgrA, the response regulator interacts with other components of *agr* system encoded by the *agrBDCA* operon and **B.** SarR transcriptional regulator with other SarA homologs. Figures were generated by STRING v 10.5 online database.⁴²

Compound **3.1** also downregulated AgrA and appeared to completely abolish expression of the histidine kinase AgrC. Downregulation of AgrA was further observed to be due to decreased expression of *agrA* mRNA. The *agr* and *sar* loci regulate virulence in *S. aureus* (Figures 4.8 and 4.9).^{43, 44} The former is composed of two divergent transcripts, RNAII and RNAIII under the control of P2 and P3 promoters respectively.⁴⁵ The RNAII transcript encodes the components of the *agr* operon (*agrBDCA*).⁴⁵ The autoinducer peptide (AIP) produced from AgrD is proteolytically processed by the membrane component, AgrB. The resulting AIP intermediate cleaved a second time before being exported. The exact mechanism of export is however unclear.^{44, 46} When a quorum is reached, AIP increases in

concentration, binds and causes the autophosphorylation of AgrC histidine kinase, which in turn phosphorylates and activates AgrA response regulator. AgrA then directs transcription from the RNAII and RNAIII transcripts. RNAIII is a major regulator of *S. aureus* virulence factor production which represses cell surface virulence factors and enhances exoproteases and toxins (Figure 4.9).^{44, 45, 47} Downregulation of AgrA would therefore imply decreased virulence since *agrA* mutation resulted in the depletion of RNAIII mRNA.⁴⁸ Consequently, beta-hemolysin, gamma-hemolysin, lipase and fibrinogen-binding protein were observed to be downregulated alongside AgrA.⁴⁹ Efforts have been made to identify inhibitors of the *agr* system as potential anti-virulence therapies. An array of molecules including analogs of AIP and small molecules have been identified (reviewed in ⁵⁰).

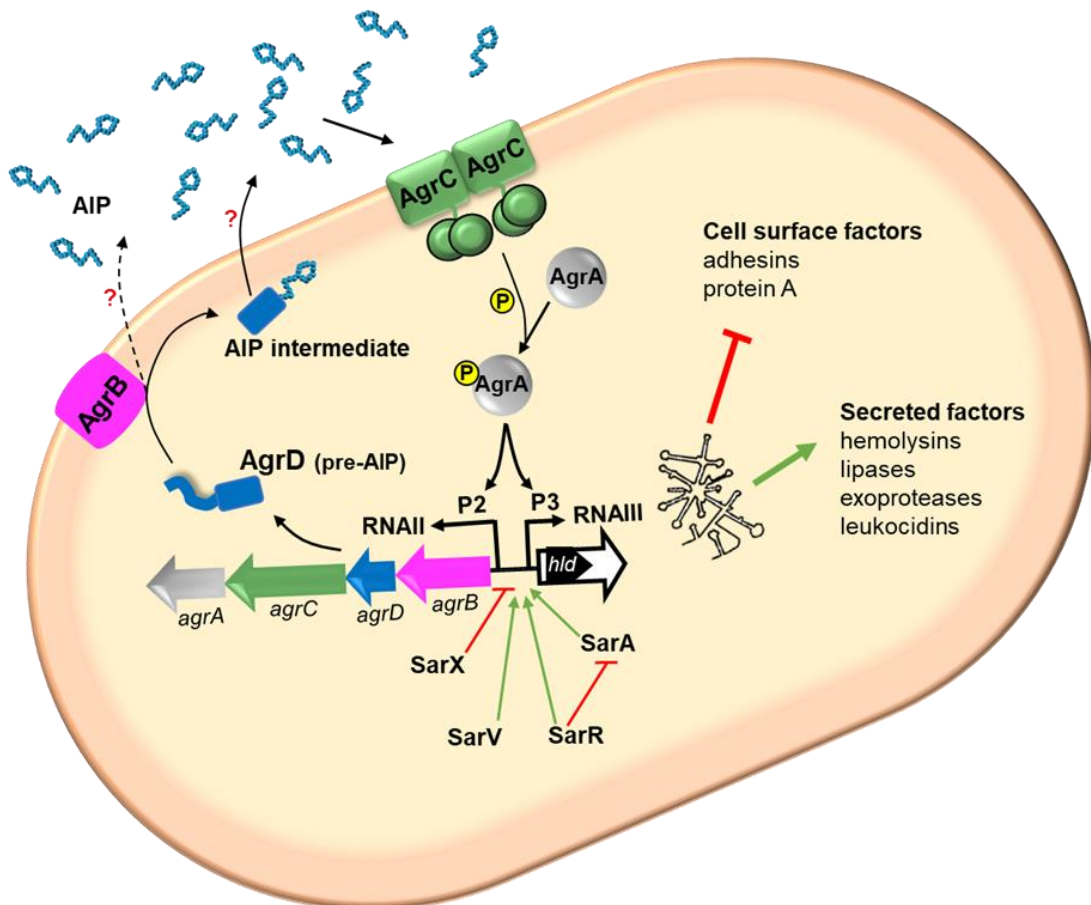


Figure 4.9. The *S. aureus agr* system. RNAIII modulates the expression of several virulence factors (upregulated factors are indicated with red lines and downregulated factors are indicated with the green lines). Regulation of *agr* by select SarA homologs is depicted as well. AgrA, AgrC, SarR and SarV were downregulated whilst SarX was upregulated in *S. aureus* when treated with compound **3.1**.

The observation that, SarX an HTH-type transcriptional regulator was upregulated in both proteomics and RT-PCR analyses, further validated the effect of compound **3.1** on inhibiting *S. aureus agr* locus. SarX is one of at least 10 homologs of SarA, a major *S. aureus* virulence regulator. SarA is needed for the transcription of RNAII and RNAIII from P2 and P3 promoters respectively. Partial characterization of some SarA homologs including SarR, SarS, SarX, SarV, SarU, SarT, Rot and MgrA has been done.⁵¹ SarX was found to repress the *agr* locus (Figure 4.9).⁵² It was demonstrated that *sarX* mutant *S. aureus* had increased levels of hemolysins and proteases due to enhanced activity of *agr* promoters.⁵² Since SarX represses *agr*, upregulating SarX will lead to decreased levels of virulence genes, such as those that encode hemolysins and proteases.⁵² Additionally, the transcriptional regulators SarR and SarV were downregulated. In late exponential and stationary phase cultures, SarR functions as a repressor for *sarA* transcription.⁵³ Analysis of a double *sarA/sarR* mutant at early growth phase revealed that SarR positively regulates the expression of genes encoded by the *agr* locus (Figure 4.9), implying that down-regulating SarR would result in decreased secreted virulence factors.⁵⁴ The transcriptional regulator SarV, which was also downregulated by compound **3.1**-treated regulates autolysis and

some virulence factor production. Northern blot and transcriptional fusion assays demonstrated that *sarV* mutant had decreased RNAII and RNAIII transcripts.⁵⁵ The study also revealed that the levels of *scdA* was lower in the *sarV* mutant. The *scdA* gene encodes the peptidoglycan hydrolyzing protein ScdA and is implicated in autolysis.⁵⁶ Consistent with these observations, we also saw decreased abundance in ScdA (Log₂FC = -2.7).

The *S. aureus* ClpX chaperone forms the ClpXP protease complex by interacting with ClpP protease to direct protein re-folding and degradation of damaged proteins. Findings from *clpX* mutants in *S. aureus* point to a function for ClpX in cell growth as *clpX* mutants have defective growth relative to wildtype.⁵⁷ In a murine skin abscess model, *clpX* mutants were observed to have attenuated virulence.⁵⁸ Additionally, the transcription of RNAIII, the *agr* effector molecule, and hence activity of AIP, were observed to be reduced in the absence of ClpX.⁵⁸ Taken together, the downregulation of AgrA, ClpX, EsaA and other virulence-related proteins could be a major contributing factor to observed anti-staphylococcal activity of compound **3.1**.

Compound **3.1** downregulated enzymes from different amino acid biosynthesis pathways. In the phosphorylated pathway of L-serine biosynthesis, the initial committed and rate limiting step is catalyzed by SerA.⁵⁹ The cellular pool of L-serine is largely controlled by the SerA-mediated pathway. The biosynthesis of pathways of purines, tryptophan, glycine, phospholipids and cysteine utilize L-serine as a precursor.^{60, 61} Compound **3.1** downregulated DapC and DapE, two successive enzymes that catalyze the second and third steps respectively in the succinylase route of lysine biosynthesis.^{62, 63} DapE is involved in the *meso*-diaminopimelate (*m*-DAP),

an essential component of peptidoglycan.⁶⁴ In *Helicobacter pylori*, *Mycobacterium smegmatis* and *M. tuberculosis*, *dapE* deletion was observed to be lethal.⁶⁵⁻⁶⁷ Consequently, DapE has been suggested as a potential antibiotic target given that lysine biosynthesis pathways are not present in human cells.⁶⁴

We also saw the upregulation of SceD (Log₂FC = 8) which was potentially caused by an increase in *sceD* mRNA expression as seen in the RT-PCR analysis. The *S. aureus* SceD is a putative lytic transglycosylase.⁶⁸ Lytic transglycosylases (LTs) are peptidoglycan hydrolases that cleave peptidoglycan to allow for biosynthesis and recycling of peptidoglycan as well as cell division.⁶⁹ The cleavage activity of LTs also creates space for membrane components such as secretion systems.⁶⁹ The LT activity of SceD in *S. aureus* was demonstrated by Stapleton *et al* in 2007.⁶⁸ The authors revealed that *sceD* mutation hindered cell separation. Expression of SceD is positively regulated by the two-component system WalKR (also called YycFG), sigma factor B and *agr* whilst SarA, LytSR and SaeRS serve as negative regulators.^{68, 70} However, little is known about the effects of increased LT activity. A continued and uncontrolled LT activity is detrimental to the cell as it could result in autolysis.^{71, 72} Others have pursued the use of peptidoglycan hydrolases as potential antibacterial strategy.^{71, 73} For example, the bacteriophage ϕ MR11-derived endolysin, MV-L was shown to completely lyse drug-resistant *S. aureus* strains such as MRSA and vancomycin-resistant *S. aureus*.⁷⁴ MV-L could synergize with vancomycin against vancomycin-intermediate resistant *S. aureus*.⁷⁴ The observed upregulation of SceD following compound **3.1** treatment potentially contributes to the synergy observed with cell wall-targeting antibiotics.

4.4 Conclusions

In summary, we found that 4-hydroxybenzylidene indolinones reduce intracellular c-di-AMP levels. We also found that GW5074 (compound **3.1**) synergized with several antibiotics from different classes β -lactams (ampicillin, cloxacillin and ceftriaxone), aminoglycosides (gentamicin and kanamycin) and fluoroquinolone (ciprofloxacin). Compound **3.1** affects levels of proteins with different functional characterizations and pathways. It was apparent that processes such as purine biosynthesis and virulence factor production were significantly downregulated. The decrease in virulence factor expression levels was characterized by downregulation of the AgrC-AgrA two-component system, transcriptional regulators SarR and SarV, and a corresponding decrease in abundance of downstream targets, such as hemolysins, lipases and proteases. Future studies will further explore the effect of compound **3.1** and related 4-hydroxybenzylidene indolinone compounds on *S. aureus* quorum sensing. Given that compound 3.1 also reduced cellular c-di-AMP, a possible integration of c-di-AMP signaling with quorum sensing needs to be examined. Additionally, the synergistic effect of combining these antibiotics with compound **3.1** in animal models of infection should be investigated.

4.5 Methods

4.5.1 Chemicals and culture methods

GW5074 was purchased from Cayman chemicals (Ann Arbor, MI, USA) and a 10 mg/mL DMSO stock solution was prepared. The antibiotics were purchased from Sigma-Aldrich (St. Louis, MO, USA). Bacteria were routinely cultured in BD™ Tryptic Soy Broth (TSB) at 37 °C with 250 rpm shaking unless otherwise stated.

4.5.2 Intracellular concentration of c-di-AMP

Overnight cultures of *E. coli* BL21 (DE3) harboring DAC plasmids were diluted 1:1000 and cultured 1:100 in LB medium and cultured until OD₆₀₀ of 0.5. The expression of the DAC was induced by adding 1 mM IPTG. Aliquots of DMSO stock solution of compounds at 10 mg/mL were added to the cultures to yield 16 µg/mL final concentration in a 10 mL culture. An equivalent percentage of DMSO was used as control. The cultures were then incubated at 37 °C with aeration for 3 hours. The cells were harvested by centrifugation at 2,500 × g for 10 min at 4 °C and washed twice with PBS. The pellets were resuspended in PBS and OD₆₀₀ determined for normalization. A 5 mL aliquot of the cell suspension was used to determine the total protein concentration. Briefly, the cells were pelleted, resuspended in 500 µL of 0.1 N NaOH and heated at 95 °C for 10 min. The lysate was centrifuged at 20,000 × g for 10 min at 4 °C and the supernatant was used to determine the protein concentration using the BCA assay. The remaining 5 mL was used for extraction of c-di-AMP. The cells were pelleted and resuspended in 300 µL of ice-cold extraction buffer (acetonitrile:methanol:water, 2:2:1) containing 1 µM cXMP as internal standard. The samples were sonicated in a sonifier waterbath at 4 °C for 6 min and left on ice for 15 min before being centrifuged at 20,000 × g for 10 min at 4 °C. The supernatant was stored on ice and pellets resuspended in 200 µL of ice-cold extraction buffer and extracted as described. A third extraction with 200 µL of extraction buffer was performed and supernatants from each sample were pooled together. The extracts were dried and resuspended in HPLC grade water and then analyzed by LC-MS/MS.

4.5.3 LC-MS/MS quantification of c-di-AMP extracts

An Agilent 6460 triple quadrupole LC-MS/MS system coupled with HPLC outfitted with Atlantis T3, 3 μ m, 2.1x150mm column was used to separate the constituents of the extract. Mobile phases of 0.1% formic acid in water (solvent A) and 0.1% formic acid in acetonitrile (solvent B) at a flow rate of 0.3 ml/min were used for the HPLC separation. A linear gradient from 100% A to 20% A was applied for the first 10 minutes followed by a 1-minute linear gradient back to 100% A. The column was re-equilibrated by isocratic flow at 100% A for an additional 4 minutes before the next run. Using the MRM analysis in the negative mode, the following transitions of analytes were detected by the triple quadrupole: cXMP: 345/151 and c-di-AMP: 657.1/328 (quantifier), 657.1/136 (identifier). The concentration of c-di-AMP was estimated from a calibration curve (Appendix A).

4.5.4 Synergy checkerboard assay

The checkerboard assay was used to determine antibiotics-compounds interactions against MRSA ATCC 33592, MRSA USA300 and VRE faecalis ATCC 51575. Briefly, antibiotics and compounds at 10 mg/mL were prepared in appropriate diluents. Compounds were diluted serially (1:2) along the ordinate whilst antibiotics were similarly diluted along the abscissa of 96-well microtiter plates. Bacteria standardized using the 0.5 McFarland standard was diluted (1:100) and added to aliquoted into respective wells. The plates were incubated in a static incubator at 37 °C for 18 – 20 hours before the MIC was determined. The fractional inhibitory concentration index (FIC) was calculated for each combination and the lowest FIC index was selected.¹⁷

For the effect of combining GW5074 with an antibiotic, the FIC of either agent was calculated as:

$$FIC_{GW5074} = \frac{\text{MIC of GW5074 in combination}}{\text{MIC of GW5074 alone}}$$

$$FIC_{antibiotic} = \frac{\text{MIC of antibiotic in combination}}{\text{MIC of antibiotic alone}}$$

The cumulative fractional inhibitory concentration index ΣFIC was calculated as:

$$\Sigma FIC = FIC_{GW5074} + FIC_{antibiotic}$$

The calculated ΣFIC indexes were interpreted as follows: synergistic ($\Sigma FIC: \leq 0.5$), additive ($\Sigma FIC: > 0.5$ and ≤ 1), indifferent ($\Sigma FIC: > 1$ and ≤ 4), antagonistic ($\Sigma FIC: > 4$).

4.5.5 Macromolecular synthesis

Overnight *S. aureus* ATCC 25923 culture was diluted 1 in 1000 in 30 mL of TSB and cultured till early exponential phase (OD₆₀₀ of 0.2 – 0.3). At the desired OD₆₀₀, 1 mL aliquots of the culture were transferred into 5 mL culture tubes and treated with increasing concentrations of GW5074 (0.25× – 2× MIC) or 8× MIC of ciprofloxacin (2 µg/mL, for DNA synthesis), vancomycin (8 µg/mL, for cell wall synthesis), rifampicin (0.32 µg/mL, for RNA synthesis) and linezolid (8 µg/mL for protein synthesis). DMSO was added to the control tubes. All tubes were incubated at 37 °C for 10 min after which radiolabeled precursors were added to respective tubes to determine the effect on macromolecular synthesis. DNA synthesis was measured by adding 1 µL of [3H]-thymidine (69.7 Ci/mmol at 0.1 mCi/mL, cat. no MT-6036,

Movarek Inc.) for 10 min whilst 1 μ L of [3H]-uridine (17.0 Ci/mmol at 0.1 mCi/mL, cat. no. MT-602, Movarek Inc.) was added to measure RNA synthesis. Cell wall synthesis was measured by adding 1 μ L of [3H]-N-acetyl-D-glucosamine (5.5 Ci/mmol at 0.1 mCi/mL, cat. no. MT-662, Movarek Inc.) for 10 min. For protein biosynthesis inhibition, the 1:1000 overnight culture dilution was incubated till OD₆₀₀ of 0.4 – 0.5. The culture was then centrifuged at 4,500 rpm for 5 min and the cell pellet resuspended in a M5T medium (1X M9 salts, 5% TSB, 0.4% glucose, 2 mM MgSO₄ and 0.1 mM CaCl₂)¹⁸ with OD₆₀₀ readjusted to 0.2. At this point, 1 mL aliquots were incubated with compound (0.25 \times – 8 \times MIC) and linezolid (16 μ g/mL, 8 \times MIC) for 10 min. A 1 μ L aliquot of [3H]-L-Leucine (60.0 Ci/mmol at 1 mCi/mL, cat. no. M672M, Movarek Inc.) was added to each tube and incubated for an additional 30 minutes. Following the respective labeling times, the macromolecules were precipitated using 1 mL of ice-cold 10% TCA for 1 hour. The samples were then filtered through a glass microfiber filter (GF/A, 25-mm; Whatman), washed with 5 mL of ice-cold 5% TCA followed by 5 mL of ice-cold distilled water. The filters were dried and then counted in a Tri-Carb 2910 TR liquid scintillation analyzer (Perkin Elmer, Waltham, MA).

4.5.6 Global proteomics analysis: sample preparation for LC-MS/MS

Exponentially growing *S. aureus* cells were treated with 2 μ g/mL of GW5074 for 3 hours. The cells were pelleted by centrifugation and washed twice with PBS. The cell pellets were homogenized in 8 M urea with Precellys[®] 24 Bead Mill Homogenizer (Bertin Corp., Rockville, MD, USA) and centrifuged at 14,000 rpm for 15 min at 4 $^{\circ}$ C. Precipitation of soluble proteins was achieved by adding five equivalents (v/v) of

pre-chilled acetone to the supernatants and incubating at -20 °C overnight. After precipitation, the protein pellets were dissolved in 8 M urea and the Pierce™ BCA Protein Assay Kit (ThermoFisher Scientific, Waltham, MA, USA) was used to determine the protein concentration. Protein (50 µg) was reduced with 5 mM dithiothreitol (DTT) at 55°C for 45 min followed by cysteine alkylation with 20 mM iodoacetamide at room temperature for 20 min and an additional 5 mM DTT for 20 min at 37 °C. Trypsin/Lys-C Mix (Promega, Madison, WI, USA) at 1:25 (w/w) enzyme-protein ratio was used to digest the protein at 37 °C overnight and passed through C18 silica micro spin columns (The Nest Group Inc., Southborough, MA, USA). The peptides were then eluted with 0.1 % formic acid (FA) in 80% acetonitrile (ACN). The eluted peptides were vacuum dried and resuspended in 0.1% FA in 3% ACN. Peptide concentration was determined with the BCA assay as above and adjusted to 0.2 µg/µL.

4.5.7 LC-MS/MS data acquisition (This was done exclusively by Dr. Uma Aryal, the Proteomics Core Facility manager at Bindley Bioscience Center in Purdue University)

A reverse-phase HPLC-ESI-MS/MS system composed of an UltiMate™ 3000 RSLCnano system coupled to a Q-Exactive (QE) High Field (HF) Hybrid Quadrupole-Orbitrap™ mass spectrometer (ThermoFisher Scientific, Waltham, MA) and a Nano-spray Flex™ ion source (Thermo Fisher Scientific) was used to analyze the samples standard data-dependent mode. A 98% purified water/2% ACN/0.01% FA solvent system was used to wash purified peptides loaded onto a trap column (300 µm ID × 5 mm, 5 µm 100 Å PepMap C18 medium) at a 5 µL/min flowrate. After 5

min, the trap column was switched in-line with the Acclaim™ PepMap™ RSLC C18 (75 μm x 15 cm, 2 μm 100 Å PepMap C18 medium, Thermo Fisher Scientific) analytical column for peptide separation. Each run constituted loading a 1 μg total peptide onto the trap column followed by a 0.3 μL/min flowrate of 0.1% formic acid (FA) in water (solvent A) and 0.1% FA in 80% ACN (solvent B) for 120 min for peptide separation at 50°C. A 5-30% linear gradient of solvent B was run for 80 min, followed by 11 min of 45 % solvent B and 2 min of 100 % solvent B with an additional 7 min of isocratic flow. Solvent A was then applied at 95 % for 20 min for column equilibration. A Top20 data-dependent MS/MS scan method was used to acquire the MS data. Injection time was set to 100 ms, resolution to 120, 000 at 200 m/z, spray voltage of 2-eV and an AGC target of 1×10^6 for a full MS spectra scan with a range of 400 – 1650 m/z. Precursor ions were fragmented at a normalized collision energy of 27 eV using a high-energy C-trap dissociation. Acquisition of MS/MS scans were done at a resolution of 15,000 at m/z 200. To avoid repeated scanning of identical peptides, we set the dynamic exclusion at 15 s.

4.5.6 Data Analysis (MaxQuant software analysis was performed by Dr. Uma Aryal. I performed the bioinformatics analysis of the data using Perseus software and OriginPro 2017 software)

The MaxQuant software (v. 1.6.0.16)⁶³⁻⁶⁵ with the Andromeda search engine was used to analyze the LC-MS/MS data. For protein identification and relative quantification, the spectra were searched against the *S. aureus* sequences on NCBI database with a minimal length of six amino acids. A precursor mass tolerance of 10 ppm, MS/MS fragment ion tolerance of 20 ppm and enzyme specificity for trypsin

and LysC (for up to two missed cleavages) were used to the database search. Also, methionine oxidation (M) was set as variable modification whilst cysteine carbamidomethylation (C) was set as a fixed modification. Peptide quantification was performed using the ‘unique plus razor peptides’. A 1% false discovery rate (FDR) was set for both peptides spectral match and proteins identification. The Perseus software¹⁹ was used for bioinformatics analysis. Since each treatment was done in triplicates, proteins identified without any LFQ intensities as well as those with just 1 LFQ intensity value were excluded from the analysis. After Log₂ transformation of the intensities and filtering of the data, a two-sample Student’s T-test was used to determine differentially abundant proteins using a 5% permutation-based FDR filter. Scatter plots were used to determine the correlation between replicates. The Z-score normalized data was used to perform hierarchical clustering and to generate the heat map analysis. The Log₂FC values (Student’s T-test difference between Log₂ intensities of GW5074 and DMSO samples) and the -Log p-values were used to generate volcano plot in OriginPro 2017 Software (OriginLab, Massachusetts, USA).

4.5.7 Total RNA isolation and RT-PCR

Exponentially growing *S. aureus* was incubated with 2 µg/mL GW5074 or DMSO for 3 h at 37 °C in triplicates. The cells were then pelleted by centrifugation at 5000 rpm for 5 min at 4 °C and resuspended in 1 mL TRIzol (Invitrogen, Carlsbad, CA) for total RNA isolation according to the manufacturer’s protocol. Residual genomic DNA was then removed by treating isolated RNA with the Turbo DNA-free kit (Ambion, Austin, TX). The isolated RNA (1 µg) was then reverse-transcribed using the Superscript II Reverse Transcriptase (ThermoFisher Scientific). The resulting cDNA were analyzed and quantified using gene-specific primers (Table 4.2) and the

QuantiTect SYBR Green PCR Kit (Qiagen, Germantown, MD) on a BioRad CFX96™ Touch Real-Time PCR Detection System following the manufacturer's protocol. The data were normalized against 16S rRNA and the p-values from student's t-test showed * ≤ 0.05 , ** ≤ 0.01 and *** ≤ 0.001

Table 4.2. Sequence of primers used in RT-PCR

Primer name	Sequence (5'-3')	Source
PurL forward	GTGAAGGTGCAGGGGTAGTC	This study
PurL reverse	ATGATTCCACCAACGCCTGT	This study
sarX forward	GGGGTGCAACATTTTGAATACTGA	This study
sarX reverse	TCTTTGCAATGCTTCATCGTT	This study
agrA forward	AACTGCACATACACGCTTACA	Thaenert <i>et al.</i> ⁷⁷
agrA reverse	GGCAATGAGTCTGTGAGATTT	Thaenert <i>et al.</i> ⁷⁷
SceD forward	GCAGTAGGTTTAGGAATCGTAGCAGGAAAT	Dubrac <i>et al.</i> ⁶⁹
SceD reverse	CTGATTCAAAGTGATAAGTAAACCCTTCAT	Dubrac <i>et al.</i> ⁶⁹
16S forward	CGGTCCAGACTCCTACGGGAGGCAGCA	Thaenert <i>et al.</i> ⁷⁷
16S reverse	GCGTGGACTACCAGGGTATCTAATCC	Thaenert <i>et al.</i> ⁷⁷

Chapter 5: Discovery of a bacteriostatic antibiotic with potency against drug-resistant bacteria

5.1 N-(1,3,4-oxadiazol-2-yl)benzamide analogs, bacteriostatic agents against

methicillin- and vancomycin-resistant bacteria

This section was a collaboration with Dr. Saleem's group at Purdue University, West Lafayette, Indiana. It was originally published as: Opoku-Temeng, C., Mohammad, H., Dayal, N., Naclerio, G.A., Abutaleb, N.S., Mohamed, S.N. and Sintim, H.O., "N-(1,3,4-oxadiazol-2-yl)benzamide analogs, bacteriostatic agents against methicillin- and vancomycin-resistant bacteria." *Eur. J. Med. Chem.* 15 (155):797-805

5.1.1 Introduction

The discovery and development of antibiotics revolutionized health care in such a way that bacterial infections, which were otherwise deadly, could be treated.^{1, 2} However, this was met with a rapid development of resistant bacterial strains that rendered many antibiotics ineffective.³ Consequently, millions of people are infected with drug-resistant bacterial strains yearly resulting in thousands of deaths. In the US, the Centers for Disease Control and Prevention in 2013 estimated that approximately 23,000 people died from infections caused by drug-resistant bacterial pathogens at an annual infection rate of about 2 million. The cost to treat such recalcitrant infections exceeds \$20 billion per year.^{4, 5}

It has been suggested that resistance to antibiotics has developed over the years via a myriad of processes including the inordinate use of antibiotics and the lack of development of new antibiotics.³ The wide gap between emergence of drug-resistant pathogens and the development of novel antibacterial therapeutics has been attributed to the non-profitable nature of the venture (it costs several millions of dollars to conduct clinical trials and the high probability of bacterial resistance emerging

against a new antibiotic hinders investment in antibiotic discovery).^{2,3} Efforts however, need to be directed towards identifying and developing novel structures as antibacterial agents with possibly novel mechanisms of action.² It is projected that in the absence of new antibacterial agents, annual mortality rates could exceed 10 million by the year 2050.⁶

As noted above, nearly 23,000 fatalities due to antibiotic-resistant infections occurs each year in the US; surprisingly, nearly half of these deaths is linked to one bacterial pathogen, methicillin-resistant *Staphylococcus aureus* (MRSA).⁵ Community-acquired methicillin-resistant *S. aureus* (CA-MRSA) is the principal causative agent for skin and soft tissue infections (SSTIs) in North America.^{7,8} Strains such as MRSA USA300 and MRSA USA400 constitute the most isolated agents in SSTIs.⁹⁻¹¹ Others including USA100 and USA200 have been primarily isolated from hospital-acquired MRSA (HA-MRSA) infections.¹² Diseases including sepsis, endocarditis, and pneumonia could also result from MRSA infection.^{13, 14} Clinical isolates of MRSA have been identified that are resistant to several antibiotics. Vancomycin, a glycopeptide antibiotic remains the reference standard for the treatment of multi-resistant MRSA infections.^{13, 15} However, there is an emergence of MRSA strains that are resistant to vancomycin including various vancomycin-intermediate *S. aureus* (VISA) and vancomycin-resistant *S. aureus* (VRSA) isolates.^{15, 16} When used alone, MRSA strains easily develop resistance to rifampicin, one alternative for treating MRSA infections. Hence rifampicin is usually administered together with a second antibiotic like fusidic acid.¹⁵ Many other anti-staphylococcal antibiotics including ciprofloxacin suffer from resistance generation.^{15, 17} There is an obvious need for

clinicians to be armed with new antibiotics that are less likely to fail due to resistance generation. Consequently, several research groups including ours have programs to understand the mechanisms of resistance and how to inhibit or reverse them.¹⁸⁻²³ Research into the development of promising antibacterial agents with potent activity against drug-resistant bacteria has also increased.^{21, 24-27}

We have identified novel structures (Figure 5.1) with potent antibacterial activities against drug-resistant Gram-positive bacteria. In particular, these molecules exhibit potent antibacterial activity against staphylococcal and enterococcal strains including MRSA, VISA, VRSA, and vancomycin-resistant *Enterococcus faecalis* and *E. faecium* (VRE). The most promising compound identified was further evaluated against multiple clinical isolates of MRSA *in vitro* and *in vivo* against MRSA USA300 in a murine wound infection model.

5.1.2 Results and Discussion

5.1.2.1 Identification of antibacterial compounds

We developed a program to identify compounds with potent activity against drug-resistant bacterial pathogens. A library of compounds (both commercially available and synthetic compounds synthesized in our laboratory) was initially screened, at a concentration of 16 µg/mL, for their ability to inhibit bacterial growth. Several compounds, which included **5.1**, **5.2**, **5.3**, **5.4 (F6)**, **5.5**, **5.6** and **5.7** (Figure 5.1) were initially screened against *S. aureus*. Compounds **5.1**, **5.2**, **5.3**, **5.4** and **5.6** significantly inhibited the growth of *S. aureus* (Figure 5.2). Compared to the DMSO control,

compound **5.5** was not active whilst compound **5.7** only slightly inhibited growth (Figure 5.2).

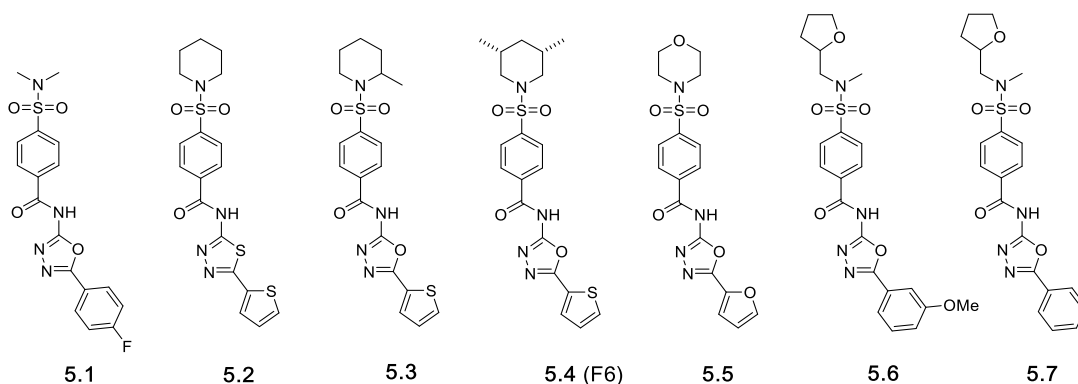


Figure 5.1. Structures of antibacterial compounds. Note: F6 (*cis* : *trans* = 10:1).

Compounds were obtained from Life Chemicals Inc. (Ontario, Canada).

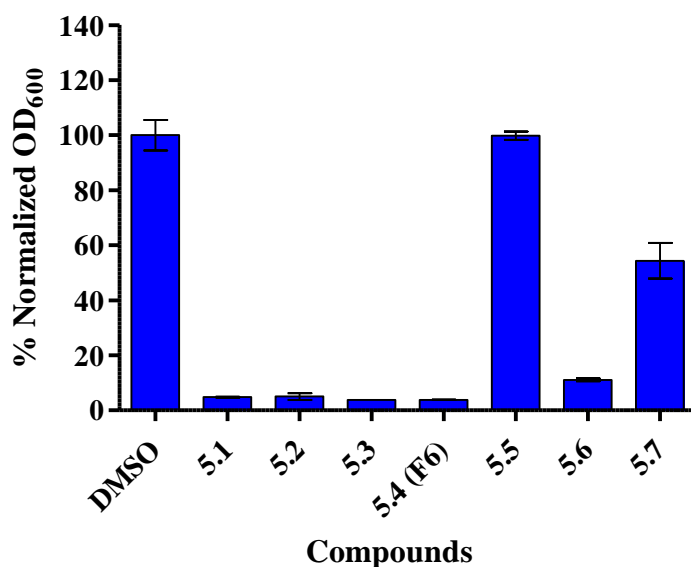


Figure 5.2. Inhibition of growth of *S. aureus* ATCC 25923 by antibacterial compounds. *S. aureus*, at early exponential growth, was treated with either DMSO or 16 $\mu\text{g/mL}$ of compounds and OD₆₀₀ measured after 24 h. Error bars represent standard error of the mean of duplicates.

To further characterize the antibacterial properties of the active compounds, we determined their minimum inhibitory concentrations (MIC) against a clinically-relevant panel of Gram-positive bacterial species including MRSA, vancomycin-sensitive *E. faecalis*, VRE and *Listeria monocytogenes*. Based on their activity from the growth inhibition experiment, we determined the MIC only for compounds **5.1**, **5.2**, **5.3**, **5.4** and **5.6**. The compounds inhibited growth of all strains tested, at concentrations ranging from 2 to 32 $\mu\text{g/mL}$ (Table 5.1).

The presence of methyl substitution on the cyclohexyl moiety of compounds **5.2**, **5.3** and **5.4** is the only structural difference present between the compounds. With the two methyl substitutions, compound **5.4** was the most potent compound identified followed by **5.3** which has one methyl substitution and then **5.2** which has an unsubstituted cyclohexyl moiety (Figure 5.1 and Table 5.1). This implies that the substitution on the cyclohexyl moiety may be important for antibacterial activity.

The most potent compound, **5.4**, was observed to inhibit growth of *S. aureus* (including MRSA), *E. faecalis* (including VRE), and *L. monocytogenes*, at concentrations ranging from 2 to 4 $\mu\text{g/mL}$. Compound **5.4** and the antibiotic vancomycin had similar MIC against *S. aureus* and MRSA (MIC = 1 – 2 $\mu\text{g/mL}$). Impressively, compound **5.4** was greater than 32 times more potent than methicillin against MRSA. It was also observed that **5.4** was more potent than vancomycin against a strain of *E. faecalis* resistant to vancomycin, with the MIC of **5.4** more than 31-fold lower than that of vancomycin.

Table 5.1. MIC ($\mu\text{g/mL}$) of compounds screened against a panel of Gram-positive bacterial pathogens.

Test agents	Bacterial Strains				
	<i>S. aureus</i> ATCC 25923	MRSA ATCC 33592	<i>E. faecalis</i> ATCC 29212	VRE (<i>E. faecalis</i>) ATCC 51575	<i>L. monocytogenes</i> ATCC 19115
5.1	16	16	32	32	32
5.2	16	16	32	32	16
5.3	8	8	16	16	16
5.4 (F6)	2	2	4	4	4
5.6	32	32	32	32	32
Vancomycin	1	1	2	>128	1
Methicillin	2	>128	ND	ND	ND

ND represents not determined

5.1.2.2 Compound **5.4** is bacteriostatic against drug-resistant Gram-positive bacteria. Having observed the potent activity of **5.4** against a single isolate of MRSA and VRE, we proceeded to confirm the compound's potent antibacterial activity against additional strains of MRSA, VISA, VRSA, and VRE (Table 5.2). Compound **5.4** was found to be active against the selected panel of clinical isolates of MRSA at a concentration of 2 $\mu\text{g/mL}$ (Table 5.2). Of note, MRSA USA300 and MRSA USA400 are the main culprits isolated from MRSA skin and soft-tissue infections in North America.^{10, 11} Additionally, **5.4** (MIC of 2 $\mu\text{g/mL}$) retained its potent antibacterial activity against clinical isolates of *S. aureus* and *E. faecium* exhibiting high-level resistance to vancomycin (MIC > 128 $\mu\text{g/mL}$), an agent of last resort for treatment of most MRSA infections³². Linezolid was potent against most clinical isolates of MRSA and VRSA at ≤ 1 $\mu\text{g/mL}$ (Table 5.2). However, linezolid was inactive against MRSA NRS119, a strain isolated as linezolid-resistant; **5.4**, in contrast retained its

potent activity against this strain (MIC = 2 µg/mL). Interestingly, compound **5.4** appears to be a bacteriostatic agent as its minimum bactericidal concentration (MBC) value exceeded >128 µg/mL. This was similar to the results obtained for linezolid, an antibiotic known to exhibit bacteriostatic activity *in vitro* against MRSA.^{33, 34}

Table 5.2. The minimum inhibitory concentration (MIC, in µg/mL) and minimum bactericidal concentration (MBC, in µg/mL) of compound **5.4** and select antibiotics.

Bacterial Strain	5.4 (F6)		Linezolid		Vancomycin	
	MIC	MBC	MIC	MBC	MIC	MBC
MRSA NRS119	2	>128	32	32	≤1	≤1
MRSA NRS123 (USA400)	2	>128	≤1	64	≤1	≤1
MRSA NRS384 (USA300)	2	>128	≤1	64	≤1	≤1
MRSA NRS385 (USA500)	2	>128	≤1	2	≤1	2
MRSA NRS386 (USA700)	2	>128	≤1	128	≤1	≤1
MRSA NRS387 (USA800)	2	>128	≤1	128	2	2
VISA NRS1	2	>128	≤1	1	4	4
VRSA VRS12	2	>128	≤1	32	>128	>128
<i>E. faecium</i> ATCC 700221 (VRE)	2	128	≤1	64	>128	>128

As observed from Table 5.2, the MBC of compound **5.4** was generally >128 µg/mL, several folds above the MIC, an indication that the compound was bacteriostatic. We sought to further ascertain whether compound **5.4** was indeed bacteriostatic. From time-kill analysis using MRSA USA300, at 6× MIC of compound **5.4** (12 µg/mL), we observed that compound **5.4** caused a 2.01-log₁₀ reduction in MRSA USA300, which was just slightly higher than the 1.85-log₁₀ reduction observed with linezolid after a 24-hour incubation period. On the other hand, the bactericidal antibiotic

vancomycin completely eradicated the MRSA USA300 inoculum within 12 hours. These observations imply that compound **5.4**, just like linezolid, exhibits *in vitro* bacteriostatic effect against MRSA USA300 (Figure 5.3).

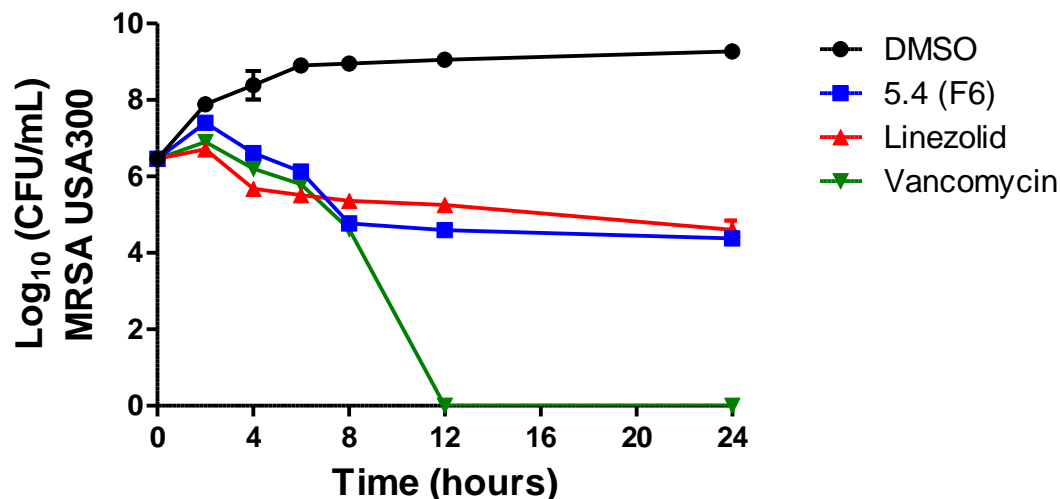


Figure 5.3. Time-kill analysis of compound **5.4** against MRSA USA300 using linezolid as a control antibiotic. MRSA USA300 was incubated with compound **5.4** (12 $\mu\text{g}/\text{mL}$) or linezolid (6 $\mu\text{g}/\text{mL}$) vancomycin (6 $\mu\text{g}/\text{mL}$) or DMSO and the number of cells estimated at the indicated time points. Experiment was performed in triplicates.

5.1.2.3 Compound **5.4** is not active against Gram-negative bacteria

We next moved to investigate whether compound **5.4** would be effective against Gram-negative bacterial pathogens as well. Hence, we determined the MIC of compound **5.4** against a selected panel of clinically-relevant Gram-negative bacterial pathogens. Compound **5.4** was not active against *Acinetobacter baumannii*, *Klebsiella pneumoniae*, *Pseudomonas aeruginosa* and *Escherichia coli* BW25113. The lack of activity against Gram-negative bacteria appears to be due to compound **5.4** being a

substrate for efflux. This can be seen by the shift in the MIC observed for compound **5.4** against wild-type *E. coli* BW25113 (MIC > 128 µg/mL) in comparison to a mutant strain (*E. coli* JW5503-1) where the AcrAB-TolC multidrug-resistant efflux pump is knocked out (MIC for **5.4** improves to 2 µg/mL). A similar result was observed with linezolid and erythromycin, two antibiotics known to be substrates for the AcrAB-TolC efflux pump in Gram-negative bacteria.^{35, 36}

Table 5.3. MIC of compound **5.4** against selected Gram-negative bacterial pathogens.

Bacterial Strain	Test agents			
	5.4 (F6)	Linezolid	Erythromycin	Colistin
<i>A. baumannii</i> ATCC 19606	128	N.D.	N.D.	≤ 1
<i>K. pneumoniae</i> BAA-1706	>128	N.D.	N.D.	≤ 1
<i>P. aeruginosa</i> ATCC 15442	>128	N.D.	N.D.	≤ 1
<i>E. coli</i> BW25113	>128	>128	32	N.D.
<i>E. coli</i> JW5503-1 ($\Delta tolC$)	2	8	≤ 1	N.D.

ND represents not determined

5.1.2.4 MRSA does not develop resistance to compound **5.4**

One of the major challenges in treatment of bacterial infections is the rapid generation of resistant pathogens. In treatment of MRSA infections, antibiotics like ciprofloxacin fail due to resistance.^{15, 16} We performed the multistep resistance selection to evaluate the ability of MRSA USA400 to develop resistance to compound **5.4** *in vitro*. The MIC of compound **5.4** remained unchanged over nine passages (Figure 5.4). A one-fold increase in the MIC of compound **5.4** was observed after the tenth passage where after no additional increase in MIC was observed up to the 14th passage. This indicates MRSA is unlikely to form rapid resistance to compound **5.4** *in vitro*, even

after multiple passages. In contrast, the MIC of ciprofloxacin, an antibiotic that targets DNA gyrase, increased three-fold after the eighth passage and continued to rapidly increase thereafter. MRSA resistance to ciprofloxacin emerged after the eleventh passage (an eight-fold increase in MIC was observed) (Figure 5.4). By the 14th passage, the MIC of ciprofloxacin increased more than 2000-fold from the original MIC value (0.25 $\mu\text{g/mL}$). The emergence of MRSA resistance to ciprofloxacin agrees with previously published reports.^{17, 29, 37}

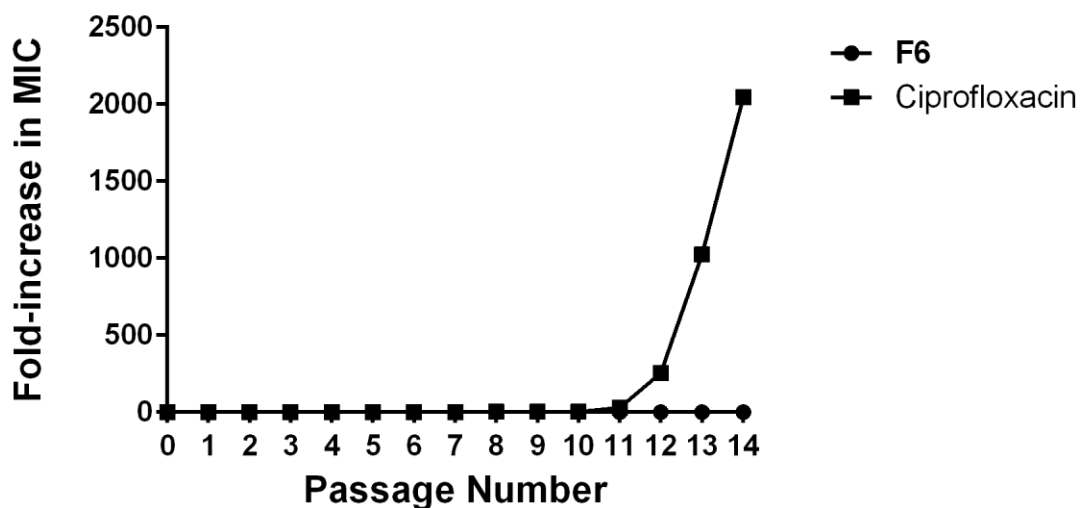


Figure 5.4. Multi-step resistance selection of compound **5.4 (F6)** and ciprofloxacin against MRSA. MRSA USA400 was serially passaged daily over a 14-day period and the broth microdilution assay was used to determine the minimum inhibitory concentration of both **F6** (compound **5.4**) and ciprofloxacin (control antibiotic) against MRSA after each successive passage. A four-fold shift in MIC would be indicative of bacterial resistance forming to the test agent.

5.1.2.5 Compound 5.4 is non-toxic against mammalian cells

As earlier stated, MRSA is responsible for SSTIs.^{7, 8} Compound 5.4 demonstrated *in vitro* potency against several important MRSA strains. Prior to evaluating compound 5.4 in an animal model of MRSA skin infection, we determined the toxicity profile of compound 5.4 against mammalian cells. The compound was incubated with murine macrophage (J774) cells and human colorectal (Caco-2) cells at concentrations ranging from 2 $\mu\text{g}/\text{mL}$ to 256 $\mu\text{g}/\text{mL}$. Compound 5.4 exhibited an excellent safety profile against both J774 and Caco-2 cells (Figure 5.5) as the compound was found to be non-toxic up to 128 $\mu\text{g}/\text{mL}$ (63-fold higher than the MIC of compound 5.4 against MRSA).

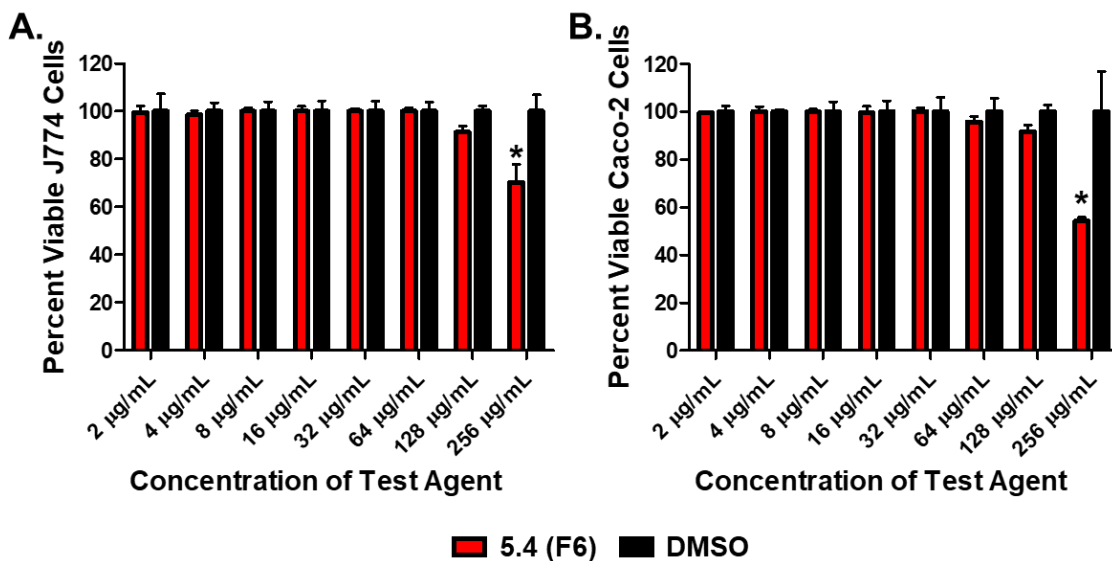


Figure 5.5. Toxicity analysis of compound 5.4 (F6) against mammalian cell lines. Percent viable mammalian cells (measured as average absorbance ratio (test agent relative to DMSO)) after exposure to compound F6 (tested in triplicate) at concentrations ranging from 2 to 256 $\mu\text{g}/\text{mL}$ against **A.** murine macrophage (J774) cells, or **B.** human colorectal (Caco-2) cells using the MTS 3-(4,5-dimethylthiazol-2-

yl)-5-(3-carboxymethoxyphenyl)-2-(4-sulfophenyl)-2H-tetrazolium) assay. Dimethyl sulfoxide (DMSO) was used as a negative control to determine a baseline measurement for the cytotoxic impact of each compound. Error bars represent standard deviation values for triplicates. A two-way ANOVA, with post hoc Sidak's multiple comparisons test, determined statistical difference (denoted by the asterisk) ($P < 0.05$) between the values obtained for compound **5.4** and DMSO (negative control, used as solvent for the compound).

5.1.2.6 Compound **5.4** reduces MRSA burden in mouse skin wound infection

Having determined that F6 was not toxic, an established mouse skin wound infection model^{38, 39} was used to assess the *in vivo* efficacy of compound **5.4**. Mice were infected with MRSA USA300, the predominant strain responsible for *S. aureus*-based SSTIs in North America. After the formation of an abscess, the wound was treated twice daily for five days with either compound **5.4**, fusidic acid, or the vehicle (petroleum jelly) alone. It was observed that compound **5.4** (0.59- \log_{10} , 72.41% reduction) was as effective as the control antibiotic fusidic acid (0.71- \log_{10} , 77.91% reduction) in reducing the burden of MRSA in the wounds of infected mice after only five days of treatment (Figure 5.6). The data garnered from the skin infection mouse model further confirms the potent antibacterial effect of compound **5.4** against MRSA.

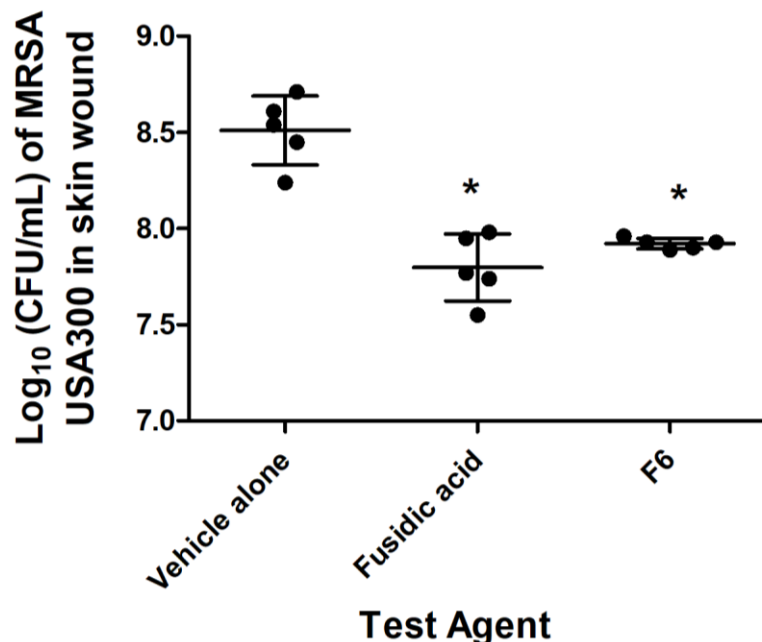


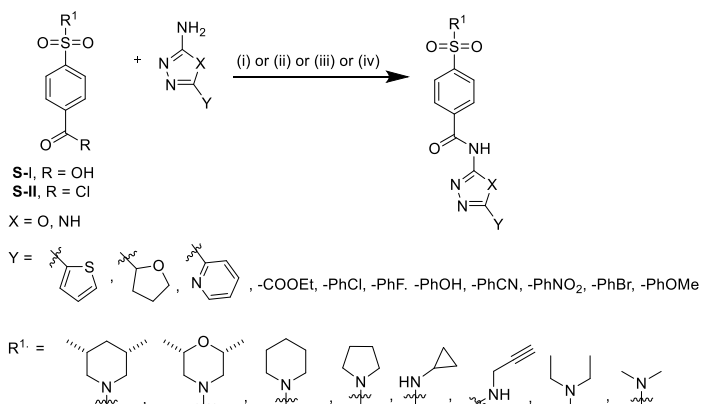
Figure 5.6. Efficacy of compound **5.4** (F6) in an *in vivo* mouse skin wound infection model. Average log₁₀ reduction in MRSA USA300 CFU/mL in wounds of mice after five days (two doses per day) of treatment. A one-way ANOVA with post-hoc Dunnet's multiple comparisons found statistical significance (*, $P < 0.05$) between mice treated with fusidic acid and compound **5.4**, compared to mice receiving the vehicle (petroleum jelly) alone.

5.1.2.7 Compound **5.4** analogs with potent antibacterial activity

With such impressive antibacterial properties, we wondered whether structural analogs of compound **5.4** could have better activity. We therefore synthesized 20 compounds (Figure 5.7) by making modifications to groups on compound **5.4** and evaluated their ability to inhibit the growth of *S. aureus* at 16 µg/mL (Figure 5.8). For compounds that showed activity against *S. aureus* in the growth inhibition assay, we proceeded to determine the MIC (Table 5.4). It was observed that installation of a

morpholine (**5.8**) instead of a piperidine or deletion of the sulfonamide group (**5.21**) abolished activity. Growth inhibition was not significantly affected upon deletion of the dimethyl-substitutions on the piperidine (**5.23**). However, from their MIC values, compound **5.22** was not as active as compound **5.4**. These suggested that the 4-((3,5-Dimethylpiperidin-1-yl)sulfonyl)benzamide was relevant for activity. Deletion of the amide linkage between the benzene ring and the oxadiazole ring resulted in compound **5.11**, which was not active. Also, activity was lost when the –O in the oxadiazole ring was replaced with –NH (**5.13**), highlighting the importance of the oxadiazole moiety. We also investigated the importance of the thiophene ring for antibacterial activity. Replacement of the thiophene ring with either a tetrahydrofuran or an acid ester resulted in inactive compounds **5.9** and **5.10** respectively. Interestingly, unlike **5.9** and **5.10**, replacement of the thiophene ring with a chlorophenyl, bromophenyl, methoxyphenyl, or fluorophenyl resulted in compounds **5.12 (F6-5)**, **5.14**, **5.19**, and **5.20** respectively, which were all found to inhibit the growth of *S. aureus*. Impressively, the MIC of these compounds against the tested bacterial pathogens ranged from 1 µg/mL to 4µg/mL (Table 5.4). Based on their MIC values, compound **5.12 (F6-5)** was the best.

A.



B.

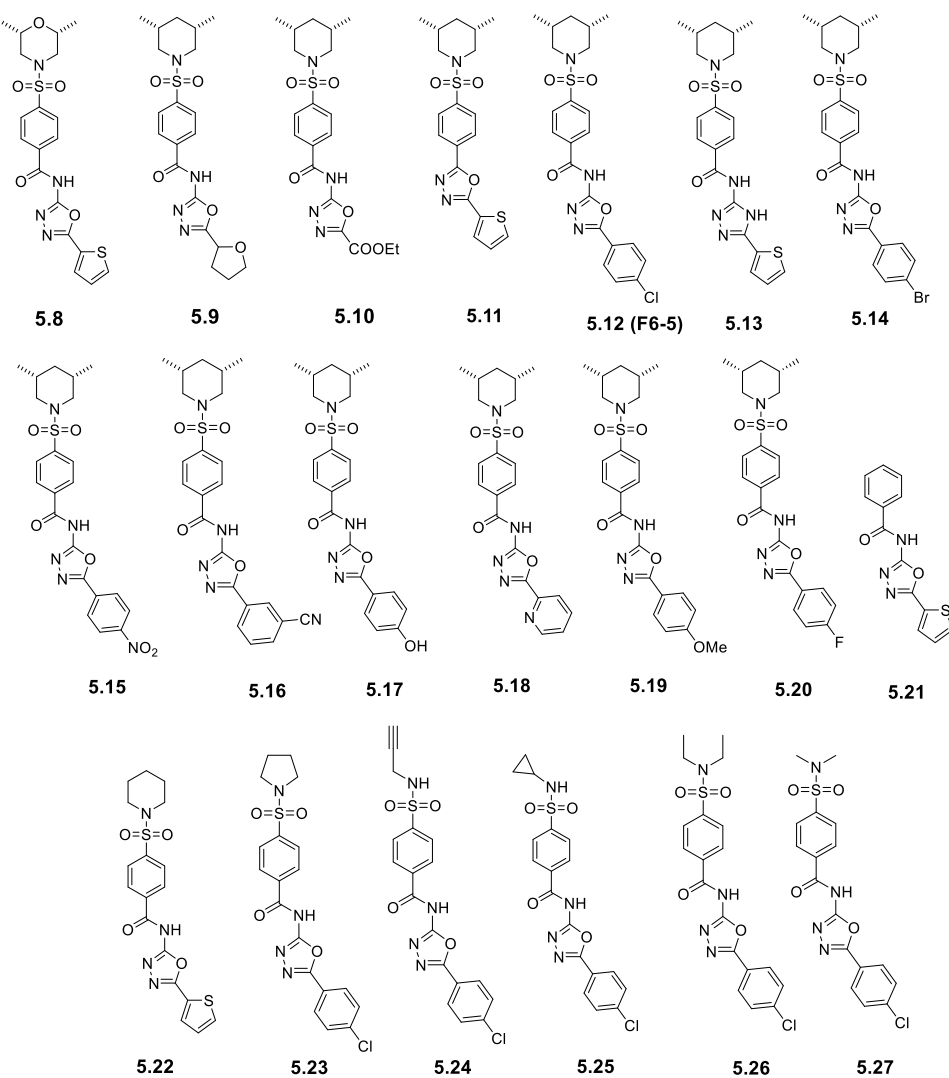


Figure 5.7. Structural analogs of compound **5.4**, synthesized in our laboratory. **A.**

Schematic representation of the synthesis of the analogs studied. Conditions used: (i)

MeLi, THF, $-78\text{ }^{\circ}\text{C}$ to rt, 14 h; (ii) EDC·HCl, DMAP, CH_2Cl_2 , rt, 16 h; (iii) a) T3P, CH_2Cl_2 , rt, 1h b) TEA, DMAP, rt, overnight; (iv) BOP reagent, DIPEA, DMF, rt, 16 h; **B**. Structures of analogs synthesized. Note: The starting material **S-I** existed as 4 :1 *cis* to *trans* form. The product obtained as **5.9** (*cis* : *trans* = 10 :1), **5.10** (*cis* : *trans* = 4 :1), **5.11** (*cis* : *trans* = 20 :1), **5.12** (*cis* : *trans* = 6 :1), **5.13** (*cis* : *trans* = 13 :1), **5.14** (*cis* : *trans* = 6:1); **5.15** (*cis* : *trans* = 5 :1), **5.16** (*cis* : *trans* = 6 :1), **5.17** (*cis* : *trans* = 4 :1), **5.18** (*cis* : *trans* = 6 :1), **5.19** (*cis* : *trans* = 6 :1), **5.20** (*cis* : *trans* = 4 :1)

Compared with compound **5.4**, the MIC of **5.12** (Table 5.4) across the panel of bacterial pathogens tested appeared to be slightly better (Table 5.1). For example, the MIC of compound **5.12** against MRSA was 1 $\mu\text{g}/\text{mL}$ compared to the MIC obtained for compound **5.12** (2 $\mu\text{g}/\text{mL}$). Furthermore, compound **5.12** had an MIC of 2 $\mu\text{g}/\text{mL}$ against VRE (*E. faecalis*) and *L. monocytogenes* compared to the MIC of compound **5.12** (4 $\mu\text{g}/\text{mL}$) against these specific bacterial pathogens. Excitingly, compound **5.12** was more active against VRE (*E. faecalis*) than vancomycin.

Given the potency of compound **5.12**, we further evaluated the importance of the piperidine moiety maintaining the other portions of compound **5.12**. Although modifications at this position did not significantly affect growth inhibition, the MIC values obtained were worse than compound **5.12**. For example, installation of a pyrrolidine ring yielded compound **5.23** with MIC values ranging from 8 $\mu\text{g}/\text{mL}$ to 16 $\mu\text{g}/\text{mL}$. Compounds with two alkyl groups on the nitrogen of the sulfonamide like the diethyl-substituted compound **5.26** and dimethyl-substituted compound **5.27** could inhibit *S. aureus* growth. However, the diethyl-substituted compound **5.26** had better

MIC values (16 $\mu\text{g/mL}$ to 32 $\mu\text{g/mL}$) than the dimethyl-substituted compound **5.27** (32 $\mu\text{g/mL}$ to 64 $\mu\text{g/mL}$). Similarly, analogs with just one alkyl group on the nitrogen of the sulfonamide (compound **5.24** and **5.25**) were less active than compound **5.12**. These observations further validate the importance of the dimethyl-substituted piperidine moiety for antibacterial activity.

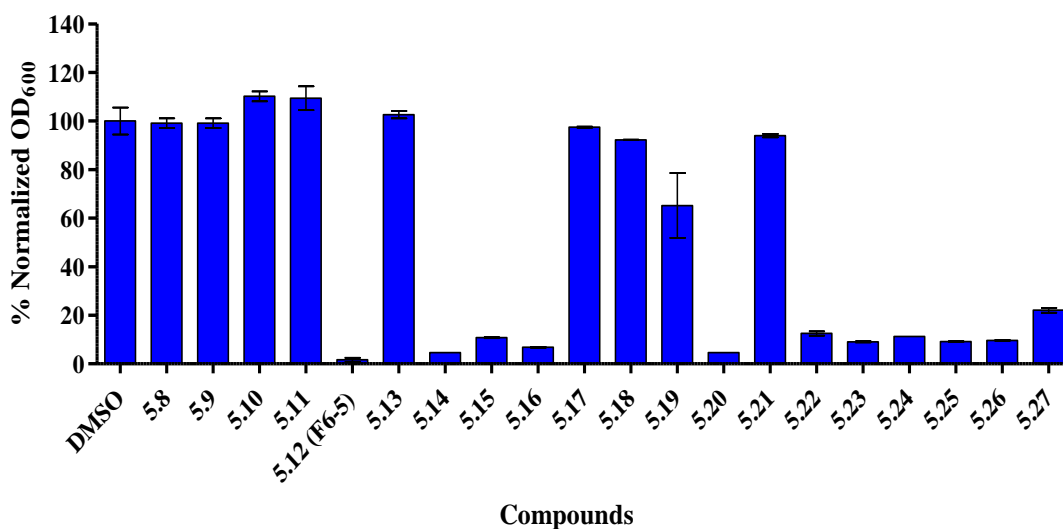
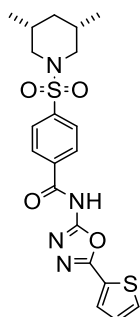


Figure 5.8. Antibacterial activity of analogs of compound **5.4**. Compounds were tested at 16 $\mu\text{g/mL}$ for their ability to inhibit *S. aureus* growth. The OD₆₀₀ of compounds were normalized to that of the DMSO control.

Table 5.4. MIC ($\mu\text{g/mL}$) of **5.12 (F6-5)** and vancomycin against a panel of Gram-positive bacterial pathogens.

Test agent	<i>S. aureus</i> ATCC 25923	MRSA ATCC 33592	<i>E. faecalis</i> ATCC29212	VRE (<i>E. faecalis</i>) ATCC 51575	<i>L. monocytogenes</i> ATCC 19115
5.12 (F6-5)	2	1	4	2	2
5.14	2	4	4	4	4
5.15	32	16	64	32	32
5.16	16	8	32	16	8
5.19	4	4	4	4	4
5.20	4	4	4	4	4
5.22	32	32	16	64	32
5.23	16	8	16	16	16
5.24	64	32	64	64	64
5.25	16	16	32	16	16
5.26	16	16	32	16	16
5.27	64	32	64	64	64
Vancomycin	1	1	2	>128	1



F6- *cis*

Figure 5.9. Structure of compound **5.4 - cis** (*cis* : *trans* = 30 :1).

Thus far the compound **5.4** compound that was initially used for screening was purchased from Life Chemicals Inc. (Ontario, Canada) as a predominantly *cis* isomer (*cis:trans* = 10:1). Analogs of compound **5.4**, which were synthesized in our lab were also predominantly *cis* (ranging from 4:1 to 20:1 *cis:trans*). To exclude the possibility that the observed antibacterial activities of the compounds were from the minor *trans* isomer and not the *cis* form, we desired to make at least one of the active compounds (**5.4**) with a higher *cis/trans* ratio than what we had obtained. To do this, we synthesized an isomerically purer compound **5.4** shown in Figure 5.9, and obtained compound **5.4-cis** (*cis:trans* is 30:1) (see supporting information). **5.4-cis** was tested for antimicrobial activity and the MIC was similar to that of the commercially available **5.4**, which had a *cis:trans* ratio of 10:1 (compare Table 5.1 with Table 5.5).

Table 5.5. Activity (MIC in $\mu\text{g/mL}$) of **5.4-cis** against select Gram-positive bacteria

Bacterial Strain	5.4-cis	Vancomycin
<i>S. aureus</i> ATCC 25923	4	2
MRSA ATCC 33592	4	2
<i>E. faecalis</i> ATCC 29212	4	2
VRE (<i>E. faecalis</i>) ATCC 51575	4	>128
<i>L. monocytogenes</i> ATCC 19115	4	1

5.1.3 Conclusions

We have identified compound **5.4** (**F6**) as a potent antibacterial agent effective against important drug-resistant Gram-positive bacterial pathogens including MRSA, VRSA, VISA, and VRE. It was observed that compound **5.4** was not active against important Gram-negative bacterial pathogens, presumably due to it being a substrate for efflux. Excitingly, resistance was not observed when MRSA was treated with compound **5.4** compared to ciprofloxacin *in vitro*. Compound **5.4** was also active *in*

in vivo in reducing the burden of MRSA in a skin wound infection model in mice. Other compounds like **5.1**, **5.2** and **5.3** were also potent. Through structural-activity relationship (SAR) studies, the relevance of various moieties for antibacterial activity was established. Particularly, the 4-((3,5-Dimethylpiperidin-1-yl)sulfonyl)benzamide and oxadiazole amine moieties were required for activity. From the SAR studies, compound **5.12 (F6-5)** emerged as a slightly more potent analog of compound **5.4** with MIC values ranging from 1 µg/mL to 4 µg/mL.

5.1.4 Materials and methods

5.1.4.1 Bacterial strains and chemical compounds

All MRSA isolates were acquired from BEI Resources. The remaining bacteria were purchased from the American Type Culture Collection (ATCC). Compounds **5.1** (cat. no. F0559-0091), **5.2** (cat. no. F0559-0342), **5.3** (cat. no. F0559-0343), **5.4** (also called **F6**; cat. no. 0559-0346), **5.5** (cat. no. 0608-0426), **5.6** (cat. no. F1821-0760) and **5.7** (cat. no. F1821-0778) were purchased from Life Chemicals Inc., (Ontario, Canada).

5.1.4.2 General synthesis of compounds

Analogs of compound **5.4 (F6)** were synthesized by Dr. Neetu Dayal and George A. Naclerio, post-doctoral fellow and graduate students respectively in the Sintim Research group.

General Considerations: unless noted otherwise, all reagents and solvents were purchased from commercial sources and used as received. The ¹H and ¹³C NMR spectra were obtained in CDCl₃ or DMSO as solvent using a 500 MHz spectrometer with Me₄Si as an internal

standard. Chemical shifts are reported in parts per million (δ) and are calibrated using residual undeuterated solvent as an internal reference. Data for ^1H NMR spectra are reported as follows: chemical shift (δ ppm) (multiplicity, coupling constant (Hz), integration). Multiplicities are reported as follows: s = singlet, d = doublet, t = triplet, q = quartet, m = multiplet, or combinations thereof. High resolution mass spectra (HRMS) were obtained using electron spray ionization (ESI) technique and as TOF mass analyzer. New compounds were characterized by ^1H NMR, ^{13}C NMR, and HRMS data. Substrate 4-((3,5-dimethylpiperidin-1-yl)sulfonyl)benzoic acid (95% purity) **S-I** was purchased from Enamine and ^1H NMR of **S-I** substrate shows a mixture of *cis* and *trans* form in a 4:1 ratio, respectively. Substrate *Cis* 3,5-Dimethyl piperidine was purchased from J & W pharma lab. All the other substrates were purchased from Enamine LLC (NJ, USA).

5.1.4.3 Screening of compounds for antibacterial activity against *S. aureus*

Library compounds and analogs of **F6** (compound **5.4**) were dissolved in DMSO at 10 mg/mL. *S. aureus* was cultured in Mueller Hinton Broth to early exponential phase at which point culture aliquots were incubated with compounds at 16 $\mu\text{g/mL}$ or DMSO in duplicates. The culture was continued at 37 $^\circ\text{C}$ for 24 hours. Aliquots (100 μL) of the cultures were dispensed into clear 96 well microtiter plates and OD_{600} was recorded. Percent normalized OD_{600} was obtained by using the equation

$$\% \text{Normalized } \text{OD}_{600} = \left(\frac{X - X_o}{X_T - X_o} \right) \times 100$$

Where for a given compound, X is the OD_{600} of culture with the compound, X_o is that of media only and X_T is the OD_{600} of the DMSO control.

5.1.4.4 Determination of the MIC and MBC

The minimum inhibitory concentration (MIC) of compounds and control antibiotics (methicillin, linezolid and vancomycin), tested from 128 $\mu\text{g/mL}$ to 1 $\mu\text{g/mL}$, was determined using the broth microdilution method²⁸ against the selected bacterial pathogens. Bacteria were cultured in cation-adjusted Mueller Hinton Broth (for strains in Tables 1 and 4) or Brain Heart Infusion broth (for *Enterococcus faecium*) or Tryptic Soy Broth (all other bacteria) in a 96-well plate at 37 °C for at least 20 hours. The MIC was classified as the lowest concentration where no visual growth of bacteria was observed. The minimum bactericidal concentration (MBC) was tested by spotting 4 μL from wells with no growth onto Tryptic Soy Agar (TSA) plates. Plates were incubated at 37 °C for at least 18 hours before recording the MBC.

5.1.4.5 Time-kill analysis

The time-kill analysis was performed as previously described.²⁹ MRSA USA300 cells in logarithmic growth phase were diluted to 2.92×10^6 colony-forming units per mL (CFU/mL) and exposed to concentrations equivalent to either $6 \times \text{MIC}$ (in triplicate) of **F6** (compound **5.4**), linezolid or vancomycin in Tryptic Soy Broth. Aliquots (100 μL) were collected from each treatment after 0, 2, 4, 8, 12, and 24 hours of incubation at 37 °C and subsequently serially diluted in phosphate-buffered saline (PBS). Bacteria were then transferred to TSA plates and incubated at 37 °C for 18-20 hours before viable CFU/mL was determined.

5.1.4.6 Toxicity profile, resistance selection and mouse study of **5.4**

Toxicity profiling, resistance selection and murine infection experiments were performed by Dr. Haroon Mohammad (post-doctoral fellow) and Nader S. Abutaleb (graduate student) from Dr. Mohamed Seleem's group, our collaborators at the College of Veterinary Medicine, Purdue University.

Toxicity profile of **5.4 (F6)**: Compound **5.4** was assayed (at concentrations ranging from 2 µg/mL to 256 µg/mL) against murine macrophage (J774) and human colorectal (Caco-2) epithelial cell lines to determine the potential toxic effect to mammalian cells *in vitro*. Caco-2 cells were cultured in Dulbecco's Modified Eagle Medium (DMEM) supplemented with 20% fetal bovine serum (FBS), non-essential amino acids (1X), and penicillin-streptomycin at 37 °C with CO₂ (5%). J774 cells were cultured in DMEM supplemented with 10% FBS. Upon reaching 85-90% confluency, cells were transferred to all wells of a 96-well tissue-culture treated plate. The cells were incubated in serum-free medium with the compounds (in triplicate) at 37 °C with CO₂ (5%) for 24 hours. Cells exposed to equivalent concentrations of DMSO served as the negative control. The assay reagent MTS 3-(4,5-dimethylthiazol-2-yl)-5-(3-carboxymethoxyphenyl)-2-(4-sulfophenyl)-2H-tetrazolium) (Promega, Madison, WI, USA) was subsequently added and the plate was incubated for four hours. Absorbance readings (at OD₄₉₀) were taken using a kinetic microplate reader (Molecular Devices, Sunnyvale, CA, USA). The quantity of viable cells after treatment with each compound was expressed as a percentage of the viability of DMSO-treated control cells (average of triplicate wells ± standard deviation). The toxicity data were analyzed via a two-way ANOVA, with post hoc

Sidak's multiple comparisons test ($P < 0.05$), utilizing GraphPad Prism 6.0 (GraphPad Software, La Jolla, CA, USA).

Multistep resistance selection: To determine if MRSA would be capable of forming resistance to compound **5.4** quickly, a multi-step resistance selection experiment was conducted, as described previously²⁹. The broth microdilution assay was utilized to determine the MIC of compound **5.4** and ciprofloxacin exposed to MRSA USA400 (NRS123) over 14 passages during a period of two weeks. Resistance was classified as a greater than four-fold increase in the initial MIC, as reported elsewhere³⁰.

Murine MRSA wound infection model: The murine MRSA skin infection was conducted as described in a previous report³¹, following the Purdue University Animal Care and Use Committee (PACUC) and carried out in strict accordance with the recommendations in the Guide for the Care and Use of Laboratory Animals of the National Institutes of Health. Three groups ($n = 5$) of eight-week old female BALB/c mice (obtained from Envigo, Indianapolis, IN, USA) were used in this study and received an intradermal injection (40 μ L) containing 1.32×10^9 CFU/mL MRSA USA300. After the formation of an abscess/open wound at the site of injection for each mouse, topical treatment was initiated with each group of mice receiving the following: fusidic acid (2%) or **5.4** (2%) twice daily for five days. One group of mice was treated with the vehicle alone (petroleum jelly, negative control). Each group of mice was individually housed in a ventilated cage with appropriate bedding, food, and water. Mice were checked at least four times daily during infection and treatment to ensure no adverse reactions were observed. Mice were humanely euthanized via CO₂ asphyxiation 12 hours after the last dose was administered. The region around the

skin wound was aseptically excised and subsequently homogenized in PBS. The homogenized tissue was then serially diluted in PBS before plating onto mannitol salt agar plates. The plates were incubated for at least 16 hours at 37 °C before viable CFU were counted and MRSA reduction in the skin wound post-treatment was determined for each group (relative to the negative control).

Chapter 6: Conclusions and future perspectives

5.1 Conclusions and future perspectives

One of the core actions suggested by the US Centers for Disease Control and Prevention to curb antibiotic resistance involves the development of new antibiotics and diagnostic tools.¹ This comes at a time where antibiotic resistance is on a rapid rise. Drug-resistant pathogens such as MRSA and VRE continue to pose significant health threats in the hospitals as well as communities. The annual cost of antibiotic resistance to the US healthcare is estimated to range from \$21 billion to \$34 billion. The introduction novel antibiotic class or scaffolds needs to be at the core of the quest for new antibiotics. New antibiotic classes could be discovered for the well-established targets including cell wall synthesis, protein synthesis, DNA and RNA synthesis.² Alternatively, identification of novel targets could lead to the discovery of novel antibiotics.

Bacteria modulate a myriad of processes by employing cyclic dinucleotide signaling.³ Cyclic di-AMP has emerged as a universal signaling molecule in Gram-positive bacteria, mycobacteria as well as some Gram-negative bacteria. Since its discovery in 2008,⁴ c-di-AMP has been associated with various physiological processes including biofilm formation,^{5, 6} peptidoglycan homeostasis, cell size regulation,⁶ and ion transport⁷ among others. The diadenylate cyclase gene encodes diadenylate cyclases (DAC) that synthesize c-di-AMP. In human pathogens like *S. aureus*, *L. monocytogenes* and *S. pneumoniae*⁸⁻¹⁰ deletion of this gene has been shown to be lethal, highlighting the essentiality of the second messenger. Increases in the cellular

concentration of c-di-AMP, has been implicated in antibiotic resistance particularly β -lactam resistance. Consequently, c-di-AMP synthesis has been suggested as a potential antibiotic target. Small molecule cell-permeable inhibitors of c-di-AMP synthesis could have therapeutic implications.

The discovery of coralyne assay set the stage for the identification of the first DAC inhibitor, bromophenol thiohydantoin.¹¹ As expected, 3'-deoxyATP which cannot be cyclized into c-di-AMP, was found to inhibit the activity of DisA.¹² Both compounds had significant limitation; bromophenol thiohydantoin is a poor inhibitor of DisA and efforts to improve its potency failed whilst the nucleotide analog is not druglike.^{13, 14} In order to probe the molecular mechanisms behind c-di-AMP signaling, potent cell permeable inhibitors of c-di-AMP synthesis will be required. During my PhD, I screened large libraries of compounds to identify potent inhibitors of DAC. Greater than 50,000 compounds were screened for *in vitro* inhibition of the DAC activity of DisA. To identify new antibacterial scaffolds, I routinely screened inhibitors against bacteria, particularly staphylococcal strains.

In chapter 2, I discussed the identification of suramin, the most potent inhibitor of DisA thus far discovered using coralyne assay. Under the same conditions (1 μ M DisA and 300 μ M ATP), suramin inhibited DisA with an IC₅₀ of 2.3 μ M compared with the 67.2 μ M observed with bromophenol thiohydantoin, approximately 30 times better than bromophenol thiohydantoin. Suramin is a polysulfonated urea derivative. However, compounds with sulfonic acid groups such as 8-aminonaphthalene-1,3,6-trisulfonic acid (ANTS), Ponceau S, 8-aminopyrene-1,3,6-trisulfonic acid (APTS) and benzothiazole-2,5-disulfonic did not inhibit DisA activity. Suramin did

not inhibit the activity of GdpP (formerly YybT), the cognate c-di-AMP PDE in *B. subtilis*.¹⁵ From fluorescence quenching experiments, suramin was observed to bind to DisA with a K_d of 5.4 μM . Although suramin potently inhibits the *in vitro* activity of DisA, it is a large anion compound with limited cell permeability. Moloud Aflakis, a graduate student in the Sintim Group recently found that suramin inhibit the cGAMP synthesis of activity of cGAS.¹⁶ The mammalian cGAMP cyclase binds ATP and so it is not surprising that its activity was inhibited by suramin.

In the second section of chapter 2, I identified tea polyphenols as DAC inhibitors of DisA activity. Theaflavin gallate, theaflavin digallate and tannic acid all inhibited DisA activity. Of the 3, tannic acid was found to be a non-specific inhibitor of DisA. The inhibition of DisA activity by the theaflavins appeared to be dependent on the number of gallate moieties. Theaflavin which contains no gallate was not active. Theaflavin gallate, with one gallate moiety inhibited DisA with an IC_{50} of 23.6 μM whilst theaflavin digallate which possessed two gallates had an IC_{50} value of 8.5 μM . However, gallic acid did not inhibit DisA activity. Inhibition of DisA by theaflavin digallate did not depend on ATP concentration as similar IC_{50} values were obtained with increasing ATP concentration. An apparent dissociation constant of 23 μM was determined for the binding of theaflavin digallate to DisA.

The identification of cell permeable DAC inhibitors is pivotal to understanding the cellular roles of c-di-AMP. I screened a library of pharmacologically active compounds and identified GW5074, a kinase inhibitor as an inhibitor of DisA. Both DAC enzymes and protein kinases bind ATP in their active site. It is therefore possible for an ATP-competitive kinase inhibitor to bind into the active site of a DAC

enzyme. GW5074 (compound **3.1**), a c-Raf inhibitor¹⁷ was identified as a DisA inhibitor using coralyne assay and the inhibition was confirmed with radioactive TLC and HPLC assay. Analysis of the analogs of compound **3.1** revealed interesting structure-activity relationship. We found that the OH group on the benzylidene moiety was important for DAC inhibition as well as the halogen substitution. Also, substitution of the indolinone moiety with hydrophilic groups afforded weak DAC inhibitors. The hydroxybenzylidene-indolinones possessed selectively killed Gram-positive bacteria over Gram-negative bacteria and also inhibited the formation of MRSA biofilms. When tested alone, we observed moderate inhibition of *S. aureus* (methicillin susceptible and methicillin-resistant) with MIC values ranging from 4 µg/mL to 16 µg/mL. Generally, the compounds were not active against vancomycin-resistant *Enterococcus faecalis* (VRE). Interestingly, I observed that they could potentiate the activity of methicillin and vancomycin against MRSA and VRE.

In chapter 4, I disclose that compound **3.1** (GW5074) and other halogenated 4-hydroxybenzylidene indolinones, decrease the intracellular concentration of c-di-AMP synthesized by the *S. aureus* DacA. A graduate student in the Sintim group, Kenneth Onyedibe is currently working on identifying more compounds that inhibit c-di-AMP synthesis. These will also be evaluated for their ability to reduce cellular c-di-AMP levels. Compounds with better potency than discussed here will allow for studying the effect of reducing cellular c-di-AMP with a small molecule. I showed that compound **3.1** synergizes with many traditional antibiotics. Analysis of the effect of compound **3.1** on macromolecular biosynthesis revealed that DNA and RNA synthesis, as well as protein and cell wall synthesis were affected.

Global proteomics analysis revealed that compound **3.1** treatment resulted in the downregulation of AgrC (a quorum sensing-related histidine kinase), AgrA (a quorum sensing-related response regulator) as well as downstream targets, such as hemolysins, lipases and proteases in *S. aureus*. We observed that the mRNA levels of *agrA* were significantly decreased in the presence of compound **3.1**, possibly explaining the observed downregulation at the protein level. The transcription of *agrA* from the *agr* operon is directed by AgrA. Hence, it may be speculated that compound **3.1** interacts with AgrA, although the upregulation of the *agr* transcriptional repressor, SarX would also lead to low levels of *agrA*.

The *agr* system regulates quorum sensing in *S. aureus*. A major question is whether c-di-AMP signaling intersects with quorum sensing in *S. aureus* and other bacteria. In the similar but distinct cyclic di-GMP, quorum sensing (QS) has been linked with the intracellular concentration of c-di-GMP in Gram-negative bacteria.¹⁸ For example, at low cell density in *Xanthomonas campestris*, RpfF hydratase is bound to the histidine kinase RpfC.¹⁸ This represses the activity of RpfF limiting the amount of diffusible signal factor (DSF) synthesized. Consequently, RpfC is not activated by DSF and this prevents the phosphorylation and activation of the HD-GYP domain-containing c-di-GMP phosphodiesterase, RpfG.¹⁸ The cellular levels of c-di-GMP are thus high under low cell density conditions. C-di-GMP then binds to and represses the transcription factor Clp, inhibiting the transcription of various virulence genes.¹⁸ Conversely, at high cell density, sensing of the DSF concentrations are high and sensing of DSF by the histidine kinase RpfC, leads to the phosphorylation and activation of RpfG, the c-di-GMP PDE.¹⁸ The PDE activation leads to decreased c-di-GMP levels, releasing the

repression of the transcriptional regulator Clp. Clp directs the transcription of various virulence factors including exopolysaccharide (EPS) biosynthesis, extracellular proteins.¹⁸ Similarly, the integration of c-di-AMP signaling with quorum sensing in the regulation of various physiological processes is plausible. From our observations, compound **3.1** reduced intracellular levels of c-di-AMP and inhibited the *agr* system. It could therefore be speculated that in *S. aureus*, low c-di-AMP levels decrease the transcription of the *agr* system with a resultant decrease in secreted virulence factors like hemolysins, lipases and exoproteases. Conversely, high c-di-AMP levels would be expected to increase *agr* expression and hence secretion of virulence factors. These could be tested with genetic mutants of DAC and PDE that create low and high cellular c-di-AMP levels respectively. Given that *agrA* mRNA levels were decreased in the presence of compound **3.1**, it would be expected that the relative expression of the components of the *agr* operon would be decreased expression in $\Delta dacA$ (lack c-di-AMP) or *dacAG206S* (low levels of c-di-AMP)¹⁹ mutants compared with wildtype *S. aureus* strains. Global proteomics analysis of such strains coupled with RT-PCR analysis will reveal any potential link between c-di-AMP signaling and quorum sensing.

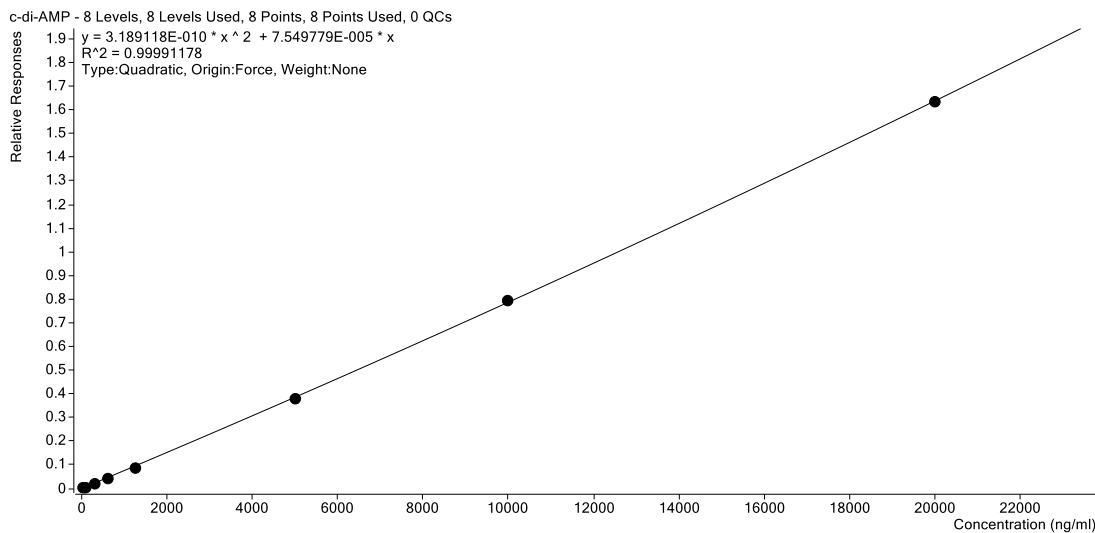
Significant downregulation of enzymes involved in the purine biosynthesis was also observed. *S. aureus* proteins involved in amino acid metabolism and peptide transport as well as metal transport were observed to be downregulated. The most upregulated protein was the peptidoglycan hydrolyase, SceD which was confirmed by RT-PCR experiments. These findings shed insights into how 4-hydroxybenzylidene indolinones kill bacteria and re-sensitize MRSA to other antibiotics. Future work will

evaluate the c-di-AMP synthesis inhibition (both direct enzyme inhibition and effect on cellular c-di-AMP level) of more analogs synthesized by Dr. Neetu Dayal, a post-doctoral fellow in the Sintim group. The antibacterial profiles of the analogs will be determined. Since compound **3.1** downregulated virulence related proteins, the effect of **3.1** and future analogs on quorum sensing in *S. aureus* will be studied. Additionally, antibiotic synergy in animal models will be studied collaboration with Dr. Saleem's group at Purdue University.

From screening a chemical library, we identified compounds with antibacterial activity. In chapter 5, I discussed one of such efforts. The most potent compounds, **F6 (5.4)** and **F6-5 (5.12)** inhibited the growth of drug-resistant Gram-positive bacterial pathogens at concentrations ranging from 1 µg/mL to 2 µg/mL. Both compounds had activity against clinical isolates of MRSA, VISA, VRSA and VRE. MRSA could not develop resistance to **F6** compared with the antibiotic ciprofloxacin. We showed that **F6** could clear MRSA from wounds of infected mice at a potency similar to the antibiotic, fusidic acid. These compounds have the potential to be translated. However, the potency against drug-resistant bacteria must be improved. A graduate student in the Sintim group, George A. Naclerio is making new analogs of the **F6** scaffold. We have identified more potent analogs that with MIC range of 0.25 – 0.5 µg/mL. The target of these compounds will also need to be identified and hence mechanism of action studies like macromolecular biosynthesis need to be evaluated. Additionally, George A. Naclerio has made a biotinylated analog that could be used in pull-down assays to identify protein(s) that the compound binds to.

Appendices

A. Calibration curve used for quantification of c-di-AMP in cell extract by LC-MS/MS.



Solutions of c-di-AMP calibrators at 39.06 to 20,000 ng/mL containing 2.5 μ M cXMP internal standard were used to generate a calibration curve. The response ratios (ratios of c-di-AMP signal to cXMP internal standard) were plotted against the c-di-AMP concentration (ng/mL) and data fitted to a quadratic regression curve.

Bibliography

Chapter 1:

1. Sengupta, S.; Chattopadhyay, M. K.; Grossart, H. P., The multifaceted roles of antibiotics and antibiotic resistance in nature. *Front. Microbiol.* **2013**, *4*, 47.
2. Ventola, C. L., The antibiotic resistance crisis: part 1: causes and threats. *P T.* **2015**, *40* (4), 277-83.
3. Frieden, T., Antibiotic Resistance Threats in the United States, 2013. Centers for Disease Control and Prevention: Atlanta, GA, USA, 2013; p 114.
4. Bhullar, K.; Waglechner, N.; Pawlowski, A.; Koteva, K.; Banks, E. D.; Johnston, M. D.; Barton, H. A.; Wright, G. D., Antibiotic resistance is prevalent in an isolated cave microbiome. *PLoS One* **2012**, *7* (4), e34953.
5. Gould, I. M.; Bal, A. M., New antibiotic agents in the pipeline and how they can help overcome microbial resistance. *Virulence* **2013**, *4* (2), 185-91.
6. Kalia, D.; Merey, G.; Nakayama, S.; Zheng, Y.; Zhou, J.; Luo, Y.; Guo, M.; Roembke, B. T.; Sintim, H. O., Nucleotide, c-di-GMP, c-di-AMP, cGMP, cAMP, (p)ppGpp signaling in bacteria and implications in pathogenesis. *Chem. Soc. Rev.* **2013**, *42* (1), 305-341.
7. Opoku-Temeng, C.; Zhou, J.; Zheng, Y.; Su, J.; Sintim, H. O., Cyclic dinucleotide (c-di-GMP, c-di-AMP, and cGAMP) signalings have come of age to be inhibited by small molecules. *Chem. Commun.* **2016**, *52* (60), 9327-9342.
8. Narang, A., Quantitative effect and regulatory function of cyclic adenosine 5'-phosphate in *Escherichia coli*. *J. Biosci.* **2009**, *34* (3), 445-63.
9. Ross, P.; Weinhouse, H.; Aloni, Y.; Michaeli, D.; Weinbergerohana, P.; Mayer, R.; Braun, S.; Devroom, E.; Vandermarel, G. A.; Vanboom, J. H.;

- Benziman, M., Regulation of cellulose synthesis in *Acetobacter xylinum* by cyclic diguanylic acid. *Nature* **1987**, 325 (6101), 279-281.
10. Witte, G.; Hartung, S.; Buettner, K.; Hopfner, K.-P., Structural biochemistry of a bacterial checkpoint protein reveals diadenylate cyclase activity regulated by DNA recombination intermediates. *Mol. Cell* **2008**, 30 (2), 167-178.
11. Davies, B. W.; Bogard, R. W.; Young, T. S.; Mekalanos, J. J., Coordinated regulation of accessory genetic elements produces cyclic di-nucleotides for *V. cholerae* virulence. *Cell* **2012**, 149 (2), 358-370.
12. Rosenberg, J.; Dickmanns, A.; Neumann, P.; Gunka, K.; Arens, J.; Kaever, V.; Stülke, J.; Ficner, R.; Commichau, F. M., Structural and biochemical analysis of the essential diadenylate cyclase CdaA from *Listeria monocytogenes*. *J. Biol. Chem.* **2015**, 290 (10), 6596-606.
13. Ablasser, A.; Goldeck, M.; Cavlar, T.; Deimling, T.; Witte, G.; Roehl, I.; Hopfner, K.-P.; Ludwig, J.; Hornung, V., cGAS produces a 2'-5'-linked cyclic dinucleotide second messenger that activates STING. *Nature* **2013**, 498 (7454), 380-384.
14. Gao, P.; Ascano, M.; Wu, Y.; Barchet, W.; Gaffney, B. L.; Zillinger, T.; Serganov, A. A.; Liu, Y.; Jones, R. A.; Hartmann, G.; Tuschl, T.; Patel, D. J., Cyclic G(2',5')pA(3',5')p is the metazoan second messenger produced by DNA-activated cyclic GMP-AMP synthase. *Cell* **2013**, 153 (5), 1094-1107.
15. Ross, P.; Weinhouse, H.; Aloni, Y.; Michaeli, D.; Weinbergerohana, P.; Mayer, R.; Braun, S.; Devroom, E.; Vandermarel, G. A.; Vanboom, J. H.;

- Benziman, M., Regulation of cellulose synthesis in *Acetobacter-xylinum* by cyclic diguanylic acid. *Nature* **1987**, 325 (6101), 279-281.
16. Hengge, R., Principles of c-di-GMP signalling in bacteria. *Nat. Rev. Microbiol.* **2009**, 7 (4), 263-273.
 17. Hengge, R.; Gründling, A.; Jenal, U.; Ryan, R.; Yildiz, F., Bacterial signal transduction by cyclic di-GMP and other nucleotide second messengers. *J. Bacteriol.* **2016**, 198 (1), 15-26.
 18. Römling, U.; Gomelsky, M.; Galperin, M. Y., C-di-GMP: the dawning of a novel bacterial signalling system. *Mol Microbiol* **2005**, 57 (3), 629-39.
 19. Römling, U.; Galperin, M. Y.; Gomelsky, M., Cyclic di-GMP: the first 25 years of a universal bacterial second messenger. *Microbiol. Mol. Biol. Rev.* **2013**, 77 (1), 1-52.
 20. Hecht, G. B.; Newton, A., Identification of a novel response regulator required for the swarmer-to-stalked-cell transition in *Caulobacter crescentus*. *J. Bacteriol.* **1995**, 177 (21), 6223-9.
 21. De, N.; Pirruccello, M.; Krasteva, P. V.; Bae, N.; Raghavan, R. V.; Sondermann, H., Phosphorylation-independent regulation of the diguanylate cyclase WspR. *PLoS Biol.* **2008**, 6 (3), 601-617.
 22. De, N.; Navarro, M. V. A. S.; Raghavan, R. V.; Sondermann, H., Determinants for the activation and autoinhibition of the diguanylate cyclase response regulator WspR. *J. Mol. Biol.* **2009**, 393 (3), 619-633.

23. Weber, H.; Pesavento, C.; Possling, A.; Tischendorf, G.; Hengge, R., Cyclic-di-GMP-mediated signalling within the sigma network of *Escherichia coli*. *Mol. Microbiol.* **2006**, *62* (4), 1014-34.
24. Bordeleau, E.; Brouillette, E.; Robichaud, N.; Burrus, V., Beyond antibiotic resistance: integrating conjugative elements of the SXT/R391 family that encode novel diguanylate cyclases participate to c-di-GMP signalling in *Vibrio cholerae*. *Environ. Microbiol.* **2010**, *12* (2), 510-23.
25. Galperin, M. Y., A census of membrane-bound and intracellular signal transduction proteins in bacteria: bacterial IQ, extroverts and introverts. *BMC Microbiol.* **2005**, *5*, 35.
26. Galperin, M. Y.; Nikolskaya, A. N.; Koonin, E. V., Novel domains of the prokaryotic two-component signal transduction systems. *FEMS Microbiol. Lett.* **2001**, *203* (1), 11-21.
27. Dahlstrom, K. M.; Giglio, K. M.; Sondermann, H.; O'Toole, G. A., The inhibitory site of a diguanylate cyclase is a necessary element for interaction and signaling with an effector protein. *J. Bacteriol.* **2016**, *198* (11), 1595-603.
28. Simm, R.; Morr, M.; Kader, A.; Nimtz, M.; Römling, U., GGDEF and EAL domains inversely regulate cyclic di-GMP levels and transition from sessility to motility. *Mol. Microbiol.* **2004**, *53* (4), 1123-34.
29. Ryjenkov, D. A.; Simm, R.; Römling, U.; Gomelsky, M., The PilZ domain is a receptor for the second messenger c-di-GMP: the PilZ domain protein YcgR controls motility in enterobacteria. *J. Biol. Chem.* **2006**, *281* (41), 30310-4.

30. Schmidt, A. J.; Ryjenkov, D. A.; Gomelsky, M., The ubiquitous protein domain EAL is a cyclic diguanylate-specific phosphodiesterase: enzymatically active and inactive EAL domains. *J. Bacteriol.* **2005**, *187* (14), 4774-81.
31. Rao, F.; Yang, Y.; Qi, Y.; Liang, Z. X., Catalytic mechanism of cyclic di-GMP-specific phosphodiesterase: a study of the EAL domain-containing RocR from *Pseudomonas aeruginosa*. *J. Bacteriol.* **2008**, *190* (10), 3622-31.
32. Jenal, U.; Malone, J., Mechanisms of cyclic-di-GMP signaling in bacteria. *Annu. Rev. Genet.* **2006**, *40*, 385-407.
33. Römling, U., Great times for small molecules: c-di-AMP, a second messenger candidate in Bacteria and Archaea. *Sci. Signal.* **2008**, *1* (33), pe39.
34. Ryan, R. P.; Dow, J. M., Intermolecular interactions between HD-GYP and GGDEF domain proteins mediate virulence-related signal transduction in *Xanthomonas campestris*. *Virulence* **2010**, *1* (5), 404-8.
35. Lovering, A. L.; Capeness, M. J.; Lambert, C.; Hopley, L.; Sockett, R. E., The structure of an unconventional HD-GYP protein from *Bdellovibrio* reveals the roles of conserved residues in this class of cyclic-di-GMP phosphodiesterases. *mBio* **2011**, *2* (5), pii: e00163-11.
36. Bellini, D.; Caly, D. L.; McCarthy, Y.; Bumann, M.; An, S. Q.; Dow, J. M.; Ryan, R. P.; Walsh, M. A., Crystal structure of an HD-GYP domain cyclic-di-GMP phosphodiesterase reveals an enzyme with a novel trinuclear catalytic iron centre. *Mol. Microbiol.* **2014**, *91* (1), 26-38.
37. Rinaldo, S.; Paiardini, A.; Stelitano, V.; Brunotti, P.; Cervoni, L.; Fernicola, S.; Protano, C.; Vitali, M.; Cutruzzolà, F.; Giardina, G., Structural basis

- of functional diversification of the HD-GYP domain revealed by the *Pseudomonas aeruginosa* PA4781 protein, which displays an unselective bimetallic binding site. *J. Bacteriol.* **2015**, *197* (8), 1525-35.
38. Amikam, D.; Galperin, M. Y., PilZ domain is part of the bacterial c-di-GMP binding protein. *Bioinformatics* **2006**, *22* (1), 3-6.
39. Merighi, M.; Lee, V. T.; Hyodo, M.; Hayakawa, Y.; Lory, S., The second messenger bis-(3'-5')-cyclic-GMP and its PilZ domain-containing receptor Alg44 are required for alginate biosynthesis in *Pseudomonas aeruginosa*. *Mol. Microbiol.* **2007**, *65* (4), 876-95.
40. Christen, M.; Christen, B.; Allan, M. G.; Folcher, M.; Jenö, P.; Grzesiek, S.; Jenal, U., DgrA is a member of a new family of cyclic diguanosine monophosphate receptors and controls flagellar motor function in *Caulobacter crescentus*. *Proc. Natl. Acad. Sci. U S A* **2007**, *104* (10), 4112-7.
41. Dubey, B. N.; Lori, C.; Ozaki, S.; Fucile, G.; Plaza-Menacho, I.; Jenal, U.; Schirmer, T., Cyclic di-GMP mediates a histidine kinase/phosphatase switch by noncovalent domain cross-linking. *Sci Adv* **2016**, *2* (9), e1600823.
42. Lori, C.; Ozaki, S.; Steiner, S.; Böhm, R.; Abel, S.; Dubey, B. N.; Schirmer, T.; Hiller, S.; Jenal, U., Cyclic di-GMP acts as a cell cycle oscillator to drive chromosome replication. *Nature* **2015**, *523* (7559), 236-9.
43. Lee, V. T.; Matewish, J. M.; Kessler, J. L.; Hyodo, M.; Hayakawa, Y.; Lory, S., A cyclic-di-GMP receptor required for bacterial exopolysaccharide production. *Mol. Microbiol.* **2007**, *65* (6), 1474-84.

44. Duerig, A.; Abel, S.; Folcher, M.; Nicollier, M.; Schwede, T.; Amiot, N.; Giese, B.; Jenal, U., Second messenger-mediated spatiotemporal control of protein degradation regulates bacterial cell cycle progression. *Genes Dev.* **2009**, *23* (1), 93-104.
45. Navarro, M. V.; De, N.; Bae, N.; Wang, Q.; Sondermann, H., Structural analysis of the GGDEF-EAL domain-containing c-di-GMP receptor FimX. *Structure* **2009**, *17* (8), 1104-16.
46. Qi, Y.; Chuah, M. L.; Dong, X.; Xie, K.; Luo, Z.; Tang, K.; Liang, Z. X., Binding of cyclic diguanylate in the non-catalytic EAL domain of FimX induces a long-range conformational change. *J. Biol. Chem.* **2011**, *286* (4), 2910-7.
47. Smith, K. D.; Lipchock, S. V.; Ames, T. D.; Wang, J.; Breaker, R. R.; Strobel, S. A., Structural basis of ligand binding by a c-di-GMP riboswitch. *Nat Struct. Mol. Biol.* **2009**, *16* (12), 1218-23.
48. Sudarsan, N.; Lee, E. R.; Weinberg, Z.; Moy, R. H.; Kim, J. N.; Link, K. H.; Breaker, R. R., Riboswitches in eubacteria sense the second messenger cyclic di-GMP. *Science* **2008**, *321* (5887), 411-3.
49. Lee, E. R.; Baker, J. L.; Weinberg, Z.; Sudarsan, N.; Breaker, R. R., An allosteric self-splicing ribozyme triggered by a bacterial second messenger. *Science* **2010**, *329* (5993), 845-8.
50. Smith, K. D.; Shanahan, C. A.; Moore, E. L.; Simon, A. C.; Strobel, S. A., Structural basis of differential ligand recognition by two classes of bis-(3'-5')-cyclic dimeric guanosine monophosphate-binding riboswitches. *Proc. Natl. Acad. Sci. U S A* **2011**, *108* (19), 7757-62.

51. Burdette, D. L.; Monroe, K. M.; Sotelo-Troha, K.; Iwig, J. S.; Eckert, B.; Hyodo, M.; Hayakawa, Y.; Vance, R. E., STING is a direct innate immune sensor of cyclic di-GMP. *Nature* **2011**, *478* (7370), 515-8.
52. Ishikawa, H.; Barber, G. N., STING is an endoplasmic reticulum adaptor that facilitates innate immune signalling. *Nature* **2008**, *455* (7213), 674-8.
53. Ishikawa, H.; Ma, Z.; Barber, G. N., STING regulates intracellular DNA-mediated, type I interferon-dependent innate immunity. *Nature* **2009**, *461* (7265), 788-92.
54. Bai, Y.; Yang, J.; Zhou, X.; Ding, X.; Eisele, L. E.; Bai, G., *Mycobacterium tuberculosis* Rv3586 (DacA) Is a diadenylate cyclase that converts ATP or ADP into c-di-AMP. *PloS One* **2012**, *7* (4).
55. Bai, Y.; Yang, J.; Eisele, L. E.; Underwood, A. J.; Koestler, B. J.; Waters, C. M.; Metzger, D. W.; Bai, G., Two DHH subfamily 1 proteins in *Streptococcus pneumoniae* possess cyclic di-AMP phosphodiesterase activity and affect bacterial growth and virulence. *J. Bacteriol.* **2013**, *195* (22), 5123-32.
56. Corrigan, R. M.; Gründling, A., Cyclic di-AMP: another second messenger enters the fray. *Nat. Rev. Microbiol.* **2013**, *11* (8), 513-524.
57. Woodward, J. J.; Iavarone, A. T.; Portnoy, D. A., c-di-AMP secreted by intracellular *Listeria monocytogenes* activates a host Type I interferon response. *Science* **2010**, *328* (5986), 1703-1705.
58. Devaux, L.; Kaminski, P. A.; Trieu-Cuot, P.; Firon, A., Cyclic di-AMP in host-pathogen interactions. *Curr. Opin. Microbiol.* **2017**, *41*, 21-28.

59. Barker, J. R.; Koestler, B. J.; Carpenter, V. K.; Burdette, D. L.; Waters, C. M.; Vance, R. E.; Valdivia, R. H., STING-dependent recognition of cyclic di-AMP mediates Type I Interferon responses during *Chlamydia trachomatis* infection. *mBio* **2013**, *4* (3), e00018-13.
60. Kaplan Zeevi, M.; Shafir, N. S.; Shaham, S.; Friedman, S.; Sigal, N.; Nir Paz, R.; Boneca, I. G.; Herskovits, A. A., *Listeria monocytogenes* multidrug resistance transporters and cyclic di-AMP, which contribute to type I interferon induction, play a role in cell wall stress. *J. Bacteriol.* **2013**, *195* (23), 5250-61.
61. Corrigan, R. M.; Abbott, J. C.; Burhenne, H.; Kaever, V.; Gründling, A., Cyclic di-AMP is a new second messenger in *Staphylococcus aureus* with a role in controlling cell size and envelope stress. *PLoS Pathog.* **2011**, *7* (9), e1002217.
62. Peng, X.; Zhang, Y.; Bai, G.; Zhou, X.; Wu, H., Cyclic di-AMP mediates biofilm formation. *Mol. Microbiol.* **2016**, *99* (5), 945-59.
63. Smith, W. M.; Pham, T. H.; Lei, L.; Dou, J.; Soomro, A. H.; Beatson, S. A.; Dykes, G. A.; Turner, M. S., Heat resistance and salt hypersensitivity in *Lactococcus lactis* due to spontaneous mutation of llmg_1816 (gdpP) induced by high-temperature growth. *Appl Environ Microbiol* **2012**, *78* (21), 7753-9.
64. Ye, M.; Zhang, J.-J.; Fang, X.; Lawlis, G. B.; Troxell, B.; Zhou, Y.; Gomelsky, M.; Lou, Y.; Yang, X. F., DhhP, a cyclic di-AMP phosphodiesterase of *Borrelia burgdorferi*, is essential for cell growth and virulence. *Infect. Immun.* **2014**, *82* (5), 1840-1849.

65. Bai, Y.; Yang, J.; Zarrella, T. M.; Zhang, Y.; Metzger, D. W.; Bai, G., Cyclic di-AMP impairs potassium uptake mediated by a cyclic di-AMP binding protein in *Streptococcus pneumoniae*. *J. Bacteriol.* **2014**, *196* (3), 614-623.
66. Rao, F.; See, R. Y.; Zhang, D.; Toh, D. C.; Ji, Q.; Liang, Z.-X., YybT is a signaling protein that contains a cyclic dinucleotide phosphodiesterase domain and a GGDEF domain with ATPase activity. *J. Biol. Chem.* **2010**, *285* (1), 473-482.
67. Commichau, F. M.; Dickmanns, A.; Gundlach, J.; Ficner, R.; Stülke, J., A jack of all trades: the multiple roles of the unique essential second messenger cyclic di-AMP. *Mol. Microbiol.* **2015**, *97* (2), 189-204.
68. Oppenheimer-Shaanan, Y.; Wexselblatt, E.; Katzhendler, J.; Yavin, E.; Ben-Yehuda, S., c-di-AMP reports DNA integrity during sporulation in *Bacillus subtilis*. *Embo Reports* **2011**, *12* (6), 594-601.
69. Bejerano-Sagie, M.; Oppenheimer-Shaanan, Y.; Berlatzky, I.; Rouvinski, A.; Meyerovich, M.; Ben-Yehuda, S., A checkpoint protein that scans the chromosome for damage at the start of sporulation in *Bacillus subtilis*. *Cell* **2006**, *125* (4), 679-690.
70. Campos, S. S.; Ibarra-Rodriguez, J. R.; Barajas-Ornelas, R. C.; Ramírez-Guadiana, F. H.; Obregón-Herrera, A.; Setlow, P.; Pedraza-Reyes, M., Interaction of apurinic/aprimidinic endonucleases Nfo and ExoA with the DNA integrity scanning protein DisA in the processing of oxidative DNA damage during *Bacillus subtilis* spore outgrowth. *J. Bacteriol.* **2014**, *196* (3), 568-78.
71. Gándara, C.; de Lucena, D. K. C.; Torres, R.; Serrano, E.; Altenburger, S.; Graumann, P. L.; Alonso, J. C., Activity and *in vivo* dynamics of *Bacillus subtilis*

- DisA are affected by RadA/Sms and by Holliday junction-processing proteins. *DNA Repair (Amst)* **2017**, *55*, 17-30.
72. Bai, Y.; Yang, J.; Zhou, X.; Ding, X.; Eisele, L. E.; Bai, G., *Mycobacterium tuberculosis* Rv3586 (DacA) is a diadenylate cyclase that converts ATP or ADP into c-di-AMP. *Plos One* **2012**, *7* (4), e35206.
73. Zhang, L.; He, Z. G., Radiation-sensitive gene A (RadA) targets DisA, DNA integrity scanning protein A, to negatively affect cyclic di-AMP synthesis activity in *Mycobacterium smegmatis*. *J. Biol. Chem.* **2013**, *288* (31), 22426-36.
74. Burghout, P.; Bootsma, H. J.; Kloosterman, T. G.; Bijlsma, J. J.; de Jongh, C. E.; Kuipers, O. P.; Hermans, P. W., Search for genes essential for pneumococcal transformation: the RADA DNA repair protein plays a role in genomic recombination of donor DNA. *J Bacteriol* **2007**, *189* (18), 6540-50.
75. Gándara, C.; Alonso, J. C., DisA and c-di-AMP act at the intersection between DNA-damage response and stress homeostasis in exponentially growing *Bacillus subtilis* cells. *DNA Repair (Amst)* **2015**, *27*, 1-8.
76. Pham, T. H.; Liang, Z. X.; Marcellin, E.; Turner, M. S., Replenishing the cyclic-di-AMP pool: regulation of diadenylate cyclase activity in bacteria. *Curr. Genet.* **2016**, 1-8.
77. Mehne, F. M. P.; Gunka, K.; Eilers, H.; Herzberg, C.; Kaefer, V.; Stuelke, J., Cyclic di-AMP homeostasis in *Bacillus subtilis*: both lack and high level accumulation of the nucleotide are detrimental for cell growth. *J. Biol. Chem.* **2013**, *288* (3), 2004-2017.

78. Luo, Y.; Helmann, J. D., Analysis of the role of *Bacillus subtilis* σ^M in β -lactam resistance reveals an essential role for c-di-AMP in peptidoglycan homeostasis. *Mol. Microbiol.* **2012**, *83* (3), 623-639.
79. Corrigan, R. M.; Campeotto, I.; Jeganathan, T.; Roelofs, K. G.; Lee, V. T.; Gründling, A., Systematic identification of conserved bacterial c-di-AMP receptor proteins. *Proc Natl Acad Sci U S A* **2013**, *110* (22), 9084-9.
80. Rosenberg, J.; Dickmanns, A.; Neumann, P.; Gunka, K.; Arens, J.; Kaever, V.; Stülke, J.; Ficner, R.; Commichau, F. M., Structural and biochemical analysis of the essential diadenylate cyclase CdaA from *Listeria monocytogenes*. *J Biol Chem* **2015**, *290* (10), 6596-606.
81. Kamegaya, T.; Kuroda, K.; Hayakawa, Y., Identification of a *Streptococcus pyogenes* SF370 gene involved in production of c-di-AMP. *Nagoya J Med Sci* **2011**, *73* (1-2), 49-57.
82. Gundlach, J.; Mehne, F. M.; Herzberg, C.; Kampf, J.; Valerius, O.; Kaever, V.; Stülke, J., An essential poison: Synthesis and degradation of cyclic di-AMP in *Bacillus subtilis*. *J. Bacteriol.* **2015**, *197* (20), 3265-74.
83. Rismondo, J.; Gibhardt, J.; Rosenberg, J.; Kaever, V.; Halbedel, S.; Commichau, F. M., Phenotypes associated with the essential diadenylate cyclase CdaA and its potential regulator CdaR in the human pathogen *Listeria monocytogenes*. *J. Bacteriol.* **2015**, *198* (3), 416-26.
84. Zhu, Y.; Pham, T. H.; Nhiep, T. H.; Vu, N. M.; Marcellin, E.; Chakrabortti, A.; Wang, Y.; Waanders, J.; Lo, R.; Huston, W. M.; Bansal, N.; Nielsen, L. K.; Liang, Z. X.; Turner, M. S., Cyclic-di-AMP synthesis by the diadenylate cyclase

CdaA is modulated by the peptidoglycan biosynthesis enzyme GlmM in *Lactococcus lactis*. *Mol. Microbiol.* **2016**, *99* (6), 1015-27.

85. Song, J. H.; Ko, K. S.; Lee, J. Y.; Baek, J. Y.; Oh, W. S.; Yoon, H. S.; Jeong, J. Y.; Chun, J., Identification of essential genes in *Streptococcus pneumoniae* by allelic replacement mutagenesis. *Mol. Cells* **2005**, *19* (3), 365-374.

86. Corrigan, R. M.; Bowman, L.; Willis, A. R.; Kaeber, V.; Gründling, A., Cross-talk between two nucleotide-signaling pathways in *Staphylococcus aureus*. *J. Biol. Chem.* **2015**, *290* (9), 5826-39.

87. Mehne, F. M.; Schröder-Tittmann, K.; Eijlander, R. T.; Herzberg, C.; Hewitt, L.; Kaeber, V.; Lewis, R. J.; Kuipers, O. P.; Tittmann, K.; Stülke, J., Control of the diadenylate cyclase CdaS in *Bacillus subtilis*: an autoinhibitory domain limits cyclic di-AMP production. *J. Biol. Chem.* **2014**, *289* (30), 21098-107.

88. Blötz, C.; Treffon, K.; Kaeber, V.; Schwede, F.; Hammer, E.; Stülke, J., Identification of the components involved in cyclic di-AMP signaling in *Mycoplasma pneumoniae*. *Front. Microbiol.* **2017**, *8*, 1328.

89. Huynh, T. N.; Woodward, J. J., Too much of a good thing: regulated depletion of c-di-AMP in the bacterial cytoplasm. *Curr. Opin. Microbiol.* **2016**, *30*, 22-9.

90. Huynh, T. N.; Luo, S. K.; Pensinger, D.; Sauer, J. D.; Tong, L.; Woodward, J. J., An HD-domain phosphodiesterase mediates cooperative hydrolysis of c-di-AMP to affect bacterial growth and virulence. *Proc. Natl. Acad. Sci. U.S.A.* **2015**, *112* (7), E747-E756.

91. Witte, C. E.; Whiteley, A. T.; Burke, T. P.; Sauer, J.-D.; Portnoy, D. A.; Woodward, J. J., Cyclic di-AMP is critical for *Listeria monocytogenes* growth, cell wall homeostasis, and establishment of infection. *mBio* **2013**, *4* (3), e00282-13.
92. Bai, Y.; Yang, J.; Eisele, L. E.; Underwood, A. J.; Koestler, B. J.; Waters, C. M.; Metzger, D. W.; Bai, G., Two DHH subfamily 1 proteins in *Streptococcus pneumoniae* possess cyclic di-AMP phosphodiesterase activity and affect bacterial growth and virulence. *J. Bacteriol.* **2013**, *195* (22), 5123-5132.
93. Yamamoto, T.; Hara, H.; Tsuchiya, K.; Sakai, S.; Fang, R.; Matsuura, M.; Nomura, T.; Sato, F.; Mitsuyama, M.; Kawamura, I., *Listeria monocytogenes* strain-specific impairment of the TetR regulator underlies the drastic increase in cyclic di-AMP secretion and beta interferon-inducing ability. *Infect. Immun.* **2012**, *80* (7), 2323-32.
94. Tang, Q.; Luo, Y.; Zheng, C.; Yin, K.; Ali, M. K.; Li, X.; He, J., Functional Analysis of a c-di-AMP-specific Phosphodiesterase MsPDE from *Mycobacterium smegmatis*. *Int. J. Biol. Sci.* **2015**, *11* (7), 813-824.
95. Zhang, L.; Li, W.; He, Z. G., DarR, a TetR-like transcriptional factor, is a cyclic di-AMP-responsive repressor in *Mycobacterium smegmatis*. *J. Biol. Chem.* **2013**, *288* (5), 3085-96.
96. Bai, Y.; Yang, J.; Zarrella, T. M.; Zhang, Y.; Metzger, D. W.; Bai, G., Cyclic di-AMP impairs potassium uptake mediated by a cyclic di-AMP binding protein in *Streptococcus pneumoniae*. *J. Bacteriol.* **2014**, *196* (3), 614-23.
97. Chin, K. H.; Liang, J. M.; Yang, J. G.; Shih, M. S.; Tu, Z. L.; Wang, Y. C.; Sun, X. H.; Hu, N. J.; Liang, Z. X.; Dow, J. M.; Ryan, R. P.; Chou, S. H.,

- Structural insights into the distinct binding mode of cyclic di-AMP with SaCpaA_RCK. *Biochem.* **2015**, *54* (31), 4936-51.
98. Moscoso, J. A.; Schramke, H.; Zhang, Y.; Tosi, T.; Dehbi, A.; Jung, K.; Gründling, A., Binding of cyclic di-AMP to the *Staphylococcus aureus* sensor kinase KdpD occurs via the universal stress protein domain and downregulates the expression of the Kdp potassium transporter. *J. Bacteriol.* **2016**, *198* (1), 98-110.
99. Freeman, Z. N.; Dorus, S.; Waterfield, N. R., The KdpD/KdpE two-component system: integrating K⁺ homeostasis and virulence. *PLoS Pathog.* **2013**, *9* (3), e1003201.
100. Huynh, T. N.; Choi, P. H.; Sureka, K.; Ledvina, H. E.; Campillo, J.; Tong, L.; Woodward, J. J., Cyclic di-AMP targets the cystathionine beta-synthase domain of the osmolyte transporter OpuC. *Mol. Microbiol.* **2016**, *102* (2), 233-243.
101. Schuster, C. F.; Bellows, L. E.; Tosi, T.; Campeotto, I.; Corrigan, R. M.; Freemont, P.; Gründling, A., The second messenger c-di-AMP inhibits the osmolyte uptake system OpuC in *Staphylococcus aureus*. *Sci. Signal.* **2016**, *9* (441), ra81.
102. Commichau, F. M.; Gibhardt, J.; Halbedel, S.; Gundlach, J.; Stülke, J., A delicate connection: c-di-AMP affects cell integrity by controlling osmolyte transport. *Trends Microbiol.* **2018**, *26* (3), 175-185.
103. Thompson, M. R.; Kaminski, J. J.; Kurt-Jones, E. A.; Fitzgerald, K. A., Pattern recognition receptors and the innate immune response to viral infection. *Viruses* **2011**, *3* (6), 920-40.
104. Mogensen, T. H., Pathogen recognition and inflammatory signaling in innate immune defenses. *Clin. Microbiol. Rev.* **2009**, *22* (2), 240-73.

105. Parvatiyar, K.; Zhang, Z.; Teles, R. M.; Ouyang, S.; Jiang, Y.; Iyer, S. S.; Zaver, S. A.; Schenk, M.; Zeng, S.; Zhong, W.; Liu, Z. J.; Modlin, R. L.; Liu, Y. J.; Cheng, G., The helicase DDX41 recognizes the bacterial secondary messengers cyclic di-GMP and cyclic di-AMP to activate a type I interferon immune response. *Nat. Immunol.* **2012**, *13* (12), 1155-61.
106. Omura, H.; Oikawa, D.; Nakane, T.; Kato, M.; Ishii, R.; Ishitani, R.; Tokunaga, F.; Nureki, O., Structural and functional analysis of DDX41: a bispecific immune receptor for DNA and cyclic dinucleotide. *Sci. Rep.* **2016**, *6*, 34756.
107. McFarland, A. P.; Luo, S.; Ahmed-Qadri, F.; Zuck, M.; Thayer, E. F.; Goo, Y. A.; Hybiske, K.; Tong, L.; Woodward, J. J., Sensing of bacterial cyclic dinucleotides by the oxidoreductase RECON promotes NF- κ B activation and shapes a proinflammatory antibacterial state. *Immunity* **2017**, *46* (3), 433-445.
108. Andrade, W. A.; Firon, A.; Schmidt, T.; Hornung, V.; Fitzgerald, K. A.; Kurt-Jones, E. A.; Trieu-Cuot, P.; Golenbock, D. T.; Kaminski, P. A., Group B Streptococcus degrades cyclic-di-AMP to modulate STING-dependent type I interferon production. *Cell Host Microbe* **2016**, *20* (1), 49-59.
109. Dey, R. J.; Dey, B.; Zheng, Y.; Cheung, L. S.; Zhou, J.; Sayre, D.; Kumar, P.; Guo, H.; Lamichhane, G.; Sintim, H. O.; Bishai, W. R., Inhibition of innate immune cytosolic surveillance by an *M. tuberculosis* phosphodiesterase. *Nat. Chem. Biol.* **2017**, *13* (2), 210-217.
110. Underwood, A. J.; Zhang, Y.; Metzger, D. W.; Bai, G., Detection of cyclic di-AMP using a competitive ELISA with a unique pneumococcal cyclic di-AMP binding protein. *J. Microbiol. Methods* **2014**, *107*, 58-62.

111. Müller, M.; Deimling, T.; Hopfner, K. P.; Witte, G., Structural analysis of the diadenylate cyclase reaction of DNA-integrity scanning protein A (DisA) and its inhibition by 3'-dATP. *Biochem. J.* **2015**, *469*, 367-374.
112. Zhou, J.; Sayre, D. A.; Zheng, Y.; Szymanski, H.; Sintim, H. O., Unexpected complex formation between coralyne and cyclic diadenosine monophosphate providing a simple fluorescent turn-on assay to detect this bacterial second messenger. *Anal. Chem.* **2014**, *86* (5), 2412-2420.
113. Xing, F.; Song, G.; Ren, J.; Chaires, J. B.; Qu, X., Molecular recognition of nucleic acids: coralyne binds strongly to poly(A). *FEBS Lett.* **2005**, *579* (22), 5035-9.
114. Persil, O.; Santai, C. T.; Jain, S. S.; Hud, N. V., Assembly of an antiparallel homo-adenine DNA duplex by small-molecule binding. *J. Am. Chem. Soc.* **2004**, *126* (28), 8644-5.
115. Zheng, Y.; Zhou, J.; Sayre, D. A.; Sintim, H. O., Identification of bromophenol thiohydantoin as an inhibitor of DisA, a c-di-AMP synthase, from a 1000 compound library, using the coralyne assay. *Chem. Commun.* **2014**, *50* (76), 11234-11237.
116. Zheng, Y.; Zhou, J.; Cooper, S. M.; Opoku-Temeng, C.; De Brito, A. M.; Sintim, H. O., Structure-activity relationship studies of c-di-AMP synthase inhibitor, bromophenol-thiohydantoin. *Tetrahedron* **2016**, *72* (25), 3554-3558.
117. Opoku-Temeng, C.; Sintim, H. O., Inhibition of cyclic diadenylate cyclase, DisA by polyphenols. *Sci. Rep.* **2016**, *6*, 25445.

118. Opoku-Temeng, C.; Sintim, H. O., Potent inhibition of cyclic diadenylate monophosphate cyclase by the antiparasitic drug, suramin. *Chem. Commun.* **2016**, 52 (19), 3754-7.
119. Opoku-Temeng, C.; Dayal, N.; Miller, J.; Sintim, H. O., Hydroxybenzylidene-indolinones, c-di-AMP synthase inhibitors, have antibacterial and anti-biofilm activities and also re-sensitize resistant bacteria to methicillin and vancomycin. *Rsc Adv.* **2017**, 7 (14), 8288-8294.
120. Gao, J.; Tao, J.; Liang, W.; Zhao, M.; Du, X.; Cui, S.; Duan, H.; Kan, B.; Su, X.; Jiang, Z., Identification and characterization of phosphodiesterases that specifically degrade 3' 3'-cyclic GMP-AMP. *Cell Research* **2015**, 25 (5), 539-550.
121. Kellenberger, C. A.; Wilson, S. C.; Hickey, S. F.; Gonzalez, T. L.; Su, Y.; Hallberg, Z. F.; Brewer, T. F.; Iavarone, A. T.; Carlson, H. K.; Hsieh, Y. F.; Hammond, M. C., GEMM-I riboswitches from *Geobacter* sense the bacterial second messenger cyclic AMP-GMP. *Proc. Natl. Acad. Sci. U S A* **2015**, 112 (17), 5383-8.
122. Zhang, X.; Shi, H.; Wu, J.; Zhang, X.; Sun, L.; Chen, C.; Chen, Z. J., Cyclic GMP-AMP Containing Mixed Phosphodiester Linkages Is An Endogenous High-Affinity Ligand for STING. *Molecular Cell* **2013**, 51 (2), 226-235.
123. Sun, L.; Wu, J.; Du, F.; Chen, X.; Chen, Z. J., Cyclic GMP-AMP synthase is a cytosolic DNA sensor that activates the type I interferon pathway. *Science* **2013**, 339 (6121), 786-791.
124. Wu, J.; Sun, L.; Chen, X.; Du, F.; Shi, H.; Chen, C.; Chen, Z. J., Cyclic GMP-AMP is an endogenous second messenger in innate immune signaling by cytosolic DNA. *Science* **2013**, 339 (6121), 826-830.

125. Li, L.; Yin, Q.; Kuss, P.; Maliga, Z.; Millan, J. L.; Wu, H.; Mitchison, T. J., Hydrolysis of 2' 3 '-cGAMP by ENPP1 and design of nonhydrolyzable analogs. *Nat. Chem.Biol.* **2015**, *11* (3), 235-235.
126. Callaway, E., Plague genome: The Black Death decoded. *Nat. News* **2011**, *478* (7370), 444-446.
127. Bush, K.; Courvalin, P.; Dantas, G.; Davies, J.; Eisenstein, B.; Huovinen, P.; Jacoby, G. A.; Kishony, R.; Kreiswirth, B. N.; Kutter, E.; Lerner, S. A.; Levy, S.; Lewis, K.; Lomovskaya, O.; Miller, J. H.; Mobashery, S.; Piddock, L. J.; Projan, S.; Thomas, C. M.; Tomasz, A.; Tulkens, P. M.; Walsh, T. R.; Watson, J. D.; Witkowski, J.; Witte, W.; Wright, G.; Yeh, P.; Zgurskaya, H. I., Tackling antibiotic resistance. *Nat. Rev. Microbiol.* **2011**, *9* (12), 894-6.
128. Pantosti, A.; Sanchini, A.; Monaco, M., Mechanisms of antibiotic resistance in *Staphylococcus aureus*. *Future Microbiol.* **2007**, *2* (3), 323-34.
129. Munita, J. M.; Arias, C. A., Mechanisms of antibiotic resistance. *Microbiol. Spectr.* **2016**, *4* (2), DOI: 10.1128/microbiolspec.VMBF-0016-2015.
130. Poole, K., Efflux-mediated antimicrobial resistance. *J. Antimicrob. Chemother.* **2005**, *56* (1), 20-51.
131. Du, D.; Wang, Z.; James, N. R.; Voss, J. E.; Klimont, E.; Ohene-Agyei, T.; Venter, H.; Chiu, W.; Luisi, B. F., Structure of the AcrAB-TolC multidrug efflux pump. *Nature* **2014**, *509* (7501), 512-5.
132. Gardete, S.; Tomasz, A., Mechanisms of vancomycin resistance in *Staphylococcus aureus*. *J. Clin. Invest.* **2014**, *124* (7), 2836-40.

133. Arthur, M.; Courvalin, P., Genetics and mechanisms of glycopeptide resistance in enterococci. *Antimicrob. Agents Chemother.* **1993**, *37* (8), 1563-71.
134. Aminov, R. I., A brief history of the antibiotic era: lessons learned and challenges for the future. *Front. Microbiol.* **2010**, *1*, 134.
135. Chellat, M. F.; Raguž, L.; Riedl, R., Targeting antibiotic resistance. *Angew. Chem. Int. Ed. Engl.* **2016**, *55* (23), 6600-26.
136. Wright, G. D., Antibiotic adjuvants: rescuing antibiotics from resistance. *Trends Microbiol.* **2016**, *24* (11), 862-871.
137. Harris, T. L.; Worthington, R. J.; Melander, C., Potent small-molecule suppression of oxacillin resistance in methicillin-resistant *Staphylococcus aureus*. *Angew. Chem. Int. Ed. Engl.* **2012**, *51* (45), 11254-7.

Chapter 2:

1. Corrigan, R. M.; Gründling, A., Cyclic di-AMP: another second messenger enters the fray. *Nat. Rev. Microbiol.* **2013**, *11* (8), 513-524.
2. Römling, U., Great times for small molecules: c-di-AMP, a second messenger candidate in Bacteria and Archaea. *Sci. Signal.* **2008**, *1* (33), pe39.
3. Witte, G.; Hartung, S.; Buettner, K.; Hopfner, K.-P., Structural biochemistry of a bacterial checkpoint protein reveals diadenylate cyclase activity regulated by DNA recombination intermediates. *Mol. Cell* **2008**, *30* (2), 167-178.

4. Bai, Y.; Yang, J.; Zhou, X.; Ding, X.; Eisele, L. E.; Bai, G., *Mycobacterium tuberculosis* Rv3586 (DacA) is a diadenylate cyclase that converts ATP or ADP into c-di-AMP. *PLoS One* **2012**, *7* (4), e35206.
5. Kamegaya, T.; Kuroda, K.; Hayakawa, Y., Identification of a *Streptococcus pyogenes* SF370 gene involved in production of c-di-AMP. *Nagoya J. Med.Sci.* **2011**, *73* (1-2), 49-57.
6. Huynh, T. N.; Luo, S. K.; Pensinger, D.; Sauer, J. D.; Tong, L.; Woodward, J. J., An HD-domain phosphodiesterase mediates cooperative hydrolysis of c-di-AMP to affect bacterial growth and virulence. *Proc. Natl. Acad. Sci. U.S.A.* **2015**, *112* (7), E747-E756.
7. Bai, Y.; Yang, J.; Eisele, L. E.; Underwood, A. J.; Koestler, B. J.; Waters, C. M.; Metzger, D. W.; Bai, G., Two DHH subfamily 1 proteins in *Streptococcus pneumoniae* possess cyclic di-AMP phosphodiesterase activity and affect bacterial growth and virulence. *J. Bacteriol.* **2013**, *195* (22), 5123-5132.
8. Witte, C. E.; Whiteley, A. T.; Burke, T. P.; Sauer, J.-D.; Portnoy, D. A.; Woodward, J. J., Cyclic di-AMP is critical for *Listeria monocytogenes* growth, cell wall homeostasis, and establishment of infection. *mBio* **2013**, *4* (3), e00282-13.
9. Kaplan Zeevi, M.; Shafir, N. S.; Shaham, S.; Friedman, S.; Sigal, N.; Nir Paz, R.; Boneca, I. G.; Herskovits, A. A., *Listeria monocytogenes* multidrug resistance transporters and cyclic di-AMP, which contribute to type I interferon induction, play a role in cell wall stress. *J. Bacteriol.* **2013**, *195* (23), 5250-61.

10. Corrigan, R. M.; Abbott, J. C.; Burhenne, H.; Kaefer, V.; Gründling, A., C-di-AMP is a new second messenger in *Staphylococcus aureus* with a role in controlling cell size and envelope stress. *PLoS Pathog.* **2011**, *7* (9), e1002217.
11. Bai, Y.; Yang, J.; Zarrella, T. M.; Zhang, Y.; Metzger, D. W.; Bai, G., Cyclic di-AMP impairs potassium uptake mediated by a cyclic di-AMP binding protein in *Streptococcus pneumoniae*. *J. Bacteriol.* **2014**, *196* (3), 614-623.
12. Luo, Y.; Helmann, J. D., Analysis of the role of *Bacillus subtilis* sM in ss-lactam resistance reveals an essential role for c-di-AMP in peptidoglycan homeostasis. *Mol. Microbiol.* **2012**, *83* (3), 623-639.
13. Woodward, J. J.; Iavarone, A. T.; Portnoy, D. A., c-di-AMP secreted by intracellular *Listeria monocytogenes* activates a host Type I interferon response. *Science* **2010**, *328* (5986), 1703-1705.
14. Song, J. H.; Ko, K. S.; Lee, J. Y.; Baek, J. Y.; Oh, W. S.; Yoon, H. S.; Jeong, J. Y.; Chun, J., Identification of essential genes in *Streptococcus pneumoniae* by allelic replacement mutagenesis. *Mol. Cells* **2005**, *19* (3), 365-374.
15. Zheng, Y.; Zhou, J.; Sayre, D. A.; Sintim, H. O., Identification of bromophenol thiohydantoin as an inhibitor of DisA, a c-di-AMP synthase, from a 1000 compound library, using the coralyne assay. *Chem. Commun.* **2014**, *50* (76), 11234-11237.
16. Müller, M.; Deimling, T.; Hopfner, K. P.; Witte, G., Structural analysis of the diadenylate cyclase reaction of DNA-integrity scanning protein A (DisA) and its inhibition by 3'-dATP. *Biochem. J.* **2015**, *469*, 367-374.

17. Zheng, Y.; Zhou, J.; Cooper, S. M.; Opoku-Temeng, C.; De Brito, A. M.; Sintim, H. O., Structure-activity relationship studies of c-di-AMP synthase inhibitor, bromophenol-thiohydantoin. *Tetrahedron* **2016**, *72* (25), 3554-3558.
18. Zhou, J.; Sayre, D. A.; Zheng, Y.; Szymanski, H.; Sintim, H. O., Unexpected complex formation between coralyne and cyclic diadenosine monophosphate providing a simple fluorescent turn-on assay to detect this bacterial second messenger. *Anal. Chem.* **2014**, *86* (5), 2412-2420.
19. Hawking, F., Suramin: with special reference to onchocerciasis. *Adv. Pharmacol. Chemother.* **1978**, *15*, 289-322.
20. Wang, C. C., Molecular mechanisms and therapeutic approaches to the treatment of African Trypanosomiasis. *Annu. Rev. Pharmacol. Toxicol.* **1995**, *35*, 93-127.
21. Avliyakov, N. K.; Lukes, J.; Kajava, A. V.; Liedberg, B.; Lundstrom, I.; Svensson, S. P. S., Suramin blocks nucleotide triphosphate binding to ribosomal protein L3 from *Trypanoplasma borreli*. *Eur. J. Biochem.* **2000**, *267* (6), 1723-1731.
22. Morgan, H. P.; McNae, I. W.; Nowicki, M. W.; Zhong, W.; Michels, P. A. M.; Auld, D. S.; Fothergill-Gilmore, L. A.; Walkinshaw, M. D., The trypanocidal drug suramin and other trypan blue mimetics are inhibitors of pyruvate kinases and bind to the adenosine site. *J. Biol. Chem.* **2011**, *286* (36), 31232-31240.
23. Kelley, L. A.; Mezulis, S.; Yates, C. M.; Wass, M. N.; Sternberg, M. J. E., The Phyre2 web portal for protein modeling, prediction and analysis. *Nat. Protoc.* **2015**, *10* (6), 845-858.

24. Lakowicz, J. R.; Weber, G., Quenching of fluorescence by oxygen - Probes for structural fluctuations in macromolecules. *Biochem.* **1973**, *12* (21), 4161-4170.
25. Lakowicz, J. R.; Weber, G., Quenching of protein fluorescence by oxygen - Detection of structural fluctuations in protein on nanosecond time scale. *Biochem.* **1973**, *12* (21), 4171-4179.
26. Bi, S.; Pang, B.; Wang, T.; Zhao, T.; Yu, W., Investigation on the interactions of clenbuterol to bovine serum albumin and lysozyme by molecular fluorescence technique. *Spectrochimica Acta Part a-Molecular and Biomolecular Spectroscopy* **2014**, *120*, 456-461.
27. Abou-Zied, O. K.; Al-Shihi, O. I. K., Characterization of subdomain IIA binding site of human serum albumin in its native, unfolded, and refolded states using small molecular probes. *J. Am. Chem. Soc.* **2008**, *130* (32), 10793-10801.
28. La Rocca, R. V.; Stein, C. A.; Danesi, R.; Myers, C. E., Suramin, a novel antitumor compound. *J. Steroid Biochem. Mol. Biol.* **1990**, *37* (6), 893-898.
29. Albulescu, I. C.; van Hoolwerff, M.; Wolters, L. A.; Bottaro, E.; Nastruzzi, C.; Yang, S. C.; Tsay, S.-C.; Hwu, J. R.; Snijder, E. J.; van Hemert, M. J., Suramin inhibits chikungunya virus replication through multiple mechanisms. *Antivir. Res.* **2015**, *121*, 39-46.
30. Nautiyal, A.; Patil, K. N.; Muniyappa, K., Suramin is a potent and selective inhibitor of *Mycobacterium tuberculosis* RecA protein and the SOS response: RecA as a potential target for antibacterial drug discovery. *J. Antimicrob. Chemother.* **2014**, *69* (7), 1834-1843.

31. Bodenreider, C.; Beer, D.; Keller, T. H.; Sonntag, S.; Wen, D.; Yap, L.; Yau, Y. H.; Shochat, S. G.; Huang, D.; Zhou, T.; Caflisch, A.; Su, X.-C.; Ozawa, K.; Otting, G.; Vasudevan, S. G.; Lescar, J.; Lim, S. P., A fluorescence quenching assay to discriminate between specific and nonspecific inhibitors of dengue virus protease. *Anal. Biochem.* **2009**, *395* (2), 195-204.
32. Trott, O.; Olson, A. J., Software news and update AutoDock Vina: Improving the speed and accuracy of docking with a new scoring function, efficient optimization, and multithreading. *J. Comput. Chem.* **2010**, *31* (2), 455-461.
33. Kalia, D.; Merey, G.; Nakayama, S.; Zheng, Y.; Zhou, J.; Luo, Y.; Guo, M.; Roembke, B. T.; Sintim, H. O., Nucleotide, c-di-GMP, c-di-AMP, cGMP, cAMP, (p)ppGpp signaling in bacteria and implications in pathogenesis. *Chem. Soc. Rev.* **2013**, *42* (1), 305-341.
34. Ross, P.; Mayer, R.; Weinhouse, H.; Amikam, D.; Huggirat, Y.; Benziman, M.; Devroom, E.; Fidler, A.; Depaus, P.; Sliedregt, L.; Vandermarel, G. A.; Vanboom, J. H., The cyclic diguanylic acid regulatory system of cellulose synthesis in *Acetobacter xylinum*. Chemical synthesis and biological activity of cyclic nucleotide dimer, trimer, and phosphothioate derivatives. *J. Biol. Chem.* **1990**, *265* (31), 18933-18943.
35. Zhang, L.; Li, W.; He, Z.-G., DarR, a TetR-like transcriptional factor, is a cyclic di-AMP-responsive repressor in *Mycobacterium smegmatis*. *J. Biol. Chem.* **2013**, *288* (5), 3085-3096.
36. Roembke, B. T.; Zhou, J.; Zheng, Y.; Sayre, D.; Lizardo, A.; Bernard, L.; Sintim, H. O., A cyclic dinucleotide containing 2-aminopurine is a general

- fluorescent sensor for c-di-GMP and 3',3'-cGAMP. *Mol. Biosyst.* **2014**, *10* (6), 1568-1575.
37. Nakayama, S.; Kelsey, I.; Wang, J.; Roelofs, K.; Stefane, B.; Luo, Y.; Lee, V. T.; Sintim, H. O., Thiazole orange-induced c-di-GMP quadruplex formation facilitates a simple fluorescent detection of this ubiquitous biofilm regulating molecule. *J. Am. Chem. Soc.* **2011**, *133* (13), 4856-4864.
38. Kim, H.-S.; Quon, M. J.; Kim, J.-a., New insights into the mechanisms of polyphenols beyond antioxidant properties; lessons from the green tea polyphenol, epigallocatechin 3-gallate. *Redox Biol.* **2014**, *2*, 187-195.
39. Ghosh, K. S.; Maiti, T. K.; Dasgupta, S., Green tea polyphenols as inhibitors of ribonuclease A. *Biochem. Biophys. Res. Commun.* **2004**, *325* (3), 807-811.
40. Khan, N.; Mukhtar, H., Tea polyphenols for health promotion. *Life Sci.* **2007**, *81* (7), 519-533.
41. Weisburger, J. H., Tea and health: A historical perspective. *Cancer Lett.* **1997**, *114* (1-2), 315-317.
42. Lorenz, M., Cellular targets for the beneficial actions of tea polyphenols. *Am. J. Clin. Nutr.* **2013**, *98* (6), 1642S-1650S.
43. Calland, N.; Sahuc, M.-E.; Belouzard, S.; Pene, V.; Bonnafous, P.; Mesalam, A. A.; Deloison, G.; Descamps, V.; Sahpaz, S.; Wychowski, C.; Lambert, O.; Brodin, P.; Duverlie, G.; Meuleman, P.; Rosenberg, A. R.; Dubuisson, J.; Rouille, Y.; Seron, K., Polyphenols inhibit Hepatitis C virus entry by a new mechanism of action. *J. Virol.* **2015**, *89* (19), 10053-10063.

44. Takahashi, O.; Cai, Z.; Toda, M.; Hara, Y.; Shimamura, T., Appearance of antibacterial activity of oxacillin against methicillin resistant *Staphylococcus aureus* (MRSA) in the presence of catechin. *Kansenshogaku zasshi*. **1995**, *69* (10), 1126-34.
45. Shoichet, B. K., Interpreting steep dose-response curves in early inhibitor discovery. *J. Med. Chem.* **2006**, *49* (25), 7274-7277.
46. Mehne, F. M. P.; Gunka, K.; Eilers, H.; Herzberg, C.; Kaefer, V.; Stuelke, J., Cyclic di-AMP homeostasis in *Bacillus subtilis*: both lack and high level accumulation of the nucleotide are detrimental for cell growth. *J. Biol. Chem.* **2013**, *288* (3), 2004-2017.
47. Rao, F.; See, R. Y.; Zhang, D.; Toh, D. C.; Ji, Q.; Liang, Z.-X., YybT is a signaling protein that contains a cyclic dinucleotide phosphodiesterase domain and a GGDEF domain with ATPase activity. *J. Biol. Chem.* **2010**, *285* (1), 473-482.
48. Goldstein, J. L.; Swain, T., The inhibition of enzymes by tannins. *Phytochemistry* **1965**, *4* ((1)), 185-192.
49. Zhao, W. H.; Hu, Z. Q.; Okubo, S.; Hara, Y.; Shimamura, T., Mechanism of synergy between epigallocatechin gallate and beta-lactams against methicillin-resistant *Staphylococcus aureus*. *Antimicrob. Agents Chemother.* **2001**, *45* (6), 1737-1742.
50. Yoo, S.; Murata, R. M.; Duarte, S., Antimicrobial traits of tea- and cranberry-derived polyphenols against *Streptococcus mutans*. *Caries Res.* **2011**, *45* (4), 327-335.
51. Xiao, H.; Liu, B.; Mo, H.; Liang, G., Comparative evaluation of tannic acid inhibiting alpha-glucosidase and trypsin. *Food Res. Int.* **2015**, *76*, 605-610.

52. Yang, E. B.; Wei, L.; Zhang, K.; Chen, Y. Z.; Chen, W. N., Tannic acid, a potent inhibitor of epidermal growth factor receptor tyrosine kinase. *J. Biochem.* **2006**, *139* (3), 495-502.
53. Murakami, S.; Muramatsu, M.; Otomo, S., Inhibitory effect of tannic acid on gastric H⁺,K⁺-ATPase. *J. Nat. Prod.* **1992**, *55* (4), 513-516.
54. Akiyama, H.; Fujii, K.; Yamasaki, O.; Oono, T.; Iwatsuki, K., Antibacterial action of several tannins against *Staphylococcus aureus*. *J. Antimicrob. Chemother.* **2001**, *48* (4), 487-491.
55. Payne, D. E.; Martin, N. R.; Parzych, K. R.; Rickard, A. H.; Underwood, A.; Boles, B. R., Tannic acid inhibits *Staphylococcus aureus* surface colonization in an IsaA-dependent manner. *Infect. Immun.* **2013**, *81* (2), 496-504.
56. Lombardo Bedran, T. B.; Morin, M.-P.; Spolidorio, D. P.; Grenier, D., Black tea extract and its theaflavin derivatives inhibit the growth of periodontopathogens and modulate interleukin-8 and beta-defensin secretion in oral epithelial cells. *Plos One* **2015**, *10* (11).
57. Friedman, M.; Henika, P. R.; Levin, C. E.; Mandrell, R. E.; Kozukue, N., Antimicrobial activities of tea catechins and theaflavins and tea extracts against *Bacillus cereus*. *J. Food Prot.* **2006**, *69* (2), 354-361.

Chapter 3:

1. de Kraker, M. E.; Stewardson, A. J.; Harbarth, S., Will 10 Million People Die a Year due to Antimicrobial Resistance by 2050? *PLoS Med* **2016**, *13* (11), e1002184.

2. Wright, G. D., Solving the Antibiotic Crisis. *ACS Infect Dis* **2015**, *1* (2), 80-4.
3. Witte, G.; Hartung, S.; Buettner, K.; Hopfner, K.-P., Structural biochemistry of a bacterial checkpoint protein reveals diadenylate cyclase activity regulated by DNA recombination intermediates. *Mol. Cell* **2008**, *30* (2), 167-178.
4. Corrigan, R. M.; Abbott, J. C.; Burhenne, H.; Kaefer, V.; Gründling, A., C-di-AMP is a new second messenger in *Staphylococcus aureus* with a role in controlling cell size and envelope stress. *PLoS Pathog.* **2011**, *7* (9), e1002217.
5. Woodward, J. J.; Iavarone, A. T.; Portnoy, D. A., c-di-AMP secreted by intracellular *Listeria monocytogenes* activates a host Type I interferon response. *Science* **2010**, *328* (5986), 1703-1705.
6. Kamegaya, T.; Kuroda, K.; Hayakawa, Y., Identification of a *Streptococcus pyogenes* SF370 gene involved in production of c-di-AMP Identification of a *Streptococcus pyogenes* SF370 gene involved in production of c-di-AMP. *Nagoya J. Med.Sci.* **2011**, *73* (1-2), 49-57.
7. Bai, Y.; Yang, J.; Zhou, X.; Ding, X.; Eisele, L. E.; Bai, G., *Mycobacterium tuberculosis* Rv3586 (DacA) is a diadenylate cyclase that converts ATP or ADP into c-di-AMP *Mycobacterium tuberculosis* Rv3586 (DacA) is a diadenylate cyclase that converts ATP or ADP into c-di-AMP. *PLoS One* **2012**, *7* (4), e35206.
8. Barker, J. R.; Koestler, B. J.; Carpenter, V. K.; Burdette, D. L.; Waters, C. M.; Vance, R. E.; Valdivia, R. H., STING-dependent recognition of cyclic di-AMP mediates Type I Interferon responses during *Chlamydia trachomatis* infection. *mBio* **2013**, *4* (3), e00018-13.

9. Luo, Y.; Helmann, J. D., Analysis of the role of Bacillus subtilis sM in ss-lactam resistance reveals an essential role for c-di-AMP in peptidoglycan homeostasis. *Molecular Microbiology* **2012**, *83* (3), 623-639.
10. Witte, C. E.; Whiteley, A. T.; Burke, T. P.; Sauer, J.-D.; Portnoy, D. A.; Woodward, J. J., Cyclic di-AMP is critical for *Listeria monocytogenes* growth, cell wall homeostasis, and establishment of infection. *mBio* **2013**, *4* (3), e00282-13.
11. Zhang, L.; Li, W.; He, Z.-G., DarR, a TetR-like transcriptional factor, is a cyclic di-AMP-responsive repressor in *Mycobacterium smegmatis* DarR, a TetR-like transcriptional factor, is a cyclic di-AMP-responsive repressor in *Mycobacterium smegmatis*. *J. Biol. Chem.* **2013**, *288* (5), 3085-3096.
12. Bai, Y.; Yang, J.; Zarrella, T. M.; Zhang, Y.; Metzger, D. W.; Bai, G., Cyclic di-AMP impairs potassium uptake mediated by a cyclic di-AMP binding protein in *Streptococcus pneumoniae* Cyclic di-AMP impairs potassium uptake mediated by a cyclic di-AMP binding protein in *Streptococcus pneumoniae*. *J. Bacteriol.* **2014**, *196* (3), 614-623.
13. Peng, X.; Zhang, Y.; Bai, G.; Zhou, X.; Wu, H., Cyclic di-AMP mediates biofilm formation. *Mol. Microbiol.* **2016**, *99* (5), 945-59.
14. Song, J. H.; Ko, K. S.; Lee, J. Y.; Baek, J. Y.; Oh, W. S.; Yoon, H. S.; Jeong, J. Y.; Chun, J., Identification of essential genes in *Streptococcus pneumoniae* by allelic replacement mutagenesis. *Molecules and Cells* **2005**, *19* (3), 365-374.
15. Chaudhuri, R. R.; Allen, A. G.; Owen, P. J.; Shalom, G.; Stone, K.; Harrison, M.; Burgis, T. A.; Lockyer, M.; Garcia-Lara, J.; Foster, S. J.; Pleasance, S. J.; Peters, S. E.; Maskell, D. J.; Charles, I. G., Comprehensive identification of

- essential *Staphylococcus aureus* genes using Transposon-Mediated Differential Hybridisation (TMDH). *BMC Genomics* **2009**, *10*, 291.
16. Walsh, C. T.; Wencewicz, T. A., Prospects for new antibiotics: a molecule-centered perspective. *Journal of Antibiotics* **2014**, *67* (1), 7-22.
 17. Opoku-Temeng, C.; Zhou, J.; Zheng, Y.; Su, J. M.; Sintim, H. O., Cyclic dinucleotide (c-di-GMP, c-di-AMP, and cGAMP) signalings have come of age to be inhibited by small molecules. *Chemical Communications* **2016**, *52* (60), 9327-9342.
 18. Zheng, Y.; Zhou, J.; Sayre, D. A.; Sintim, H. O., Identification of bromophenol thiohydantoin as an inhibitor of DisA, a c-di-AMP synthase, from a 1000 compound library, using the coralyne assay. *Chem. Commun.* **2014**, *50* (76), 11234-11237.
 19. Opoku-Temeng, C.; Sintim, H. O., Potent inhibition of cyclic diadenylate monophosphate cyclase by the antiparasitic drug, suramin. *Chem. Commun.* **2016**, *52* (19), 3754-7.
 20. Opoku-Temeng, C.; Sintim, H. O., Inhibition of cyclic diadenylate cyclase, DisA by polyphenols. *Sci. Rep.* **2016**, *6*, 25445.
 21. Lambert, J. D.; Yang, C. S., Mechanisms of cancer prevention by tea constituents. *J Nutr* **2003**, *133* (10), 3262S-3267S.
 22. Müller, M.; Deimling, T.; Hopfner, K. P.; Witte, G., Structural analysis of the diadenylate cyclase reaction of DNA-integrity scanning protein A (DisA) and its inhibition by 3'-dATP. *Biochem. J.* **2015**, *469*, 367-374.
 23. Zhou, J.; Sayre, D. A.; Zheng, Y.; Szmazinski, H.; Sintim, H. O., Unexpected complex formation between coralyne and cyclic diadenosine

- monophosphate providing a simple fluorescent turn-on assay to detect this bacterial second messenger. *Anal. Chem.* **2014**, *86* (5), 2412-2420.
24. Chin, P. C.; Liu, L.; Morrison, B. E.; Siddiq, A.; Ratan, R. R.; Bottiglieri, T.; D'Mello, S. R., The c-Raf inhibitor GW5074 provides neuroprotection *in vitro* and in an animal model of neurodegeneration through a MEK-ERK and Akt-independent mechanism. *J Neurochem* **2004**, *90* (3), 595-608.
25. Lei, Y.; Cao, Y. X.; Xu, C. B.; Zhang, Y., The Raf-1 inhibitor GW5074 and dexamethasone suppress sidestream smoke-induced airway hyperresponsiveness in mice. *Respir. Res.* **2008**, *9*, 71.
26. Davies, D., Understanding biofilm resistance to antibacterial agents. *Nat Rev Drug Discov* **2003**, *2* (2), 114-22.
27. CDC Antibiotic resistance threats in the United States, 2013. Report CS239559-B. www.cdc.gov/drugresistance/threats-report-2013.
28. Lister, J. L.; Horswill, A. R., *Staphylococcus aureus* biofilms: recent developments in biofilm dispersal. *Front Cell Infect Microbiol* **2014**, *4*, 178.
29. Worthington, R. J.; Richards, J. J.; Melander, C., Small molecule control of bacterial biofilms. *Org Biomol Chem* **2012**, *10* (37), 7457-74.
30. Yeagley, A. A.; Su, Z.; McCullough, K. D.; Worthington, R. J.; Melander, C., N-substituted 2-aminoimidazole inhibitors of MRSA biofilm formation accessed through direct 1,3-bis(tert-butoxycarbonyl)guanidine cyclization. *Org Biomol Chem* **2013**, *11* (1), 130-7.
31. O'Toole, G. A., Microtiter dish biofilm formation assay. *J Vis Exp* **2011**, (47).

32. Kalan, L.; Wright, G. D., Antibiotic adjuvants: multicomponent anti-infective strategies. *Expert Rev Mol Med* **2011**, *13*, e5.
33. Laxminarayan, R.; Duse, A.; Wattal, C.; Zaidi, A. K.; Wertheim, H. F.; Sumpradit, N.; Vlieghe, E.; Hara, G. L.; Gould, I. M.; Goossens, H.; Greko, C.; So, A. D.; Bigdeli, M.; Tomson, G.; Woodhouse, W.; Ombaka, E.; Peralta, A. Q.; Qamar, F. N.; Mir, F.; Kariuki, S.; Bhutta, Z. A.; Coates, A.; Bergstrom, R.; Wright, G. D.; Brown, E. D.; Cars, O., Antibiotic resistance-the need for global solutions. *Lancet Infect. Dis.* **2013**, *13* (12), 1057-98.
34. Wright, G. D., Antibiotic adjuvants: rescuing antibiotics from resistance. *Trends Microbiol* **2016**, *24* (11), 862-871.
35. Harris, T. L.; Worthington, R. J.; Melander, C., Potent small-molecule suppression of oxacillin resistance in methicillin-resistant *Staphylococcus aureus*. *Angew. Chem. Int. Ed. Engl.* **2012**, *51* (45), 11254-7.
36. Yamazaki, H.; Nonaka, K.; Masuma, R.; Omura, S.; Tomoda, H., Xanthoradones, new potentiators of imipenem activity against methicillin-resistant *Staphylococcus aureus*, produced by *Penicillium radicum* FKI-3765-2: I. Taxonomy, fermentation, isolation and biological properties. *J. Antibiot. (Tokyo)* **2009**, *62* (8), 431-4.
37. Brackett, C. M.; Melander, R. J.; An, I. H.; Krishnamurthy, A.; Thompson, R. J.; Cavanagh, J.; Melander, C., Small-molecule suppression of β -lactam resistance in multidrug-resistant gram-negative pathogens. *J. Med. Chem.* **2014**, *57* (17), 7450-8.

38. Chiosis, G.; Boneca, I. G., Selective cleavage of D-Ala-D-Lac by small molecules: re-sensitizing resistant bacteria to vancomycin. *Science* **2001**, *293* (5534), 1484-7.
39. Zheng, Y.; Tsuji, G.; Opoku-Temeng, C.; Sintim, H. O., Inhibition of *P. aeruginosa* c-di-GMP phosphodiesterase RocR and swarming motility by a benzoisothiazolinone derivative. *Chem. Sci.* **2016**, *7* (9), 6238-6244.
40. Orhan, G.; Bayram, A.; Zer, Y.; Balci, I., Synergy tests by E test and checkerboard methods of antimicrobial combinations against *Brucella melitensis*. *J Clin. Microbiol.* **2005**, *43* (1), 140-3.

Chapter 4:

1. Frieden, T., Antibiotic resistance threats in the United States, 2013. Centers for Disease Control and Prevention: Atlanta, GA, USA, 2013; p 114.
2. Nathan, C.; Cars, O., Antibiotic resistance - problems, progress, and prospects. *N. Engl. J. Med.* **2014**, *371* (19), 1761-1763.
3. O'Neill, J., *Review on antimicrobial resistance: Tackling a crisis for the health and wealth of nations*. London, United Kingdom, 2014.
4. Wright, G. D., Solving the antibiotic crisis. *ACS Infect. Dis.* **2015**, *1* (2), 80-4.
5. Gould, I. M.; Bal, A. M., New antibiotic agents in the pipeline and how they can help overcome microbial resistance. *Virulence* **2013**, *4* (2), 185-91.
6. Ventola, C. L., The antibiotic resistance crisis: part 1: causes and threats. *P T.* **2015**, *40* (4), 277-83.

7. Wright, G. D., Antibiotic adjuvants: rescuing antibiotics from resistance. *Trends Microbiol.* **2016**, *24* (11), 862-871.
8. Kalan, L.; Wright, G. D., Antibiotic adjuvants: multicomponent anti-infective strategies. *Expert Rev. Mol. Med* **2011**, *13*, e5.
9. Melander, R. J.; Melander, C., Antibiotic Adjuvants. In *Antibacterials: Volume I*, Fisher, J. F.; Mobashery, S.; Miller, M. J., Eds. Springer International Publishing: Cham, 2017; pp 89-118.
10. Ahmed, A.; Azim, A.; Gurjar, M.; Baronia, A. K., Current concepts in combination antibiotic therapy for critically ill patients. *Indian J. Crit. Care Med.* **2014**, *18* (5), 310-4.
11. Rahal, J. J., Novel antibiotic combinations against infections with almost completely resistant *Pseudomonas aeruginosa* and *Acinetobacter* species. *Clinical Infectious Diseases* **2006**, *43*, S95-S99.
12. Chong, C. R.; Sullivan, D. J., New uses for old drugs. *Nature* **2007**, *448* (7154), 645-6.
13. Opoku-Temeng, C.; Dayal, N.; Miller, J.; Sintim, H. O., Hydroxybenzylidene-indolinones, c-di-AMP synthase inhibitors, have antibacterial and anti-biofilm activities and also re-sensitize resistant bacteria to methicillin and vancomycin. *Rsc Adv.* **2017**, *7* (14), 8288-8294.
14. Witte, G.; Hartung, S.; Buettner, K.; Hopfner, K.-P., Structural biochemistry of a bacterial checkpoint protein reveals diadenylate cyclase activity regulated by DNA recombination intermediates. *Mol. Cell* **2008**, *30* (2), 167-178.

15. Sambanthamoorthy, K.; Sloup, R. E.; Parashar, V.; Smith, J. M.; Kim, E. E.; Semmelhack, M. F.; Neiditch, M. B.; Waters, C. M., Identification of small molecules that antagonize diguanylate cyclase enzymes to inhibit biofilm formation. *Antimicrob. Agents Chemother.* **2012**, *56* (10), 5202-5211.
16. Kim, B.; Park, J. S.; Choi, H. Y.; Yoon, S. S.; Kim, W. G., Terrein is an inhibitor of quorum sensing and c-di-GMP in *Pseudomonas aeruginosa*: a connection between quorum sensing and c-di-GMP. *Sci. Rep.* **2018**, *8*.
17. EUCAST, Terminology relating to methods for the determination of susceptibility of bacteria to antimicrobial agents. *Clin. Microbiol. Infect.* **2000**, *6* (9), 503-508.
18. Cotsonas King, A.; Wu, L., Macromolecular synthesis and membrane perturbation assays for mechanisms of action studies of antimicrobial agents. *Curr. Protoc. Pharmacol.* **2009**, Chapter 13, Unit 13A.7.
19. Tyanova, S.; Temu, T.; Sinitcyn, P.; Carlson, A.; Hein, M. Y.; Geiger, T.; Mann, M.; Cox, J., The Perseus computational platform for comprehensive analysis of (prote)omics data. *Nat. Methods* **2016**, *13* (9), 731-40.
20. Frees, D.; Savijoki, K.; Varmanen, P.; Ingmer, H., Clp ATPases and ClpP proteolytic complexes regulate vital biological processes in low GC, Gram-positive bacteria. *Mol. Microbiol.* **2007**, *63* (5), 1285-95.
21. Zolkiewski, M., A camel passes through the eye of a needle: protein unfolding activity of Clp ATPases. *Mol. Microbiol.* **2006**, *61* (5), 1094-100.
22. Buist, G.; Steen, A.; Kok, J.; Kuipers, O. P., LysM, a widely distributed protein motif for binding to (peptido)glycans. *Mol. Microbiol.* **2008**, *68* (4), 838-47.

23. Rasmussen, R. V.; Fowler, V. G.; Skov, R.; Bruun, N. E., Future challenges and treatment of *Staphylococcus aureus* bacteremia with emphasis on MRSA. *Future Microbiol.* **2011**, *6* (1), 43-56.
24. Grundmann, H.; Aires-de-Sousa, M.; Boyce, J.; Tiemersma, E., Emergence and resurgence of methicillin-resistant *Staphylococcus aureus* as a public-health threat. *Lancet* **2006**, *368* (9538), 874-85.
25. Stapleton, P. D.; Taylor, P. W., Methicillin resistance in *Staphylococcus aureus*: mechanisms and modulation. *Sci. Prog.* **2002**, *85* (Pt 1), 57-72.
26. Conlon, B. P.; Nakayasu, E. S.; Fleck, L. E.; LaFleur, M. D.; Isabella, V. M.; Coleman, K.; Leonard, S. N.; Smith, R. D.; Adkins, J. N.; Lewis, K., Activated ClpP kills persisters and eradicates a chronic biofilm infection. *Nature* **2013**, *503* (7476), 365-70.
27. Subramanian, D.; Natarajan, J., Network analysis of *S. aureus* response to ramoplanin reveals modules for virulence factors and resistance mechanisms and characteristic novel genes. *Gene* **2015**, *574* (1), 149-62.
28. Schwan, W. R.; Polanowski, R.; Dunman, P. M.; Medina-Bielski, S.; Lane, M.; Rott, M.; Lipker, L.; Wescott, A.; Monte, A.; Cook, J. M.; Baumann, D. D.; Tiruveedhula, V. V. N. P.; Witzigmann, C. M.; Mikel, C.; Rahman, M. T., Identification of *Staphylococcus aureus* cellular pathways affected by the stilbenoid lead Drug SK-03-92 using a microarray. *Antibiotics (Basel)* **2017**, *6* (3).
29. Kriegeskorte, A.; Block, D.; Drescher, M.; Windmüller, N.; Mellmann, A.; Baum, C.; Neumann, C.; Lorè, N. I.; Bragonzi, A.; Liebau, E.; Hertel, P.; Seggewiss, J.; Becker, K.; Proctor, R. A.; Peters, G.; Kahl, B. C., Inactivation of

- thyA in *Staphylococcus aureus* attenuates virulence and has a strong impact on metabolism and virulence gene expression. *MBio* **2014**, 5 (4), e01447-14.
30. Yee, R.; Cui, P.; Shi, W.; Feng, J.; Zhang, Y., Genetic screen reveals the role of purine metabolism in *Staphylococcus aureus* persistence to rifampicin. *Antibiotics (Basel)* **2015**, 4 (4), 627-42.
31. Ji, Y.; Zhang, B.; Van, S. F.; Horn; Warren, P.; Woodnutt, G.; Burnham, M. K.; Rosenberg, M., Identification of critical staphylococcal genes using conditional phenotypes generated by antisense RNA. *Science* **2001**, 293 (5538), 2266-9.
32. Valentino, M. D.; Foulston, L.; Sadaka, A.; Kos, V. N.; Villet, R. A.; Santa Maria, J.; Lazinski, D. W.; Camilli, A.; Walker, S.; Hooper, D. C.; Gilmore, M. S., Genes contributing to *Staphylococcus aureus* fitness in abscess- and infection-related ecologies. *MBio* **2014**, 5 (5), e01729-14.
33. Lan, L.; Cheng, A.; Dunman, P. M.; Missiakas, D.; He, C., Golden pigment production and virulence gene expression are affected by metabolisms in *Staphylococcus aureus*. *J. Bacteriol.* **2010**, 192 (12), 3068-77.
34. Meng, L. M.; Nygaard, P., Identification of hypoxanthine and guanine as the co-repressors for the purine regulon genes of *Escherichia coli*. *Mol. Microbiol.* **1990**, 4 (12), 2187-92.
35. Weng, M.; Nagy, P. L.; Zalkin, H., Identification of the *Bacillus subtilis* pur operon repressor. *Proc. Natl. Acad. Sci. U.S.A.* **1995**, 92 (16), 7455-9.

36. Jönsson, K.; McDevitt, D.; McGavin, M. H.; Patti, J. M.; Höök, M., *Staphylococcus aureus* expresses a major histocompatibility complex class II analog. *J. Biol. Chem.* **1995**, *270* (37), 21457-60.
37. Kreikemeyer, B.; McDevitt, D.; Podbielski, A., The role of the map protein in *Staphylococcus aureus* matrix protein and eukaryotic cell adherence. *Int. J. Med. Microbiol.* **2002**, *292* (3-4), 283-95.
38. Lee, L. Y.; Miyamoto, Y. J.; McIntyre, B. W.; Höök, M.; McCrea, K. W.; McDevitt, D.; Brown, E. L., The *Staphylococcus aureus* Map protein is an immunomodulator that interferes with T cell-mediated responses. *J. Clin. Invest.* **2002**, *110* (10), 1461-71.
39. Pallen, M. J., The ESAT-6/WXG100 superfamily -- and a new Gram-positive secretion system? *Trends Microbiol.* **2002**, *10* (5), 209-12.
40. Burts, M. L.; Williams, W. A.; DeBord, K.; Missiakas, D. M., EsxA and EsxB are secreted by an ESAT-6-like system that is required for the pathogenesis of *Staphylococcus aureus* infections. *Proc. Natl. Acad. Sci. U. S. A.* **2005**, *102* (4), 1169-74.
41. Aly, K. A.; Anderson, M.; Ohr, R. J.; Missiakas, D., Isolation of a membrane protein complex for Type VII Secretion in *Staphylococcus aureus*. *J. Bacteriol.* **2017**, *199* (23).
42. Szklarczyk, D.; Morris, J. H.; Cook, H.; Kuhn, M.; Wyder, S.; Simonovic, M.; Santos, A.; Doncheva, N. T.; Roth, A.; Bork, P.; Jensen, L. J.; von Mering, C., The STRING database in 2017: quality-controlled protein-protein association networks, made broadly accessible. *Nucleic Acids Res.* **2017**, *45* (D1), D362-D368.

43. Chien, Y.; Cheung, A. L., Molecular interactions between two global regulators, sar and agr, in *Staphylococcus aureus*. *J. Biol. Chem.* **1998**, *273* (5), 2645-52.
44. Wang, B.; Muir, T. W., Regulation of virulence in *Staphylococcus aureus*: molecular mechanisms and remaining puzzles. *Cell Chem. Biol.* **2016**, *23* (2), 214-224.
45. Novick, R. P., Autoinduction and signal transduction in the regulation of staphylococcal virulence. *Mol. Microbiol.* **2003**, *48* (6), 1429-49.
46. Koenig, R. L.; Ray, J. L.; Maleki, S. J.; Smeltzer, M. S.; Hurlburt, B. K., *Staphylococcus aureus* AgrA binding to the RNAlII-agr regulatory region. *J. Bacteriol.* **2004**, *186* (22), 7549-55.
47. Reyes, D.; Andrey, D. O.; Monod, A.; Kelley, W. L.; Zhang, G.; Cheung, A. L., Coordinated regulation by AgrA, SarA, and SarR to control agr expression in *Staphylococcus aureus*. *J. Bacteriol.* **2011**, *193* (21), 6020-31.
48. Gray, B.; Hall, P.; Gresham, H., Targeting agr- and agr-Like quorum sensing systems for development of common therapeutics to treat multiple gram-positive bacterial infections. *Sensors (Basel)* **2013**, *13* (4), 5130-66.
49. Gordon, C. P.; Williams, P.; Chan, W. C., Attenuating *Staphylococcus aureus* virulence gene regulation: a medicinal chemistry perspective. *J. Med. Chem.* **2013**, *56* (4), 1389-404.
50. Cheung, A. L.; Bayer, A. S.; Zhang, G.; Gresham, H.; Xiong, Y. Q., Regulation of virulence determinants in vitro and in vivo in *Staphylococcus aureus*. *FEMS Immunol. Med. Microbiol.* **2004**, *40* (1), 1-9.

51. Manna, A. C.; Cheung, A. L., Expression of SarX, a negative regulator of agr and exoprotein synthesis, is activated by MgrA in *Staphylococcus aureus*. *J. Bacteriol.* **2006**, *188* (12), 4288-99.
52. Manna, A.; Cheung, A. L., Characterization of sarR, a modulator of sar expression in *Staphylococcus aureus*. *Infect. Immun.* **2001**, *69* (2), 885-96.
53. Manna, A. C.; Cheung, A. L., Transcriptional regulation of the agr locus and the identification of DNA binding residues of the global regulatory protein SarR in *Staphylococcus aureus*. *Mol. Microbiol.* **2006**, *60* (5), 1289-301.
54. Manna, A. C.; Ingavale, S. S.; Maloney, M.; van Wamel, W.; Cheung, A. L., Identification of sarV (SA2062), a new transcriptional regulator, is repressed by SarA and MgrA (SA0641) and involved in the regulation of autolysis in *Staphylococcus aureus*. *J. Bacteriol.* **2004**, *186* (16), 5267-80.
55. Brunskill, E. W.; de Jonge, B. L.; Bayles, K. W., The *Staphylococcus aureus* *scaA* gene: a novel locus that affects cell division and morphogenesis. *Microbiol.* **1997**, *143* (Pt 9), 2877-82.
56. Olivares, A. O.; Baker, T. A.; Sauer, R. T., Mechanistic insights into bacterial AAA+ proteases and protein-remodelling machines. *Nat Rev Microbiol* **2016**, *14* (1), 33-44.
57. Frees, D.; Qazi, S. N.; Hill, P. J.; Ingmer, H., Alternative roles of ClpX and ClpP in *Staphylococcus aureus* stress tolerance and virulence. *Mol. Microbiol.* **2003**, *48* (6), 1565-78.

58. Okamura, E.; Hirai, M. Y., Novel regulatory mechanism of serine biosynthesis associated with 3-phosphoglycerate dehydrogenase in *Arabidopsis thaliana*. *Sci. Rep.* **2017**, *7* (1), 3533.
59. Grant, G. A., Contrasting catalytic and allosteric mechanisms for phosphoglycerate dehydrogenases. *Arch. Biochem. Biophys.* **2012**, *519* (2), 175-85.
60. Locasale, J. W.; Grassian, A. R.; Melman, T.; Lyssiotis, C. A.; Mattaini, K. R.; Bass, A. J.; Heffron, G.; Metallo, C. M.; Muranen, T.; Sharfi, H.; Sasaki, A. T.; Anastasiou, D.; Mullarky, E.; Vokes, N. I.; Sasaki, M.; Beroukhim, R.; Stephanopoulos, G.; Ligon, A. H.; Meyerson, M.; Richardson, A. L.; Chin, L.; Wagner, G.; Asara, J. M.; Brugge, J. S.; Cantley, L. C.; Vander Heiden, M. G., Phosphoglycerate dehydrogenase diverts glycolytic flux and contributes to oncogenesis. *Nat. Genet.* **2011**, *43* (9), 869-74.
61. Triassi, A. J.; Wheatley, M. S.; Savka, M. A.; Gan, H. M.; Dobson, R. C.; Hudson, A. O., L,L-diaminopimelate aminotransferase (DapL): a putative target for the development of narrow-spectrum antibacterial compounds. *Front. Microbiol.* **2014**, *5*, 509.
62. Grant Pearce, F.; Hudson, A. O.; Loomes, K.; Dobson, R. C. J., Dihydrodipicolinate synthase: structure, dynamics, function, and evolution. *Subcell. Biochem.* **2017**, *83*, 271-289.
63. Gillner, D. M.; Becker, D. P.; Holz, R. C., Lysine biosynthesis in bacteria: a metallodesuccinylase as a potential antimicrobial target. *J. Biol. Inorg. Chem.* **2013**, *18* (2), 155-63.

64. Karita, M.; Etterbeek, M. L.; Forsyth, M. H.; Tummuru, M. K.; Blaser, M. J., Characterization of *Helicobacter pylori* dapE and construction of a conditionally lethal dapE mutant. *Infect. Immun.* **1997**, *65* (10), 4158-64.
65. Pavelka, M. S.; Jacobs, W. R., Biosynthesis of diaminopimelate, the precursor of lysine and a component of peptidoglycan, is an essential function of *Mycobacterium smegmatis*. *J. Bacteriol.* **1996**, *178* (22), 6496-507.
66. Sasseti, C. M.; Boyd, D. H.; Rubin, E. J., Genes required for mycobacterial growth defined by high density mutagenesis. *Mol. Microbiol.* **2003**, *48* (1), 77-84.
67. Stapleton, M. R.; Horsburgh, M. J.; Hayhurst, E. J.; Wright, L.; Jonsson, I. M.; Tarkowski, A.; Kokai-Kun, J. F.; Mond, J. J.; Foster, S. J., Characterization of IsaA and SceD, two putative lytic transglycosylases of *Staphylococcus aureus*. *J. Bacteriol.* **2007**, *189* (20), 7316-25.
68. Dik, D. A.; Marous, D. R.; Fisher, J. F.; Mobashery, S., Lytic transglycosylases: concinnity in concision of the bacterial cell wall. *Crit. Rev. Biochem. Mol. Biol.* **2017**, *52* (5), 503-542.
69. Dubrac, S.; Boneca, I. G.; Poupel, O.; Msadek, T., New insights into the WalK/WalR (YycG/YycF) essential signal transduction pathway reveal a major role in controlling cell wall metabolism and biofilm formation in *Staphylococcus aureus*. *J. Bacteriol.* **2007**, *189* (22), 8257-69.
70. Szweda, P.; Schielmann, M.; Kotlowski, R.; Gorczyca, G.; Zalewska, M.; Milewski, S., Peptidoglycan hydrolases-potential weapons against *Staphylococcus aureus*. *Appl. Microbiol. Biotechnol.* **2012**, *96* (5), 1157-74.

71. Scheurwater, E.; Reid, C. W.; Clarke, A. J., Lytic transglycosylases: bacterial space-making autolysins. *Int. J. Biochem. Cell Biol.* **2008**, *40* (4), 586-91.
72. Sharma, A. K.; Kumar, S.; K, H.; Dhakan, D. B.; Sharma, V. K., Prediction of peptidoglycan hydrolases- a new class of antibacterial proteins. *BMC Genomics* **2016**, *17*, 411.
73. Rashel, M.; Uchiyama, J.; Ujihara, T.; Uehara, Y.; Kuramoto, S.; Sugihara, S.; Yagy, K.; Muraoka, A.; Sugai, M.; Hiramatsu, K.; Honke, K.; Matsuzaki, S., Efficient elimination of multidrug-resistant *Staphylococcus aureus* by cloned lysin derived from bacteriophage phi MR11. *J. Infect. Dis.* **2007**, *196* (8), 1237-47.
74. Cox, J.; Hein, M. Y.; Lubner, C. A.; Paron, I.; Nagaraj, N.; Mann, M., Accurate proteome-wide label-free quantification by delayed normalization and maximal peptide ratio extraction, termed MaxLFQ. *Mol. Cell. Proteomics* **2014**, *13* (9), 2513-26.
75. Cox, J.; Mann, M., MaxQuant enables high peptide identification rates, individualized p.p.b.-range mass accuracies and proteome-wide protein quantification. *Nat. Biotechnol.* **2008**, *26* (12), 1367-72.
76. Cox, J.; Neuhauser, N.; Michalski, A.; Scheltema, R. A.; Olsen, J. V.; Mann, M., Andromeda: a peptide search engine integrated into the MaxQuant environment. *J. Proteome Res.* **2011**, *10* (4), 1794-805.
77. Thänert, R.; Goldmann, O.; Beineke, A.; Medina, E., Host-inherent variability influences the transcriptional response of *Staphylococcus aureus* during in vivo infection. *Nat. Commun.* **2017**, *8*, 14268.

Chapter 5:

1. Gould, I. M.; Bal, A. M., New antibiotic agents in the pipeline and how they can help overcome microbial resistance. *Virulence* **2013**, *4* (2), 185-91.
2. Wright, G. D., Something old, something new: revisiting natural products in antibiotic drug discovery. *Can. J. Microbiol.* **2014**, *60* (3), 147-54.
3. Ventola, C. L., The antibiotic resistance crisis: part 1: causes and threats. *P T* **2015**, *40* (4), 277-83.
4. Bush, K.; Courvalin, P.; Dantas, G.; Davies, J.; Eisenstein, B.; Huovinen, P.; Jacoby, G. A.; Kishony, R.; Kreiswirth, B. N.; Kutter, E.; Lerner, S. A.; Levy, S.; Lewis, K.; Lomovskaya, O.; Miller, J. H.; Mobashery, S.; Piddock, L. J.; Projan, S.; Thomas, C. M.; Tomasz, A.; Tulkens, P. M.; Walsh, T. R.; Watson, J. D.; Witkowski, J.; Witte, W.; Wright, G.; Yeh, P.; Zgurskaya, H. I., Tackling antibiotic resistance. *Nat. Rev. Microbiol.* **2011**, *9* (12), 894-6.
5. Frieden, T., Antibiotic Resistance Threats in the United States, 2013. Centers for Disease Control and Prevention: Atlanta, GA, USA, 2013; p 114.
6. de Kraker, M. E.; Stewardson, A. J.; Harbarth, S., Will 10 million people die a year due to antimicrobial resistance by 2050? *PLoS Med.* **2016**, *13* (11), e1002184.
7. Gorak, E. J.; Yamada, S. M.; Brown, J. D., Community-acquired methicillin-resistant *Staphylococcus aureus* in hospitalized adults and children without known risk factors. *Clin. Infect. Dis.* **1999**, *29* (4), 797-800.
8. Stevens, A. M.; Hennessy, T.; Baggett, H. C.; Bruden, D.; Parks, D.; Klejka, J., Methicillin-Resistant *Staphylococcus aureus* carriage and risk factors for

- skin infections, Southwestern Alaska, USA. *Emerg. Infect. Dis.* **2010**, *16* (5), 797-803.
9. David, M. Z.; Rudolph, K. M.; Hennessy, T. W.; Boyle-Vavra, S.; Daum, R. S., Molecular epidemiology of methicillin-resistant *Staphylococcus aureus*, rural southwestern Alaska. *Emerg. Infect. Dis.* **2008**, *14* (11), 1693-9.
10. Johnson, J. K.; Khoie, T.; Shurland, S.; Kreisel, K.; Stine, O. C.; Roghmann, M. C., Skin and soft tissue infections caused by methicillin-resistant *Staphylococcus aureus* USA300 clone. *Emerg. Infect. Dis.* **2007**, *13* (8), 1195-200.
11. Golding, G. R.; Levett, P. N.; McDonald, R. R.; Irvine, J.; Quinn, B.; Nsungu, M.; Woods, S.; Khan, M.; Ofner-Agostini, M.; Mulvey, M. R.; Partnership, N. A. R., High rates of *Staphylococcus aureus* USA400 infection, Northern Canada. *Emerg. Infect. Dis.* **2011**, *17* (4), 722-5.
12. Klevens, R. M.; Morrison, M. A.; Nadle, J.; Petit, S.; Gershman, K.; Ray, S.; Harrison, L. H.; Lynfield, R.; Dumyati, G.; Townes, J. M.; Craig, A. S.; Zell, E. R.; Fosheim, G. E.; McDougal, L. K.; Carey, R. B.; Fridkin, S. K.; Investigators, A. B. C. s. A. M., Invasive methicillin-resistant *Staphylococcus aureus* infections in the United States. *JAMA* **2007**, *298* (15), 1763-71.
13. Drew, R. H., Emerging options for treatment of invasive, multidrug-resistant *Staphylococcus aureus* infections. *Pharmacotherapy* **2007**, *27* (2), 227-49.
14. Lowy, F. D., *Staphylococcus aureus* infections. *N. Engl. J. Med.* **1998**, *339* (8), 520-32.
15. Rayner, C.; Munckhof, W. J., Antibiotics currently used in the treatment of infections caused by *Staphylococcus aureus*. *Intern. Med. J.* **2005**, *35* Suppl 2, S3-16.

16. Thati, V.; Shivannavar, C. T.; Gaddad, S. M., Vancomycin resistance among methicillin-resistant *Staphylococcus aureus* isolates from intensive care units of tertiary care hospitals in Hyderabad. *Indian J. Med. Res.* **2011**, *134* (5), 704-8.
17. Gilbert, D. N.; Kohlhepp, S. J.; Slama, K. A.; Grunkemeier, G.; Lewis, G.; Dworkin, R. J.; Slaughter, S. E.; Leggett, J. E., Phenotypic resistance of *Staphylococcus aureus*, selected Enterobacteriaceae, and *Pseudomonas aeruginosa* after single and multiple *in vitro* exposures to ciprofloxacin, levofloxacin, and trovafloxacin. *Antimicrob. Agents Chemother.* **2001**, *45* (3), 883-92.
18. Wright, G. D., Solving the Antibiotic Crisis. *ACS Infect. Dis.* **2015**, *1* (2), 80-4.
19. Wright, G. D., Antibiotic adjuvants: rescuing antibiotics from resistance. *Trends Microbiol.* **2016**, *24* (11), 862-871.
20. Epanand, R. M.; Walker, C.; Epanand, R. F.; Magarvey, N. A., Molecular mechanisms of membrane targeting antibiotics. *Biochim. Biophys. Acta* **2016**, *1858* (5), 980-7.
21. Opoku-Temeng, C.; Dayal, N.; Miller, J.; Sintim, H. O., Hydroxybenzylidene-indolinones, c-di-AMP synthase inhibitors, have antibacterial and anti-biofilm activities and also re-sensitize resistant bacteria to methicillin and vancomycin. *Rsc Adv.* **2017**, *7* (14), 8288-8294.
22. Devasahayam, G.; Scheld, W. M.; Hoffman, P. S., Newer antibacterial drugs for a new century. *Expert Opin. Investig. Drugs* **2010**, *19* (2), 215-34.
23. Arias, C. A.; Murray, B. E., Antibiotic-resistant bugs in the 21st century--a clinical super-challenge. *N. Engl. J. Med.* **2009**, *360* (5), 439-43.

24. Huggins, W. M.; Minrovic, B. M.; Corey, B. W.; Jacobs, A. C.; Melander, R. J.; Sommer, R. D.; Zurawski, D. V.; Melander, C., 1,2,4-Triazolidine-3-thiones as narrow spectrum antibiotics against multidrug-resistant *Acinetobacter baumannii*. *ACS Med. Chem. Lett.* **2017**, *8* (1), 27-31.
25. Harris, T. L.; Worthington, R. J.; Melander, C., Potent small-molecule suppression of oxacillin resistance in methicillin-resistant *Staphylococcus aureus*. *Angew. Chem. Int. Ed. Engl.* **2012**, *51* (45), 11254-7.
26. Panchaud, P.; Bruyère, T.; Blumstein, A. C.; Bur, D.; Chambovey, A.; Ertel, E. A.; Gude, M.; Hubschwerlen, C.; Jacob, L.; Kimmerlin, T.; Pfeifer, T.; Prade, L.; Seiler, P.; Ritz, D.; Rueedi, G., Discovery and optimization of isoquinoline ethyl ureas as antibacterial agents. *J. Med. Chem.* **2017**, *60* (9), 3755-3775.
27. Wang, B.; Huang, W.; Zhou, J.; Tang, X.; Chen, Y.; Peng, C.; Han, B., Drug design based on pentaerythritol tetranitrate reductase: synthesis and antibacterial activity of Pogostone derivatives. *Org. Biomol. Chem.* **2017**, *15* (31), 6548-6556.
28. CLSI, *Methods for dilution antimicrobial susceptibility tests for bacteria that grow aerobically - Ninth Edition: Approved Standard M07-A9*. Wayne, PA, 2012.
29. Mohammad, H.; Younis, W.; Ezzat, H. G.; Peters, C. E.; AbdelKhalek, A.; Cooper, B.; Pogliano, K.; Pogliano, J.; Mayhoub, A. S.; Seleem, M. N., Bacteriological profiling of diphenylureas as a novel class of antibiotics against methicillin-resistant *Staphylococcus aureus*. *PLoS One* **2017**, *12* (8), e0182821.

30. Farrell, D. J.; Robbins, M.; Rhys-Williams, W.; Love, W. G., Investigation of the potential for mutational resistance to XF-73, retapamulin, mupirocin, fusidic acid, daptomycin, and vancomycin in methicillin-resistant *Staphylococcus aureus* isolates during a 55-passage study. *Antimicrob. Agents Chemother.* **2011**, *55* (3), 1177-81.
31. Mohammad, H.; Cushman, M.; Seleem, M. N., Antibacterial evaluation of synthetic thiazole compounds in vitro and in vivo in a methicillin-resistant *Staphylococcus aureus* (MRSA) skin infection mouse model. *PLoS One* **2015**, *10* (11), e0142321.
32. van Hal, S. J.; Fowler, V. G., Is it time to replace vancomycin in the treatment of methicillin-resistant *Staphylococcus aureus* infections? *Clin. Infect. Dis.* **2013**, *56* (12), 1779-88.
33. Wise, R.; Andrews, J. M.; Boswell, F. J.; Ashby, J. P., The in-vitro activity of linezolid (U-100766) and tentative breakpoints. *J. Antimicrob. Chemother.* **1998**, *42* (6), 721-8.
34. MacGowan, A. P., Pharmacokinetic and pharmacodynamic profile of linezolid in healthy volunteers and patients with Gram-positive infections. *J. Antimicrob. Chemother.* **2003**, *51 Suppl 2*, ii17-25.
35. Piddock, L. J., Multidrug-resistance efflux pumps - not just for resistance. *Nat. Rev. Microbiol.* **2006**, *4* (8), 629-36.
36. Opperman, T. J.; Nguyen, S. T., Recent advances toward a molecular mechanism of efflux pump inhibition. *Front. Microbiol.* **2015**, *6*, 421.

37. D'Lima, L.; Friedman, L.; Wang, L.; Xu, P.; Anderson, M.; Debabov, D., No decrease in susceptibility to NVC-422 in multiple-passage studies with methicillin-resistant *Staphylococcus aureus*, *S. aureus*, *Pseudomonas aeruginosa*, and *Escherichia coli*. *Antimicrob. Agents Chemother.* **2012**, *56* (5), 2753-5.
38. Mohamed, M. F.; Seleem, M. N., Efficacy of short novel antimicrobial and anti-inflammatory peptides in a mouse model of methicillin-resistant *Staphylococcus aureus* (MRSA) skin infection. *Drug Des. Devel. Ther.* **2014**, *8*, 1979-83.
39. Thangamani, S.; Mohammad, H.; Abushahba, M. F.; Hamed, M. I.; Sobreira, T. J.; Hedrick, V. E.; Paul, L. N.; Seleem, M. N., Exploring simvastatin, an antihyperlipidemic drug, as a potential topical antibacterial agent. *Sci. Rep.* **2015**, *5*, 16407.

Chapter 6:

1. Frieden, T., Antibiotic Resistance Threats in the United States, 2013. Centers for Disease Control and Prevention: Atlanta, GA, USA, 2013; p 114.
2. Epand, R. M.; Walker, C.; Epand, R. F.; Magarvey, N. A., Molecular mechanisms of membrane targeting antibiotics. *Biochim. Biophys. Acta* **2016**, *1858* (5), 980-7.
3. Opoku-Temeng, C.; Dayal, N.; Miller, J.; Sintim, H. O., Hydroxybenzylidene-indolinones, c-di-AMP synthase inhibitors, have antibacterial and anti-biofilm activities and also re-sensitize resistant bacteria to methicillin and vancomycin. *RSC Adv.* **2017**, *7* (14), 8288-8294.

4. Witte, G.; Hartung, S.; Buettner, K.; Hopfner, K.-P., Structural biochemistry of a bacterial checkpoint protein reveals diadenylate cyclase activity regulated by DNA recombination intermediates. *Mol. Cell* **2008**, *30* (2), 167-178.
5. Peng, X.; Zhang, Y.; Bai, G.; Zhou, X.; Wu, H., Cyclic di-AMP mediates biofilm formation. *Mol. Microbiol.* **2016**, *99* (5), 945-59.
6. Corrigan, R. M.; Abbott, J. C.; Burhenne, H.; Kaefer, V.; Gründling, A., C-di-AMP is a new second messenger in *Staphylococcus aureus* with a role in controlling cell size and envelope stress. *PLoS Pathog.* **2011**, *7* (9), e1002217.
7. Bai, Y.; Yang, J.; Zarrella, T. M.; Zhang, Y.; Metzger, D. W.; Bai, G., Cyclic di-AMP impairs potassium uptake mediated by a cyclic di-AMP binding protein in *Streptococcus pneumoniae*. *J. Bacteriol.* **2014**, *196* (3), 614-623.
8. Woodward, J. J.; Iavarone, A. T.; Portnoy, D. A., c-di-AMP secreted by intracellular *Listeria monocytogenes* activates a host Type I interferon response. *Science* **2010**, *328* (5986), 1703-1705.
9. Song, J. H.; Ko, K. S.; Lee, J. Y.; Baek, J. Y.; Oh, W. S.; Yoon, H. S.; Jeong, J. Y.; Chun, J., Identification of essential genes in *Streptococcus pneumoniae* by allelic replacement mutagenesis. *Mol. Cells* **2005**, *19* (3), 365-374.
10. Corrigan, R. M.; Bowman, L.; Willis, A. R.; Kaefer, V.; Gründling, A., Cross-talk between two nucleotide-signaling pathways in *Staphylococcus aureus*. *J. Biol. Chem.* **2015**, *290* (9), 5826-39.
11. Zheng, Y.; Zhou, J.; Sayre, D. A.; Sintim, H. O., Identification of bromophenol thiohydantoin as an inhibitor of DisA, a c-di-AMP synthase, from a

- 1000 compound library, using the coralyne assay. *Chem. Commun.* **2014**, 50 (76), 11234-11237.
12. Müller, M.; Deimling, T.; Hopfner, K. P.; Witte, G., Structural analysis of the diadenylate cyclase reaction of DNA-integrity scanning protein A (DisA) and its inhibition by 3'-dATP. *Biochem. J.* **2015**, 469, 367-374.
13. Zheng, Y.; Tsuji, G.; Opoku-Temeng, C.; Sintim, H. O., Inhibition of *P. aeruginosa* c-di-GMP phosphodiesterase RocR and swarming motility by a benzoisothiazolinone derivative. *Chem. Sci.* **2016**, 7 (9), 6238-6244.
14. Zheng, Y.; Zhou, J.; Cooper, S. M.; Opoku-Temeng, C.; De Brito, A. M.; Sintim, H. O., Structure-activity relationship studies of c-di-AMP synthase inhibitor, bromophenol-thiohydantoin. *Tetrahedron* **2016**, 72 (25), 3554-3558.
15. Rao, F.; See, R. Y.; Zhang, D.; Toh, D. C.; Ji, Q.; Liang, Z.-X., YybT is a signaling protein that contains a cyclic dinucleotide phosphodiesterase domain and a GGDEF domain with ATPase activity. *J. Biol. Chem.* **2010**, 285 (1), 473-482.
16. Wang, M.; Soorshjani, M. A.; Mikek, C.; Opoku-Temeng, C.; Sintim, H. O., Suramin potently inhibits cGAMP synthase, cGAS, in THP1 cells to modulate IFN- β levels. *Future Med. Chem.* **2018**, 10 (11), 1301-1317.
17. Lackey, K.; Cory, M.; Davis, R.; Frye, S. V.; Harris, P. A.; Hunter, R. N.; Jung, D. K.; McDonald, O. B.; McNutt, R. W.; Peel, M. R.; Rutkowske, R. D.; Veal, J. M.; Wood, E. R., The discovery of potent cRaf1 kinase inhibitors. *Bioorg Med Chem Lett* **2000**, 10 (3), 223-6.
18. Srivastava, D.; Waters, C. M., A tangled web: regulatory connections between quorum sensing and cyclic Di-GMP. *J. Bacteriol.* **2012**, 194 (17), 4485-93.

19. Zeden, M. S.; Schuster, C. F.; Bowman, L.; Zhong, Q.; Williams, H. D.; Gründling, A., Cyclic di-adenosine monophosphate (c-di-AMP) is required for osmotic regulation in. *J. Biol. Chem.* **2018**, *293* (9), 3180-3200.